Engineering and integration of pathways for anaerobic redox-cofactor balancing in yeast

van Aalst, A.C.A.

DOI
10.4233/uuid:9a149309-2339-40c5-9151-032d70b91dbe

Publication date
2023

Document Version
Final published version

Citation (APA)
van Aalst, A. C. A. (2023). *Engineering and integration of pathways for anaerobic redox-cofactor balancing in yeast*. [Dissertation (TU Delft), Delft University of Technology]. https://doi.org/10.4233/uuid:9a149309-2339-40c5-9151-032d70b91dbe

Engineering and integration of pathways for anaerobic redox-cofactor balancing in yeast

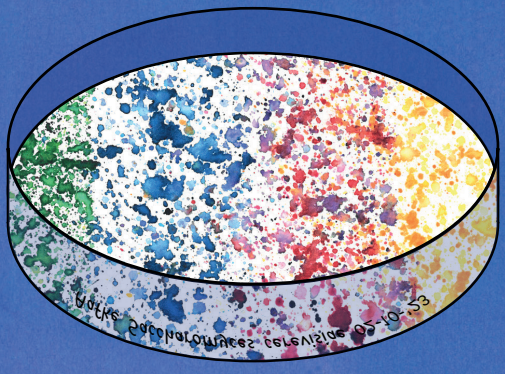

Aafke C.A. van Aalst

Engineering and integration of pathways for anaerobic redox-cofactor balancing in yeast

Dissertation

for the purpose of obtaining the degree of doctor

at Delft University of Technology

by the authority of the Rector Magnificus prof. dr. ir. T.H.J.J. van der Hagen,

Chair of the Board for Doctorates

to be defended publicly on

Monday 2 October 2023 at 12:00 o'clock

by

Aafke Cornelie Albertine VAN AALST

Master of Science in Life Science and Technology, Delft University of Technology, The Netherlands

born in Breda, The Netherlands

This dissertation has been approved by the promotors.

Composition of the doctoral committee:

Rector Magnificus	Chairperson
prof. dr. J. T. Pronk	Delft University of Technology, promotor
prof. dr. ir. J. G. Daran	Delft University of Technology, promotor

Independent members:

prof. dr. V. Siewers	Chalmers University of Technology
prof. dr. R.A. Weusthuis	Wageningen University & Research
prof. dr. ir. H.J. Noorman	Delft University of Technology / DSM
dr. M. Chow	IFF

Other member:

dr. ir. R. Mans	Hyasynth Bio, Canada

Reserve member:

prof. dr. ir. P.A.S. Daran-Lapujade	Delft University of Technology

The research presented in this thesis was performed at the Industrial Microbiology Section, Department of Biotechnology, Faculty of Applied Sciences, Delft University of Technology, The Netherlands. The project was financed by DSM Bio-based Products & Services B.V.

Cover	A.C.A. van Aalst
Layout	A.C.A. van Aalst
Printed by	Ridderprint | www.ridderpint.nl
ISBN	978-94-6483-352-2

Table of contents

Summary

The production of ethanol from sugars with the yeast *Saccharomyces cerevisiae* remains the process in industrial biotechnology with the largest product volume (ca. 100 million litres annually in 2022). Bioethanol provides an alternative to fossil transport fuels, but as the price of the feedstock can account for up to 70% of the total production costs, the bioethanol industry generally operates at low profit margins. To be able to compete with the economics of the petrochemical industry, maximization of the ethanol yield on sugar is essential. Carbon losses occur due to the formation of biomass and glycerol, which can account for at least 8% of the product. Under anaerobic conditions, formation of yeast biomass and glycerol are coupled via redox-cofactor balances, as a net generation of NADH during biomass formation needs to be compensated by NADH-dependent formation of glycerol from sugar. **Chapter 1** of this thesis discusses past research and recent advances in pathway engineering strategies for maximizing ethanol yields on the sugars glucose and sucrose. In particular, attention is paid to engineering strategies that alter the ratio of ethanol, biomass and glycerol formation in *S. cerevisiae*.

A particularly interesting strategy to reduce glycerol formation depends on functional implementation in *S. cerevisiae* of phosphoribulokinase (PRK) and ribulose-1,5-bisphosphate carboxylase/oxygenase (RuBisCO), which together create a non-oxidative bypass of glycolysis. In an earlier proof-of-principle study, in slow-growing sugar-limited chemostat cultures (D = 0.05 h^{-1}), the implementation of PRK and RuBisCO was shown to enable the use of CO_2, whose production is stoichiometrically linked to alcoholic fermentation, as an alternative electron acceptor. In these cultures, the glycerol yield on sugar of an engineered strain carrying these modifications was 90% lower than that of the reference strain, while its ethanol yield on sugar was 10% higher. Building on this strategy, the yeast metabolic network of PRK-RuBisCO yeast strains was further engineered to improve specific growth rates in anaerobic batch cultures. This resulted in a PRK-RuBisCO strain that was optimized for high ethanol yield, low glycerol yield and fast growth. In industrial bioethanol production, high ethanol concentrations and/or nutrient depletion cause a progressively decreasing growth rate of the yeast cells during the fermentation process. Therefore, in **Chapter 2**, the performance of the optimized PRK-RuBisCO strain was investigated in anaerobic chemostat cultures grown at submaximal growth rates (D = 0.05, 0.1 and 0.25 h^{-1}). In slow-growing anaerobic chemostat cultures (D = 0.05 h^{-1}), an engineered PRK-RuBisCO strain produced 80-fold more acetaldehyde and 30-fold more acetate

than a reference strain. This observation indicated an imbalance between *in vivo* activities of the PRK-RuBisCO bypass and the rate of formation of NADH in biosynthesis. Reducing the capacity of PRK and RuBisCO was shown to lead to 79% and 40% reduction in acetaldehyde and acetate production per glucose, respectively, in slow-growing cultures (D = 0.05 h^{-1}) compared to the original PRK-RuBisCO strain. Moreover, the resulting strain displayed a 72% lower glycerol yield and a 12% higher ethanol yield than a non-engineered *S. cerevisiae* strain in anaerobic batch cultures. Employing a growth-rate-dependent promoter to express *PRK* highlighted the potential of adjusting gene expression in engineered strains to adapt to growth-rate variations in industrial batch processes.

Another strategy to reduce glycerol formation depends on the introduction of an acetate-to-ethanol reduction pathway based on heterologous acetylating acetaldehyde dehydrogenase (A-ALD). Previously, this strategy was shown to be able to replace glycerol formation as 'redox sink' and improve ethanol yields in media containing high concentrations of acetate. Acetate concentrations in feedstock for first-generation bioethanol production are, however, insufficient to completely replace glycerol formation. For optimal performance in industrial settings, yeast strains should ideally first fully convert acetate and, subsequently, continue low-glycerol fermentation via an alternative reduction pathway. **Chapter 3** focusses on the performance of engineered *S. cerevisiae* strains that harbour a functional A-ALD pathway as well as a functional PRK-RuBisCO pathway. However, anaerobic batch cultures of a strain carrying both pathways showed inferior acetate reduction relative to a strain carrying only the A-ALD pathway. The negative impact of the PRK-RuBisCO pathway on acetate reduction was attributed to sensitivity of the reversible A-ALD reaction to high intracellular acetaldehyde concentrations. Complete A-ALD-mediated acetate reduction by a dual-pathway strain, was achieved upon reducing PRK abundance by a C-terminal extension of its amino acid sequence. Yields of glycerol and ethanol on glucose were 55% lower and 6% higher, respectively, than those of a non-engineered reference strain. This outcome represents a first proof-of-principle for effectively converting feedstocks with low acetate content into ethanol while removing all acetate from the growth medium.

In contrast to the previous chapters, which focused on metabolic engineering strategies in mono-cultures, **Chapter 4** investigates potential advantages of the use of co-cultures to balance *in vivo* activity of different heterologous reduction pathways with the *in vivo* demand for NADH reoxidation. Co-cultivation of the previously characterized PRK-RuBisCO strain and A-ALD strain in anaerobic batch cultures on glucose, resulted in 84% and 72% lower acetate and acetaldehyde production,

respectively, than in corresponding monocultures of the PRK-RuBisCO strain. Moreover, on acetate-containing medium, the co-culture was able to fully convert all acetate into ethanol, and our results show that the kinetics of the co-cultivation process can be optimized by tuning the relative inoculum sizes of the two strains. At an inoculation ratio of 0.8:1 of the A-ALD-based and PRK-RuBisCO-based strains, respectively, the co-culture displayed a 6% higher ethanol yield and a 47% lower glycerol yield compared to mono-cultures of a non-engineered reference strain on acetate-containing medium. Further engineering of the A-ALD strain to completely block the glycerol reduction pathway, resulted in a strain completely dependent on acetate for its growth. Subsequent co-cultivation with this strain at an inoculation ratio of 1.0:1, resulted in a 7% higher ethanol yield and an 82% lower glycerol yield relative to mono-cultures of a non-engineered reference strain. The findings presented in this chapter illustrate the potential of employing defined consortia of engineered yeast strains for anaerobic ethanol production.

Previously described redox-engineering strategies for improving ethanol yield from glucose in *S. cerevisiae* cultures aim to approach the theoretical maximum yield of 2 moles of ethanol per mol of glucose. This ethanol yield can only be surpassed when additional electrons (e.g. in the form of NADH) are fed into the fermentation pathway. Sorbitol, a six-carbon polyol whose oxidation to pyruvate via glycerol yields one more NADH than conversion of glucose into pyruvate, provides an interesting model system for investigating this concept. **Chapter 5** explores the ability of an engineered yeast strain carrying the PRK-RuBisCO glycolytic bypass to anaerobically (co-)ferment sorbitol. In anaerobic, slow-growing chemostat cultures on glucose-sorbitol mixtures ($D = 0.025\ h^{-1}$), functional expression of PRK-RuBisCO-pathway genes enabled a 12-fold higher rate of sorbitol co-consumption than observed in a sorbitol-consuming reference strain. Moreover, this strain displayed a 91% lower glycerol production, which, in combination with the increased sorbitol conversion, resulted in a 15% higher ethanol yield. This study demonstrates the increased flexibility of redox-cofactor metabolism in anaerobic *S. cerevisiae* cultures. Moreover, these results are the first steps towards improved product yields in yeast-based anaerobic processes by facilitating the introduction of additional electrons.

Samenvatting

De productie van ethanol uit suikers met behulp van de gist *Saccharomyces cerevisiae* is, op volumebasis, nog steeds het proces in de industriële biotechnologie met de hoogste jaarlijkse productie. De huidige industriële productieprocessen zijn voornamelijk gebaseerd op de microbiële fermentatie van suikers afkomstig uit mais of suikerriet. Bio-ethanol biedt een alternatief voor fossiele transportbrandstoffen, maar doordat de prijs van de grondstoffen tot wel 70% van de totale productie kosten kan bedragen, opereert de bio-ethanol industrie met lage winstmarges. Om te kunnen concurreren met de petrochemische industrie, is maximalisatie van de ethanolopbrengst op suiker essentieel. Tijdens de productie van bio-ethanol gaat koolstof verloren als gevolg van de vorming van biomassa en glycerol, die samen ten minste 8% van het gevormde product kunnen uitmaken. Onder anaerobe condities zijn de vorming van biomassa en glycerol gekoppeld via redox-cofactorbalansen, aangezien NADH die gegenereerd wordt tijdens de vorming van biomassa opnieuw geoxideerd moet worden via NADH-afhankelijke vorming van glycerol uit suiker. **Hoofdstuk 1** van dit proefschrift bespreekt eerdere onderzoeken en recente ontwikkelingen in 'metabolic engineering'-strategieën om de ethanolopbrengst uit de suikers glucose en sucrose te maximaliseren. Hierbij wordt in het bijzonder aandacht besteed aan strategieën voor het aanpassen van de verhouding tussen ethanol productie, biomassavorming en glycerolvorming in *S. cerevisiae*.

Een zeer interessante strategie om de vorming van glycerol te verminderen, is gebaseerd op de functionele implementatie van phosphoribulokinase (PRK) en ribulose-1,5-bisfosfaat carboxylase/oxygenase (RuBisCO) in *S. cerevisiae*. Hiermee wordt een niet-oxidatieve omleiding van de glycolyse gecreëerd, die gebruik maakt van CO_2 als een alternatieve elektronacceptor. In een eerdere ''proof-of-principle'' studie werd in langzaam groeiende chemostaatculturen ($D = 0{,}05\ h^{-1}$) aangetoond dat de implementatie van PRK en RuBisCO leidde tot een 90% lagere glycerolopbrengst en een 10% hogere opbrengst van ethanol dan in een niet-gemodificeerde stam. Vervolgens werd het metabolisme van PRK-RuBisCO-stammen verder aangepast om dezelfde verbeteringen te behalen in snel groeiende anaerobe batchculturen. Dit resulteerde in een PRK-RuBisCO-stam die geoptimaliseerd was voor hoge ethanolopbrengst, lage glycerolproductie en snelle groei. Tijdens industriële bio-ethanolproductie neemt de groeisnelheid van de gist geleidelijk af door hoge ethanolconcentratie en/of uitputting van voedingsstoffen. Daarom worden in **Hoofdstuk 2** de prestaties van de geoptimaliseerde PRK-RuBisCO-stam onderzocht

bij submaximale specifieke groeisnelheden in anaerobe chemostaatculturen (D = 0,05, 0,1 en 0,25 h^{-1}). In langzaam groeiende anaerobe chemostaatculturen (D = 0,05 h^{-1}) produceerde een genetisch gemodificeerde PRK-RuBisCO-stam 80 keer meer acetaldehyde en 30 keer meer acetaat dan een referentiestam. Deze waarneming suggereerde een discrepantie tussen de *in vivo* activiteit van de PRK-RuBisCO-route en de snelheid van de vorming van NADH in de biosynthese. Het verminderen van de capaciteit van PRK en RuBisCO leidde tot reducties van respectievelijk 79% en 40% in de productie van acetaldehyde en acetaat per hoeveelheid glucose in langzaam groeiende culturen (D = 0,05 h^{-1}) in vergelijking met de oorspronkelijke PRK-RuBisCO-stam. Bovendien vertoonde de resulterende stam een 72% lager glycerolrendement en een 12% hoger ethanolrendement dan een niet-genetisch gemodificeerde *S. cerevisiae*-stam in anaerobe batchculturen. Het gebruik van een groeisnelheids-afhankelijke promotor om de expressie van *PRK* te reguleren, benadrukte het belang van dynamische regulatie om genexpressie aan te passen aan de dynamische condities tijdens een bio-ethanol proces.

Een andere strategie om de vorming van glycerol te verminderen, is gebaseerd op heterologe acetylerende acetaldehyde dehydrogenase (A-ALD). Expressie van dit enzym maakt een acetaat-naar-ethanol route mogelijk, waardoor de vorming van glycerol als 'redox-sink' vervangen kan worden en de ethanolopbrengst verbeterd kan worden in media met hoge concentraties acetaat. De concentraties acetaat in eerste-generatie grondstoffen voor ethanolproductie zijn echter onvoldoende om de vorming van glycerol volledig te vervangen. Voor optimale prestaties onder industriële condities zouden giststammen idealiter eerst acetaat volledig moeten omzetten en vervolgens een alternatieve redox-strategie moeten gebruiken voor fermentatie met lage glycerolproductie. **Hoofdstuk 3** richt zich op de prestaties van genetisch gemodificeerde *S. cerevisiae*-stammen die zowel een functionele A-ALD-route als een functionele PRK-RuBisCO-route bevatten. Echter, anaerobe batchculturen van een stam met beide routes vertoonden verminderde acetaatreductie ten opzichte van een stam die alleen de A-ALD-route tot expressie bracht. Het negatieve effect van de PRK-RuBisCO-route op acetaatreductie werd toegeschreven aan de gevoeligheid van de reversibele A-ALD-reactie voor intracellulair acetaldehyde. Volledige A-ALD-acetaatreductie door een stam met beide routes werd bereikt door de hoeveelheid PRK te verminderen met behulp van een C-terminale verlenging van de aminozuursequentie. De opbrengsten van glycerol en ethanol op glucose waren respectievelijk 55% lager en 6% hoger dan die van een niet-genetisch gemodificeerde referentiestam. Dit resultaat vormt een eerste ‘proof-of-principle’ voor het efficiënt omzetten van grondstoffen met een lage acetaatconcentratie in ethanol.

In tegenstelling tot de voorgaande hoofdstukken, die zich richtten op onderzoek in monoculturen, richt **Hoofdstuk 4** zich op de mogelijke voordelen van het gebruik van co-culturen. Hierbij werd onderzocht of co-culturen gebruikt kunnen worden om de *in vivo* activiteit van verschillende heterologe reductie-routes in balans te brengen met de *in vivo* behoefte aan NADH-reoxidatie. Co-cultivatie van de eerder gekarakteriseerde PRK-RuBisCO-stam en de A-ALD-stam in anaerobe batchculturen op glucose resulteerde in respectievelijk 84% en 72% lagere productie van acetaat en acetaldehyde dan in monoculturen van de PRK-RuBisCO-stam. Bovendien kon de co-cultuur op medium met acetaat al het acetaat volledig omzetten in ethanol, en kon de kinetiek van het co-cultivatieproces geoptimaliseerd worden door de ratio van de twee stammen in het inoculum te variëren. Bij een inoculatieverhouding van 0,8:1 van de A-ALD-stam en de PRK-RuBisCO-stam had de co-cultuur een 6% hogere ethanolopbrengst en een 47% lagere glycerolopbrengst in vergelijking met een niet-genetisch gemodificeerde referentiestam. Verdere aanpassingen van de A-ALD-stam om de glycerolroute volledig te blokkeren, resulteerde in een stam die compleet afhankelijk is van acetaat voor de groei. Een co-cultuur met de PRK-RuBisCO-stam en de nieuwe A-ALD-stam, geïnoculeerd met een verhouding van 1,4:1, liet een 7% hogere ethanolopbrengst en een 82% lagere glycerolopbrengst zien, in vergelijking met monoculturen van een niet-genetisch gemodificeerde referentiestam. De bevindingen in dit hoofdstuk laten het potentieel zien van het gebruik van gedefinieerde consortia van genetisch gemodificeerde giststammen in de anaerobe ethanolproductie.

Eerder beschreven strategieën voor het verbeteren van de ethanolopbrengst uit glucose in *S. cerevisiae*-culturen hadden als doel om de theoretische maximale opbrengst van 2 mol ethanol per mol glucose te benaderen. Deze ethanolopbrengst kan alleen worden overtroffen wanneer extra elektronen (bijvoorbeeld in de vorm van NADH) aan de fermentatieroute worden toegevoegd. Sorbitol, een C_6-polyol waarvan de oxidatie tot pyruvaat via glycerol één extra NADH oplevert ten opzichte van de omzetting van glucose tot pyruvaat, biedt een interessant model voor het onderzoeken van dit concept. **Hoofdstuk 5** onderzoekt de mogelijkheid om anaeroob sorbitol om te zetten, met een genetisch gemodificeerde giststam die de PRK-RuBisCO-route tot expressie brengt. In anaerobe, langzaam groeiende chemostaatculturen op glucose-sorbitolmengsels ($D = 0{,}025\ h^{-1}$), kon de PRK-RuBisCO-stam 12 keer meer sorbitol omzetten per tijdseenheid dan een referentiestam. Bovendien vertoonde deze stam een 91% lagere glycerolproductie, hetgeen in combinatie met de verhoogde sorbitolomzetting resulteerde in een 15% hogere ethanolopbrengst. Dit onderzoek laat de verbeterde flexibiliteit van het redox-cofactor-metabolisme in anaerobe *S. cerevisiae*-culturen zien. Deze studie is een eerste

stap naar het mogelijk maken van introductie van extra elektronen, om ethanolopbrengsten in anaerobe processen verder te verbeteren.

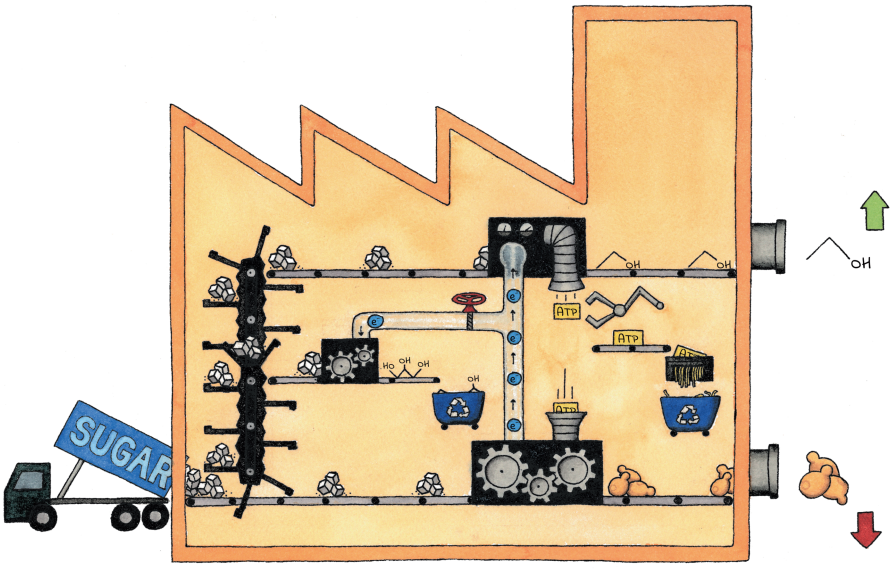

Visual abstract created by Sophie C. de Valk

Chapter 1

Introduction

Pathway engineering strategies for improved product yield in yeast-based industrial ethanol production

Aafke C. A. van Aalst[#], Sophie C. de Valk[#], Walter M. van Gulik, Mickel L. A. Jansen, Jack T. Pronk and Robert Mans

[#]These authors contributed equally

This chapter is essentially as published in Synthetic and Systems Biotechnology (2022) 7(1): 554-566.

Background

In 2020, 99 billion litres of ethanol were produced by yeast-based fermentation of agriculture-derived carbohydrates (1). Of this volume, approximately 30% was produced from Brazilian cane sugar (mainly consisting of sucrose) and approximately 54% from corn starch-derived glucose, mainly in the United States of America (1). Ethanol is predominantly used as a renewable 'drop-in' transport fuel and ethanol-based value chains towards other compounds, including jet fuel and polyethylene, are under development (2, 3).

Despite a plethora of academic and industrial studies on alternative microbial platforms (4), *Saccharomyces cerevisiae* remains the organism of choice for industrial ethanol production from carbohydrates. Factors that contribute to its popularity include rapid fermentation of glucose and sucrose to ethanol, insensitivity to phages, a long history of safe use in food applications and a high tolerance to ethanol. Ethanol concentrations in corn-starch-based, very-high-gravity fermentation processes can reach up to 21% (v/v) (5, 6). In bulk fermentation processes such as ethanol production, where costs of the carbohydrate feedstock can account for up to 70% of the total production costs (7), every detectable improvement of the ethanol yield on sugar is economically relevant. The extensive toolbox for genetic modification of *S. cerevisiae* (8) is therefore intensively used to explore options for maximizing ethanol yields by engineering its metabolic network.

In *S. cerevisiae*, anaerobic metabolism of glucose or sucrose starts with their conversion to pyruvate via the ATP-generating Embden-Meyerhof glycolytic pathway (9). NADH generated by this oxidative pathway is re-oxidized by the combined action of pyruvate decarboxylase (Pdc1, Pdc5, Pdc6, EC 4.1.1.1: pyruvate → acetaldehyde + CO_2) and NAD^+-dependent alcohol dehydrogenases (predominantly Adh1, EC 1.1.1.1: acetaldehyde + NADH → ethanol + NAD^+ (10)) (Fig. 1). This native yeast pathway for alcoholic fermentation perfectly conserves the degree of reduction of sugars (11) and almost completely captures their heat of combustion in ethanol (-2840 kJ per mol of glucose versus -2734 kJ per two moles of ethanol). Clearly, if alcoholic fermentation was the only relevant metabolic process in industrial ethanol production, attempts to improve ethanol yields on sugars as sole carbon and electron sources would be futile. Metabolic engineering strategies for improving ethanol yields are therefore directly or indirectly related to another cellular process that occurs during industrial ethanol production: anaerobic growth.

In the absence of growth, survival of yeast cells requires cellular maintenance metabolism, which encompasses use of ATP for growth-independent processes that

maintain structural integrity and viability (12). In anaerobic yeast cultures, this ATP is exclusively generated via alcoholic fermentation (Fig. 1). In contrast, growth of yeast cells not only requires ATP but also organic precursors for biomass components, whose biosynthetic pathways compete for carbon with ethanol production (Fig. 1). Anaerobic growth occurs in all current industrial processes for ethanol production and the resulting surplus yeast biomass is valorized by its inclusion in a byproduct stream sold as an animal feed supplement (13).

Growth is coupled to formation of glycerol, a second important byproduct of anaerobic yeast metabolism, by redox-cofactor metabolism. Formation of *S. cerevisiae* biomass from sugar, ammonium or urea and other nutrients is coupled to a net reduction of NAD^+ to NADH (14, 15) (Fig. 1). Anaerobic *S. cerevisiae* cultures cannot re-oxidize this NADH by mitochondrial respiration and instead rely on NADH-dependent reduction of the glycolytic intermediate dihydroxyacetone-phosphate to glycerol-3-phosphate, in a reaction catalyzed by NAD^+-dependent glycerol-3-phosphate dehydrogenase (Gpd1, Gpd2, EC 1.1.1.8 (16, 17)). Glycerol-3-phosphate is then hydrolyzed by glycerol-3-phosphate-phosphatase (Gpp1, Gpp2, EC 3.1.3.21 (18)) to yield phosphate and glycerol (Fig. 1). In processes based on wild-type *S. cerevisiae* strains, approximately 4% of the potential ethanol yield on carbohydrate feedstocks was estimated to be lost to glycerol (19). Based on current ethanol production volumes, this loss would correspond to approximately 4 billion litres of ethanol per year.

The aim of this chapter is to review the current body of knowledge on pathway engineering strategies that focus on maximizing ethanol yields on glucose or sucrose by altering the ratio of ethanol, biomass and glycerol formation in *S. cerevisiae*. This scope excludes a large body of metabolic engineering research aimed at expanding the sugar- and polysaccharide substrate range of *S. cerevisiae* to enable its nascent application for industrial-scale fermentation of lignocellulosic hydrolysates generated from agricultural residues or energy crops (reviewed in (4, 20-22)). However, the discussed strategies can, in principle, be applied in such 'second-generation' bioethanol processes as well as in 'first-generation' processes based on corn starch or cane sugar, once other metabolic engineering strategies have been successfully addressed.

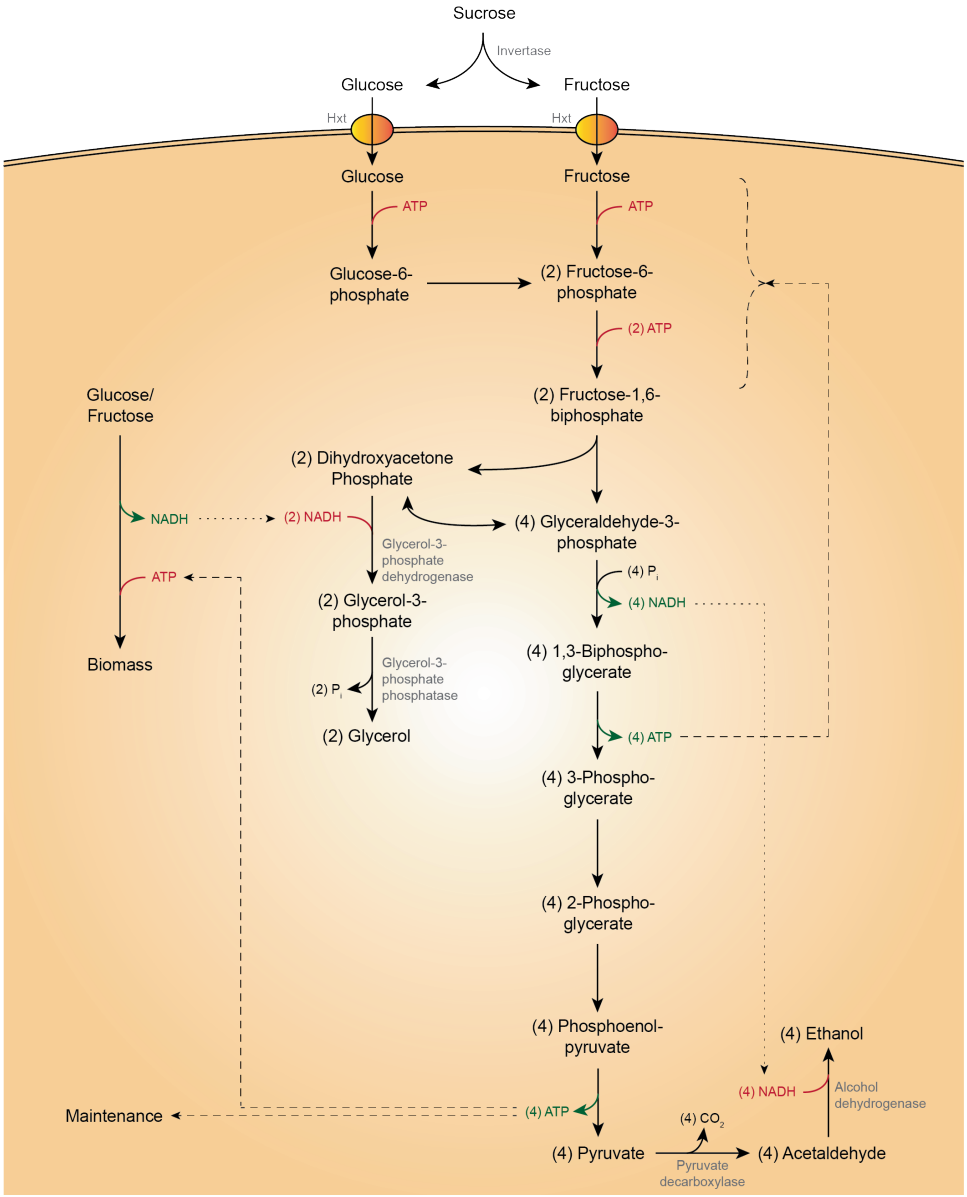

Figure 1: Schematic representation of the distribution of substrate over biomass, glycerol, ethanol and CO_2 in anaerobically growing *S. cerevisiae*. NADH/NAD$^+$ redox-cofactor coupling and use of ATP for sugar phosphorylation, biomass formation and maintenance are indicated by dotted and dashed arrows, respectively. Glucose, fructose and (after hydrolysis) sucrose are converted into pyruvate via the Emden-Meyerhoff glycolysis, yielding 2 NADH and 2 ATP per glucose equivalent. ATP is used for cellular maintenance and synthesis of biomass (growth). NADH is primarily re-oxidized via alcoholic fermentation, but a surplus of NADH formed during biomass synthesis is re-oxidized via the production of glycerol.

Process conditions

Growth of anaerobic laboratory cultures of wild-type *S. cerevisiae* strains under different conditions provided insight in how distribution of sugar over biomass, glycerol and ethanol can be influenced and has therefore been a key source of inspiration for the design of metabolic engineering strategies. In anaerobic, sugar-limited cultures of *S. cerevisiae*, maintenance-energy requirements are essentially growth-rate independent (23-25). The fraction of the consumed sugar that is fermented to ethanol therefore increases with decreasing specific growth rate (12) (Fig. 2A). This correlation is clearly demonstrated in anaerobic retentostat cultures of *S. cerevisiae*, in which all biomass is retained in the culture and only cell-free effluent leaves the reactor. In such systems, near-theoretical ethanol yields on glucose were demonstrated during prolonged growth at near-zero specific growth rates (23).

As an alternative to reducing the specific growth rate, the fraction of the sugar substrate that is fermented to ethanol by actively growing anaerobic cultures to meet maintenance-energy requirements can be increased by changing cultivation conditions. In particular, addition of weak organic acids such as lactate, acetate, propionate or benzoate to anaerobic batch and chemostat cultures grown at low pH, was shown to lead to lower biomass yields and higher ethanol yields (15, 26-30). These results reflect an increased maintenance energy requirement for intracellular pH homeostasis, caused by an influx of protons into the yeast cytosol as a result of weak acid diffusion (Fig. 2B) (31). In anaerobic yeast cultures, countering this 'weak acid uncoupling' and maintenance of intracellular pH homeostasis critically depends on ATP-dependent proton export by the plasma membrane ATPase (Pma1, EC 7.1.2.1) (Fig. 2D) (32, 33). These observations clearly indicate the potential of modifying maintenance-energy requirements as a means to improve ethanol yields. Practical issues such as costs of adding organic acids and their subsequent removal from process effluents, as well as potential synergies of weak organic acid and ethanol toxicity (34, 35), preclude direct application of weak organic acid uncoupling in industrial bioethanol production. Feedstocks for 'second-generation' bioethanol production already contain inhibitors such as acetic acid, furfural and hydroxymethyl-2-furaldehyde (21, 36-38), which cause increased ATP requirements for cellular maintenance. In addition, high concentrations of ethanol also in themselves affect maintenance energy requirements by increasing permeability of the yeast plasma membrane to protons and thereby activating Pma1 (39, 40).

Experiments on disaccharide metabolism by anaerobic *S. cerevisiae* cultures provided a first demonstration that ethanol yields can be modified by changing the mechanism of sugar import. In contrast to transport of glucose, which occurs via facilitated

diffusion by Hxt transporters (41, 42), uptake of its dimer maltose by *S. cerevisiae* is mediated by Malx1 transporters and involves symport with a single proton (32, 43). After intracellular hydrolysis of maltose by a Malx2 maltase (EC 3.2.1.20, maltose + H_2O → 2 glucose), alcoholic fermentation of the resulting two glucose molecules yields 4 molecules of ATP. However, since one of these ATP molecules has to be used to enable expulsion of the symported proton by Pma1, which has a stoichiometry of 1 H^+/ATP (32, 43), the net ATP yield from maltose fermentation is only 1.5 ATP per glucose equivalent (Fig. 2C). Indeed, based on hexose units, ethanol and biomass yields of *S. cerevisiae* in anaerobic maltose-limited chemostat cultures were shown to be 16% higher and 25% lower, respectively, than in corresponding glucose-limited cultures (33). These observations inspired metabolic engineering studies that were focused on sucrose-containing feedstock for bioethanol production.

During growth on ammonium or urea (19, 44), a significant part of the 'surplus' NADH generated in biosynthesis is derived from the synthesis of amino acids from these nitrogen sources and sugar. Several studies reported lower glycerol yields and higher ethanol yields on sugar in anaerobic cultures grown with amino acids or yeast extract as the nitrogen source (45-47). Although use of amino acids as industrial nitrogen source is not an economically viable proposition, these observations highlighted the potential for engineering redox-cofactor metabolism to improve ethanol yields.

Engineering of energy coupling

Introduction of futile cycles

Several metabolic engineering strategies have been explored to increase the use of sugar for cellular maintenance energy requirements by introducing metabolic 'futile cycles', whose net effect is the hydrolysis of ATP to ADP and inorganic phosphate with a concomitant release of heat (Fig. 2E). Such 'ATP wasting' cycles can either be introduced by constitutive expression of ATPases or by creating more complicated futile cycles that cause a net hydrolysis of ATP. Overexpression of the soluble F1 unit of the *Escherichia coli* H^+-ATPase in *S. cerevisiae* (48, 49) led to a 10% increase of the anaerobic ethanol yield on glucose relative to a reference strain, but also caused a 26% decrease of the specific growth rate (49). Overexpression of *PHO5* or *PHO8*, which encode aspecific phosphatases (EC 3.1.3.1/2) (50, 51) was similarly reported to cause increased ATP turn-over. *PHO8* overexpression was reported to cause a 17% higher ethanol yield on glucose, without affecting growth rate (51). Simultaneous activity of ATP-generating glycolytic and ATP-consuming gluconeogenic enzymes leads to textbook examples of futile metabolic cycles. Though not tested with the specific aim to improve ethanol yields, overexpression of the gluconeogenic enzyme fructose-1,6-

bisphosphatase (Fbp1, EC 3.1.3.11: fructose-1,6-bisphosphate + H_2O → fructose-6-phosphate + P_i) increased glucose consumption (19%) and CO_2 (10%) and ethanol (14%) production rates of aerobic suspensions of non-growing cells (52). An even more pronounced effect on the ethanol production rate (22%) was found when the gluconeogenic enzyme phosphoenolpyruvate carboxykinase (PEPCK, EC 4.1.1.49: oxaloacetate + ATP → phosphoenolpyruvate + ADP + CO_2) was simultaneously overexpressed (52, 53). More recently, *E. coli* PEPCK (*pckA*) was overexpressed together with the yeast anaplerotic enzyme pyruvate carboxylase (Pyc2, EC 6.4.1.1: pyruvate + ATP + CO_2 → oxaloacetate + ADP + Pi) (54). Simultaneous activity of these enzymes results in hydrolysis of two ATP molecules for the formation of phosphoenolpyruvate (PEP) from pyruvate. Since, in glucose-grown cultures, the glycolytic enzyme pyruvate kinase (Pyk2, Cdc19, EC 2.7.1.40) converts PEP back to pyruvate with the formation of only a single ATP, the net result of this futile cycle is the hydrolysis of one ATP. The potential of this strategy was demonstrated by more ethanol production, related to yeast biomass, by the overexpression strain than by the control strain (54).

An inherent risk of the constitutive expression of futile cycles is that, in industrial processes, situations may occur in which a too large drain of the cellular ATP content can no longer be compensated for by faster alcoholic fermentation. In extreme situations, net ATP synthesis might even decrease below maintenance energy-requirements and cause cell death. Careful 'tuning' of the *in vivo* activity of engineered futile cycles can, in principle, address this problem in cultures grown under constant conditions in the laboratory. However, such tuning would be much more difficult to achieve in large-scale industrial processes, which are highly dynamic, for example as a consequence of changing sugar and ethanol concentrations. Application-oriented pathway-engineering studies therefore mostly focus on strategies that, instead, aim at a fixed, stoichiometric reduction of the ATP yield from ethanol fermentation.

Decreasing the ATP stoichiometry of yeast glycolysis

The bacterium *Zymomonas mobilis* employs the Entner-Doudoroff (ED) pathway for alcoholic fermentation. Instead of the 2 mol ATP (mol glucose)$^{-1}$ generated in yeast glycolysis, this pathway has a net ATP yield of only 1 mol ATP (mol glucose)$^{-1}$ (55, 56). As a consequence, high ethanol yields can be achieved in growing *Z. mobilis* cultures (55, 56). A now expired patent proposed functional expression of the ED pathway in *S. cerevisiae* (Fig. 2F) (57). However, experimental studies failed to achieve the high *in vivo* activities of 6-phosphogluconate dehydratase (PGDH, EC 4.2.1.12: 6-phosphogluconate → 2-dehydro-3-deoxy-gluconate-6-phosphate) in *S. cerevisiae* that would be required to demonstrate an impact on ethanol yield (58, 59). A limiting

activity of PGDH, which contains an [4Fe-4S] iron-sulfur cluster (60), was attributed to the well-documented difficulties in synthesizing heterologous iron-sulfur-cluster enzymes in the yeast cytosol (61).

An alternative approach to reduce the ATP yield of glycolysis in *S. cerevisiae* was based on functional expression of a heterologous, non-phosphorylating, $NADP^+$-dependent glyceraldehyde-3-phosphate dehydrogenase (GAPN, EC 1.2.1.9: glyceraldehyde-3-phosphate + $NADP^+$ → 3-phosphoglycerate + NADPH), which bypasses the ATP-generating phosphoglycerate kinase reaction (Pgk1, EC 2.7.2.3: 1,3-biphosphoglycerate + ADP → 3-phosphoglycerate + ATP) (62-64). Strains engineered with this strategy increased the ethanol yield in anaerobic cultures by 3% (62) and 7.6% (63). This increase was partly attributed to a lower ATP yield of glycolysis and partly to changes in redox-cofactor metabolism.

Altering topology and energy coupling of disaccharide metabolism and transport
In contrast to maltose which, as described above, is taken up by proton symport prior to hydrolysis (32, 33, 43), sucrose metabolism in wild-type *S. cerevisiae* strains is predominantly initiated by its extracellular hydrolysis to glucose and fructose, catalysed by invertase (Suc2, EC 3.2.1.26) (Fig. 1) (65, 66). After uptake via facilitated diffusion, mediated by Hxt transporters (67), these hexoses are oxidized to pyruvate by yeast glycolysis.

Due to the presence of a second start codon in the *SUC2* transcript, a small fraction of the expressed invertase is retained in the cytosol (65) while, moreover, the Mal11 (Agt1) maltose-proton symporter is also able to import sucrose (68, 69). Replacement of the native *SUC2* gene by a constitutively expressed, truncated *SUC2* gene that no longer encoded the N-terminal excretion sequence of Suc2 led to a near-complete targeting of invertase to the yeast cytosol (Fig. 2G) (70). Adaptive laboratory evolution of an engineered *S. cerevisiae* strain synthesizing this internal invertase ('iSuc2') in anaerobic, sucrose-limited chemostat cultures yielded an evolved strain with increased expression of *MAL11*. When compared under identical conditions in anaerobic chemostat cultures, the evolved strain showed an 11% higher ethanol yield and a 30% lower biomass yield on sucrose than the reference strain (70). These results were in good agreement with predictions based on stoichiometric models of yeast metabolism and mirrored earlier comparisons of biomass and product yields of wild-type *S. cerevisiae* grown anaerobically on maltose and glucose (33). Using a similar strategy, it should also be possible to decrease the ATP yield of monosaccharide dissimilation by replacing the endogenous facilitated diffusion transporters by proton symporters (71, 72).

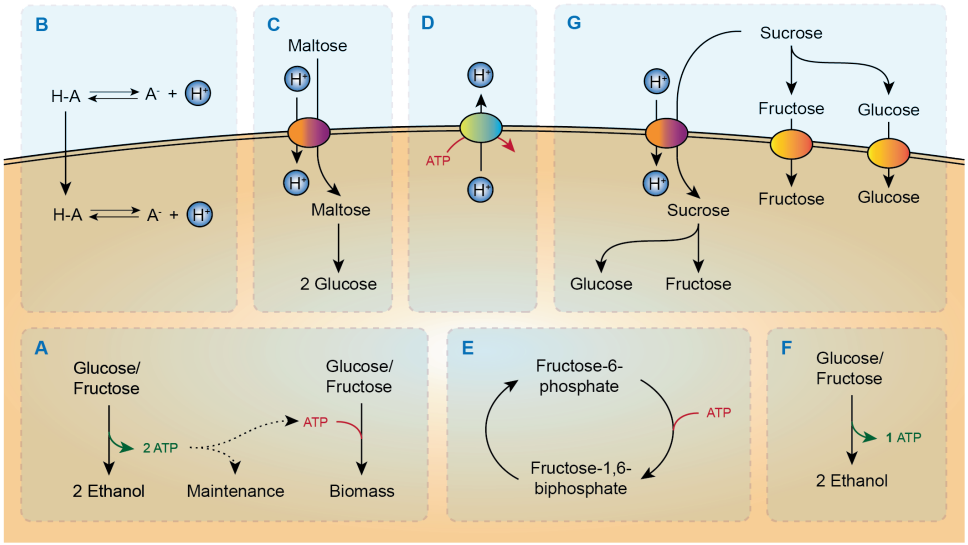

Figure 2: Schematic representation of energy metabolism in *S. cerevisiae* and strategies to improve ethanol yield on sugar. A: Alcoholic fermentation of glucose or fructose. B: Maintenance energy requirements can be increased by presence of weak organic acids in culture medium. C: The net ATP yield (mol ATP/mol glucose equivalent) of maltose utilization is lower than that of glucose, since maltose transport is proton coupled, whereas glucose is transported via facilitated diffusion. D: Plasma membrane ATPase exports protons at the cost of ATP. E: Example of a futile cycle, e.g. a set of reactions that leads to net hydrolysis of ATP, that can be introduced in order to enforce 'ATP wasting'. F: The Enter-Doudoroff glycolytic pathway yields only 1 ATP per glucose equivalent, instead of 2 ATP. G: Intracellular targeting of invertase (iSuc2) combined with uptake of sucrose by proton symport (left) lowers the ATP yield compared to wildtype *S. cerevisiae*, where sucrose is hydrolyzed extracellularly, after which the resulting monosaccharides are taken up via facilitated diffusion (right).

Engineering of redox metabolism

Multiple pathway engineering strategies for improving ethanol yield on sugars aim to minimize production of glycerol. In aerobic *S. cerevisiae* cultures, generation of glycerol-3-phosphate by the Gpd1 and Gpd2 glycerol-3-phosphate dehydrogenases is non-essential due to the presence of an alternative route for glycerolipid synthesis that involves 1-acyldihydroxyacetone-phosphate as intermediate (73). In contrast, due to the essential role of glycerol formation in NADH redox-cofactor balancing in non-respiratory cultures, double deletion of *GPD1* and *GPD2* prevents anaerobic growth (74, 75). Anaerobic growth of *gpd1Δ gpd2Δ* strains can be rescued by supplementation of compounds such as acetaldehyde or acetoin, which can be reduced by intracellular NADH-dependent dehydrogenases (74, 75). Glycerol-

negative mutants are highly sensitive to osmotic stress due to the key role of glycerol in osmotolerance of *S. cerevisiae* (74, 76).

In anaerobic, glucose-limited cultures of *S. cerevisiae* grown on synthetic media with ammonium as nitrogen source, approximately 12 mmol of glycerol is formed per gram of biomass dry weight (74, 77), which closely matches calculated requirements for NADH re-oxidation (78). Strain-dependent diversity in glycerol production may reflect different biomass composition, formation of metabolites whose formation is coupled to a net generation of NADH (e.g. acetate (75)) and/or activity of the γ-butyric acid (GABA) shunt (79). 'Tuning' of *in vivo* activities of glycerol-3-phosphate dehydrogenase, by deletion of either *GPD1* or *GPD2* or by promoter engineering, has in different wild-type *S. cerevisiae* strain backgrounds and under different (semi-) anaerobic cultivation conditions, been shown to affect specific growth rates, glycerol and ethanol yields (Fig. 3B) (19, 74, 75, 80). While biomass synthesis in *S. cerevisiae* results in a net reduction of NAD^+ to NADH, it requires a net oxidation of NADPH to $NADP^+$ (81, 82). Based on this observation, Anderlund *et al*. (1999) (83) and Nissen *et al*. (2001) (84) explored whether expression of heterologous soluble transhydrogenases (EC 1.6.1.1: NADPH + NAD^+ → $NADP^+$ + NADH) from *E. coli* or *Azotobacter vinelandii*, respectively, could convert the 'surplus' NADH generated by anaerobic *S. cerevisiae* cultures into NADPH and thereby lower glycerol production. Physiological analysis of the resulting strains revealed that, instead, intracellular concentrations of reduced and oxidized forms of these cofactors favoured the reverse reaction, thus resulting in higher glycerol yields and a lower ethanol yields than in the corresponding reference strains (83, 84).

Engineering redox-cofactor coupling of nitrogen assimilation

Based on observations that amino acid synthesis from ammonium or urea is a key contributor to the 'excess' NADH formed in yeast biosynthesis, an early redox engineering study (19) focused on Gdh1, the $NADP^+$-dependent glutamate dehydrogenase (EC 1.4.1.4) that catalyses the key reaction in ammonium assimilation by nitrogen-sufficient *S. cerevisiae* cultures: (2-oxoglutarate + NH_4^+ + NADPH → glutamate + $NADP^+$, Fig. 3A). Theoretical analysis predicted that making ammonium assimilation NADH-dependent could reduce glycerol production in anaerobic cultures by half. In one strategy, deletion of *GDH1* was combined with constitutive overexpression of *GLN1* and *GLT1*, which encode ATP-dependent glutamine synthetase (GS, EC 6.3.1.2: glutamate + NH_4^+ + ATP → glutamine + ADP + P_i) and NADH-dependent glutamate-2-oxoglutarate aminotransferase (EC 1.4.1.14: glutamine + 2-oxoglutarate + NADH + H^+ → 2 glutamate + NAD^+ (GOGAT), respectively. In anaerobic bioreactor batch cultures, a resulting engineered strain grew at 90% of

the specific growth rate of the reference strain, while its glycerol yield on glucose was 38% lower and its ethanol yield was 10% higher (85). The increased ethanol yield was attributed to a combination of reduced NADH formation and increased ATP consumption in ammonium assimilation. In a second strategy, deletion of *GDH1* was combined with overexpression of the NADH-dependent glutamate dehydrogenase *GDH2* (EC 1.4.1.2: 2-oxoglutarate + NH_4^+ + NADH → glutamate + NAD^+). This approach led to a 30% lower glycerol yield. However, the ethanol yield was hardly affected and the biomass yield was 12% higher than that of the reference strain. This observation was attributed to a reduced loss of carbon via CO_2 formation in the oxidative pentose-phosphate pathway (19), which is the main source of NADPH in *S. cerevisiae* (86, 87). Since NADH re-oxidation in the first step of ammonium assimilation cannot completely replace glycerol formation, the GS-GOGAT strategy, as successfully implemented by Nissen *et al*. (2000) (85), left room for further reduction of glycerol yields.

Expression of $NADP^+$-dependent, non-phosphorylating glyceraldehyde 3-phosphate dehydrogenase (gapN)

In *S. cerevisiae*, the oxidative step in glycolysis is catalysed by the strictly NAD^+-dependent oxidation of glyceraldehyde-3-phosphate to 1,3-diphosphoglycerate by isoenzymes of glyceraldehyde-3-phosphate dehydrogenase (Tdh1, 2 or 3, EC 1.2.1.12). Based on stoichiometric modelling of the yeast metabolism, Bro *et al*. (2006) (62) identified expression of a heterologous non-phosphorylating, $NADP^+$-dependent glyceraldehyde-3-phosphate dehydrogenase (GAPN), which generates 3-phosphoglycerate instead of 1,3-diphosphoglycerate, as a promising option to increase ethanol yields (Fig. 3C). Initial experimental verification of this model prediction by expression of *Streptococcus mutans gapN* showed a 40% lower glycerol yield in anaerobic, glucose-grown batch cultures than in a reference strain. No negative impact on specific growth rate or biomass yield was observed, but also the ethanol yield on glucose was not significantly altered (62)(Table 1). Subsequent studies in which expression of *Bacillus cereus gapN* was tested, reported a 3.5% higher final ethanol concentration and a 23% reduction of the glycerol yield on sugar relative to a reference strain (64). Expression of *Bacillus cereus gapN* in combination with deletion of *GPD1*, yielded a strain that exhibited a 49% lower glycerol yield and 8% higher ethanol yield than the wild-type reference strain. However, the engineered strain was found to be highly sensitive to osmotic stress, thereby precluding its use in high-gravity industrial ethanol fermentation. When osmotolerance was restored by overexpression of *TPS1* and *TPS2*, which encode trehalose-6-phosphate synthase (EC 2.4.1.15: glucose-6-phosphate + UDP-glucose → UDP + trehalose-6-phosphate) and trehalose-6-phosphate phosphatase (EC 3.1.3.12: trehalose-6-phosphate + H_2O →

trehalose + P_i), near-wild-type anaerobic growth rates were reported along with an up to 8% higher ethanol yield and 73% lower glycerol yield, respectively (63)(Table1). In a further study (88), expression of *gapN* from *Streptococcus mutans* was combined with deletion of *FPS1*, which encodes a membrane channel protein involved in glycerol export, in some strains combined with overexpression of *UTR1*, which encodes *S. cerevisiae* NADH kinase (EC 2.7.1.86: ATP + NADH → ADP + P_i + NADPH) (89). While lower glycerol yields and higher ethanol yields were observed in micro-aerobic cultures, the engineered strains were unable to grow under fully anaerobic conditions.

NADH-dependent reduction of acetate to ethanol

In many fermentative bacteria, acetylating acetaldehyde dehydrogenase (A-ALD, EC1.2.1.10: acetyl-CoA + NADH + H^+ → acetaldehyde + CoA + NAD^+) catalyses a key reaction in alcoholic fermentation, that is followed by NADH-dependent reduction of acetaldehyde to ethanol (90). The potential of using the combination of A-ALD and yeast alcohol dehydrogenase to re-oxidize NADH in anaerobic *S. cerevisiae* cultures, and thereby replace glycerol as NADH redox sink for ethanol, was explored by expressing the A-ALD-encoding *E. coli* gene *mhpF* in a *gpd1Δ gpd2Δ* strain (91). Like other *gpd1Δ gpd2Δ S. cerevisiae* strains, the resulting strain did not grow anaerobically on glucose as sole carbon source. However, anaerobic growth was restored by addition of acetate to growth media (Fig. 3E). In anaerobic *S. cerevisiae* cultures, acetate is activated to acetyl-CoA by the acetyl-CoA synthethase isoenzyme Acs2 (EC 6.2.1.1: acetate + ATP + CoA → acetyl-CoA + AMP + PP_i, (92)). In anaerobic bioreactor batch cultures supplemented with 2 g L^{-1} acetate, the engineered strain did not produce glycerol and showed a 13% higher apparent ethanol yield on glucose (note that part of the produced ethanol was derived from acetate rather than from glucose). Under these conditions, the *mhpF*-expressing strain grew at 44% of the specific growth rate of the *GPD1 GPD2* reference strain (91). Introduction, in the same *gpd1Δ gpd2Δ* genetic background, of a single copy of an expression cassette for *eutE*, an alternative *E. coli* A-ALD gene, increased specific growth rate to 84% of that of the reference strain (93).

When *E. coli* EutE was expressed in a *GPD1 GPD2 S. cerevisiae* strain, a mere 10% reduction of the amount of glycerol produced per gram biomass was observed in anaerobic, glucose-grown batch cultures supplemented with acetate. This observation indicated that the native glycerol pathway effectively competed with *E. coli* EutE for NADH in this genetic context. Deletion of *GPD2*, which encodes the redox-regulated isoenzyme of glycerol-3-phosphate dehydrogenase in *S. cerevisiae*, led to a 80% reduction of glycerol production, with a corresponding increase in acetate consumption (93).

Acetate is a common constituent and inhibitor of yeast performance in the hydrolysates of lignocellulosic biomass that are explored as feedstocks for 'second-generation' yeast-based ethanol production (94). Since, in such processes, expression of A-ALD offers an option to convert an inhibitor into additional product, further pathway engineering strategies were explored to increase the amount of NADH available for acetate reduction and to improve robustness of engineered *gpd1Δ gpd2Δ*, A-ALD-based strains. To enable additional NADH generation, the native *S. cerevisiae* $NADP^+$-dependent 6-phosphogluconate dehydrogenases Gnd1 and Gnd2 (EC 1.1.1.44: 6-phosphogluconate + $NADP^+$ → ribulose-5-phosphate + CO_2 + NADPH) were replaced by the NAD^+-dependent enzyme GndA from *Methylobacillus flagellates* (EC 1.1.1.343). To force flux through the resulting, now partially NADH-coupled oxidative pentose-phosphate pathway, *ALD6*, which encodes $NADP^+$-dependent acetaldehyde dehydrogenase (EC 1.2.1.5: acetaldehyde + $NADP^+$ → acetate + NADPH), was deleted. This metabolic engineering strategy resulted in a 29% higher acetate consumption per gram biomass than in the parental *gpd1Δ gpd2Δ*, *eutE*-expressing strain (95). Relative to a congenic *GPD1 GPD2* reference strain, the engineered strain showed a 13% higher ethanol yield and a 29% lower specific growth rate.

An alternative strategy to boost the acetate-reducing capacity of *eutE*-expressing strains focused on changing the cofactor preference of alcohol dehydrogenase, which in *S. cerevisiae* is strictly NADH-dependent (96). Relative to an industrial *S. cerevisiae* strain expressing *Bifidobacterium adolescentis eutE* in a *gpd1Δ gpd2Δ* background, a further engineered strain that expressed an NADPH-dependent alcohol dehydrogenase from *Entamoeba histolytica*, combined with overexpression of *S. cerevisiae* NADP-dependent glucose-6-P dehydrogenase (Zwf1, EC 1.1.1.49: glucose-6-phosphate + $NADP^+$ → 6-phospho-glucono-1,5-lactone + NADPH) and acetyl-CoA synthetase (Acs2) showed an almost 3-fold higher acetate consumption (96).

A different strategy to increase the potential for acetate reduction by A-ALD-based strains is to enable anaerobic co-conversion of glycerol, which is left in the final phases of fermentation or obtained from post-distillation stills (97), to ethanol. In the patent literature, an NADH-specific glycerol dehydrogenase from *E. coli* (*gldA*, EC 1.1.1.6: glycerol + NAD^+ → dihydroxyacetone + NADH + H^+) was expressed together with an additional copy of *DAK1*, encoding dihydroxyacetone kinase (EC 2.7.1.29: dihydroxyacetone + ATP → dihydroxyacetone phosphate + ADP) (98, 99). Combined with enzymes from the lower half of glycolysis, pyruvate decarboxylase and alcohol dehydrogenase, GldA and Dak1 enable conversion of glycerol to ethanol with the formation of one mol of NADH (Fig. 3H). When, besides sugars, glycerol and acetate are present as an additional substrate in A-ALD-dependent cultures, glycerol

conversion to ethanol acts as source of NADH enabling more acetate reduction. Indeed, high apparent ethanol yields of 0.48-0.50 gram ethanol per gram of glucose were reported for *S. cerevisiae* strains in which *gldA* and *DAK1* overexpression was combined with expression of *E. coli mhpF* or *eutE* (98, 99).

Integration of acetyl-CoA reduction by A-ALD in yeast sugar metabolism

Organic acid concentrations in 'first-generation' feedstocks for yeast-based ethanol production are generally around 1.3 g L^{-1} (37, 100), which limits the potential impact of the replacement of glycerol production by reduction of exogenous acetate via an engineered A-ALD pathway. In such settings, NADH re-oxidation by A-ALD could still replace glycerol production if acetyl-CoA is formed from glucose by pathways that yield fewer than two moles of NADH per mol of acetyl-CoA. The patent literature describes two strategies to achieve this goal, of which the first is based on heterologous expression of a gene encoding bacterial pyruvate formate-lyase (PFL; EC 2.3.1.54: pyruvate → acetyl-CoA + formate) in A-ALD-dependent *S. cerevisiae* (101, 102) (Fig. 3E). PFL, which is an oxygen-sensitive enzyme, was shown to be able to functionally replace the native pathway for acetyl-CoA synthesis in anaerobic *S. cerevisiae* cultures (103, 104). Synthesis of acetyl-CoA via glycolysis and PFL yields only one NADH per acetyl-CoA and thus enables a net reduction of one NADH when combined with ethanol production via A-ALD and yeast alcohol dehydrogenase. To prevent NADH formation by the yeast formate dehydrogenases Fdh1 and Fdh2 (EC 1.17.1.9: formate + NAD^+ → CO_2 + NADH; (105)), it was proposed to delete *FDH1* and *FDH2* from PFL/A-ALD carrying strains (101, 102).

A second strategy for coupling A-ALD to sugar metabolism proposed in the patent literature (106) is based on generation of acetyl-CoA through phosphoketolase (EC 4.1.2.9) and phosphotransacetylase (EC 2.3.1.8) (Fig. 3F). In this strategy, xylulose-5-phosphate is first formed from glucose in a redox-cofactor neutral manner via the enzymes of the non-oxidative pentose-phosphate pathway. This sugar phosphate is then converted into glyceraldehyde-3-phosphate and acetyl-phosphate by a heterologously expressed gene encoding phosphoketolase (PK, EC 4.1.2.9: xylulose-5-phosphate + P_i → acetyl-phosphate + glyceraldehyde-3-phosphate + H_2O). Subsequently, a heterologously expressed gene encoding phosphotransacetylase (PTA, EC 2.3.1.8: acetyl-phosphate + CoA → acetyl-CoA + P_i) converts acetyl phosphate to acetyl-CoA. This pathway has been successfully used for the ATP-efficient generation of acetyl-CoA as a precursor for aerobic product formation by engineered *S. cerevisiae* strains (107, 108). While the exact impact on ethanol yields will depend on strain and process characteristics, both pathways have the theoretical potential to completely replace the role of glycerol formation in NADH re-oxidation.

Expression of Calvin-cycle enzymes

Phosphoribulokinase (PRK, EC 2.7.1.19: ribulose-5-phosphate + ATP → ribulose-1,5-biphosphate + ADP) and ribulose-1,5-bisphosphate carboxylase/oxygenase (RuBisCO, EC 4.1.1.39: ribulose-1,5-biphosphate + CO_2 + H_2O → 2 glyceraldehyde-3-phosphate + $2H^+$) are the two key enzymes of the Calvin cycle for autotrophic CO_2 fixation. By capturing CO_2, these enzymes together have the potential to generate a redox-cofactor-neutral bypass of the oxidative glyceraldehyde-3-phosphate dehydrogenase reaction in glycolysis when ribulose-5-phosphate, the substrate of phosphoribulokinase, is generated from glucose via the reactions of the non-oxidative pentose-phosphate pathway (Fig. 3D). In theory, this bypass should enable the use of ethanol formation as a redox sink for NADH generated in biosynthetic reactions. This hypothesis was tested by Guadalupe-Medina *et al*. (2013) (109), who demonstrated the presence of a functionally active RuBisCO in cell extracts of an engineered *S. cerevisiae* strain that co-expressed the *Thiobacillus denitrificans* type-II RuBisCO CbbM with the *E. coli* chaperonins GroEL and GroES. Co-expression of *cbbM*, *groEL*, *groES* with spinach *PRK* encoding phosphoribulokinase was shown to result in a 90% lower glycerol yield and a 10% higher ethanol yield in anaerobic, sugar-limited chemostat cultures grown at a dilution rate of 0.05 h^{-1} and sparged with CO_2-enriched nitrogen (109). In line with the low affinity of CbbM for CO_2 (110), a less pronounced effect on glycerol and ethanol yields was observed when cultures were sparged with pure nitrogen gas.

Papapetridis *et al.* (2018) (77) observed that an *S. cerevisiae* strain that combined constitutive expression of the genes encoding for PRK, RuBisCO, GroEL and GroES showed only a modest reduction of glycerol in fast-growing anaerobic batch cultures on glucose than the slow-growing chemostat cultures studied by Guadalupe-Medina *et al.* (2013) (109). To improve competition of the RuBisCO pathway for NADH with the native glycerol pathway, *GPD2* was deleted and the genes encoding the four key enzymes of the non-oxidative pentose phosphate pathway were overexpressed. In addition, *PRK* was expressed from a weaker, anaerobically inducible promoter to avoid reported toxic effects of PRK overactivity in microorganisms (111, 112) during aerobic pre-cultivation. The resulting strain retained a wild-type growth rate in anaerobic, glucose-grown batch cultures, while showing an 86% lower glycerol yield and 15% higher ethanol yield on glucose than a congenic reference strain (77).

The strategies discussed above were first designed to reduce or eliminate the need for glycerol formation in alcoholic fermentation of disaccharides or hexoses. However, they can similarly be employed in conversion of other sugars into ethanol. Xylose-utilizing *S. cerevisiae* have been engineered either based on the synthesis of the fungal

xylose reductase (XR, EC 1.1.1.307: xylose + NAD(P)H → xylitol + $NAD(P)^+$) and xylitol dehydrogenase (XDH, EC 1.1.1.9: xylitol + NAD^+ → xylulose + NADH), or the synthesis of a bacterial xylose isomerase (EC 5.3.1.5: xylose → xylulose). A key challenge in the strategy based on XR and XDH is that XR typically prefers NADPH as cofactor, while XDH exclusively uses NAD^+ (113). As a consequence of this cofactor imbalance, xylitol is formed as a byproduct. Changing the cofactor preference of ammonium assimilation as demonstrated by Nissen *et al*. (2000) (85), facilitated re-oxidation of NADH generated in the XDH reaction and improved ethanol yield in an XR-XDH-based *S. cerevisiae* strain (114). Combined functional expression of the genes encoding PRK and RuBisCO (115, 116); phosphoketolase and phosphotransacetylase (117); or GAPN (62) were similarly applied to improve redox co-factor balancing in XR-XDH-based strains and, thereby, ethanol yields on xylose.

Table 1: Reported impacts on glycerol production, maximum specific growth rate and ethanol production in anaerobic batch cultures of *S. cerevisiae* strains subjected to different pathway engineering strategies aimed at reducing glycerol production and improving ethanol yield. Depending on the studies, changes in product yields were either expressed per amount of substrate or per amount of biomass. Subscript x denotes dry biomass, ↑ indicates overexpression of native *S. cerevisiae* genes, glc = glucose.

Strategy	**Genotype**	**Glycerol yield**	**Growth rate**	**Ethanol yield**	**Reference**
Altered cofactor specificity of ammonium assimilation	*gdh1Δ GLN1↑GLT1↑*	-38% ($g\ g_{glc}^{-1}$)	-10%	+10% ($g\ g_{glc}^{-1}$)	(19)
	gdh1Δ GDH2↑	-30% ($g\ g_{glc}^{-1}$)	-5%	+3% ($g\ g_{glc}^{-1}$)	(19)
NADH-dependent reduction of acetate to ethanol (Ec = *E. coli*)	*gpd1Δ gpd2Δ* Ec*mphF*	-100% ($g\ g_{x}^{-1}$)	-56%	+13% ($g\ g_{glc}^{-1}$)	(91)
	gpd1Δ gpd2Δ Ec*eutE*	-100% ($g\ g_{x}^{-1}$)	-7%	+9% ($g\ g_{glc}^{-1}$)	(95)
NADH-dependent reduction of acetate to ethanol with increased NADH generation via pentose-phosphate pathway	*gnd2Δ gnd1Δ gndAΔ ald6Δ gpd1Δ gpd2Δ* Ec*eutE*	-100% ($g\ g_{x}^{-1}$)	-29%	+11% ($g\ g_{glc}^{-1}$)	(95)
NADH re-oxidation via expression of Calvin-cycle enzymes, optimized for anaerobic growth rate (So = *Spinacia oleracea*, Td = *Thiobacillus denitrificans*)	*gpd2Δ RPE1↑TKL1↑ TAL1↑ NQM1↑ RKI1↑ TKL2↑* So*PRK* Td*cbbM* (9 copies) Ec*groES,* Ec*groEL*	-86% ($g\ g_{x}^{-1}$)	0%	+15% ($g\ g_{glc}^{-1}$)	(77)
Reduced NADH and ATP formation in glycolysis by expression of *gapN* (Sm = *Streptococcus mutans*)	Sm*gapN*	-40% ($g\ g_{glc}^{-1}$)	0%	+2% ($g\ g_{glc}^{-1}$)	(62)
	gpd1Δ Sm*gapN TPS1↑ TPS2↑*	-73 % ($g\ g_{glc}^{-1}$)	0%	+8% ($g\ g_{glc}^{-1}$)	(63)

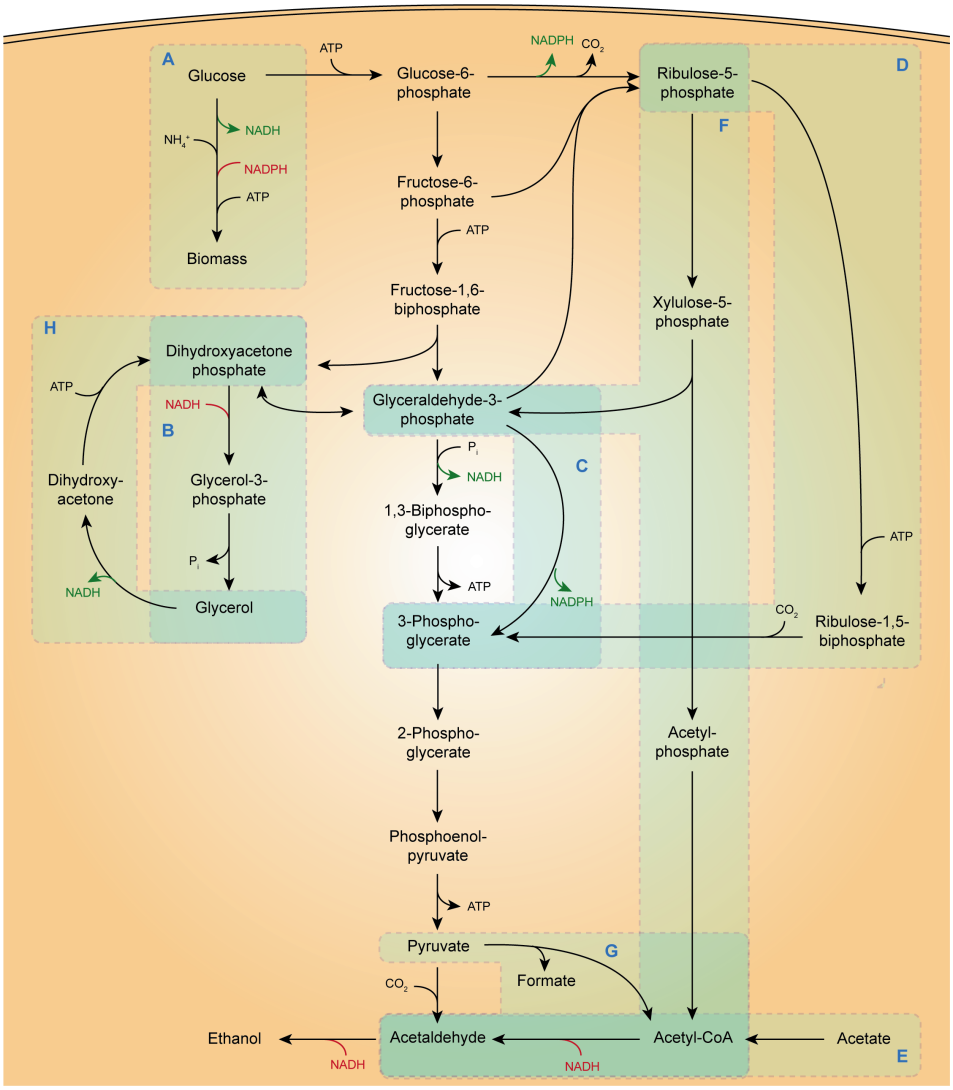

Figure 3: Schematic representation of pathway engineering strategies for minimizing formation of glycerol during anaerobic growth of *S. cerevisiae*. A: Biosynthetic reactions: replacing the $NADP^+$-dependent step by an NADH-dependent step in ammonium assimilation, can reduce the NADH production in biosynthetic reactions. B: Native glycerol pathway. C: Bypass of NAD^+-dependent glyceraldehyde-3-phosphate dehydrogenase by heterologous non-phosphorylating, $NADP^+$-dependent glyceraldehyde-3-phosphate dehydrogenase (GAPN). D: Non-oxidative bypass of glycolysis by heterologous phosphoribulokinase and ribulose-1,5-bisphosphate carboxylase/oxygenase. E: Re-oxidation of NADH via heterologous acetylating acetaldehyde dehydrogenase (A-ALD), using exogenous acetate as electron acceptor. F: Re-oxidation of NADH enabled by heterologous A-ALD, phosphoketolase and phosphotransacetylase. G: Re-oxidation of NADH enabled by heterologous A-ALD and pyruvate-formate lyase. H: Combined expression of genes encoding a heterologous NADH-dependent glycerol dehydrogenase and the native dihydroxyacetone kinase enables ethanol formation from glycerol when combined with strategies D, E, F and/or G.

Model-based comparison of maximum theoretical impact of individual engineering strategies

Experimentally determined ethanol yields achieved with the pathway engineering strategies discussed in this review (Table 1) can be influenced by experimental conditions as well as by the *S. cerevisiae* genetic background into which genetic modifications were introduced, for example due to different biomass compositions. To eliminate these factors, different pathway strategies were implemented in a stoichiometric model of the core metabolic network of *S. cerevisiae* (118) and used to calculate growth stoichiometries of anaerobic, sugar-grown cultures (Table 2). Although the resulting estimates cannot be used to predict performance of strategies in specific strain backgrounds or processes, they do enable comparison of the maximum impact of the different strategies and identification of trade-offs.

To evaluate pathway engineering strategies aimed at reducing the ATP yield from sugar fermentation, two scenarios were simulated. In the first, glucose import required a net input of 0.5 ATP, which corresponds to the ATP yield per hexose unit in strains that combine sucrose-proton symport with intracellular sucrose hydrolysis (70). The second scenario, in which glucose import required 1 ATP, corresponds to a situation in which hexose transport occurs via symport with a proton or, alternatively, glucose is fermented via an alternative glycolytic pathway with a net ATP yield of 1 mol per mol glucose (e.g. the Entner-Doudoroff pathway) in combination with a glucose facilitator. At a specific growth rate of 0.30 h^{-1}, simulation of these scenarios gave predicted increases of ethanol yield on hexose equivalents of 8.1% and 16.2%, respectively (Table 2). Due to a larger impact of a constant maintenance-energy requirement at low growth rate (23, 119), predicted benefits of these engineering strategies declined as the specific growth rate approached zero (Table 2). An important consequence of these two strategies was that, at each specific growth rate, specific rates of sugar conversion were 33% and 100% higher, respectively, than in the reference situation (Supplementary Table 1). Especially at high specific growth rates, which are important for supporting high volumetric productivities in industrial batch processes, achieving such high conversion rates may be challenging due to the requirement for a large resource allocation to glycolytic proteins (120, 121) or for membrane space to accommodate the required number of sugar transporters (122). In addition, concomitant reductions of the biomass yield on sugar by 25% and 50%, respectively (Supplementary Table 2) may cause economic trade-offs when surplus yeast biomass is sold as a co-product for application in animal feed products (13).

To assess the maximum theoretical impact on ethanol yield of the strategies focused on redox-cofactor balancing, glycerol production was set to zero, so that re-oxidation

of NADH generated in biosynthesis occurred exclusively via the engineered pathways. At a specific growth rate of 0.3 h^{-1}, the PFL-A-ALD, PK-PTA-A-ALD and PRK-Rubisco strategies yielded predicted improvements of the ethanol yield on glucose of 8.7%, 9.7% and 11.9%, respectively. The predicted differences between the impacts of the three strategies can be predominantly attributed to the different net ATP and ethanol yields for NADH re-oxidation via these pathways. Due to different ATP and carbon efficiencies of these heterologous pathways, implementation of these redox engineering strategies in the stoichiometric model also led to higher predicted biomass yields on glucose and correspondingly lower specific rates of glucose consumption (Supplementary Tables 1 and 2). Thus, in contrast to strategies aimed at reducing the ATP stoichiometry of sugar fermentation, their industrial implementation should not be affected by a potentially limited capacity of sugar fermentation and/or transport or by a trade-off with revenues from surplus yeast biomass. As observed for the strategies aimed at engineering ATP coupling of sugar dissimilation, the impact of the redox-engineering strategies on ethanol yield declined with decreasing specific growth rate and, at the lowest simulated growth rate (0.001 h^{-1}), the predicted increase of ethanol yield on glucose was only approximately 1%.

For several of the strategies, experimental studies (Table 1) yielded larger improvements of the ethanol yield than the maximum theoretical improvements shown in Table 2. In addition to differences in biomass composition and ethanol yields of reference *S. cerevisiae* strains, these differences may reflect unintended impacts of genetic modifications on cellular energy requirements. For example, high-level prodcution of heterologous proteins has been associated with increased cellular energy requirements (123, 124) which, in anaerobic cultures can contribute to higher ethanol yields. In addition, alteration of the expression of genes encoding membrane proteins may potentially lead to increased ATP dissipation, for exampling by futile cycling of glucose through overproduced Mal11 and Hxt transporters.

Table 2: Maximum impact of different pathway engineering strategies for improving ethanol yields, estimated with a stoichiometric model of the core metabolic network of *S. cerevisiae* (118). Assumptions on biomass composition, maintenance-energy requirements, as well as modifications to the model that were implemented to simulate each of the metabolic engineering strategies, are described in Supplementary Materials. For the strategies focused on NADH re-oxidation, glycerol production was set at zero and oxidation of surplus NADH from biosynthetic reactions was entirely routed through the engineered pathways.

Specific growth rate (h^{-1})	$Y_{ethanol/hexose}$ (mol/mol)					
	Reference	**Altered ATP coupling of sugar dissimilation**		**Alternative pathways for re-oxidation of NADH**		
	Wild type	H^+ symport/ intracellular hydrolysis of sucrose	H^+ symport of glucose	PFL-A-ALD	PK-PTA-A-ALD	PRK-RuBisCO
0.3	1.51	1.63 (8%)	1.76 (16%)	1.64 (9%)	1.66 (10%)	1.69 (12%)
0.1	1.54	1.66 (8%)	1.77 (15%)	1.67 (8%)	1.69 (10%)	1.71 (11%)
0.03	1.62	1.72 (6%)	1.81 (12%)	1.74 (7%)	1.76 (9%)	1.78 (10%)
0.01	1.75	1.81 (4%)	1.87 (7%)	1.84 (5%)	1.86 (6%)	1.86 (6%)
0.001	1.95	1.97 (1%)	1.98 (1%)	1.97 (1%)	1.98 (1%)	1.98 (1%)

Scope of this thesis

As outlined in this introduction, multiple pathway engineering strategies have been demonstrated to improve ethanol yields on sugars in exponentially growing anaerobic laboratory cultures of *S. cerevisiae* by altering the ratio of the formation of ethanol, biomass and glycerol. However, observations made under laboratory conditions are not necessarily representative for industrial processes. In particular, industrial batch processes for ethanol production involve growth-rate dynamics caused by depletion of nutrients and/or accumulation of ethanol that may affect the impact of engineering strategies. During the later phases of such processes, when ethanol formation is increasingly uncoupled from biomass formation and instead mainly contributes to energy requirements, impact of redox-engineering strategies may even become negligible.

The impact of specific growth rate on the performance of yeast strains with an engineered redox metabolism is the focus of **Chapter 2**. The goal of this study was to investigate the performance of a PRK-RuBisCO-dependent *S. cerevisiae* strain, which had previously been optimized for fast growth at high specific growth rates, at submaximal growth rates. At low specific growth rates, which coincide with a lower rate of NADH generation from biosynthetic conditions, the engineered strain produced acetaldehyde and acetate as byproducts. This byproduct formation is

undesirable in industrial contexts and was attributed to an *in vivo* overcapacity of the non-oxidative glycolytic bypass via PRK and RuBisCO. The same chapter explores metabolic engineering strategies to mitigate this byproduct formation.
While engineered acetate-reducing *S. cerevisiae* strains can efficiently couple reoxidation of NADH to the conversion of acetate into ethanol, concentrations of acetate in feedstocks for 'first-generation' are typically too low for strains to fully rely on acetate reduction for reoxidation of 'surplus' NADH from biosynthetic processes. To investigate whether this limitation can be eliminated by further metabolic engineering, **Chapter 3** focuses on the performance of engineered *S. cerevisiae* strains that harbour a functional PRK-RuBisCO pathway as well as an acetate reduction pathway. The ideal scenario pursued with this study was to develop strains that can reduce any acetate available in the growth medium to ethanol and then seamlessly switch to NADH reoxidation via the PRK-RuBisCO bypass.

While **Chapter 2** focused on metabolic engineering of a single culture to balance activity of the PRK-RuBisCO bypass with the *in vivo* demand for NADH reoxidation, **Chapter 4** investigates an alternative approach to mitigate byproduct formation and, thereby, optimize product yields in cultures of PRK-RuBisCO-synthezizing yeast strains. This alternative strategy was based on co-cultivation of the previously characterized acetaldehyde- and acetate-producing PRK-RuBisCO-based *S. cerevisiae* strain with a second engineered strain capable of reducing acetate and acetaldehyde to ethanol.

Previously described redox-engineering strategies for improving ethanol yield from glucose in *S. cerevisiae* cultures aim to approach the theoretical yield of 2 moles of ethanol per mol of glucose that is dictated by conservation laws. Increasing this yield to above 2 moles of ethanol per mol of substrate is only theoretically possible when additional electrons (e.g. in the form of NADH) can be fed into the fermentation pathway. Sorbitol, a six-carbon polyol that is more reduced than glucose and which can therefore not be anaerobically fermented to ethanol, provides an interesting model system for investigating this concept. **Chapter 5** describes experiments aimed at testing the ability of an engineered yeast strain carrying the PRK-RuBisCO glycolytic bypass to anaerobically (co-)ferment sorbitol.

Supplementary information

Additional supplementary information

Available online via: https://doi.org/10.1016/j.synbio.2021.12.010.

Table S1: Estimated biomass-mass specific rates of hexose consumption for different pathway-engineering strategies to improve ethanol yields (see Table 2 for estimated maximum impacts on ethanol yield), calculated with a stoichiometric model of the core metabolic network of *S. cerevisiae* (118). For the three strategies focused on NADH reoxidation, glycerol production was set at zero and oxidation of surplus NADH from biosynthetic reactions was entirely routed through the engineered pathways.

Specific growth rate (h^{-1})	**$-q_{hexose}$ ($mmol/Cmol_x/h$)**					
	Reference	**Altered ATP coupling of sugar dissimilation**		**Alternative pathways for reoxidation of NADH**		
	Wild type	H^+ symport/ intracellular hydrolysis of sucrose	H^+ symport of glucose	PFL-A-ALD	PK-PTA-A-ALD	PRK-RuBisCO
0.3	402	536	803	307	278	308
0.1	143	190	285	111	102	111
0.03	52.1	69.4	104	42.6	39.7	42.7
0.01	26.2	34.9	52.3	23.0	22.0	23.0
0.001	14.5	19.3	29.0	14.2	14.1	14.2

Table S2: Estimated biomass yields on hexose units for different pathway-engineering strategies to improve ethanol yields (see Table 2 for estimated maximum impacts on ethanol yield), calculated with a stoichiometric model of the core metabolic network of *S. cerevisiae* (118). For the three strategies focused on NADH reoxidation, glycerol production was set at zero and oxidation of surplus NADH from biosynthetic reactions was entirely routed through the engineered pathways. Subscript x denotes yeast biomass.

Specific growth rate (h^{-1})	**$Y_{x/hexose}$ (g_x/g)**					
	Reference	**Altered ATP coupling of sugar dissimilation**		**Alternative pathways for reoxidation of NADH**		
	Wild type	H^+ symport/ intracellular hydrolysis of sucrose	H^+ symport of glucose	PFL-A-ALD	PK-PTA-A-ALD	PRK-RuBisCO
0.3	0.109	0.082	0.055	0.143	0.158	0.143
0.1	0.103	0.077	0.051	0.132	0.145	0.132
0.03	0.085	0.063	0.042	0.103	0.111	0.103
0.01	0.056	0.042	0.028	0.064	0.067	0.064
0.001	0.010	0.008	0.005	0.010	0.010	0.010

Model-based estimation of the impact of pathway engineering strategies on growth stoichiometry

Quantitative estimates of the impact of different pathway engineering strategies on ethanol yield, biomass-specific rate of glucose consumption and biomass yield in anaerobic, glucose-grown cultures were generated with a compartmented stoichiometric network model for growth of *Saccharomyces cerevisiae* (125), with the following modifications:

Calculations were based on a growth-rate independent rate of ATP turnover for cellular maintenance (m_{ATP}) of 1 mmol (g biomass)$^{-1}$ h^{-1} (126) and a growth-coupled ATP cost of 0.5 mol (Cmol biomass)$^{-1}$.

Molecular and elemental composition of *S. cerevisiae* biomass was assumed to correspond to the statistically reconciled composition calculated by Lange and Heijnen (2001) (127) for glucose-limited cultures grown at a dilution rate of 0.10 h^{-1} (1 Cmol biomass = 26.4 g).

Pathway engineering strategies were simulated by introducing the following modifications:

<u>H^+ symport and subsequent intracellular hydrolysis of sucrose</u>

This scenario was simulated by coupling import of glucose, which in the reference model occurs via facilitated diffusion (no coupling with proton translocation), to the inward translocation of 0.5 H^+

<u>H^+ symport of glucose</u>

This scenario was simulated by coupling import of glucose, which in the reference model occurs via facilitated diffusion (no coupling with proton translocation), to the inward translocation of 1.0 H^+

<u>Expression of pyruvate-formate lyase (PFL) and acetylating acetaldehyde dehydrogenase (A-ALD)</u>

To simulate this scenario, the following changes were introduced in the model:

- the rate of glycerol production ($q_{glycerol}$) was set to 0
- NAD^+-dependent acetaldehyde dehydrogenase was removed from the model
- PFL was added to the model: pyruvate → formate + acetyl-CoA
- A-ALD was added to the model: acetyl-CoA + NADH → acetaldehyde + NAD^+
- formate export was assumed to occur by uniport of the formate anion

Expression of phosphoketolase (PK), phosphotransacetylase (PTA) and acetylating acetaldehyde dehydrogenase (A-ALD):

- the rate of glycerol production ($q_{glycerol}$) was set to 0
- NAD^+-dependent acetaldehyde dehydrogenase (cACTAL deh(NAD)) was removed from the model
- PK was added to the model: xylulose-5P + P_i → glyceraldehyde-3P + acetyl-P
- PTA was added to the model: acetyl-P + CoA → acetyl-CoA + P_i
- A-ALD was added to the model: acetyl-CoA + NADH → acetaldehyde + NAD^+

Expression of phosphoribulokinase (PRK) and ribulose-1,5-bisphosphate carboxylase/oxygenase (Rubisco):

- the rate of glycerol production ($q_{glycerol}$) was set at 0
- PRK was added to the model: ribulose-5P + ATP → ribulose-1,5P + ADP
- Rubisco was added to the model: ribulose-1,5P + CO_2 → 2 3P-glycerate

Chapter 2

Quantification and mitigation of byproduct formation by low-glycerol-producing *Saccharomyces cerevisiae* strains containing Calvin-cycle enzymes

Aafke C.A. van Aalst, Mickel L.A. Jansen, Robert Mans, and Jack T. Pronk

This chapter is essentially as published in Biotechnology for Biofuels and Bioproducts (2023) 16(1): 1-17.

Abstract

Anaerobic *Saccharomyces cerevisiae* cultures require glycerol formation to re-oxidize NADH formed in biosynthetic processes. Introduction of the Calvin-cycle enzymes phosphoribulokinase (PRK) and ribulose-1,5-bisphosphate carboxylase/oxygenase (RuBisCO) has been shown to couple re-oxidation of biosynthetic NADH to ethanol production and improve ethanol yield on sugar in fast-growing batch cultures. Since growth rates in industrial ethanol-production processes are not constant, performance of engineered strains was studied in slow-growing cultures.

In slow-growing anaerobic chemostat cultures (D = 0.05 h^{-1}), an engineered PRK-RuBisCO strain produced 80-fold more acetaldehyde and 30-fold more acetate than a reference strain. This observation suggested an imbalance between *in vivo* activities of PRK-RuBisCO and formation of NADH in biosynthesis. Lowering the copy number of the RuBisCO-encoding *cbbM* expression cassette from 15 to 2 reduced acetaldehyde and acetate production by 67% and 29%, respectively. Additional C-terminal fusion of a 19 amino acid tag to PRK reduced its protein level by 13-fold while acetaldehyde and acetate production decreased by 94% and 61%, respectively, relative to the 15x *cbbM* strain. These modifications did not affect glycerol production at 0.05 h^{-1} but caused a 4.6 fold higher glycerol production per amount of biomass in fast-growing (0.29 h^{-1}) anaerobic batch cultures than observed for the 15x *cbbM* strain. In another strategy, the promoter of *ANB1*, whose transcript level positively correlated with growth rate, was used to control PRK synthesis in a 2x *cbbM* strain. At 0.05 h^{-1}, this strategy reduced acetaldehyde and acetate production by 79% and 40%, respectively, relative to the 15x *cbbM* strain, without affecting glycerol production. The maximum growth rate of the resulting strain equalled that of the reference strain, while its glycerol production was 72% lower.

Acetaldehyde and acetate formation by slow-growing cultures of engineered *S. cerevisiae* strains carrying a PRK-RuBisCO bypass of yeast glycolysis was attributed to an *in vivo* overcapacity of PRK and RuBisCO. Reducing the capacity of PRK and/or RuBisCO was shown to mitigate this undesirable byproduct formation. Use of a growth-rate-dependent promoter for PRK expression highlighted the potential of modulating gene expression in engineered strains to respond to growth-rate dynamics in industrial batch processes.

Background

With an estimated annual production of 103 billion litres in 2021 (1), bioethanol remains the largest-volume product of industrial biotechnology. Although alternative microbial production platforms based on autotrophic conversion of carbon monoxide and/or carbon dioxide are in the ascendant (128), ethanol is still predominantly produced via fermentation of plant-derived glucose and sucrose by the yeast *Saccharomyces cerevisiae* (129, 130). In these yeast-based processes, costs of the carbohydrate feedstock make up more than half of the total production costs (7). Therefore, maximizing the ethanol yield on feedstock is an economically important goal.

Alcoholic fermentation of glucose and sucrose by *S. cerevisiae* starts with the ATP-yielding Embden-Meyerhof glycolytic pathway (9), whose product pyruvate is converted to ethanol and carbon dioxide by the combined action of pyruvate decarboxylase and alcohol dehydrogenase (10). This native yeast pathway for sugar fermentation is redox-neutral and generates ATP. Its maximum product yield of 2 moles of ethanol per mol of glucose corresponds to the theoretical maximum yield based on conservation laws (131). Indeed, near-theoretical ethanol yields on glucose were demonstrated during prolonged cultivation of *S. cerevisiae* at near-zero specific growth rates in anaerobic retentostat cultures (23). In such non-growing cultures, sugar is almost exclusively used to generate ATP for cellular maintenance rather than for supporting yeast growth. Ethanol production in industrial fermentation processes is, however, accompanied by anaerobic growth, which requires the use of sugar for biomass formation. In addition, formation of *S. cerevisiae* biomass from sugars and ammonium or urea leads to a net reduction of NAD^+ to NADH (78). Under anaerobic conditions, re-oxidation of this 'surplus' NADH occurs by reduction of dihydroxyacetone-phosphate to glycerol-3-phosphate, which, upon hydrolysis, yields glycerol and phosphate (15). In non-engineered *S. cerevisiae* strains, glycerol formation can account for a loss of up to 4% of the carbohydrate feedstock (19).

Multiple metabolic engineering strategies have been designed to reduce glycerol formation and, thereby, improve ethanol yield, (see (132) for a recent review). A pioneering study focussed on changing the cofactor preference in ammonia assimilation by replacing the $NADP^+$-dependent glutamate dehydrogenase with an NAD^+-dependent enzyme (85), with the aim to reduce the surplus of NADH formed in biosynthesis. While this approach led to a significant reduction of glycerol production, the amount of NADPH required for ammonia assimilation is smaller than the surplus of NADH for biosynthesis (81). Other metabolic engineering strategies therefore focussed on engineering central carbon metabolism to couple oxidation of surplus

NADH to the formation of ethanol instead of glycerol. Some of these strategies were based on generation of acetyl-CoA followed by its reduction to ethanol by the concerted action of a heterologous NAD^+-dependent acetylating acetaldehyde dehydrogenase and the native yeast alcohol dehydrogenase. As long as formation of acetyl-CoA yields fewer than 2 moles of NADH per mol of acetyl-CoA, such pathways can replace glycerol formation as a means to reoxidize 'surplus' NADH. This requirement can be met by heterologous expression of a gene encoding pyruvate-formate lyase (98, 101), by combined expression of genes encoding phosphoketolase and phosphotransacetylase (106) or, alternatively, by supplementation of acetic acid (91, 93), which can be converted to acetyl-CoA by native yeast acetyl-CoA synthetase.

The present study focuses on an alternative strategy, for which a proof-of-concept was provided by Guadalupe-Medina *et al.* (109). In this strategy, genes encoding the Calvin-cycle enzymes phosphoribulokinase (PRK) and ribulose-1,5-bisphosphate carboxylase/oxygenase (RuBisCO) were heterologously expressed in *S. cerevisiae* along with *Escherichia coli* genes encoding the chaperonins GroEL and GroES (Fig. 1)(*PRK*, *cbbM*, *groES/groEL*). In slow-growing sugar-limited chemostat cultures (0.05 h^{-1}), the glycerol yield on sugar of an engineered strain carrying these modifications was 90% lower than that of the reference strain, while its ethanol yield on sugar was 10% higher. This strategy, which is based on a bypass of the oxidative reaction in glycolysis that involves both Calvin-cycle enzymes, has since also been applied to reoxidize 'surplus' NADH generated by other metabolic processes in yeast (115, 116).

Building on the initial proof-of-principle experiments, the yeast metabolic network of PRK-RuBisCO-based strains was further engineered to improve specific growth rates in anaerobic batch cultures (77). Overexpression of the structural genes for enzymes of the non-oxidative pentose-phosphate pathway (non-ox PPP↑; p*TDH3-RPE1*, p*PGK1-TKL1*, p*TEF1-TAL1*, p*PGI1-NQM1*, p*TPI1-RKI1* and p*PYK1-TKL2*) was implemented to increase supply of ribulose-5-phosphate, while multiple copies of a bacterial *cbbM* RuBisCO expression cassette were integrated in the yeast genome to improve conversion of ribulose-5-bisphosphate into 3-phosphoglycerate. Moreover, *GPD2*, which encodes an isoenzyme of NAD^+-dependent glycerol-3-phosphate dehydrogenase, was deleted to reduce competition for biosynthetic NADH in fast growing cultures. Finally, expression of the spinach *PRK* gene from the anaerobically inducible *DAN1* promoter (133, 134) limited toxic effects of PRK during aerobic pre-cultivation. The resulting PRK-RuBisCO *S. cerevisiae* strain (IMX1489; Δ*gpd2*, non-ox PPP↑, p*DAN1-PRK*, 15x *cbbM*, *groES/groEL*) showed essentially the same maximum growth rate on glucose as a non-engineered reference strain in anaerobic batch

bioreactors while showing an 86% lower glycerol yield and an over 10% higher ethanol yield than the reference strain (77).

The results obtained with fast-growing anaerobic batch cultures of an optimized PRK-RuBisCO strain were promising. However, in industrial ethanol fermentation, the specific growth rate is not high throughout the process but, instead, decreases as the ethanol concentration reaches inhibitory levels and/or non-sugar nutrients are depleted (37, 135). The goal of the present study was therefore to investigate performance of a PRK-RuBisCO strain that was optimized for high ethanol yield and fast growth (specific growth rate of 0.29 h^{-1}) at submaximal specific growth rates (0.05, 0.1 and 0.25 h^{-1}) in anaerobic chemostat cultures. As these slow-growing cultures showed substantial production of acetaldehyde and acetate, we explored metabolic engineering strategies to reduce or prevent an apparent *in vivo* overcapacity of the key enzymes of the PRK-RuBisCO bypass and, thereby, of the formation of these undesirable byproducts.

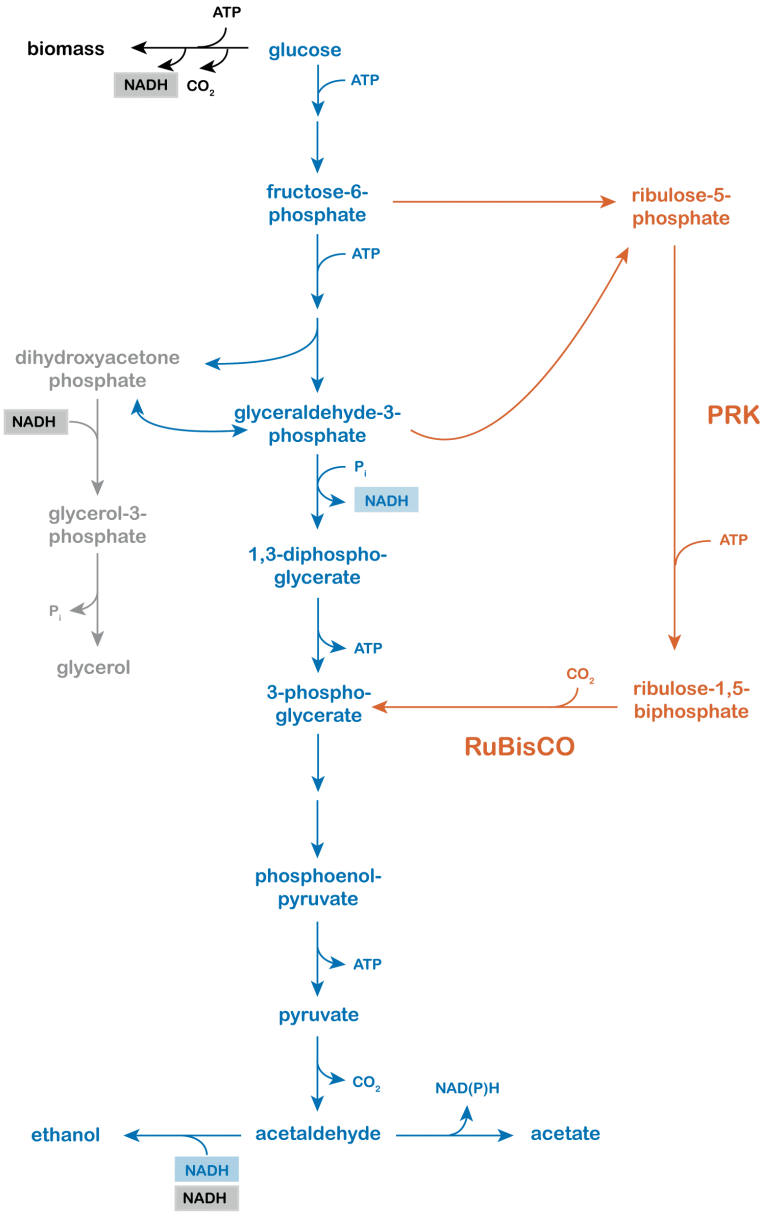

Figure 1: Simplified schematic representation of ethanol and biomass formation by an engineered strain of *Saccharomyces cerevisiae* by heterologous expression of genes encoding the Calvin-cycle enzymes PRK and RuBisCO. Black: biosynthetic reactions with a net input of ATP and a net production of CO_2 and NADH. Blue: redox-neutral conversion of glucose to ethanol by glycolysis, pyruvate decarboxylase and alcohol dehydrogenase. Blue: NAD(P)H-dependent conversion of acetaldehyde into acetate. Orange: non-oxidative pentose phosphate pathway, heterologously expressed PRK-RuBisCO pathway and subsequent NADH-requiring ethanol formation. Grey: native glycerol reduction pathway.

Results

Acetaldehyde and acetate as key byproducts in slow-growing anaerobic cultures of a PRK-RuBisCO S. cerevisiae strain

To investigate the impact of the specific growth rate on product yields of a PRK-RuBisCO-based *S. cerevisiae* strain, anaerobic glucose-limited chemostat cultures of strain IMX1489 (Δ*gpd2* non-ox PPP↑ p*DAN1-PRK* 15x *cbbM* g*roES/groEL* (77); non-ox PPP↑ indicates overexpression of native *S. cerevisiae* genes encoding enzymes of the non-oxidative pentose-phosphate pathway) were grown at dilution rates of 0.05 h^{-1}, 0.1 h^{-1} and 0.25 h^{-1}. Biomass and product yields of these cultures were compared with those of cultures of the congenic reference strain IME324, which carried none of the genetic modifications introduced into strain IMX1489. In addition, exponentially growing anaerobic batch cultures of the two strains were compared.

At all three dilution rates, chemostat cultures of the PRK-RuBisCO-synthesizing strain IMX1489 produced much less glycerol per amount of biomass formed than the reference strain (Fig. 2, Table 1). This observation showed that, at all three dilution rates, the PRK-RuBisCO-pathway replaced glycerol formation as main mechanism for oxidation of 'surplus' NADH derived from biosynthesis (78). The relative impact of the PRK-RuBisCO pathway on glycerol formation was largest at low specific growth rates (Figure 2, Table 1). At a dilution rate of 0.05 h^{-1}, the amount of glycerol produced per amount of biomass by strain IMX1489 was only 3.5% of that of the reference strain, as compared to 10% at a dilution rate of 0.25 h^{-1} and 18% in exponentially growing batch cultures (Table 1, Table 2).

Despite the near-complete elimination of glycerol formation in chemostat cultures of strain IMX1489 grown at 0.05 h^{-1}, the ethanol yield on glucose in these cultures was only 3.0% higher than observed in similar cultures of the reference strain. This difference was smaller than observed in chemostat cultures grown at a dilution rate of 0.25 h^{-1} and in exponentially growing batch cultures (9.5% and 8.7%, respectively, Table 1, Table 2). At all three dilution rates, strain IMX1489 showed a higher acetate yield on glucose than the reference strain IME324, with the highest relative difference being observed at 0.05 h^{-1}. At this low dilution rate, acetate was a minor byproduct in cultures of the reference strain (0.002 mol acetate per mol glucose), while strain IMX1489 showed a 22-fold higher acetate yield (0.045 mol acetate per mol glucose) (Table 1, Fig. 2). The smallest difference was found in exponentially growing batch cultures, in which strain IMX1489 showed an only 40% higher acetate yield than the reference strain (Table 2).

A distinct smell of the off-gas of chemostat cultures indicated that strain IMX1489 produced acetaldehyde. To quantify this volatile metabolite (boiling temperature 20 °C, (136)), culture broth was rapidly sampled into a 2,4-dinitrophenylhydrazine (2,4-DNPH) solution (103) and acetaldehyde in the gas phase was measured after sparging bioreactor off-gas through a 2,4-DNPH solution. Low acetaldehyde yields on glucose (≤ 0.001 mol acetaldehyde per mol glucose; Table 1) were found in chemostat cultures of the reference strain IME324. Acetaldehyde yields of strain IMX1489 were much higher, with the highest values observed at dilution rates of 0.05 h^{-1} and 0.10 h^{-1} (0.056 and 0.071 mol acetaldehyde (mol glucose)$^{-1}$, respectively). In these cultures, concentrations of acetaldehyde of up to 6.5 mM were measured in the culture broth (Additional file 1: accessible online). This concentration is within the toxicity range for yeasts (137) and may explain why biomass yields of strain IMX1489 at these dilution rates were 6 to 7% lower than those of the reference strain IME324. Acetaldehyde yields on glucose of chemostat cultures at 0.25 h^{-1} and anaerobic batch cultures of strain IMX1489 were lower (0.020 mol (mol glucose)$^{-1}$ and 0.015 mol (mol glucose)$^{-1}$, respectively) than observed in slow-growing chemostat cultures. Biomass yields in those cultures were similar to those of the control strain. To investigate whether acetate and acetaldehyde production by the PRK-RuBisCO strain depended on the nutrient-limitation regime, anaerobic nitrogen-limited chemostat cultures were grown at 0.1 h^{-1}. Also in those cultures, strain IMX1489 showed a much higher acetaldehyde yield on glucose than the reference strain IME324 (Fig. S1).

Based on the high yields of acetate and acetaldehyde in anaerobic cultures of the PRK-RuBisCO strain IMX1489, we hypothesized that the rate of pyruvate generation via the PRK-RuBisCO bypass (Fig. 1) exceeded the rate of 'surplus' NADH formation in biosynthesis. In such a scenario, limited availability of NADH would prevent complete reduction of acetaldehyde generated in the irreversible pyruvate-decarboxylase reaction by NADH-dependent alcohol dehydrogenase. The excess acetaldehyde could then either be excreted or converted to acetate by (NAD(P)$^+$-dependent acetaldehyde dehydrogenases (Ald6, Ald5 and Ald4 (138)). This hypothesis is consistent with the observed high acetaldehyde and acetate yields in slow-growing cultures since, under the assumption of a constant biomass composition, the biomass-specific rate of NADH formation in biosynthesis is proportional to the specific growth rate (78).

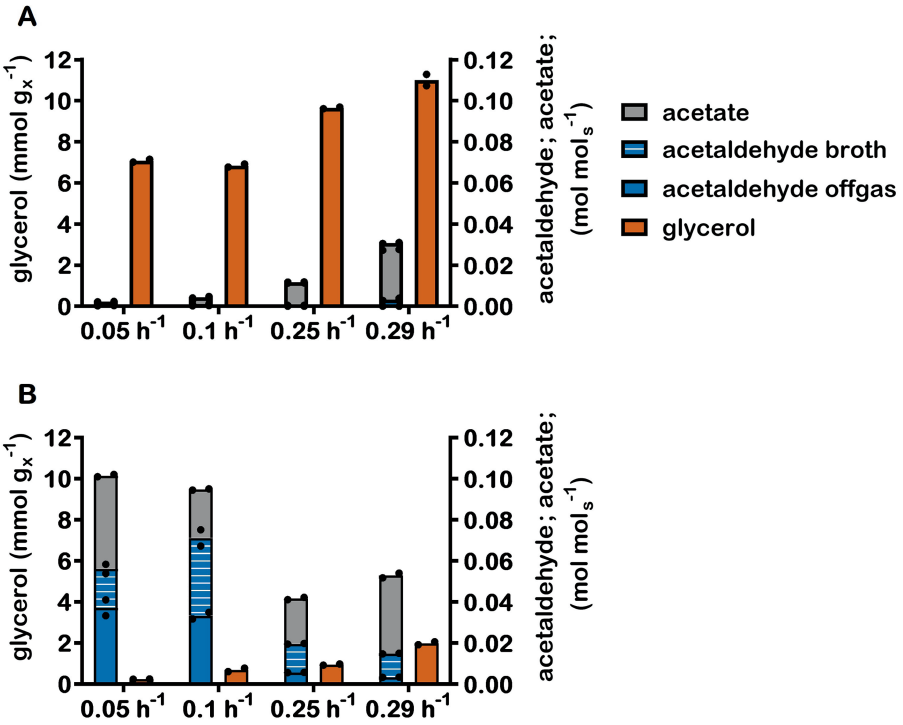

Figure 2: Yields of acetaldehyde and acetate on glucose and stoichiometric relationships between glycerol production and formation of biomass (denoted by x) in anaerobic chemostat cultures of *S. cerevisiae* strains IME324 (A: reference strain lacking PRK-RuBisCO bypass) and IMX1489 (B: Δ*gpd2* non-ox PPP↑ p*DAN1-PRK* 15x *cbbM groES/groEL*) at 0.05 h^{-1}, 0.1 h^{-1} and at 0.25 h^{-1} and anaerobic batch cultures at maximum specific growth rates (0.31 h^{-1} and 0.29 h^{-1}). Non-ox PPP↑ indicates the integration of the expression cassettes of p*TDH3-RPE1*, p*PGK1-TKL1*, p*TEF1-TAL1*, p*PGI1-NQM1*, p*TPI1-RKI1* and p*PYK1-TKL2.* Values represent means and individual values of measurements on independent steady-state duplicate cultures.

Table 1: Yields of biomass, acetaldehyde, acetate and ethanol on glucose and ratio of glycerol production and biomass (x) formation in anaerobic chemostat cultures of *S. cerevisiae* strains IME324 (reference strain lacking PRK-RuBisCO bypass) and IMX1489 (Δ*gpd*, non-ox PPP↑ p*DAN1-PRK* 15x *cbbM* g*roES/groEL*) at 0.05 h^{-1}, 0.1 h^{-1} and at 0.25 h^{-1}. Values represent average ± mean deviation of measurements on independent steady-state duplicate cultures. Electron recoveries were calculated as balances of degree of reduction of substrates and products (11).

Strain	**IME324**			**IMX1489**		
Relevant genotype	Reference			Δ*gpd2* p*DAN1-PRK* 15x *cbbM*		
Dilution rate (h^{-1})	**0.05**	**0.1**	**0.25**	**0.05**	**0.1**	**0.25**
Biomass/glucose (g_x g^{-1})	0.084 ± 0.002	0.096 ± 0.004	0.093 ± 0.001	0.078 ± 0.001	0.090 ± 0.001	0.093 ± 0.001
Ethanol/glucose (mol mol^{-1})	1.539 ± 0.010	1.590 ± 0.039	1.487 ± 0.001	1.585± 0.010	1.574 ± 0.018	1.630 ± 0.007
Acetaldehyde/glucose (mol mol^{-1})	0.001 ± 0.000	0.001 ± 0.000	0.000 ± 0.000	0.056 ± 0.002	0.071 ± 0.003	0.020 ± 0.000
Acetate/glucose (mol mol^{-1})	0.002 ± 0.000	0.003 ± 0.001	0.011 ± 0.000	0.045 ± 0.001	0.024 ± 0.000	0.022 ± 0.001
Glycerol/glucose (mol mol^{-1})	0.108 ± 0.001	0.118 ± 0.003	0.161 ± 0.000	0.004 ± 0.000	0.011 ± 0.002	0.016 ± 0.001
Glycerol/biomass (mmol g_x^{-1})	7.10 ± 0.10	6.85 ± 0.10	9.65 ± 0.06	0.25 ± 0.00	0.70 ± 0.12	0.96 ± 0.04
Electron recovery (%)	95-95	98-102	98-98	95-95	96-97	97-98

Table 2: Anaerobic bioreactor batch cultures of *S. cerevisiae* strains carrying different genetic modifications. Specific growth rates and yields of ethanol, acetaldehyde and acetate on glucose and ratio between glycerol and biomass (x) formation were calculated from at least 6 sampling points in the exponential growth phase. Biomass yield was determined based on the measured concentrations of biomass and glucose of the first and last timepoint. Values represent averages ± mean deviations of measurements on independent duplicate cultures for each strain. Electron recoveries were calculated as balances of degree reduction of substrates and products (11). Abbrevations: gluc, glucose; glyc, glycerol; acetal, acetaldehyde.

Strain Relevant genotype	**IME324** Reference	**IMX1489** Δ*gpd2* p*DAN1-PRK* 15x *cbbM*	**IMX2736** Δ*gpd2* p*DAN1-PRK* 2x *cbbM*	**IMX2701** Δ*gpd2* p*DAN1-PRK*-PEST 2x *cbbM*	**IMX2593** Δ*gpd2* p*DAN1-PRK*-19aa 2x *cbbM*	**IMX2608** Δ*gpd2* p*ANB1-PRK* 2x *cbbM*
Biomass/gluc (g_x g^{-1})	0.091 ± 0.001	0.091 ± 0.001	0.095 ± 0.001	0.090 ± 0.001	0.094 ± 0.002	0.094 ± 0.001
μ_{max} (h^{-1})	0.32 ± 0.01	0.29 ± 0.00	0.29 ± 0.01	0.25 ± 0.00	0.29 ± 0.00	0.29 ± 0.00
Ethanol/gluc (mol mol^{-1})	1.473 ± 0.046	1.601 ± 0.001	1.626 ± 0.008	1.544 ± 0.001	1.602 ± 0.007	1.647 ± 0.011
Acetal/gluc (mol mol^{-1})	0.003 ± 0.001	0.015 ± 0.000	0.007 ± 0.001	0.001 ± 0.000	0.003 ± 0.002	0.004 ± 0.001
Acetate/gluc (mol mol^{-1})	0.027 ± 0.000	0.038 ± 0.001	0.034 ± 0.001	0.013 ± 0.001	0.019 ± 0.002	0.025 ± 0.002
Glyc/gluc (mol mol^{-1})	0.202 ± 0.004	0.033 ± 0.001	0.037 ± 0.002	0.153 ± 0.003	0.086 ± 0.002	0.052 ± 0.005
Glyc/biomass (mmol g_x^{-1})	11.3 ± 0.55	1.99 ± 0.07	1.86 ± 0.07	9.08 ± 0.06	5.05 ± 0.20	3.12 ± 0.25
Electron recovery (%)	100-101	98-98	100-101	101-102	100-101	100-100

Reduced acetaldehyde and acetate production in strains with a lower copy number of the RuBisCO-encoding expression cassette

To maximize the positive impact of the engineered PRK-RuBisCO-bypass on ethanol yield, production of acetate and acetaldehyde, resulting from a too high activity of this pathway, should be minimized. In strain IMX1489, multiple copies of the *cbbM* expression cassette were introduced in tandem (139) to facilitate amplification of the number of *cbbM* expression cassettes by homologous recombination. Such homologous recombination can also lead to a reduction of the *cbbM* copy number but, since adjacent copies of the *cbbM* cassette were divergently oriented, could not lead to a copy number below two. Short-read whole-genome sequencing (WGS) and long-read sequencing estimated the copy number in strain IMX1489 at 13 and 15 copies, respectively (140). However, strain IMX2736 and other strains derived from

IMX2288, which was obtained by removing the gRNA plasmid from strain IMX1489, contained only 2 copies. Strain IMX2736, which did not reveal mutations in open reading frames relative to strain IMX1489, was therefore used to study the impact of a reduced *cbbM* copy number on byproduct formation. In slow-growing anaerobic chemostat cultures (0.05 h^{-1}), the 7-fold lower copy number of *cbbM* in strain IMX2736 coincided with a 3-fold lower abundance of the CbbM protein than in strain IMX1489 (0.70 ± 0.01% and 2.20 ± 0.01 % of total protein, respectively, in duplicate anaerobic chemostats of each strain grown at 0.05 h^{-1}). In contrast, PRK abundance was not significantly different (Fig. 3B). In these slow-growing chemostat cultures, acetaldehyde and acetate yields of strain IMX2736 were 67% and 29% lower, respectively, than those of strain IMX1489 (p*DAN1-PRK* 15x *cbbM*), while ethanol yield was 4% higher (Table 3). The 12.8% higher biomass yield of strain IMX2736 may reflect alleviation of acetaldehyde toxicity.

Despite its 7-fold lower *cbbM* copy number, IMX2736 did not show a lower specific growth rate or higher glycerol yield per amount of biomass than strain IMX1489 in anaerobic batch cultures (Table 2, Fig. 4). In addition, acetate and acetaldehyde yields on glucose in anaerobic batch cultures of strain IMX2736 were 10.5% and 53% lower, respectively, than in similar cultures of strain IMX1489, while the ethanol yield was 1.5% higher (Table 2). As observed in slow-growing chemostat cultures, a lower production of acetaldehyde and acetate in strain IMX2736 coincided with a higher biomass yield on glucose relative to strain IMX1489.

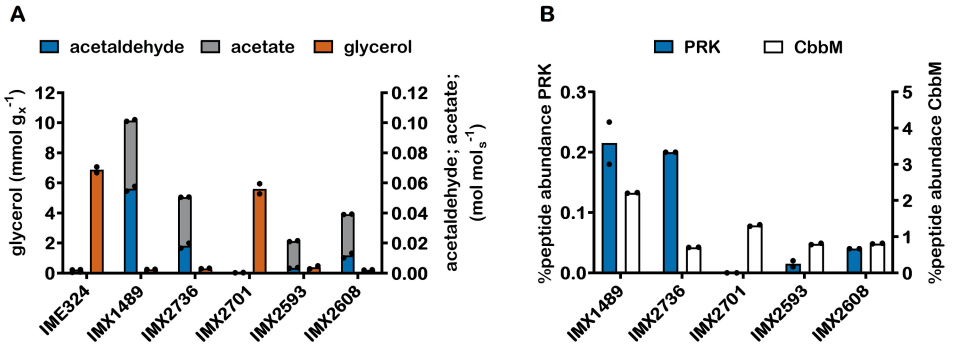

Figure 3: Glycerol, acetate and acetaldehyde production (A) and PRK and CbbM-derived peptide abundance determined by LC-MS and displayed as the percentage of PRK or CbbM protein in the total protein pool (B) in anaerobic chemostat cultures of IME324 (reference strain lacking PRK-RuBisCO bypass), IMX1489 (Δ*gpd2*, non-ox PPP↑ p*DAN1-PRK* 15x *cbbM groES/groEL*), IMX2736 (Δ*gpd2* non-ox PPP↑ p*DAN1-PRK* 2x *cbbM groES/groEL*), IMX2701 (Δ*gpd2* non-ox PPP↑ p*DAN1-PRK-CLN2*$_{PEST}$ 2x *cbbM groES/groEL*), IMX2593 (Δ*gpd2* non-ox PPP↑ p*DAN1-PRK*-19aa 2x *cbbM groES/groEL*) and IMX2608 (Δ*gpd2* non-ox PPP↑ p*ANB1-PRK* 2x *cbbM groES/groEL*) at a dilution rate of 0.05 h^{-1}. Values represent means and individual values of measurements on independent steady-state duplicate cultures.

Table 3: Yields of biomass, acetaldehyde, acetate and ethanol on glucose and ratio between glycerol production and biomass formation in anaerobic glucose-limited chemostat cultures of *S. cerevisiae* strains carrying different genetic modifications at a dilution rate of 0.05 h^{-1}. Values represent averages ± mean deviations of measurements on independent steady-state duplicate cultures. Electron recoveries were calculated as balances of degree of reduction of substrates and products (11). Abbrevations: gluc, glucose; glyc, glycerol; acetal, acetaldehyde.

Strain Relevant genotype	**IME324** Reference	**IMX1489** Δ*gpd2* p*DAN1-PRK* 15x *cbbM*	**IMX2736** Δ*gpd2* p*DAN1-PRK* 2x *cbbM*	**IMX2701** Δ*gpd2* p*DAN1-PRK*-PEST 2x *cbbM*	**IMX2593** Δ*gpd2* p*DAN1-PRK*-19aa 2x *cbbM*	**IMX2608** Δ*gpd2* p*ANB1-PRK* 2x *cbbM*
Biomass/gluc (g_x g^{-1})	0.084 ± 0.002	0.078 ± 0.001	0.088 ± 0.002	0.085 ± 0.000	0.089 ± 0.002	0.090 ± 0.000
Ethanol/gluc (mol mol^{-1})	1.539 ± 0.010	1.585 ± 0.010	1.648 ± 0.005	1.549 ± 0.004	1.651 ± 0.034	1.626 ± 0.002
Acetal/gluc (mol mol^{-1})	0.001 ± 0.000	0.056 ± 0.002	0.018 ± 0.002	0.000 ± 0.000	0.004 ± 0.000	0.012 ± 0.002
Acetate/gluc (mol mol^{-1})	0.002 ± 0.000	0.045 ± 0.001	0.032 ± 0.002	0.000 ± 0.000	0.018 ± 0.000	0.027 ± 0.000
Glyc/gluc (mol mol^{-1})	0.108 ± 0.001	0.004 ± 0.000	0.005 ± 0.000	0.086 ± 0.006	0.006 ± 0.002	0.003 ± 0.000
Glyc/biomass (mmol g_x^{-1})	7.10 ± 0.10	0.25 ± 0.00	0.31 ± 0.01	5.60 ± 0.41	0.39 ± 0.14	0.21 ± 0.01
Electron recovery (%)	95-95	95-95	97-98	95-95	95-97	96-96

C-terminal tags to reduce abundancy of PRK

C-terminal PEST sequences, which are rich in proline (P), glutamic acid (E), serine (S) and threonine (T), have been described to enhance proteasome-mediated protein turnover (141). This regulation mechanism could, in principle, not only reduce PRK levels in growing cultures but, in particular, support fast PRK degradation once growth and protein synthesis in industrial processes slows down. Regulation of PRK activity at a post-translational level is also attractive because it is not expected to interfere with oxygen-dependent expression of *PRK* from the p*DAN1* promoter, which was used to prevent toxicity of high levels of PRK during aerobic pre-cultivation (142).

When the DNA sequence encoding the 178 amino acid C-terminal $CLN2_{PEST}$ sequence (141) was C-terminally fused to *PRK* in strain IMX2701 (p*DAN1-PRK-*$CLN2_{PEST}$ 2x *cbbM*), PRK levels were below the detection limit of the proteomics analysis (Figure

3B). This extreme reduction of PRK protein levels relative to those in strain IMX2736 (p*DAN1-PRK* 2x *cbbM*) was reflected in a 19-fold and 5-fold higher glycerol formation per amount of biomass in chemostat cultures grown at 0.05 h^{-1} and in anaerobic batch cultures, respectively (Table 2, Table 3). In addition, strain IMX2701 showed a 14% lower specific growth rate in anaerobic batch cultures than strain IMX2736 (Table 2, Fig. 4D). This observation is consistent with a limited capacity for anaerobic reoxidation of cytosolic NADH which, at the extremely low PRK level in strain IMX2701 (Fig. 3B), predominantly depends on sole remaining glycerol-3-phosphate isoenzyme Gpd1 in the engineered strains.

While constructing fusions of *PRK* with the *CLN2$_{PEST}$*-tag, we unintentionally obtained a fusion of *PRK* with a frameshifted PEST-sequence that led to extension of PRK with a 19 amino acid translation product. This extension, which we labelled 19aa, showed no notable sequence similarity with the *CLN2$_{PEST}$* sequence (Table S2). However, chemostat cultures of strain IMX2593 (p*DAN1-PRK*-19aa 2x *cbbM*) grown at 0.05 h^{-1} showed a 13-fold lower PRK protein level than strain IMX2736 (p*DAN1-PRK* 2x *cbbM*). Despite this strongly reduced PRK protein level, strain IMX2593 still showed an 18-fold lower glycerol production per amount of biomass than the reference strain IME324. Moreover, acetaldehyde and acetate yields on glucose in the chemostat cultures of strain IMX2593 were 81% and 45% lower, respectively, than in corresponding cultures of strain IMX2736. In exponentially growing batch cultures of strain IMX2593, glycerol formation per amount of biomass was 30% higher than in batch cultures of IMX2736, but still 55% lower than in batch cultures of the reference strain (IME324) (Table 2, Fig. 4E).

To explore how the 19 amino acid C-terminal '19aa' tag affected protein levels, it was fused to the C-terminus of eGFP. The resulting yeast strain showed an almost 2-fold lower fluorescence signal (Fig. S2; 0 min) than a strain synthesizing non-tagged eGFP gene. Both tagged and non-tagged eGFP remained stable upon addition of the protein-synthesis inhibitor cycloheximide (143) (Fig. S2). In contrast, a strain synthesizing an *egfp-CLN2$_{PEST}$* fusion, whose steady-state fluorescence was 7-fold lower than that of a strain synthesizing non-tagged GFP, showed a fast decline of fluorescence after cycloheximide addition (Fig. S2). These results indicated that the 19aa tag did not substantially affect protein degradation kinetics.

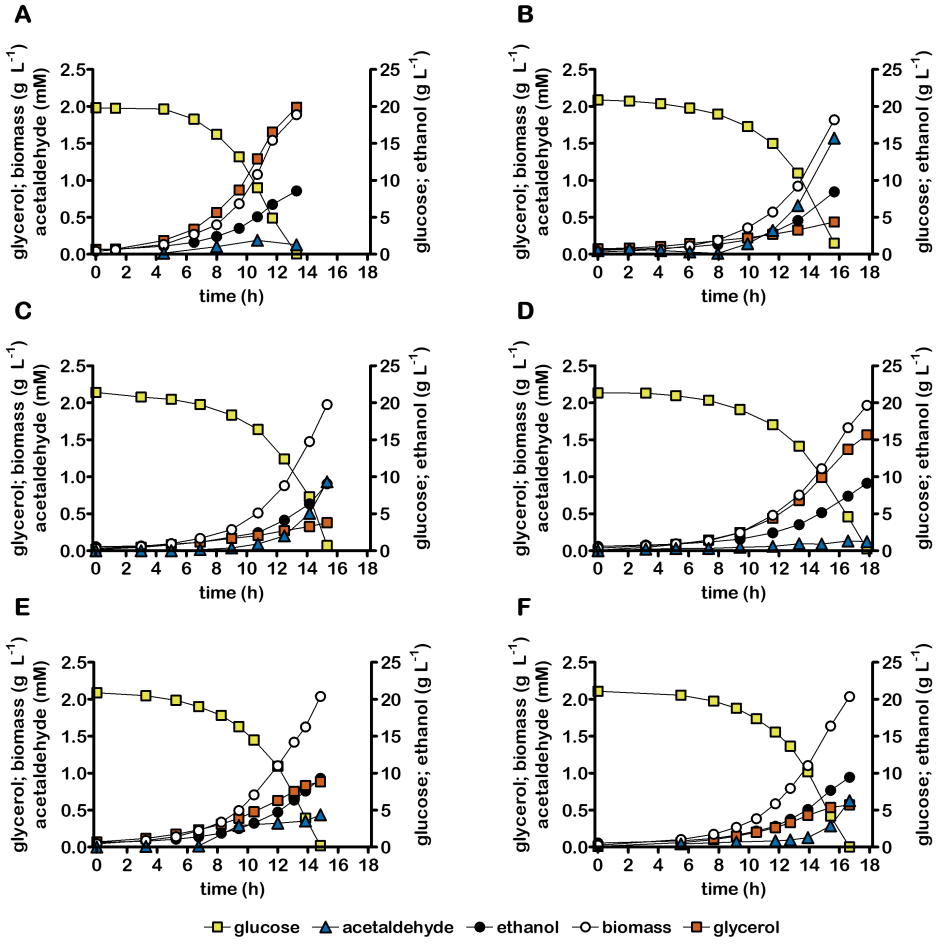

Figure 4: Growth, glucose consumption, ethanol formation, acetaldehyde formation and glycerol formation in anaerobic bioreactor batch cultures of *S. cerevisiae* strains IME324 (reference strain lacking PRK-RuBisCO bypass) (A), IMX1489 (*Δgpd2* non-ox PPP↑ p*DAN1-PRK* 15x *cbbM groES/groEL*)(B), IMX2736 (*Δgpd2* non-ox PPP↑ p*DAN1-PRK* 2x *cbbM groES/groEL*)(C), IMX2701 (*Δgpd2* non-ox PPP↑ p*DAN1-PRK-CLN2$_{PEST}$* 2x *cbbM groES/groEL*)(D), IMX2593 (*Δgpd2* non-ox PPP↑ p*DAN1-PRK*-19aa 2x *cbbM groES/groEL*)(E) and IMX2608 (*Δgpd2* non-ox PPP↑ p*ANB1-PRK* 2x *cbbM groES/groEL*)(F) Cultures were grown anaerobically at pH 5 and at 30 °C on synthetic medium containing 20 g L^{-1} glucose. Representative cultures of independent duplicate experiments are shown, corresponding replicate of each culture shown in Figure S3.

Promoter selection for PRK results in reduced overflow metabolism

While a C-terminal '19aa' tag decreased PRK protein levels and formation of acetaldehyde and acetate, this mode of regulation of PRK synthesis is essentially static. Ideally, *in vivo* activity of the PRK-RuBisCO-pathway should be dynamically adapted to the rate of growth-coupled NADH formation in biosynthesis. To enable adaptation of *PRK* expression to specific growth rate, we explored the use of an anaerobically induced, growth-rate dependent promoter.

Transcriptome data from anaerobic, glucose-limited chemostat cultures of strains IMX1489 and IME324 grown at 0.05, 0.1 and 0.25 h^{-1} were used to identify genes whose anaerobic transcript levels positively correlated with specific growth rate and whose transcript level at 0.25 h^{-1} was at least 50% of the transcript level of *PRK* observed upon its expression from the *DAN1* promoter. The search was further narrowed by excluding genes that were also expressed in aerobic cultures of the congenic reference strain CEN.PK113-7D (data set of Regenberg *et al.* (144); Fig. 5). This search yielded only *ANB1*, which encodes a translation initiation factor (145). Expression of *PRK* from a 1000 bp *ANB1* promoter fragment yielded strain IMX2608 (*Δgpd2* non-ox PPP↑ p*ANB1-PRK* 2x *cbbM GroES/GroEL*).

In anaerobic chemostat cultures grown at 0.05 h^{-1}, acetaldehyde and acetate yields on glucose of this strain were 36% and 15% lower than in corresponding cultures of strain IMX2736. In anaerobic bioreactor batch cultures, strain IMX2608 showed a two-fold lower PRK protein level than strain IMX2736, which expressed *PRK*-19aa (Additional File 4: available online). In these batch cultures, the specific growth rates of the two strains were not significantly different. Acetaldehyde and acetate yields of strain IMX2608 in anaerobic batch cultures were approximately 40% and 25% lower than in those of strain IMX2736 and not significantly different from those in batch cultures of the reference strain IME324 (Table 2). While the glycerol yield per amount of biomass of strain IMX2608 was 57% higher than in cultures of strain IMX2736, it was still 72% lower than observed in batch cultures of the reference strain IME324 (Table 2, Fig. 4F).

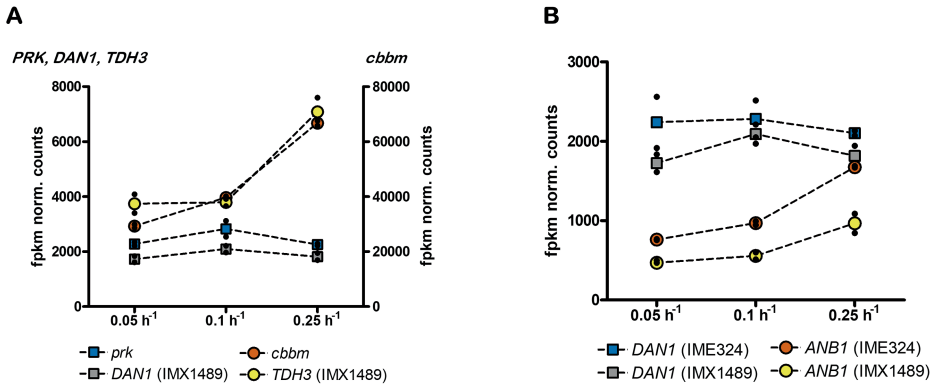

Figure 5: fpkm normalized counts of *PRK*, *DAN1*, *cbbM* and *TDH3* obtained from transcriptome data of chemostat cultures of strain IMX1489 (*Δgpd2* non-ox PPP↑ p*DAN1-PRK* 15x *cbbM groES/groEL*) (A) and fpkm normalized counts of *DAN1* and *ANB1* obtained from transcriptome data of chemostat cultures of strain IMX1489 and IME324 (reference strain lacking PRK-RuBisCO bypass) (B) at dilution rates of 0.05 h^{-1}, 0.1 h^{-1} and 0.25 h^{-1}. Values represent means and individual values of measurements on independent steady-state duplicate cultures.

Discussion

An engineered non-oxidative glycolytic bypass mediated by the Calvin-cycle enzymes PRK and RuBisCO can replace glycerol formation as main mechanism for re-oxidation of biosynthesis-derived NADH in anaerobic *S. cerevisiae* cultures and, thereby, improve ethanol yields on sugar (77). Our results show that, especially at low specific growth rates, strains carrying the PRK-RuBisCO glycolytic bypass produced more acetaldehyde and acetate than a reference strain. This enhanced byproduct formation was hypothesized to reflect an imbalance between *in vivo* activity of the PRK-RuBisCO bypass and generation of NADH in biosynthesis. Consistent with this hypothesis, reduction of PRK and/or RuBisCO synthesis by engineered strains led to a lower production of acetaldehyde and acetate. Slow-growing anaerobic cultures of a similarly engineered *S. cerevisiae* strain were recently shown to co-ferment glucose and sorbitol (140). Since sorbitol co-fermentation required a higher flux through the PRK-RuBisCO bypass, these results are also in line with an 'overcapacity' of this pathway during slow anaerobic growth on glucose.

As generation of acetaldehyde and acetate goes at the expense of maximum achievable ethanol yield gains of the PRK-RuBisCO strain, the observed byproduct formation is undesirable for industrial application. Furthermore, slow-growing cultures of a PRK-RuBisCO strain that carried 15 copies of the expression cassette for RuBisCO reached acetaldehyde concentrations that were within the toxicity range for yeast (137). Loss

of carbon to acetaldehyde and acetate goes at the expense of the ethanol yield on sugar and, in addition, production of acetaldehyde in large-scale processes may raise environmental (146) and health (147) issues. We therefore explored metabolic engineering strategies to mitigate byproduct formation.

Reducing the copy number of the expression cassette for RuBisCO led to lower acetaldehyde and acetate production in slow-growing anaerobic cultures and, concomitantly, a higher ethanol yield on glucose (strain IMX2736; Fig. 3, Table 3). Further reduction of acetaldehyde and acetate production was tested by reducing the PRK protein level. One of the strategies used for decreasing PRK levels was based on a serendipitously discovered C-terminal tag, which was found to reduce acetaldehyde and acetate production both in fast and slow-growing cultures (strain IMX2593; Fig. 3, Table 2, Table 3). However, this engineering strategy, resulting in 'static' regulation of *PRK* expression, also led to higher glycerol yields in fast-growing cultures (Table 2, Figure 4), thus reflecting a trade-off between performance at low and high specific growth rates.

The 19aa tag affected steady-state protein level without modification of transcriptional regulation. In the case of PRK, conserving transcriptional regulation by an oxygen-responsive promoter was important as it prevents toxicity of PRK in aerobic pre-cultures (77, 142). Of the nineteen nucleotide triplets that encode the 19aa tag, four occur at a frequency that is below 50% of that of the most frequently occurring synonymous triplet (Table S3). However, it cannot be excluded that factors other than codon usage cause the reduced protein abundance of PRK and GFP observed upon addition of the 19aa tag. Resolving this issue would require analyses of protein and transcript levels, as well as protein activity in strains carrying C-terminal tags with different codon usage. Irrespective of the responsible mechanism, tuning of protein levels and/or activity by C-terminal tagging may be a simple, flexible strategy in scenarios that require conservation of transcriptional regulation of an expression cassette, for example because few suitable promoters are available. Flexibility of this approach could be increased by high-throughput screening of libraries of short C-terminal tags for different impacts on protein levels. In *E. coli*, different protein degradation tags were obtained by mutagenizing a known C-terminal tag based on the *Mesoplasma florum* tmRNA system (148). In *S. cerevisiae*, the PEST-tag was used to similarly decrease protein stability (149-151) but, in the present study, a PRK-PEST fusion led to too low levels of PRK (Figure 3).

Conditions in large-scale ethanol fermentation processes are inherently dynamic due to changes in the concentrations of sugar, nitrogen source, ethanol and other

compounds (152). In industrial contexts, the capacity of the PRK-RuBisCO bypass should therefore ideally be dynamically adapted to the actual rate of NADH generation in biosynthesis. The potential of such dynamic regulation strategies was demonstrated by expressing the *PRK* gene from the promoter of *ANB1*, whose transcript levels in anaerobic chemostat cultures positively correlated with specific growth rate (Fig. 5; (145)). While yields of acetate and acetaldehyde in slow-growing cultures of the resulting *pANB1-PRK* strain IMX2608 were not as low as in strain IMX2593, which is based on the 'static' regulation of PRK (Table 3), they were similar to those in fast-growing cultures of the non-engineered reference strain IME324 (Table 2). In addition, the p*ANB1-PRK* strain showed a strong reduction of glycerol production and high ethanol yield in anaerobic batch cultures relative to this reference strain (Table 2).

Rather than relying on native yeast promoters such as *ANB1*, dynamic regulation of *PRK* expression might be coupled to synthetic regulatory circuits (153). In this context, regulation of *PRK* expression by cytosolic NADH/NAD^+ ratio (154) would be particularly interesting. The NADH-responsive transcriptional repressor Rex, which has a high affinity for its co-repressor NADH, naturally occurs in gram-positive bacteria and was previously applied as redox biosensor in bacteria and mammalian cells (155-157). Rex or similar transcriptional regulators may be applied to construct regulatory circuits that couple *PRK* expression to NADH availability. Alternatively, dynamic regulation of *PRK* expression or PRK degradation might be coupled to the intracellular acetaldehyde concentration. YqhC, an *E. coli* transcriptional activator whose many ligands include acetaldehyde, mediates upregulation of transcription in the presence of acetaldehyde (158-160). Dynamic regulatory circuits for *PRK* based on YqhC could be coupled to a dCas9 (161) or an mRNA interference module (162) to control transcription or translation respectively of *PRK* or could activate auxin-mediated degradation of the PRK protein (163). Implementation of these allosterically regulated transcription factors (aTF) into eukaryotic cells can be achieved via heterologous expression of the gene encoding the transcription factor and insertion of the aTF operator site into a native promoter (164, 165). Although this strategy usually requires extensive optimization in eukaryotic hosts (166, 167) and has not yet been applied to anaerobic yeast cell factories, aTF based biosensors may hold promise for tuning pathway expression in yeast redox engineering strategies.

Byproduct formation in yeast strains engineered for reduced glycerol formation is not necessarily a unique characteristic of *S. cerevisiae* strains carrying a PRK-RuBisCO bypass. In an alternative strategy based on heterologous phosphoketolase and phosphotransacetylase (106, 108), acetyl-CoA is generated via acetyl-phosphate. The

subsequent reduction of acetyl-CoA to acetaldehyde via acetylating acetaldehyde dehydrogenase requires NADH, while an additional NADH is required to further reduce acetaldehyde to ethanol. By analogy to the situation in PRK-RuBisCO-based strains, a too high activity of phosphoketolase, phosphotransacetylase and/or acetylating acetaldehyde dehydrogenase could theoretically also lead to accumulation of acetaldehyde (and acetate). Yet another strategy for glycerol reduction relies on the heterologous pyruvate-formate lyase and acetylating acetaldehyde dehydrogenase (98, 101), which together convert pyruvate into acetaldehyde and formate. While formation of acetaldehyde from glucose via this pathway is redox-cofactor neutral, its subsequent reduction to ethanol requires NADH. Slow anaerobic growth of engineered yeast strains that rely on this pathway for reoxidation of 'surplus' NADH from biosynthesis, combined with a high activity of pyruvate-formate lyase and acetylating acetaldehyde dehydrogenase, might therefore also result in acetaldehyde accumulation.

Redox-cofactor engineering strategies are typically designed based on pathway stoichiometry, which for organisms such as *S. cerevisiae* can be easily modelled by metabolic network models (118). Our results underline the importance of also considering pathway kinetics and process dynamics in redox-cofactor based engineering studies and show the potential of dynamic regulation mechanisms to optimize microbial performance in industrial processes.

Materials and methods

Strains, media and maintenance

S. cerevisiae strains used in this study were derived from the CEN.PK lineage (168, 169). Synthetic medium (SM), prepared as described previously (29), contained 3.0 g L^{-1} KH_2PO_4, 0.5 g L^{-1} $MgSO_4 \cdot 7H_2O$, 5.0 g L^{-1} $(NH_4)_2SO_4$, 1.0 ml L^{-1} trace-element solution and 1.0 mL L^{-1} vitamin solution. Shake-flask, bioreactor-batch and glucose-limited chemostat cultures were grown on SM supplemented with 20 g L^{-1} glucose (SMD). In synthetic medium for nitrogen-limited chemostat cultivation (170), the concentration of $(NH_4)_2SO_4$ was reduced to 1.0 g L^{-1}, 5.3 g L^{-1} K_2SO_4 was added and the glucose concentration was increased to 59 g L^{-1}. Anaerobic growth media were supplemented with ergosterol (10 mg L^{-1}) and Tween 80 (420 mg L^{-1}) (15). Complex medium (YPD) contained 10 g L^{-1} Bacto yeast extract (Thermo Fisher Scientific, Waltham MA), 20 g L^{-1} Bacto peptone (Thermo Fisher Scientific) and 20 g L^{-1} glucose. *Escherichia coli* XL1-Blue cultures were grown on lysogeny broth (LB) (171) containing 10 g L tryptone (Brunschwig Chemie B.V., Amsterdam, The Netherlands), 5.0 g L^{-1} yeast extract and 10 g L^{-1} NaCl, where indicated supplemented with 100 mg L^{-1} ampicillin (Merck,

Darmstadt, Germany). *E. coli* strains were grown overnight at 37 °C in 15 mL tubes containing 5 mL LB, shaken at 200 rpm in an Innova 4000 Incubator (Eppendorf AG, Hamburg, Germany). Agar (20 g L^{-1}; Becton Dickinson, Breda, The Netherlands) was added to obtain solid-medium plates. *S. cerevisiae* plate cultures were incubated at 30 °C until colonies appeared (2-3 d), while *E. coli* plates were incubated overnight at 37 °C. Frozen stock cultures were prepared by freezing samples from fully grown batch cultures at -80 °C after addition of 30% (v/v) glycerol.

Plasmid and cassette construction

Plasmids and oligonucleotide primers used in this study, the latter either HPLC or PAGE purified or desalted (DST), are listed in Table 4 and Table S1 (available online), respectively. Phusion High-Fidelity DNA polymerase and Dreamtaq polymerase (Thermo Fisher Scientific) were used for PCR amplification of DNA fragments for further assembly and for diagnostic PCR reactions, respectively, according to the supplier's instructions. PCR-amplified DNA fragments were purified from gels using the ZymoClean Gel DNA recovery kit (Zymoclean, D2004, Zymo Research, Irvine, CA) or directly from PCR reaction mixtures using a GeneJET PCR purification kit (Thermo Fisher Scientific) following supplier's protocols. Plasmids were assembled with the *in vitro* Gibson method, using the HiFi DNA Assembly Master Mix (New England Biolabs, Ipswich, MA), essentially as recommended by the manufacturer but with a downscaled 5-µL reaction volume. XL-1 Blue cells were transformed by heat shock (172) with 1 µL of assembly mix. Assembled plasmids were isolated from *E. coli* cultures with a GenElute Plasmid kit (Sigma-Aldrich, St. Louis, MO) and used to transform *S. cerevisiae* strains. Yeast genomic DNA was isolated as described by Lõoke et al. (2011)(173).

A unique gRNA sequence targeting p*DAN1*-*PRK*-t*PGK1* was designed as described in BoxS4 in the supplementary materials in the publication by Mans et al. (2018)(174). To construct plasmid pUDR760, which expresses the unique *PRK*-targeting gRNA, the pROS10 backbone was PCR amplified with primer 5793 (double binding) and the plasmid insert was amplified using primer 17610 (double binding) and pROS10 as template for both reactions (175), after which pUDR760 was assembled by Gibson Assembly. A DNA repair fragment for eliminating a *PRK* expression cassette, while simultaneously restoring the *SGA1* target site into which it had been integrated, was PCR amplified from genomic DNA of *S. cerevisiae* IMX581 with primers 11404/17612. *DAN1* and *ANB1* promoter fragments were PCR amplified from genomic DNA of strain IMX581 with primer pairs 7978/7931 and 17929/17930, respectively. Genomic DNA of strain IMX581 was also used as template for amplification of the 534 3'-terminal nucleotides of *CLN2*, which contain the $CLN2_{PEST}$ sequence (141). Primer pairs

18391/17628 used in this amplification were designed to add flanking sequences with homology to *PRK* and t*PGK1*, respectively. A DNA fragment that resulted in frame-shift of the *CLN2$_{PEST}$* sequence added to the *PRK* ORF, was inadvertently obtained with primers 17627/17628 and will be referred to as '19aa'. The *PRK* ORF was amplified from pUDE046 with primer pair 7932/17626 to add flanks with homology to p*DAN1* and 19aa-tag, with 7932/18392 to add flanks homologous to p*DAN1* and *CLN2$_{PEST}$*, with 7932/7081 for adding flanks homologous to p*DAN1* and t*PGK1* and with 17983/7081 to add flanks with homology to p*ANB1* and t*PGK1*. A *PGK1* terminator fragment was amplified from genomic DNA of strain IMX581 with primer pair 7084/11205 or 17629/11205 to add flanks homologous to *PRK* and to *CLN2$_{PEST}$* and 19aa-tag, respectively. Complete expression cassettes of p*DAN1-PRK-tPGK1,* p*DAN1-PRK-CLN2$_{PEST}$*-t*PGK1*, p*DAN1-PRK*-[19aa]-t*PGK1* and p*ANB1-PRK-tPGK1* were assembled by *in vivo* homologous recombination (176).

A linearized backbone of p426-*GPD* (177) was amplified with primers 10546/10547. The *egfp* insert was ordered from GeneArt and amplified with primers 11584/11585. The insert was assembled with the p426-*GPD* fragment to obtain pUDE672. For construction of pUDE682, three fragments were amplified with primers 15651/18945, 16503/18946 and 5975/15645 with pUDE672 as template and one fragment using primers 18943/18944 and genomic DNA of IMX581 as template. Gibson assembly of the four fragments yielded pUD682, which carries a p*GPD-egfp-CLN2*$_{pest}$-t*CYC1* cassette. To obtain pUDE681, which encodes a p*GPD-egfp*-[19aa]-t*CYC1* cassette, pUDE672 was amplified with primers 5975/15645, 18948/15651 and 18947/16503.

Table 4: plasmids used in this study. *Kl* denotes *Kluyveromyces lactis*.

Plasmid	Characteristics	Origin
p426-*GPD*	2 µm ori, *URA3*, p*TDH3* -t*CYC1* (empty vector)	(177)
pROS10	2 µm ori , *KIURA3*, gRNA.*CAN1*-gRNA.*ADE2*	(175)
pUDR103	2 µm ori, *KIURA3*, p*SNR52*-gRNA.*SGA1*-t*SUP4*	(77)
pUDR760	2 µm ori, *KIURA3*, p*SNR52*-gRNA.*PRK*-t*SUP4*	This study
pUDE046	2 µm ori, *TRP1*, p*GAL1-PRK*-t*CYC1*	(109)
pUDE672	2 µm ori, *URA3*, p*TDH3-eGFP*-t*CYC1*	This study
pUDE1119	2 µm ori, *URA3*, p*TDH3-eGFP*-[19aa]-t*CYC1*	This study
pUDE1120	2 µm ori, *URA3*, p*TDH3-eGFP-CLN2*$_{PEST}$-t*CYC1*	This study

Yeast strain construction

Yeast strains were transformed with lithium-acetate method (178) and transformation mixtures were plated on SMD plates. Correct Cas9-mediated integration (175) and/or assembly of DNA fragments was verified by diagnostic PCR. gRNA-expression plasmids were removed by overnight growth in liquid, non-selective YPD and subsequent isolation of single colonies on YPD plates. Plasmid loss was checked by streaking colonies on selective (SMD) and non-selective (YPD) plates. A single verified colony, restreaked thrice, was grown on non-selective liquid medium and stored at -80 °C.

Strain IMX2288 was obtained by removing pUDR103 from *S. cerevisiae* IMX1489 (Δ*gpd2* p*DAN1-PRK* 15x *cbbM* pUDR103). After sequencing it was verified that strain IMX2288 and all strains made from this strain contained 2 copies of *cbbM* while IMX1489 contained 15 copies of *in tandem* integrated *cbbM*. Co-transformation of strain IMX2288 with pUDR760 (targeting *PRK*) and the repair fragment (encoding the *sga1* target sequence) yielded strain IMX2545 (Δ*gpd2* 2x *cbbM*), after removal of pUDR760, which was used for construction of multiple congenic strains with different *PRK*-cassettes.

Co-transformation of strain IMX2545 with pUDR103 together with p*DAN1* sequence, *PRK*-ORF, 19aa-tag sequence and the t*PGK1* fragment, yielded strain IMX2593 (Δ*gpd2* p*DAN1-PRK*-19aa 2x *cbbM* pUDR103). To construct strain IMX2608 (Δ*gpd2* p*ANB1-PRK* 2x *cbbM* pUDR103), strain IMX2545 was transformed with pUDR103 together with the promoter sequence of *ANB1*, *PRK*-ORF and t*PGK1*. Strain IMX2701 (Δ*gpd2* p*DAN1-PRK-CLN2*$_{PEST}$ 2x *cbbM* pUDR103) was obtained by transformation of strain IMX2545 with pUDR103 and p*DAN1*, *PRK*-ORF, *CLN2*$_{PEST}$ and t*PGK1*. Transformation of strain IMX2545 with pUDR103 together with the promoter sequence of *DAN1*, *PRK*-ORF and t*PGK1* resulted in strain IMX2736 (Δ*gpd2* p*DAN1-PRK* 2x *cbbM* pUDR103).

Strains IME678, IME681 and IME682 were obtained by transforming strain IMX581 with pUDE672, pUDE1119 and pUDE1120, respectively.

Table 5: *S. cerevisiae* strains used in this study. Non-ox PPP↑ indicates the integration of the expression cassettes of p*TDH3-RPE1*, p*PGK1-TKL1*, p*TEF1-TAL1*, p*PGI1-NQM1*, p*TPI1-RKI1* and p*PYK1-TKL2. Kl* denotes *Kluyveromyces lactis.*

Strain name	Relevant genotype	Parental strain	Origin
CEN.PK113-7D	*MATa URA3*	-	
CEN.PK113-5D	*MATa ura3-52*	-	
IMX581	*MATa ura3-52 can1::cas9-natNT2*	CEN.PK113-5D	(175)
IMX1489	*MATa ura3-52 can1::cas9-natNT2 gpd2::*non-ox PPP↑ *sga1::*(p*DAN1-PRK, cbbM* (15 copies), *groES*, *groEL*) pUDR103 (*KlURA3*)	IMX581	(77, 140)
IMX2288	*MATa ura3-52 can1::cas9-natNT2 gpd2::*non-ox PPP↑ *sga1::*(p*DAN1-PRK, cbbM* (2 copies), *groES*, *groEL*)	IMX1489	This study
IMX2545	*MATa ura3-52 can1::cas9-natNT2 gpd2::*non-ox PPP↑ *sga1::*(*sga1*-gRNA site, *cbbM* (2 copies), *groES*, *groEL)*	IMX2288	This study
IMX2593	*MATa ura3-52 can1::cas9-natNT2 gpd2::*non-ox PPP↑ *sga1::*(p*DAN1-PRK*-19aa*, cbbM* (2 copies), *groES*, *groEL*) pUDR103 (*KlURA3*)	IMX2545	This study
IMX2608	*MATa ura3-52 can1::cas9-natNT2 gpd2::*non-ox PPP↑ *sga1::*(p*ANB1-PRK, cbbM* (2 copies), *groES*, *groEL*) pUDR103 (*KlURA3*)	IMX2545	This study
IMX2701	*MATa ura3-52 can1::cas9-natNT2 gpd2::*non-ox PPP↑ *sga1::*(p*DAN1-PRK-CLN2$_{PEST}$, cbbM* (2 copies), *groES*, *groEL*) pUDR103 (*KlURA3*)	IMX2545	This study
IMX2736	*MATa ura3-52 can1::cas9-natNT2 gpd2::*non-ox PPP↑ *sga1::*(p*DAN1-PRK, cbbM* (2 copies), *groES*, *groEL*) pUDR103 (*KlURA3*)	IMX2545	This study
IME678	*MATa ura3-52 can1::cas9-natNT2* pUDE672 (*URA3*)	IMX581	This study
IME681	*MATa ura3-52 can1::cas9-natNT2* pUDE1119 (*URA3*)	IMX581	This study
IME682	*MATa ura3-52 can1::cas9-natNT2* pUDE1120 (*URA3*)	IMX581	This study

Shake-flask cultivation

Aerobic shake-flask cultures of *S. cerevisiae* were grown at 30 °C in 500-mL round-bottom flasks containing 100 mL medium, placed in an Innova incubator (Eppendorf Nederland B.V., Nijmegen, The Netherlands) and shaken at 200 rpm. Anaerobic shake-flask cultures were grown in 50-mL round-bottom flasks containing 30 mL medium, incubated at 30 °C in a Bactron anaerobic chamber (Sheldon Manufacturing Inc., Cornelius, OR) under an atmosphere of 5% (v/v) H_2, 6% (v/v) CO_2 and 89% (v/v) N_2, on a IKA KS 260 basic shaker (Dijkstra Verenigde BV, Lelystad, The Netherlands) at 200 rpm (179).

Bioreactor cultivation

Anaerobic batch and chemostat cultures of *S. cerevisiae* strains were grown in 2-L bioreactors with a 1-L working volume (Applikon, Delft, The Netherlands), at 30 °C and at a stirrer speed of 800 rpm. Culture pH was maintained at 5.0 by automatic addition of 2 M KOH. Loss of water by evaporation was minimized by cooling of the off-gas to 4 °C in a condenser. Bioreactors were sparged with a 90:10 mixture of N_2 and CO_2 at a rate of 0.5 L min^{-1}. Cultures were grown on SM supplemented with glucose, at concentrations of 20 g L^{-1} for batch cultures, 25 g L^{-1} for chemostat cultures and 59 g L^{-1} for nitrogen-limited cultures (on modified SM, see above). Antifoam C (Sigma Aldrich) was added to bioreactor media at a concentration of 0.2 g L^{-1}. Oxygen diffusion into the bioreactors was minimized by the use of Norprene tubing and Viton O-rings (179). Frozen stock cultures (1-mL samples) were used to inoculate aerobic shake-flasks on SMD. After incubation for 8-12 h, these starting cultures were used to inoculate shake-flask pre-cultures, which, upon reaching an OD_{660} between 3 and 6, were used to inoculate bioreactor cultures at an initial OD_{660} of approximately 0.2.

Acetaldehyde determination

Analysis of acetaldehyde concentrations was based on a previously described protocol (103). A solution of 0.2 M 4-dinitrophenylhydrazine in phosphoric acid (DNPH; Sigma-Aldrich) was diluted in acetonitrile (VWR International, Louvain, Belgium) to obtain a solution of 0.9 g L^{-1} DNPH in acetonitrile. Sampling tubes containing 5.00 mL (exact volume determined by weighing) of the resulting derivatization solution were stored at -20 °C and placed in a cryostat at -40 °C at least one hour before sampling. For analyses of acetaldehyde concentration in culture liquid, 1 mL of complete broth (including biomass) was sampled directly into 5.00 mL of derivatization solution using a rapid-sampling set-up (180). After mixing on a Vortex Genie II (Scientific Industries inc., Bohemia, NY), the samples were incubated on a Nutating Mixer (VWR International) at 4 °C for 1-3 h. The weight was determined before and after sampling, to be able to determine the dilution factor. After centrifugation, the supernatant was

stored at -80 °C until analysis by HPLC. To measure acetaldehyde in bioreactor off-gas, the off-gas stream of a bioreactor was led through two bottles connected in series, each containing approximately 400 mL derivatization solution. The time period over which acetaldehyde was trapped and the exact volumes of the derivatization before and after were determined to enable corrections for evaporation. Samples from the two bottles were directly analysed by HPLC. Saturation of the derivatization solution in the first bottle was assessed by measuring the acetaldehyde-2,4-dinitrophenylhydrazine adduct (A-DNPH) in the second bottle. HPLC analysis was performed on a Waters WAT086344 silica-based reverse-phase C18 column operated at room temperature with a hydrophobic stationary phase, at a flow rate of 1 mL min^{-1}. The mobile phase was made increasingly hydrophobic by linearly changing its composition from 100% MilliQ water to 100% acetonitrile (VWR international) over a period of 20 min. A-DNPH (Sigma-Aldrich) was dissolved in acetonitrile to a standard solution of 50.9 mg L^{-1}, from which a calibration curve was prepared.

Analytical methods

Biomass dry weight measurements, analyses of metabolite concentrations and correction for ethanol evaporation from bioreactor cultures were performed as described previously (91). Metabolite concentrations in steady-state chemostat cultures were analysed after rapid quenching of the culture samples using cold steel beads (181). High concentration of CO_2 in the inlet gas hindered the accurate determination of carbon balances (77, 109). Therefore, balances of the degree of reduction of substrates and products were used to calculate electron recoveries (11). For organic compounds that only contain carbon, hydrogen and/or oxygen, degree of reduction (γ) represents the number of electrons released upon complete oxidation to CO_2, H_2O and or H^+. These oxidized compounds are assigned a γ of zero, which yields values of γ for H, C and O of 1, 4 and 2, respectively and for positive and negative charge of −1 and 1, respectively. To simplify construction of degree-of-reduction balances, the nitrogen source was assigned $\gamma = 0$ which, with NH_4^+ as nitrogen source, implied that $\gamma = 3$ for N. Calculations were based on an estimated composition and degree of reduction of yeast biomass (182).

Transcriptome analysis

For transcriptome analysis, culture samples containing 100 to 160 mg of cells were sampled directly into liquid nitrogen to prevent mRNA turnover (183). Within 2 weeks after sampling, samples were transferred to a mixture of phenol/chloroform and TEA buffer for long-term storage at -80 °C (184). Total RNA extraction was performed using a phenolic acid/chloroform method as described previously (185). Quality of the RNA was assessed by RNA screen tape using a Tapestation (Agilent

technologies, Santa Clara, CA). RNA concentration was determined with a Qubit (Thermo Fisher Scientific). Paired-end sequencing was performed on a Truseq Stranded mRNA 150-bp insert library using Illumina SBS technology (Macrogen, Amsterdam, The Netherlands). Sequencing reads were aligned to the CEN.PK113-7D genome using STAR (186). The expression was quantified by featureCounts (version 1.6.0) (187) and normalized to FPKM counts by applying the rpkm function from the edgeR package (188).

Flow cytometry

GFP fluorescence was detected by flow cytometry. After growth on SMD to an OD_{660} of between 2 and 4 in aerobic shake-flask cultures, cycloheximide (25 mg L^{-1}) was added to arrest protein synthesis and cells were suspended to $\sim 1.0 \cdot 10^6$ cells per mL of Isoton II Diluent (Beckman Coulter, Woerden, The Netherlands). At least 10,000 cells were analyzed for green fluorescence (FL-1, 530/30 nm BP filter) after excitation by a 488 nm laser on a BD-Accuri C6 flow cytometer (Becton Dickinson, Franklin Lakes, New Jersey). Cells of *S. cerevisiae* IME324 were used to optimize gating of non-fluorescent cells in experiments with strains IME678, IME681 and IME682. The raw data and applied gating can be found in the supplementary materials (available online).

Protein extraction and proteome analysis

For proteome analysis, 5 mg (dry weight) of cells were harvested from late-exponential-phase (OD_{660} between 8 and 10) anaerobic bioreactor batch cultures on SMD (20 g L^{-1} glucose), or from steady-state anaerobic chemostat cultures grown at 0.05 h^{-1}, 0.10 h^{-1} or 0.25 h^{-1}. Cells were washed once and then resuspended in 5.00 mL ice-cold 1% NaCl. After storage at −80 °C, the frozen samples were processed as described previously (77). All LC–MS/MS results were searched against the *S. cerevisiae* protein database (UniProt), to which the amino acid sequences of the heterologous enzymes (PRK, CbbM) were manually added.

Genome sequencing

Genomic DNA was isolated from yeast cultures grown on YPD medium with a blood & cell culture DNA kit with 100/G genomics-tips (Qiagen, Hilden, Germany) according to supplier's instructions. Short-read whole-genome sequencing was performed in-house or commercially (Macrogen, Amsterdam; GenomeScan, Leiden) on a 350-bp insert TruSeq PCR-free library using the MiSeq platform (Illumina, San Diego, CA). Genomic libraries were either prepared in-house with a Nextera DNA Flex Library Prep kit (Illumina, San Diego, CA) and sequenced using the MiSeq platform (Illumina, San Diego, CA), or a 350-bp insert TruSeq PCR-free library was prepared and

sequenced commercially using Illumina SBS technology (Macrogen; GenomeScan). Sequence reads were mapped against the CEN.PK113-7D genome, supplemented with an additional virtual contig encompassing the sequences of chromosomally integrated expression cassettes for non-native genes (p*DAN1-PRK*-t*CPS1*, p*ANB1-PRK*-t*CPS1*, p*DAN1-PRK-CLN2*$_{PEST}$-t*CPS1*, p*DAN1-PRK*-tag-t*CPS1* p*TDH3-cbbM*-t*CYC1*, p*TEF1-groEL*-t*ACT1*, and p*TPI1-groES*-tPGI1) and processed as described previously (139). The copy number of *cbbM* was estimated through comparison of the read depth of *cbbM* to the average read depth for all chromosomes.

Long-read sequencing was performed in-house using the MinION platform using R10.3 flow cells, for 48 hours (Oxford Nanopore Technologies, Oxford, UK). Genomic libraries were prepared using Oxford Nanopore Sequencing kit SQK-LSK109, according to manufacturer's instructions. Basecalling was performed using Guppy version 4.5.4 (Oxford Nanopore Technologies), ran with options --flowcell FLO-MIN111 and --kit SQK-LSK109. Resulting basecalled files were demultiplexed by applying Guppy_barcoder (Oxford Nanopore Technologies) with option--barcode_kits EXP-NBD104. The demultiplexed sample were assembled using canu version 2.0 (189).

Availability of data and materials

Short read DNA sequencing data of the *S. cerevisiae* strains IMX2288, IMX2593, IMX2701 and IMX2736 and long read DNA sequencing data of the *S. cerevisiae* strains IMX1489 and IMX2608 were deposited at NCBI under BioProject accession number PRJNA906461. Transcriptomics datasets of IMX1489 and IME324 of anaerobic steady state C-limited chemostat cultures at 0.05 h^{-1}, 0.1 h^{-1} and 0.25 h^{-1} and N-limited chemostat cultures at 0.1 h^{-1} were uploaded to GEO under accession number GSE221392. All measurement data used to prepare Figure 2, Figure 3, Figure 4, Figure 5, Table 1, Table 2 and Table 3 of the manuscript are available in Additional file 1, Additional file 2, Additional file 3, Additional file 4 and Additional file 5, which are accessible online via https://doi.org/10.1186/s13068-023-02329-9.

Funding

This work was supported by DSM Bio-based Products & Services B.V. (Delft, The Netherlands).

Acknowledgements

We thank Rosalie Wouters for the discussions about dynamic regulation of *PRK*. We thank Rinke van Tatenhove-Pel for her help with analysis of the flow cytometer data. We thank Pilar de la Torres for her help with RNA extraction and Marcel van den Broek for his help with analysis of the DNA and RNA sequencing data. We thank Erik de Hulster for his help with the acetaldehyde trapping and Marijke Luttik for her help with the subsequent HPLC analysis.

Supplementary information

Additional supplementary information

Available online via: https://doi.org/10.1186/s13068-023-02329-9.

Table S2: DNA sequences and predicted amino acid sequences of *CLN2$_{PEST}$* and frameshifted *CLN2$_{PEST}$* (19aa). The DNA sequence of the serendipity tag is underlined in both DNA sequences.

		Sequence 5'→ 3'
CLN2$_{PEST}$	*DNA sequence*	GCATCCAACTTGAACATTTCGAGAAAGCTTACCATATCAACCCCA TCATGCTCTTTCGAAAATTCAAATAGCACATCCATTCCTTCGCCC GCTTCCTCATCTCAAAGCCACACTCCAATGAGAAACATGAGCTCA CTCTCTGATAACAGCGTTTTCAGCCGGAATATGGAACAATCATCA CCAATCACTCCAAGTATGTACCAATTTGGTCAGCAGCAGTCAAAC AGTATATGTGGTAGCACCGTTAGTGTGAATAGTCTGGTGAATAC AAATAACAAACAAAGGATCTACGAACAAATCACGGGTCCTAACA GCAATAACGCAACCAATGATTATATTGATTTGCTAAACCTAAAT GAGTCTAACAAGGAAAACCAAAATCCCGCAACGGCGCATTACCTC AATGGGGGCCCACCCAAGACAAGCTTCATTAACCATGGAATGTTC CCCTCGCCAACTGGGACCATAAATAGCGGTAAATCTAGCAGTGCC TCATCTTTAATTTCTTTTGGTATGGGCAATACCCAAGTAATATAG
	Protein sequence	ASNLNISRKLTISTPSCSFENSNSTSIPSPASSSQSHTPMRNMSSLSD NSVFSRNMEQSSPITPSMYQFGQQQSNSICGSTVSVNSLVNTNNK QRIYEQITGPNSNNATNDYIDLLNLNESNKENQNPATAHYLNGGP PKTSFINHGMFPSPTGTINSGKSSSASSLISFGMGNTQVI
19aa	*DNA sequence*	GAACATTTCGAGAAAGCTTACCATATCAACCCCATCATGCTCTTT CGAAAATTCAAATAG
	Protein sequence	EHFEKAYHINPIMLFRKFK

Table S3: Frequency of the triplets encoding the 19 amino acid C-terminal extension of PRK in the yeast genome. Information on triplet frequency in the *S. cerevisiae* genome was derived from https://www.genscript.com/tools/codon-frequency-table.

Triplet	Amino acid	Frequency of triplet ‰	Number of triplets for amino acid	Frequency rank	Frequency synonymous triplet(s) ‰	% of frequency most abundant synonomous triplet
GAA	E	45.9	2	1	19.1	100
CAT	H	13.7	2	1	7.8	100
TTC	F	18.2	2	2	26.1	69.7
GAG	E	19.1	2	2	45.9	41.6
AAA	K	42.2	2	1	30.8	100
GCT	A	21.1	4	1	16.2, 12.5, 6.1	100
TAC	Y	14.7	2	2	18.8	78.2
CAT	H	13.7	2	1	7.8	100
ATC	I	17.1	3	3	30.2, 17.8	56.6
AAC	N	24.9	2	2	36.0	69.1
CCC	P	6.8	4	3	18.2, 13.6, 5.2	37.4
ATC	I	17.1	3	3	30.2, 17.8	56.6
ATG	M	20.9	1	1	-	100
CTC	L	5.4	4	4	13.4, 12.2, 10.4	40.2
TTT	F	26.1	2	1	18.2	100
CGA	R	3.0	4	3	6.5, 2.6, 1.7	46.2
AAA	K	42.2	2	1	30.8	100
TTC	F	18.2	2	2	26.1	69.7
AAA	K	42.2	2	1	30.8	100

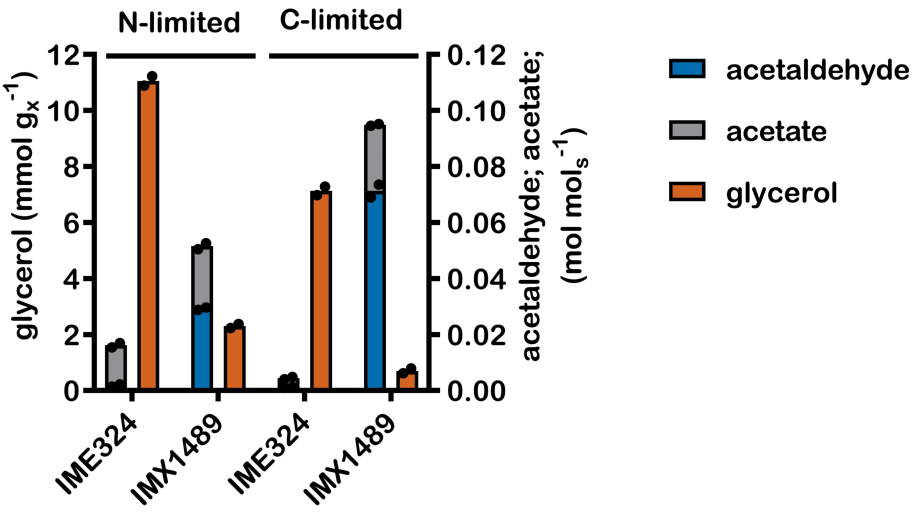

Figure S1: Yields of acetaldehyde and acetate on glucose and stoichiometric relationships between glycerol production and biomass formation in anaerobic nitrogen-limited and glucose-limited chemostat cultures of *S. cerevisiae* strains IME324 (reference strain lacking PRK-RuBisCO bypass) and IMX1489 (Δ*gpd2* non-ox PPP↑ p*DAN1-PRK* 15x *cbbM GroES/GroEL*), at a dilution rate of 0.1 h^{-1}. Values represent means and individual values of measurements on independent steady-state duplicate cultures. Non-ox PPP↑ indicates the integration of the expression cassettes of p*TDH3-RPE1*, p*PGK1-TKL1*, p*TEF1-TAL1*, p*PGI1-NQM1*, p*TPI1-RKI1* and p*PYK1-TKL2*.

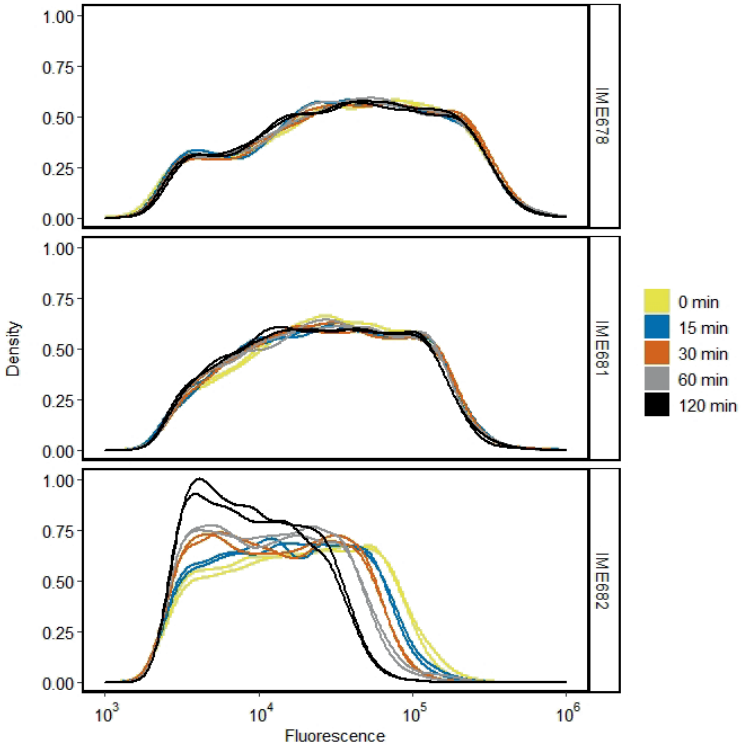

Figure S2: Fluorescence intensity plots of exponentially growing aerobic shake-flask cultures of *S. cerevisiae* strains IME678 (*egfp*), IME681 (*egfp*-19aa) and IME682 (*egfp-CLN2*$_{PEST}$) on SMD (pH=6), measured over time after the addition of cycloheximide. Data used in this plot were obtained by gating the raw flow-cytometry data as shown Supplemental Information S1 (Additional file 7; available online).

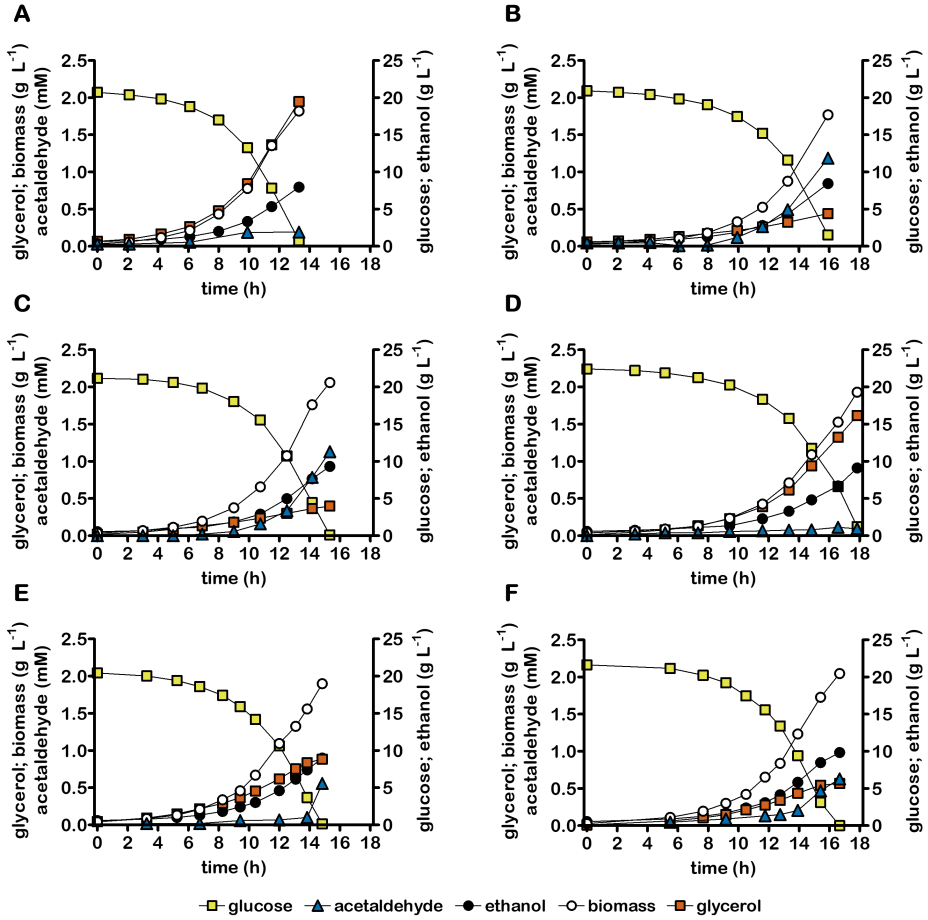

Figure S3: Growth, glucose consumption, ethanol formation, acetaldehyde formation and glycerol formation in anaerobic bioreactor batch cultures of *S. cerevisiae* strains IME324 (reference strain) (A), IMX1489 (*Δgpd2* non-ox PPP↑ p*DAN1-PRK* 15x *cbbM GroES/GroEL*)(B), IMX2736 (*Δgpd2* non-ox PPP↑ p*DAN1-PRK* 2x *cbbM GroES/GroEL*)(C), IMX2701 (*Δgpd2* non-ox PPP↑ p*DAN1-PRK-CLN2*$_{PEST}$ 2x *cbbM GroES/GroEL*)(D), IMX2593 (*Δgpd2* non-ox PPP↑ p*DAN1*-prk-19aa 2x *cbbM GroES/GroE*L)(E) and IMX2608 (*Δgpd2* non-ox PPP↑ p*ANB1-PRK* 2x *cbbM GroES/GroEL*)(F). Cultures were grown anaerobically at pH 5 and at 30 °C on synthetic medium containing 20 g L^{-1} glucose. Non-ox PPP↑ indicates the integration of the expression cassettes of p*TDH3-RPE1*, p*PGK1-TKL1*, p*TEF1-TAL1*, p*PGI1-NQM1*, p*TPI1-RKI1* and p*PYK1-TKL2*. Representative cultures of independent duplicate experiments are shown, corresponding replicate of each culture shown in Fig. 3.

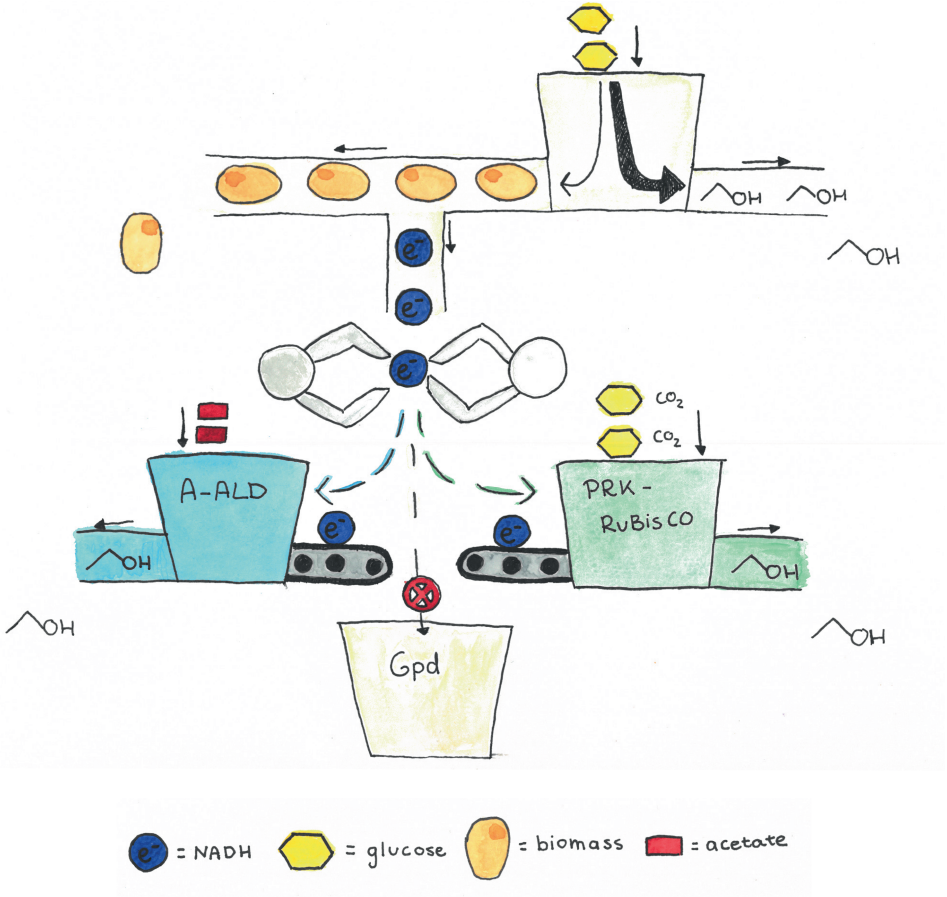
OH
OH
OH
e⁻
e⁻
e⁻
CO_2
CO_2
A-ALD
PRK -
RuBisCO
e⁻
e⁻
OH
OH
OH
OH
Gpd
= NADH
= glucose
= biomass
= acetate

Chapter 3

Optimizing the balance between heterologous acetate- and CO_2-reduction pathways in anaerobic cultures of *Saccharomyces cerevisiae* strains engineered for low glycerol production

Aafke C.A. van Aalst, Ellen H. Geraats, Mickel L.A. Jansen, Robert Mans, and Jack T. Pronk

This chapter is essentially as published on bioRxiv (2023), 05: 21.541164.

Abstract

In anaerobic *Saccharomyces cerevisiae* cultures, NADH-cofactor balancing by glycerol formation constrains ethanol yields. Introduction of an acetate-to-ethanol reduction pathway based on heterologous acetylating acetaldehyde dehydrogenase (A-ALD) can replace glycerol formation as 'redox-sink' and improve ethanol yields in acetate-containing media. Acetate concentrations in feedstock for first-generation bioethanol production are, however, insufficient to completely replace glycerol formation. An alternative glycerol reduction strategy bypasses the oxidative reaction in glycolysis by introducing phosphoribulokinase (PRK) and ribulose-1,5-bisphosphate carboxylase/oxygenase (RuBisCO). For optimal performance in industrial settings, yeast strains should ideally first fully convert acetate and, subsequently, continue low-glycerol fermentation via the PRK-RuBisCO pathway. However, anaerobic batch cultures of a strain carrying both pathways showed inferior acetate reduction relative to a strain carrying only the A-ALD pathway. Complete A-ALD-mediated acetate reduction by a dual-pathway strain, grown anaerobically on 50 g L^{-1} glucose and 5 mmol L^{-1} acetate, was achieved upon reducing PRK abundance by a C-terminal extension of its amino acid sequence. Yields of glycerol and ethanol on glucose were 55% lower and 6% higher, respectively, than those of a non-engineered reference strain. The negative impact of the PRK-RuBisCO pathway on acetate reduction was attributed to sensitivity of the reversible A-ALD reaction to intracellular acetaldehyde concentrations.

Background

Ethanol, predominantly produced by yeast-based fermentation of renewable carbohydrate feedstocks, can serve as a renewable automotive fuel and as precursor for a range of other products, including ethylene and jet fuel (2, 3). In industrial ethanol production, the sugar feedstock can account for up to 70% of the overall process costs (7). Maximizing the yield of ethanol on sugar is therefore of paramount importance for process economics. The current global fermentative production of ca. 100 Mton ethanol y^{-1} (1) almost exclusively relies on the yeast *Saccharomyces cerevisiae*. Ethanol yields in yeast-based industrial processes can reach up to 92% of the theoretical maximum (190), with loss of substrate carbon primarily due to formation of yeast biomass and glycerol (85).

In anaerobic cultures of wild-type *S. cerevisiae*, glycerol formation via the NAD^+-dependent glycerol-3-phosphate dehydrogenases Gpd1 and Gpd2 is essential for re-oxidation of 'surplus' NADH formed in biosynthetic processes (14, 15). Multiple strategies have been explored to alter the metabolic network of *S. cerevisiae* to reduce NADH formation in biosynthetic reactions and/or rearrange yeast carbon metabolism to couple NADH re-oxidation to the formation of ethanol instead of glycerol (reviewed in (132)). Some of the latter engineering strategies can completely replace glycerol formation in anaerobic laboratory cultures. However, because of the importance of glycerol in yeast osmotolerance (76), application-oriented engineering strategies typically aim at a strong reduction of glycerol formation rather than at its complete elimination (132).

Introduction of a heterologous acetylating acetaldehyde dehydrogenase (A-ALD) into *S. cerevisiae* enables the NADH-dependent reduction of acetyl-CoA to acetaldehyde, which can subsequently be reduced to ethanol by the native yeast alcohol dehydrogenase (91). Coupling this reaction to heterologous pathways involving either phosphoketolase and phosphotransacetylase (106) or pyruvate-formate lyase (101, 102) can couple a net oxidation of NADH to the conversion of glucose to ethanol. Alternatively, in acetate-containing media, A-ALD-synthesizing yeast strains can use exogenous acetate, which can be activated to acetyl-CoA by native yeast acetyl-CoA synthetase. Introduction of the *Escherichia coli* A-ALD *eutE* in *S. cerevisiae*, combined with deletion of *GPD2*, led to a 5-fold lower ratio between glycerol and biomass formation in anaerobic, acetate-supplemented cultures than in the non-engineered parental strain, without affecting specific growth rate (93). However, the combined activity of native acetyl-CoA synthetase (Acs2,(92)), acetaldehyde dehydrogenases (Ald6, Ald5 and Ald4 (138)) and A-ALD can theoretically form an ATP-hydrolysing

reaction cycle (95). Additional deletion of *ALD6* is therefore often applied in A-ALD-based redox-cofactor engineering strategies (93, 95, 191).

Development of metabolic engineering strategies aimed at reduction of exogenous acetate to ethanol is predominantly inspired by industrial fermentation of lignocellulosic hydrolysates, in which acetate concentrations can exceed 5 g L^{-1} (192) and negatively affect yeast fermentation (27, 193). In first-generation feedstocks such as corn mash, acetate concentrations of up to 1.2 g L^{-1} are reported (37, 100, 194), while glucose concentrations in industrial fermentation processes can reach 300 g L^{-1} (152, 195). During such fermentations, 12-15 g L^{-1} of glycerol is produced (19, 196). To replace the redox-cofactor-balancing role of this amount of glycerol, approximately 4 g L^{-1} of acetate would be required. First-generation feedstocks for ethanol production therefore typically do not contain enough acetate to replace all the glycerol produced.

Ideally, an engineered yeast strain for first-generation processes should reduce all available acetate to ethanol and, after acetate depletion, continue fast anaerobic growth with a low glycerol yield by using another engineered, acetate-independent redox-balancing pathway. An engineered pathway meeting this description is based on bypassing the oxidative reaction in glycolysis by introducing the Calvin-cycle enzymes phosphoribulokinase (PRK) and ribulose-1,5-bisphosphate carboxylase/oxygenase (RuBisCO) (77, 109). Performance of this pathway as a redox-cofactor balancing pathway in yeast was improved by overexpression of structural genes for enzymes of the non-oxidative pentose-phosphate pathway (non-ox PPP↑; p*TDH3-RPE1*, p*PGK1-TKL1*, p*TEF1-TAL1*, p*PGI1-NQM1*, p*TPI1-RKI1* and p*PYK1-TKL2*) and deletion of *GPD2* (77). In addition, multiple copies of an expression cassette for bacterial *cbbM* RuBisCO were integrated in the yeast genome to improve conversion of ribulose-5-bisphosphate into 3-phosphoglycerate (77). While, initially, up to 15 copies of the *cbbM* cassette were integrated (77), a later study indicated that 2 copies were sufficient (197). Expression of a spinach *PRK* gene from the anaerobically inducible *DAN1* promoter limited toxic effects of PRK during aerobic pre-cultivation (77). The resulting PRK-RuBisCO-synthesizing *S. cerevisiae* strain (IMX2736; Δ*gpd2*, non-ox PPP↑, p*DAN1-PRK*, 2x *cbbM*, *GroES/GroEL*) showed essentially the same maximum growth rate on glucose as a non-engineered reference strain in anaerobic batch bioreactors while exhibiting a 96% lower glycerol yield and a 10% higher ethanol yield on glucose than the reference strain (197).

The A-ALD and PRK-RuBisCO-based strategies have both been shown to re-oxidize surplus NADH in anaerobic yeast cultures (77, 93) and, in particular in Δ*gpd2* genetic

backgrounds, to efficiently compete for NADH with the native glycerol pathway. However, interaction of these two strategies upon their implementation of a single yeast strain has not yet been investigated. The goal of the present study is therefore to study growth and product formation in acetate-containing media of dual-pathway *S. cerevisiae* strains that express both the A-ALD pathway and the PRK-RuBisCO pathway. To this end, engineered strains were grown in anaerobic bioreactor cultures on glucose, using media in which acetate concentrations were either sufficient or insufficient to complete re-oxidation of surplus NADH by acetate reduction. Based on observed patterns of growth and (by)product formation, further engineering was aimed at improving acetate reduction via A-ALD in PRK-RuBisCO-synthesizing strains.

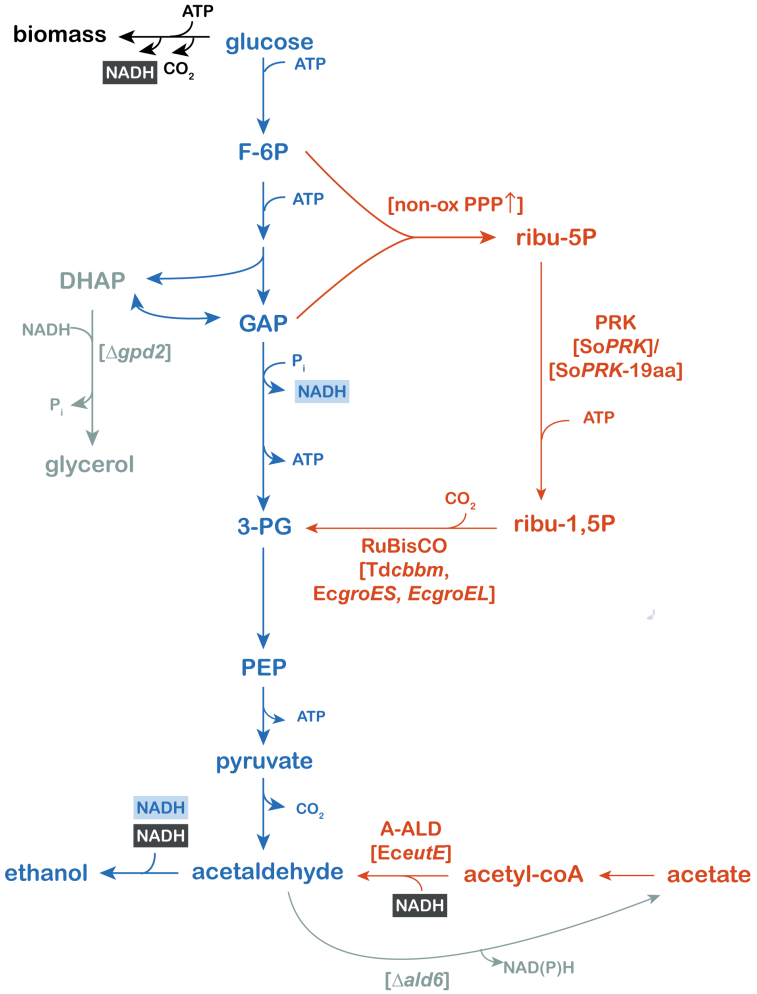

Figure 1: Simplified schematic representation of ethanol and biomass formation from glucose and acetate by an engineered strain of *Saccharomyces cerevisiae* via heterologous expression of genes encoding the enzymes phosphoribulokinase (PRK), ribulose-1,5-bisphosphate carboxylase/oxygenase (RuBisCO) and acetylating acetaldehyde dehydrogenase (A-ALD). Genetic modifications are indicated between square brackets. Blue: native reactions of the redox-neutral conversion of glucose to ethanol via glycolysis and alcoholic fermentation. Black: biosynthetic reactions with a net input of ATP and a net production of CO_2 and NADH. Orange: heterologous reduction pathways for NADH recycling either via a non-oxidative bypass of glycolysis via PRK-RuBisCO or via acetyl-coA reduction via A-ALD using exogenous acetate. Grey: native pathways which are (partially) impaired by deletion of a key gene. Heterologous genes encode the following enzymes: Ec*eutE*, *E. coli* A-ALD; So*PRK*, *S. oleracea* PRK; Td*cbbM*, *T. denitrificans* RuBisCO; Ec*groEL* and Ec*groES*, *E. coli* GroEL and GroES. Abbreviations indicate the following metabolites: F-6P, fructose-6-phosphate; GAP, glyceraldehyde-3-P; DHAP, dihydroxyacetone phosphate, 3-PG, 3-phosphoglycerate; PEP, phosphoenolpyruvate; ribu-5P, ribuolose-5-phosphate; ribu-1,5P, ribulose-1,5-bisphosphate. 19aa indicates a 19 amino acid C-terminal extension (197). Non-ox PPP↑ indicates the overexpression of the native *RPE1*, *TKL1*, *TAL1*, *NQM1*, *RKI1* and *TKL2* from the non-oxidative pentose phosphate pathway.

Results

Suboptimal acetate conversion by a yeast strain harbouring both an A-ALD-based acetate-reduction and PRK-RuBisCO pathway

S. cerevisiae Δgpd2 strains expressing a bacterial gene encoding A-ALD can use exogenous acetate as electron acceptor for anaerobic re-oxidation of 'surplus' NADH generated in biosynthesis (15). Consistent with earlier reports (93), *S. cerevisiae* IMX2503 (*Δald6 Δgpd2 eutE*) produced 76% less glycerol per amount of biomass formed than the reference strain IME324 (*ALD6 GPD2*) when grown in anaerobic bioreactor batch cultures on 20 g L^{-1} glucose and 50 mmol L^{-1} acetate (Table 1, Fig. 2A and 2B). This acetate concentration was approximately 5-fold higher than what was calculated to be required for complete re-oxidation of surplus NADH via A-ALD-mediated acetate reduction (91, 132). Specific growth rates of the two strains were not significantly different, but strain IMX2503 showed a 6.7% higher ethanol yield on glucose than the reference strain. Slow, EutE-independent consumption of acetate by the reference strain (Table 1) was previously attributed to the use of acetate-derived acetyl-CoA as a biosynthetic precursor (198).

S. cerevisiae IMX2502 (*Δgpd2 Δald6 eutE* non-ox PPP↑ *PRK* 2x *cbbM groES/groEL*) combined the genetic modifications in the acetate-reducing strain IMX2503 with introduction of a non-oxidative bypass of glycolysis via phosphoribulokinase (PRK) and ribulose-1,5-bisphosphate carboxylase/oxygenase (RuBisCO, CbbM) (197). Under the conditions described above, this strain showed an even lower rate of acetate consumption than the reference strain IME324 (Table 1). Apparently, simultaneous presence of the two engineered pathways prevented efficient acetate reduction via EutE. However, strain IMX2502 produced 79% less glycerol per amount of biomass than the reference strain IME324, indicating that the PRK-RuBisCO bypass actively contributed to re-oxidation of surplus NADH.

Despite its low glycerol formation, strain IMX2502 displayed a mere 4% higher ethanol yield than the reference strain IME324 and a slightly lower ethanol yield than the acetate-reducing strain IMX2503 (Table 1). This increase is approximately 55% lower than theoretically predicted (132) and reported (197) for anaerobic glucose-grown cultures of a congenic 'PRK-RuBisCO-only' strain. This lower-than-anticipated ethanol yield of strain IMX2502 coincided with production of up to 2.7 ± 0.1 mmol L^{-1} acetaldehyde, a byproduct that was not detected in cultures of the acetate-reducing strain IMX2503 and the reference strain IME324 (Table 1). Formation of acetaldehyde and acetate by slow-growing cultures of PRK-RuBisCO-based *S. cerevisiae* strains was previously attributed to an *in vivo* overcapacity of the non-oxidative bypass of glycolysis (197). The acetaldehyde yield on glucose of strain IMX2502 was 3.6-fold

higher than previously reported for anaerobic glucose-grown batch cultures of a congenic PRK-RuBisCO-strain (0.007 ± 0.001 mol acetaldehyde (mol glucose)$^{-1}$, (197)).

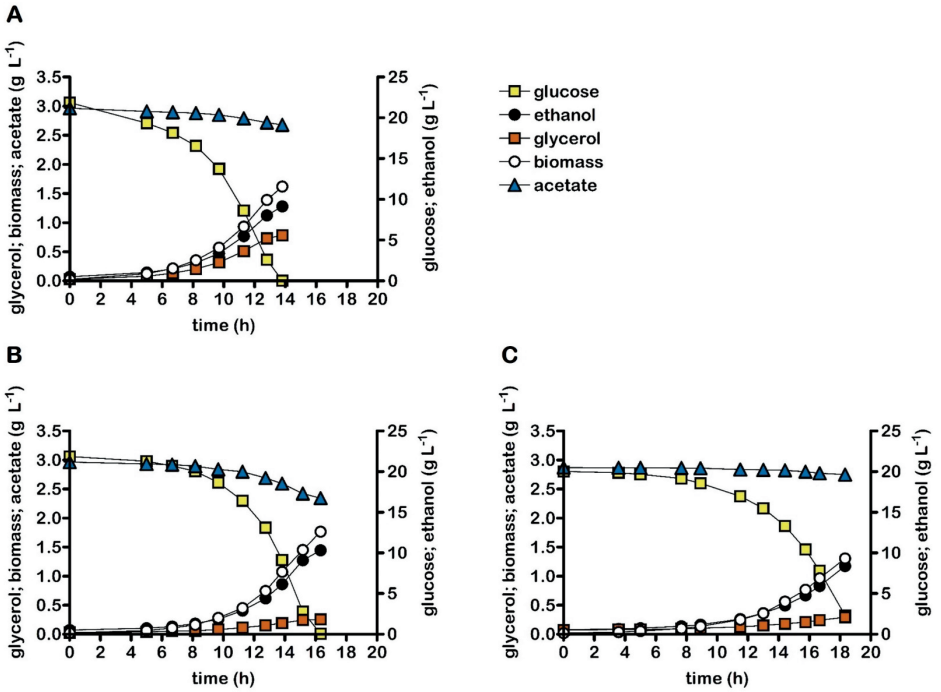

Figure 2: Concentrations of biomass, ethanol, glycerol and acetate in anaerobic bioreactor batch cultures of *S. cerevisiae* strains IME324 (reference strain, A), IMX2503 (*Δgpd2 Δald6* p*TDH3-eutE*, B), IMX2502 (non-ox PPP↑ *Δgpd2 Δald6* p*TDH3-eutE* p*DAN1-PRK* 2x p*TDH3-cbbM* p*TPI1-groES* p*TEF1-groEL*, C). Cultures were grown anaerobically at pH 5.0 and at 30 °C on synthetic medium containing 20 g L^{-1} glucose and 50 mmol L^{-1} acetate. Non-ox PPP↑ indicates the integration of the expression cassettes of p*TDH3-RPE1*, p*PGK1-TKL1*, p*TEF1-TAL1*, p*PGI1-NQM1*, p*TPI1-RKI1* and p*PYK1-TKL2*. Representative cultures of independent duplicate experiments are shown, corresponding replicate of each culture shown in Fig. S2.

Table 1: Specific growth rate, stochiometries of biomass and (by)product formation and biomass-specific acetate consumption rates in anaerobic bioreactor batch cultures of *S. cerevisiae* strains IME324 (reference strain), IMX2503 (*Δgpd2 Δald6* p*TDH3-eutE*) and IMX2502 (non-ox PPP↑ *Δgpd2 Δald6* p*TDH3-eutE* p*DAN1-PRK* 2x p*TDH3-cbbM* p*TPI1-groES pTEF1-groEL*). Cultures were grown on synthetic medium with 20 g L^{-1} glucose and 50 mmol L^{-1} acetate at pH 5 and at 30 °C and sparged with a 90:10 mixture of N_2 and CO_2. Stoichiometries of biomass and metabolite production formation were calculated from at least 6 sampling points in the exponential growth phase, while biomass yield was determined based on biomass and glucose determinations at the first and last time point. Values represent averages ± mean deviations of measurements on independent duplicate cultures. Since the high concentration of CO_2 in the inlet gas precluded construction of carbon balances, degree-of-reduction balances were used to verify data consistency (11). Non-ox PPP↑ indicates the integration of the expression cassettes of p*TDH3-RPE1*, p*PGK1-TKL1*, p*TEF1-TAL1*, p*PGI1-NQM1*, p*TPI1-RKI1* and p*PYK1-TKL2*. Symbols: μ, specific growth rate; g_x, gram biomass; Y, yield; $q_{acetate}$: biomass-specific rate of acetate consumption in exponential growth phase.

Strain Relevant genotype	**IME324** reference	**IMX2503** *gpd2Δ ald6Δ eutE*	**IMX2502** *gpd2Δ ald6Δ eutE PRK 2x cbbM*
μ (h^{-1})	0.31 ± 0.00	0.32 ± 0.00	0.25 ± 0.01
$Y_{biomass/glucose}$ (g_x g^{-1})	0.071 ± 0.003	0.081 ± 0.001	0.072 ± 0.001
$Y_{ethanol/glucose}$ (mol mol^{-1})	1.65 ± 0.02	1.76 ± 0.01	1.71 ± 0.00
$Y_{acetaldehyde/glucose}$ (mol mol^{-1})	<0.005	<0.005	0.026 ± 0.001
$Y_{glycerol/glucose}$ (mol mol^{-1})	0.117 ± 0.000	0.033 ± 0.000	0.024 ± 0.002
$Y_{acetate/glucose}$ (mol mol^{-1})	-0.032 ± 0.004	-0.084 ± 0.002	-0.023 ± 0.001
Glycerol production (mmol g_x^{-1})	8.5 ± 0.1	2.1 ± 0.1	1.8 ± 0.1
Acetate consumption (mmol g_x^{-1})	2.3 ± 0.3	5.7 ± 0.3	1.7 ± 0.1
$q_{acetate}$ (mmol g_x^{-1} h^{-1})	-0.7 ± 0.0	-1.8 ± 0.1	-0.4 ± 0.0
Electron recoveries (%)	99-101	99-100	100-101

Performance of engineered strains at low acetate-to-glucose ratios

To explore performance of engineered strains at acetate-to-glucose ratios that are more representative for those in first-generation feedstocks such as corn mash, anaerobic bioreactor batch cultures were grown on 50 g L^{-1} glucose and 5 mmol L^{-1} acetate (Fig. 3, Table 2). Biomass and ethanol yields on glucose of the reference strain IME324 in these cultures were 32% higher and 10% lower, respectively, than in cultures grown at the higher acetate-to-glucose ratio (Tables 1 and 2). These results are in line with a higher maintenance-energy requirement in cultures grown at 50 mmol L^{-1} acetate, caused by weak-acid uncoupling of the plasma-membrane pH gradient (31).

Expressed per amount of formed biomass, acetate consumption by strain IME324 was ca. 10-fold lower than in cultures grown at the higher acetate-to-glucose ratio (Tables 1 and 2, respectively) and over two-thirds of the added 5 mmol L^{-1} acetate remained unused (Fig. 3A). In contrast, cultures of strain IMX2503 (*Δald6 Δgpd2 eutE*) completely consumed acetate under these conditions (Fig. 3B). However, strain

IMX2503 showed a mere 12% lower overall glycerol production per amount of biomass formed than the reference strain IME324 (Table 2), as compared to a 76% lower value in cultures grown at a high acetate-to-glucose ratio (Table 1). Consistent with the small difference in glycerol yield, ethanol yields on glucose of the two strains measured in cultures grown at the low acetate-to-glucose ratio were not significantly different. These results are consistent with the dynamics of acetate consumption in the low-acetate cultures of strain IMX2503, which showed a progressive decrease of the biomass-specific rate of acetate consumption during the first phase of batch cultivation (Additional file 3, supplementary Fig. S1). This may reflect the high K_m (ca. 8.8 mM) of Acs2, the sole acetyl-coenzyme A synthetase isozyme synthesized in anaerobic batch cultures of *S. cerevisiae* (92). The decreasing biomass-specific rate of acetate conversion of strain IMX2503 forced a progressively larger fraction of surplus NADH to be reoxidized via Gpd1-dependent glycerol formation. When, after only approximately half of the glucose had been consumed, acetate was depleted (Fig. 3B), this requirement became absolute and, as in wild-type *S. cerevisiae* (19), further anaerobic growth became strictly coupled to glycerol production.

In cultures of the dual-pathway-strain IMX2502 (*Δgpd2 Δald6 eutE* non-ox PPP↑ *PRK* 2x *cbbM groES/groEL*) grown at a low acetate-to-glucose ratio, glycerol production per amount of biomass was 65% and 49% lower, respectively, than in corresponding cultures of the reference strain IME324 and the acetate-reducing strain IMX2503 (Table 2). However, acetate consumption expressed per amount of biomass formed by strain IMX2502 was 2.6-fold lower than in cultures of strain IMX2503 (Table 2) and, upon glucose depletion, not all acetate had been consumed (Fig. 3C). A 6 to 7% gap in the degree-of-reduction balance for low-acetate cultures of the dual-pathway-strain IMX2502 (Table 2) probably suggested that, as observed for cultures of this strain grown at a high acetate-to-glucose ratio (Table 1), acetaldehyde was formed as a byproduct. This interpretation was also consistent with an only slightly (2%) higher ethanol yield on glucose and a 14% lower biomass yield relative to the reference strain IME324 (Table 2).

Table 2: Stoichiometries of biomass and (by)product formation and biomass, ethanol, glycerol and acetate yield on glucose of anaerobic bioreactor batch cultures of *S. cerevisiae* strains IME324 (reference strain), IMX2503 (*Δgpd2 Δald6* p*TDH3-eutE*), IMX2502 (non-ox PPP↑ *Δgpd2 Δald6* p*TDH3-eutE* p*DAN1-PRK* 2x p*TDH3-cbbM* p*TPI1-groES pTEF1-groEL*) and IMX2723 (non-ox PPP↑ *Δgpd2 Δald6* p*TDH3-eutE* p*DAN1-PRK*-19aa 2x p*TDH3-cbbM* p*TPI1-groES pTEF1-groEL*). Cultures were grown on synthetic medium with 50 g L^{-1} of glucose and 5.0 mmol L^{-1} acetate at pH 5 and at 30 °C and sparged with a 90:10 mixture of N_2 and CO_2. Stoichiometries of biomass and metabolite production were calculated using the first two and last two sampling points, and the stoichiometry of biomass and acetate consumption was calculated using sample points before acetate depletion. Since the high concentration of CO_2 in the inlet gas precluded construction of accurate carbon balances, degree-of-reduction balances were used to verify data consistency (11). Symbols: x, biomass; Y, yield. Values represent averages ± mean deviations of measurements on independent duplicate cultures.

Strain Relevant genotype	**IME324** Reference	**IMX2503** *Δgpd2 Δald6 eutE*	**IMX2502** *Δgpd2 Δald6 eutE PRK* 2x *cbbM*	**IMX2723** *Δgpd2 Δald6 eutE PRK*-19aa (197) 2x *cbbM*
$Y_{biomass/glucose}$ (g_x g^{-1})	0.084 ± 0.000	0.083 ± 0.000	0.073 ± 0.001	0.087 ± 0.001
$Y_{ethanol/glucose}$ (mol mol $^{-1}$)	1.55 ± 0.01	1.58 ± 0.00	1.59 ± 0.02	1.64 ± 0.02
$Y_{glycerol/glucose}$ (mol mol $^{-1}$)	0.150 ± 0.000	0.125 ± 0.000	0.053 ± 0.000	0.070 ± 0.002
$Y_{acetate/glucose}$ (mol mol^{-1})	-0.004 ± 0.000	-0.067 ± 0.002	-0.021 ± 0.002	-0.053 ± 0.009
Glycerol production (mmol g_x^{-1})	9.9 ± 0.0	8.2 ± 0.0	4.3 ± 0.1	4.5 ± 0.1
Acetate consumption (mmol g_x^{-1})	0.2 ± 0.0	3.5 ± 0.2	1.4 ± 0.2	2.5 ± 0.0
Electron recovery	99-99	99-99	94-94	99-99

Tuning the PRK-RuBisCO pathway for improved acetate conversion in an A-ALD-based acetate-reducing yeast strain

The results presented above show that, at both high and low acetate-to-glucose ratios, presence of a functional PRK-RuBisCO pathway in an A-ALD-based acetate-reducing *S. cerevisiae* strain impeded *in vivo* acetate reduction. We recently reported that a 19 amino acid C-terminal extension ('19aa') of the heterologous PRK protein reduced its abundance in engineered yeast strains. This modification was shown to mitigate an overcapacity of the PRK-RuBisCO pathway that led to formation of acetaldehyde and acetate in slow-growing cultures (197). To investigate whether this modification could also affect interference of the PRK-RuBisCO pathway with the A-ALD-mediated reduction of exogenous acetate, strain IMX2723 (*Δgpd2 Δald6 eutE* non-ox PPP↑ p*DAN1-PRK*-19aa *cbbM groES/groEL*) was grown in anaerobic batch cultures on 50 g L^{-1} glucose and 50 mmol L^{-1} acetate. In contrast to strain IMX2502, in which the PRK protein did not carry the C-terminal extension, strain IMX2723 consumed all acetate added to the medium and did not show a gap in degree-of-reduction balances or reduced biomass yield (Fig. 3D, Table 2). In addition, it showed a lower glycerol yield

than the acetate-reducing strain IMX2503 and, relative to the reference strain IME324, it showed a 6% higher ethanol yield on glucose.

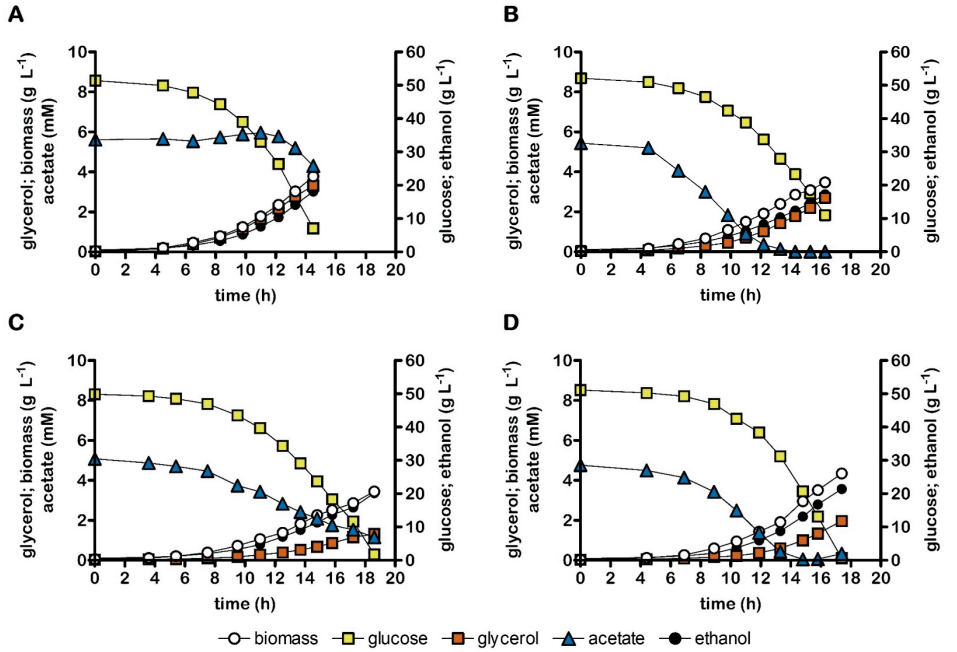

Figure 3: Concentrations of biomass, ethanol, glycerol and acetate in anaerobic bioreactor batch cultures of *S. cerevisiae* strains IME324 (reference strain, A), IMX2503 (*Δgpd2 Δald6* p*TDH3-eutE*, B), IMX2502 (non-ox PPP↑ *Δgpd2 Δald6* p*TDH3-eutE* p*DAN1-PRK* 2x p*TDH3-cbbM* p*TPI1-groES* p*TEF1-groEL*, C), and IMX2723 (non-ox PPP↑ *Δgpd2 Δald6* p*TDH3-eutE* p*DAN1-PRK*-19aa (197) 2x p*TDH3-cbbM* p*TPI1-groES pTEF1-groEL*, D). Cultures were grown anaerobically at pH 5.0 and at 30 °C on synthetic medium containing 50 g L^{-1} glucose and 5.0 mmol L^{-1} acetate. Representative cultures of independent duplicate experiments are shown, corresponding replicate of each culture shown in Fig. S3.

Discussion

Previous studies demonstrated that, in *Δgpd2* genetic backgrounds, the A-ALD-based acetate-reduction pathway and the PRK-RuBisCO pathway can each efficiently compete for NADH with the remaining glycerol production pathway and, thereby, enable improved ethanol yields in anaerobic *S. cerevisiae* cultures (77, 93). Here, introduction of both pathways in a single *S. cerevisiae* strain was shown to strongly impede *in vivo* activity of acetate reduction via the A-ALD pathway. In addition, anaerobic batch cultures of the dual-pathway strain produced high levels of acetaldehyde, a byproduct that was previously found in slow-growing cultures of strains carrying the PRK-RuBisCO pathway (197).

Acetaldehyde produced by the PRK-RuBisCO pathway might influence *in vivo* activity of the reversible A-ALD reaction ($\Delta G^{0'}$ = 17.6 kJ mol^{-1} for the reductive reaction (199). Its reactants NADH/NAD^+ and acetyl-CoA/CoA are conserved moieties, whose concentration ratios are likely to be constrained by their involvement in a large number of metabolic reactions. An estimate of the maximum permissive acetaldehyde concentration for acetyl-CoA reduction ($\Delta G_R' = 0$), based on reported NADH:NAD^+ and acetyl-CoA:CoA ratios in glucose-grown yeast cultures (Additional file 3), yielded a value of 0.35 mmol L^{-1} acetaldehyde. Assuming that acetaldehyde diffuses freely out of the yeast cell, the acetaldehyde concentration measured in the fermentation broth was assumed to be the same as the intracellular acetaldehyde concentration. Acetaldehyde concentrations in glucose-acetate grown anaerobic batch cultures of the dual pathway strain IMX2502 were an order of magnitude higher (1.0 to 2.8 mmol L^{-1}, Additional file 1) than this estimated value. In contrast, acetaldehyde concentrations in cultures of the 'single-pathway' acetate-reducing strain IMX2503 did not exceed 0.35 mmol L^{-1} (Additional file 1). This analysis supports the interpretation that the elevated acetaldehyde concentrations in cultures of the dual-pathway strain rendered a net reduction of acetyl-CoA to acetaldehyde by A-ALD thermodynamically impossible.

Acetaldehyde concentrations in anaerobic batch cultures of the dual-pathway strain IMX2502 exceeded those reported for anaerobic batch cultures of congenic 'PRK-RuBisCO-only' strains (197). This difference may be related to the deletion of *ALD6*, which encodes cytosolic $NADP^+$-dependent acetaldehyde dehydrogenase. *ALD6* was deleted in A-ALD-containing strains, including the dual pathway strain, to prevent a cytosolic ATP-dissipating futile cycle, consisting of A-ALD, Ald6 and the acetyl-CoA synthetase. This futile cycle was implicated in delayed growth of A-ALD-based strains in high-osmolarity media (95). In the dual-pathway context, eliminating a key enzyme for acetaldehyde conversion may be less desirable and further research is needed to investigate whether and how expression levels of *ALD6* affect acetaldehyde production by PRK-RuBisCO-based strains.

To simulate the low acetate-to-glucose ratios in first-generation feedstocks for industrial ethanol production, we used a medium containing 50 g L^{-1} glucose and 5 mmol L^{-1} acetate (corresponding to 0.3 g L^{-1} acetic acid). At this low initial concentration of acetate, the biomass-specific rate of acetate conversion by strain IMX2503 (*Δgpd2 Δald6 eutE*) declined as the acetate concentration decreased (Additional file 3, supplementary Fig. S1), which indicated a suboptimal affinity of this strain for acetate. While acetate concentrations in industrial media can be 3- to 4-fold higher (37, 100, 194), improvement of the kinetics of acetate reduction may be

required for fast and complete acetate conversion. This could for example be achieved via expression of acetyl-CoA synthetases with better affinity for acetate than the anaerobically expressed isoenzyme Acs2. A candidate protein could be the native Acs1, which is not synthesized under anaerobic conditions and has a 30-fold lower Km than Acs2 (0.32 and 8.8 mmol L^{-1}, respectively (92)). However, Acs1 is subject to glucose catabolite inactivation (143), which complicates its application in glucose-grown batch cultures. Alternatively, highly active heterologous acetyl-CoA synthetases, such as an optimized variant of the *Salmonella enterica* enzyme (200-202) may be applied. Alternatively, strains with improved affinity for acetate, potentially also due to changes in acetate transport across the plasma membrane, may be obtained by laboratory evolution (203). Such experiments could for example be based on anaerobic, acetate-limited chemostat cultures of A-ALD-dependent *Δgpd1 Δgpd2* strains (204).

A C-terminal extension of the heterologous PRK was previously shown to reduce acetaldehyde production in slow-growing cultures of PRK-RuBisCO-carrying *S. cerevisiae* (197). The same strategy for 'tuning' activity of the PRK-RuBisCO pathway enabled complete conversion of acetate in media with low acetate-to-glucose ratios, while maintaining a low glycerol yield and high ethanol yield after acetate depletion. This result provides a first proof-of-principle for efficient conversion of feedstocks for industrial bioethanol production with a low acetate content, thereby preventing continual increase of acetate via recycle water (205) and improving ethanol yield. However, controlling pathway activity by modification of the abundance of a single enzyme is likely to be a too static approach for application under industrial conditions. Strategies to dynamically regulate expression of the PRK-RuBisCO and A-ALD pathways in response to changes in medium composition could, for example, be based on the design and construction of synthetic regulatory loops based on prokaryotic sensor proteins for acetaldehyde and acetate, such as *Bacillus subtilis* AlsR, which activates transcription in response to acetate (206, 207).

Materials and Methods

Growth media and strain maintenance

S. cerevisiae strains constructed and/or used in this study all originate from the CEN.PK lineage (Table 4) (168, 208). Yeast strains were propagated in YPD medium (10 g L^{-1} Bacto yeast extract (Thermo Fisher Scientific, Waltham MA), 20 g L^{-1} Bacto™ peptone (Thermo Fisher Scientific), 20 g L^{-1} glucose) or synthetic medium with vitamins (SM; 3.0 g L^{-1} KH_2PO_4, 0.5 g L^{-1} $MgSO_4 \cdot 7H_2O$, 5.0 g L^{-1} $(NH_4)_2SO_4$, (29)) prepared and sterilized as described previously. Concentrated solutions of glucose

were autoclaved separately for 20 min at 110 °C and supplemented to SM to a final concentration of 20 g L^{-1} or 50 g L^{-1}. For growth of uracil-auxotrophic strains, 150 mg L^{-1} uracil was added to SM by adding a concentrated uracil solution (3.75 g L^{-1}) autoclaved at 120 °C for 20 min (209). To select for presence of an acetamidase marker cassette (210), $(NH_4)_2SO_4$ was replaced by 6.6 g L^{-1} K_2SO_4 and 0.6 g L^{-1} filter-sterilized acetamide. Where indicated, acetic acid (≥99.8%, Honeywell, Charlotte NC) was added to media to a concentration of 0.3 g L^{-1} or 3 g L^{-1}. A concentrated stock solution of Tween 80 (polyethylene glycol sorbitan monoelate; Merck, Darmstadt, Germany) and ergosterol (98%; Acros Organics-Thermo Fisher Scientific) (420 g L^{-1} Tween and 10 g L^{-1} ergosterol) was prepared in absolute ethanol (Supelco: Sigma-Aldrich, St. Louis MI). For anaerobic cultivation, 1 mL of this solution was added per litre of medium (179). *Escherichia coli* XL1-Blue stock cultures were propagated in lysogeny broth (LB) medium (171). For strain maintenance, glycerol (30% v/v final concentration) was added to late exponential phase cultures and stored at -80 °C. Solid media were prepared by adding 20 g L^{-1} Bacto agar (Becton Dickinson, Breda, The Netherlands) to mineral salts solutions. Vitamin solution, glucose and when required acetamide were added to SM-agar media after cooling to 60 °C. *S. cerevisiae* cultures on agar plates were incubated at 30 °C until colonies appeared (1-5 days) and *E. coli* cultures on plates were incubated overnight at 37 °C.

Construction of plasmids and expression cassettes

DNA fragments for construction of plasmids and expression cassettes were PCR amplified with Phusion High Fidelity DNA Polymerase (Thermo Fisher Scientific) according to the manufacturer's manual. Diagnostic colony PCR was performed using DreamTaq polymerase (Thermo Fisher Scientific). DNA fragments were separated by electrophoresis on 1% (w/v) agarose (Sigma-Aldrich) gels in 1xTAE (40 mM Tris-acetate pH 8.0 and 1 mM EDTA). Fragments were isolated from gels with the Zymoclean Gel DNA Recovery kit (Zymo Research, Irvine CA) or isolated from PCR mixes with a GeneJET kit (Thermo Fisher Scientific). DNA concentrations were measured with a NanoDrop 2000 spectrophotometer (wavelength 260 nm; Thermo Fisher Scientific). Plasmid assembly was performed by *in vitro* Gibson assembly using a HiFi DNA Assembly Master Mix (New England Biolabs, Ipswich MA), downscaled to 5 µL reaction volume. 1 µL of reaction mixture was used for heat-shock transformation (211) of *E. coli* XL-1 Blue. Plasmids were isolated from *E. coli* XL-I Blue transformants with the Sigma GenElute Plasmid Kit (Sigma-Aldrich) according to the manufacturer's instructions. Plasmids used and constructed in this study are listed in Table 3 and oligonucleotide primers are listed in Table S1 (available online).

Table 3: Plasmids used in this study. Kl denotes Kluyveromyces lactis

Plasmid name	Characteristics	Origin
p426_TEF	2 µm ori, *URA3*, p*TEF1*-t*CYC1* (empty vector)	(177)
pMEL10	2 µm ori, *KIURA*, gRNA-*CAN1*.Y	(175)
pMEL11	2 µm ori, *AmdS*, gRNA-*CAN1*.Y	(175)
pROS10	2 µm ori , *KIURA3*, gRNA-*CAN1*.Y gRNA-*ADE2*.Y	(175)
pUDI076	pRS406-*TDH3*p-*eutE-CYC1t*	(95)
pUDR103	2 µm ori, *KIURA3*, gRNA-*SGA1*.Y	(77)
pUDR264	2 µm ori, *AmdS,* gRNA.*ALD6*.Y	(95)
pUDR744	2 µm ori, *KIURA3,* gRNA.*GPD2*.Y gRNA.*GPD2*.Y	This work

A unique Cas9-recognition sequence in *GPD2* was identified as described previously (175). pUDR744 was constructed by PCR amplification of pROS10 with primer 5793 to obtain a linear backbone, and PCR amplification of pROS10 with primer 7839 to obtain the insert fragment containing the *GPD2* gRNA. The plasmid was then assembled by *in vitro* Gibson Assembly. A p*TDH3-eutE*-t*CYC1* integration cassette was obtained by PCR amplification with primers 16615/16616 with pUDI076 as template, adding 60 bp terminal sequences homologous to sequences directly upstream and downstream of the coding region of *ALD6*. A dsDNA repair fragment for *GDP2* deletion was obtained by mixing primers 6969/6970 in a 1:1 molar ratio, heating the mixture to 95 °C for 5 min and subsequently cooling down at room temperature.

Yeast genome editing

The lithium-acetate method (178) was used for yeast transformation. Correct Cas9-mediated integration or deletion was routinely verified by diagnostic PCR and single-colony isolates were restreaked thrice on SMD (SM with 20 g L^{-1} glucose) and stored at -80 °C.

IMX2303 was constructed by co-transforming strain IMX2288 with pUDR264 and repair fragment p*TDH3-eutE*-t*CYC1* (with homologous flanks to the upstream and downstream sequence of *ALD6* open reading frame). Transformants were selected on SMD with acetamide and uracil. To restore uracil prototrophy , strain IMX2303 was transformed with the *URA3*-carrying plasmid p426-*TEF* (empty vector), yielding strain IMX2502.

Strain IMX2503 was constructed by co-transforming IMX581 with gRNA-plasmids pUDR744 (targeting *GPD2*) and pUDR264 (targeting *ALD6*) and repair fragments for *GPD2* deletion (dsDNA homologous to the upstream and downstream sequence of *GPD2* open reading frame) and p*TDH3-eutE*-t*CYC1* (with homologous flanks to the upstream and downstream sequence of *ALD6* open reading frame). Transformants

were selected on SMD with acetamide. pUDR264 was removed by selection on SMD, while pUDR744 was retained to support uracil prototrophy.

Strain IMX2723 was obtained from IMX2593 by co-transforming with gRNA-plasmid pUDR264 and repair fragment p*TDH3-eutE*-t*CYC1*. Transformants were selected on SMD with acetamide. pUDR264 was removed by selection on SMD, while pUDR103 was retained to support uracil prototrophy.

Table 4: *S. cerevisiae* strains used in this study. *Kl* denotes *Kluyveromyces lactis*. Non-ox PPP↑ indicates the integration of the expression cassettes of p*TDH3-RPE1*, p*PGK1-TKL1*, p*TEF1-TAL1*, p*PGI1-NQM1*, p*TPI1-RKI1* and p*PYK1-TKL2.*

Strain name	Relevant genotype	Parental strain	Origin
CEN.PK113-5D	*MATa ura3-52*	-	(168)
IMX581	*MATa ura3-52 can1::cas9-natNT2*	CEN.PK113-5D	(175)
IME324	*MAT*a *ura3-52 can1::cas9-natNT2* p426-*TEF* (*URA3*)	IMX581	(77)
IMX2288	*MATa ura3-52 can1::cas9 natNT2 gpd2*:: non-ox PPP↑ *sga1*::(p*DAN1-PRK, cbbM (2 copies) groEL, groES)*	-	(197)
IMX2303	*MATa ura3-52 can1::cas9 natNT2 gpd2*::non-ox PPP↑ *sga1*::(p*DAN1-PRK, cbbM (2 copies) groEL, groES) ald6::eutE*	IMX2288	This study
IMX2502	*MATa ura3-52 can1::cas9 natNT2 gpd2*::non-ox PPP↑ *sga1*::(p*DAN1-PRK, cbbM (2 copies) groEL, groES*) *ald6::eutE* p426-*TEF* (*URA3*)	IMX2302	This study
IMX2503	*MATa ura3-52 can1::cas9 natNT2 ald6::eutE Δgpd2* pUDR774 (*KlURA3*)	IMX581	This study
IMX2593	*MATa ura3-52 can1::cas9-natNT2 gpd2*::non-ox PPP↑ *sga1*::(p*DAN1-PRK*-19aa*, cbbM (2 copies) groEL, groES*) pUDR103 (*KlURA3*)	-	(197)
IMX2723	*MATa ura3-52 can1::cas9-natNT2 gpd2*::non-ox PPP↑ *sga1*::(p*DAN1-PRK*-19aa*, cbbM (2 copies) groEL, groES*) *ald6::eutE* pUDR103 (*KlURA3*)	IMX2593	This study

Aerobic shake-flask cultivation

Shake-flask cultures were grown at 30 °C in 500-mL round-bottom shake-flasks containing 100 mL medium, placed in an Innova incubator shaker (Eppendorf Nederland B.V., Nijmegen, The Netherlands) and shaken at 200 rpm.

Bioreactor cultivation

Anaerobic bioreactor batch cultivation was conducted at 30 °C in 2-L bioreactors (Applikon Getinge, Delft, The Netherlands), with a working volume of 1 L. Culture pH

was kept constant at 5.0 by automatic addition of 2 M KOH. All bioreactor cultures were grown on synthetic medium supplemented with vitamins, glucose, acetic acid, the anaerobic growth factors Tween 80 (420 mg L^{-1}) and ergosterol (10 mg L^{-1}), and 0.2 g L^{-1} antifoam C (Sigma-Aldrich). Cultures were sparged at 0.5 L min^{-1} with an N_2/CO_2 (90/10%) gas mixture. The outlet gas stream was cooled to 4 °C in a condenser to minimize evaporation. Oxygen diffusion was minimized by use of Norprene tubing (Saint-Gobain, Amsterdam, The Netherlands) and Viton O-rings (ERIKS, Haarlem, The Netherlands)(179). Inocula were prepared in 500-mL shake-flasks containing 100 mL SMD. The first starter culture was inoculated with a frozen stock culture, grown aerobically for 15-18 h at 30 °C and used to inoculate precultures on SMD. Upon reaching mid-exponential phase (OD_{660} of 3-5), these were used to inoculate bioreactor cultures at an initial OD_{660} of 0.25-0.40.

Analytical methods

Growth was monitored by biomass dry weight measurements (109) and by measuring optical density at 660 nm (OD_{660}) on a Jenway 7200 spectrophotometer. Metabolite concentrations were determined by high-performance liquid chromatography (109). A first-order evaporation rate constant of 0.008 h^{-1} was used to correct ethanol concentrations for evaporation (109). Acetaldehyde concentrations were determined in the off-gas and the broth by derivatization using 2,4-DNPH as described previously (197). As carbon recoveries could not be accurately calculated due to the high concentration of CO_2 in the inlet gas of bioreactor cultures, electron recoveries based on degree of reduction of relevant compounds (11) were used instead.

Whole genome sequencing

Genomic DNA was isolated from aerobic shake-flask cultures (100 mL) on SMD of *S. cerevisiae* strain IMX2503 and IMX2303, at late exponential-phase (OD_{660} of 10-15), using a Qiagen Blood & Cell Culture DNA kit and 100/G Genomics-tips (Qiagen, Hilden, Germany). Short-read paired-end whole genome sequencing was performed commercially on a 350-bp PCR-free insert library using Illumina SBS technology (Macrogen; Amsterdam, The Netherlands). Sequence reads were mapped against the genome of *S. cerevisiae* CEN.PK113-7D (212) to which a virtual contig containing p*TDH3-eutE* had been added, and processed as described previously (140).

Availability of data and materials

Short read DNA sequencing data of the *Saccharomyces cerevisiae* strains IMX2503 and IMX2303 were deposited at NCBI under BioProject accession number PRJNA972872. All measurement data used to prepare Figure 2, Figure 3, Table 1 and Table 2 of the

manuscript and Figure S1, Figure S2 and Figure S3 of the supplementary materials are available in Additional file 1 and Additional file 2, which can be accessed online via https://doi.org/10.1101/2023.05.21.541164.

Funding

This work was supported by DSM Bio-based Products & Services B.V. (Delft, The Netherlands).

Supplementary information

Additional supplementary information

Available online via: https://doi.org/10.1101/2023.05.21.541164.

Additional information S1

Here, we estimate the threshold concentration of acetaldehyde at which A-ALD can operate in the reductive direction (equation I). For this estimation, we used equation II. By implementing a zero Gibbs free energy change (i.e. thermodynamic equilibrium, so no net reduction or oxidation), equation II was rewritten to equation III. We used a $\Delta G^{0'}$ of 17600 J mol^{-1} (199), R is 8.3145 J mol^{-1} K^{-1} and T is 303.15 K. For the CoA:acetyl-CoA-ratio, a value of 3.8 was used based on measurements from aerobic batch cultures of *S. cerevisiae* (213). A value of 10.1 was used for the NAD^+:NADH ratio, based on a published estimate for anaerobic *S. cerevisiae* cultures (214). This approach yielded a threshold concentration of 0.35 mM acetaldehyde (i.e., based on the assumed CoA:acetyl-CoA and NAD^+:NADH ratios, A-ALD cannot operate in yeast cells in the direction indicated in equation 1 when the acetaldehyde concentration exceeds 0.35 mM).

$$acetyl - CoA + NADH + H^+ \rightarrow acetaldehyde + CoA + NAD^+ \quad \text{(equation I)}$$

$$\Delta_{R,red}G = \Delta_{R,red}G^{0\prime} + RT \ln\left([acetaldehyde] * \frac{[NAD^+]}{[NADH]} * \frac{[CoA]}{[acetyl-CoA]}\right) \quad \text{(equation II)}$$

$$[acetaldehyde] = e^{-\frac{\Delta_{R,red}G^{0\prime}}{RT}} * \frac{[NADH]}{[NAD^+]} * \frac{[acetyl-CoA]}{[CoA]} \quad \text{(equation III)}$$

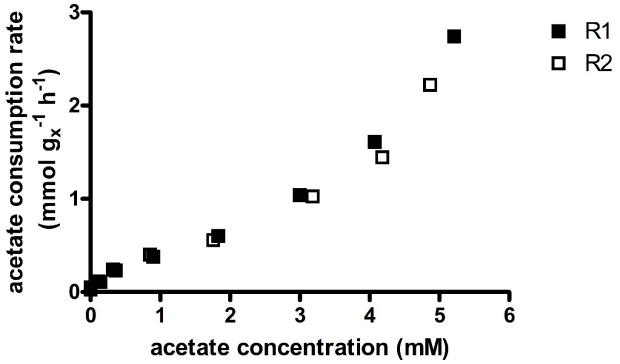

Figure S1: Biomass-specific acetate-consumption rate at different acetate concentrations in anaerobic bioreactor batch cultures of *S. cerevisiae* strain IMX2503 (*Δgpd2 Δald6 eutE*). Cultures were grown on synthetic medium containing 50 g L^{-1} glucose and 5 mmol L^{-1} acetate, at pH 5.0, 30°C and sparged with a 90:10 mixture of N_2 and CO_2. Cultures were grown in duplicate, represented by R1 and R2. Symbol: g_x, gram biomass. The biomass-specific acetate-consumption rates were calculated by fitting third-power polynomial spline through a plot of the acetate concentrations at each timepoint. The derivative of the function was used to calculate the acetate-consumption rate at each acetate concentration, which was subsequently normalized using the biomass concentration at each timepoint to obtain the biomass-specific acetate consumption rates.

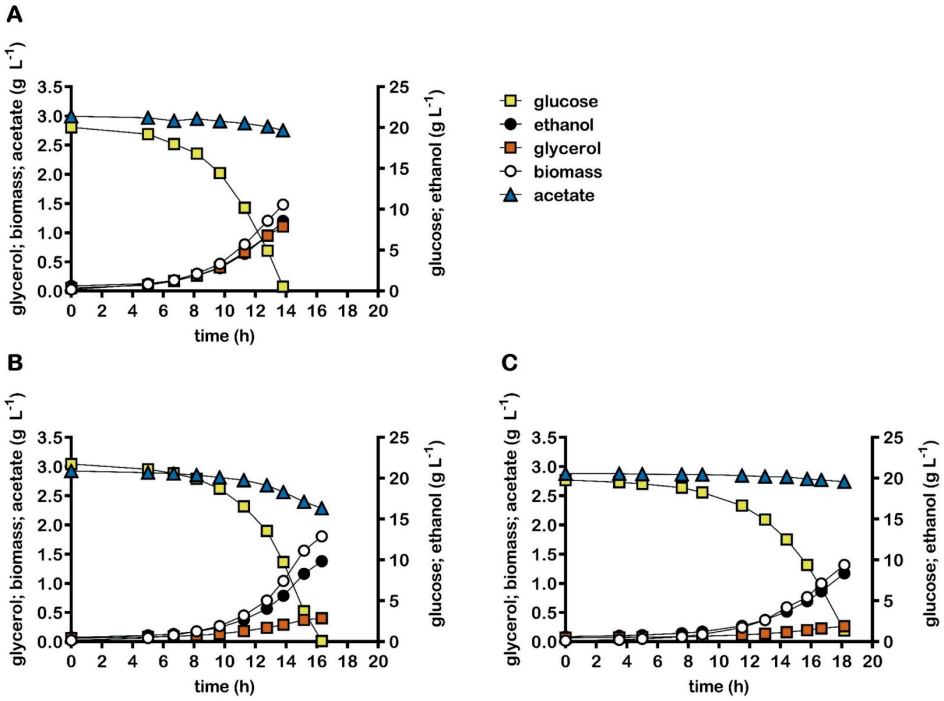

Figure S2: Concentrations of biomass, ethanol, glycerol and acetate in anaerobic bioreactor batch cultures of *S. cerevisiae* strains IME324 (reference strain, A), IMX2503 (*Δgpd2 Δald6* p*TDH3-eutE*, B), IMX2502 (non-ox PPP↑ *Δgpd2 Δald6* p*TDH3-eutE* p*DAN1-PRK* 2x p*TDH3-cbbM* p*TPI1-groES* p*TEF1-groEL*, C). Cultures were grown anaerobically at pH 5.0 and at 30 °C on synthetic medium containing 20 g L^{-1} glucose and 50 mmol L^{-1} acetate. Non-ox PPP↑ indicates the integration of the expression cassettes of p*TDH3-RPE1*, p*PGK1-TKL1*, p*TEF1-TAL1*, p*PGI1-NQM1*, p*TPI1-RKI1* and p*PYK1-TKL2*. Representative cultures of independent duplicate experiments are shown, corresponding replicate of each culture shown in Fig. 2.

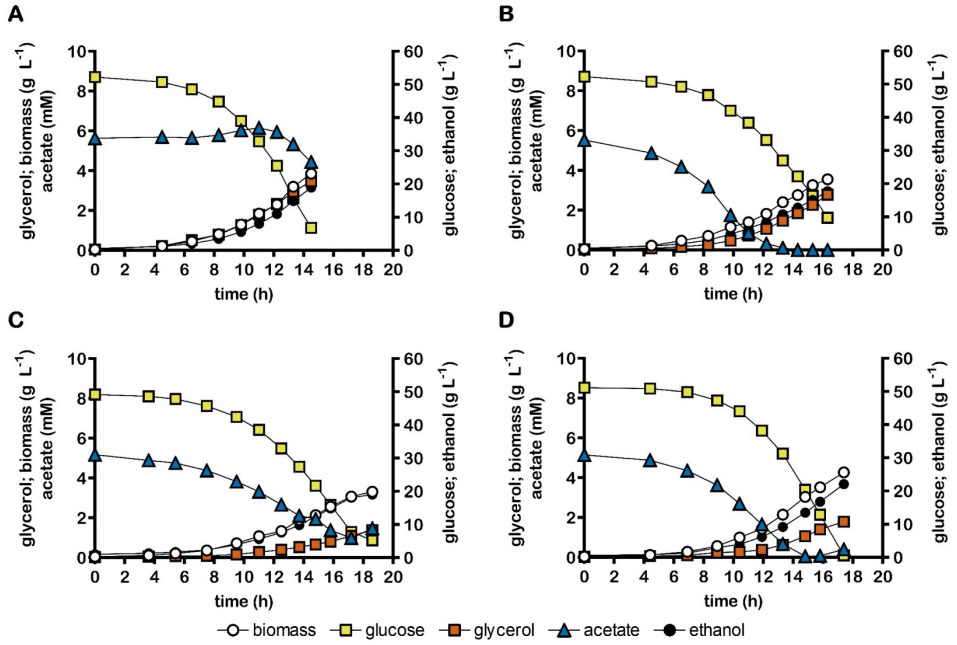

Figure S3: Concentrations of biomass, ethanol, glycerol and acetate in anaerobic bioreactor batch cultures of S. cerevisiae strains IME324 (reference strain, A), IMX2503 (*Δgpd2 Δald6 eutE*, B), IMX2502 (non-ox PPP↑ *Δgpd2 Δald6* p*TDH3-eutE* p*DAN1-PRK* 2x p*TDH3-cbbM* p*TPI1-groES* p*TEF1-groEL*, C), and IMX2723 (non-ox PPP↑ *Δgpd2 Δald6* p*TDH3-eutE* p*DAN1-PRK*-19aa (197) 2x p*TDH3-cbbM* p*TPI1-groES pTEF1-groEL*, D). Cultures were grown anaerobically at pH 5.0 and at 30 °C on synthetic medium containing 50 g L^{-1} glucose and 5.0 mmol L^{-1} acetate. Representative cultures of independent duplicate experiments are shown, corresponding replicate of each culture shown in Fig. 3.

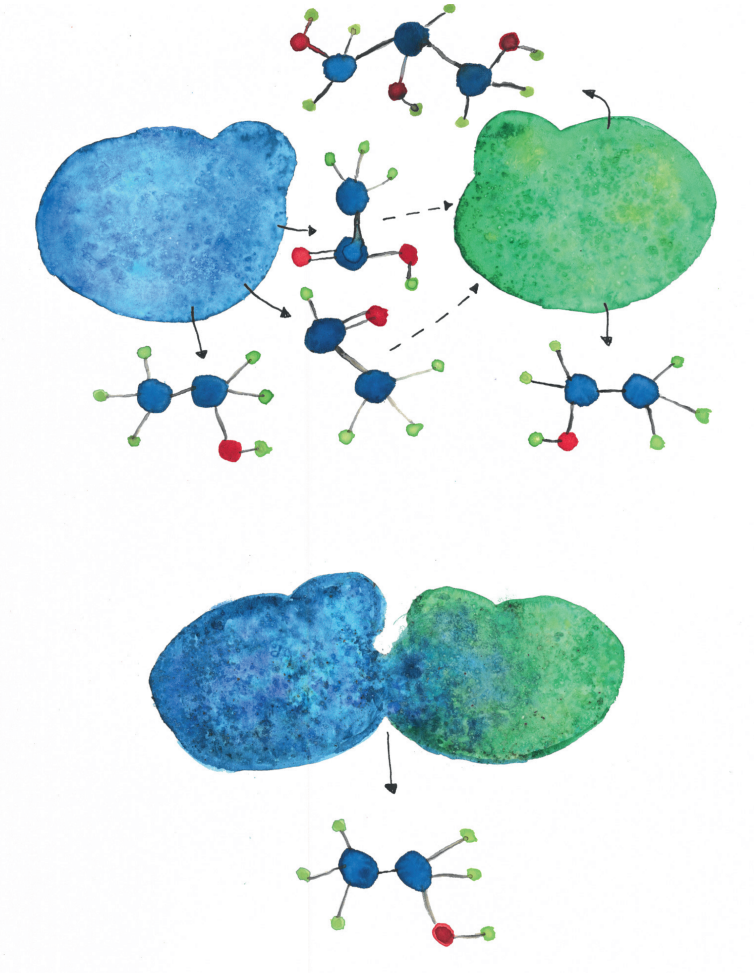

Chapter 4

Co-cultivation of *Saccharomyces cerevisiae* strains combines advantages of different metabolic engineering strategies for improved ethanol yield

Aafke C.A. van Aalst, Igor S. van der Meulen, Mickel L.A. Jansen, Robert Mans, and Jack T. Pronk

This chapter is essentially as published on BioRxiv (2023), 7: 04.547682.

Abstract

Glycerol is the major organic byproduct of industrial ethanol production by the yeast *Saccharomyces cerevisiae*. Improved ethanol yields have been achieved with engineered *S. cerevisiae* strains in which heterologous pathways replace glycerol formation as the predominant mechanism for anaerobic re-oxidation of surplus NADH generated in biosynthetic reactions. Functional expression of heterologous phosphoribulokinase (PRK) and ribulose-1,5-bisphosphate carboxylase/oxygenase (RuBisCO) genes enables yeast cells to couple a net oxidation of NADH to the conversion of glucose to ethanol. In another strategy, NADH-dependent reduction of exogenous acetate to ethanol is enabled by introduction of a heterologous acetylating acetaldehyde dehydrogenase (A-ALD). This study explores potential advantages of co-cultivating engineered PRK-RuBisCO-based and A-ALD-based strains in anaerobic bioreactor batch cultures. Co-cultivation of these strains, which in monocultures showed reduced glycerol yields and improved ethanol yields, strongly reduced the formation of acetaldehyde and acetate, two byproducts that were formed in anaerobic monocultures of a PRK-RuBisCO-based strain. In addition, co-cultures on medium with low acetate-to-glucose ratios that mimicked those in industrial feedstocks completely removed acetate from the medium. Kinetics of co-cultivation processes and glycerol production could be optimized by tuning the relative inoculum sizes of the two strains. Co-cultivation of a PRK-RuBisCO strain with a *Δgpd1 Δgpd2* A-ALD strain, which was unable to grow in the absence of acetate and evolved for faster anaerobic growth in acetate-supplemented batch cultures, further reduced glycerol formation but led to extended fermentation times. These results demonstrate the potential of using defined consortia of engineered *S. cerevisiae* strains for high-yield, minimal-waste ethanol production.

Background

Saccharomyces cerevisiae is extensively used for industrial production of ethanol, the largest-volume product of industrial biotechnology (1). Yeast-based ethanol production predominantly occurs in the United States of America and Brazil, using hydrolyzed corn starch or cane sugar, respectively, as main feedstocks (1). The majority of US fuel alcohols is made by batch fermentation (130), in which biomass and glycerol are the major byproducts (19, 85). Anaerobic fermentation of glucose or sucrose starts by oxidation of these sugars to pyruvate via the Embden-Meyerhof glycolysis, yielding ATP and NADH (9). Reduction of pyruvate by pyruvate decarboxylase and NAD^+-dependent alcohol dehydrogenase re-oxidizes the NADH formed in glycolysis and completes the conversion of sugars into ethanol and carbon dioxide (10).

In *S. cerevisiae*, formation of biomass and glycerol are coupled via redox-cofactor balances. Biomass formation leads to a net production of NADH. In anaerobic cultures, this 'surplus' NADH can neither be re-oxidized by mitochondrial respiration nor by the redox-cofactor-balanced pathway for ethanol production. Instead, anaerobic yeast cultures rely on the NADH-dependent reduction of the glycolytic intermediate dihydroxyacetone-phosphate to glycerol-3-phosphate (15). This reaction is catalyzed by Gpd1 and Gpd2 (16) and followed by the hydrolysis of glycerol-3-phosphate to glycerol and phosphate by Gpp1 and Gpp2 (18). As approximately 4% of the potential ethanol yield in industrial processes is estimated to be lost to glycerol (19), multiple metabolic engineering strategies have focused on reducing glycerol formation by engineering of yeast redox metabolism (132).

Introduction of the heterologous genes encoding phosphoribulokinase (PRK) and ribulose-1,5-bisphosphate carboxylase/oxygenase (RuBisCO) into *S. cerevisiae*, along with *Escherichia coli* genes encoding the chaperonins GroES and GroEL (*PRK*, *cbbM*, *groES*/*groEL*), enables a non-oxidative bypass of glycolysis (77). Ribulose-5-phospate can be generated via the non-oxidative pentose pathway, thereby creating a redox-cofactor neutral bypass from sugars to 3-phosphoglycerate. This concept has been implemented and optimized to allow for fast-growing low-glycerol-producing *S. cerevisiae* strains with an up to 10% higher ethanol yield on glucose in fast-growing anaerobic laboratory cultures (0.29 h^{-1}; (77)).

In industrial corn-starch-based alcoholic fermentation, the specific growth rate decreases as the ethanol concentration reaches inhibitory levels and/or non-sugar nutrients are depleted (37, 215). A recent study showed that, in slow-growing anaerobic chemostat cultures (0.05 h^{-1}), a PRK-RuBisCO strain produced up to 80-fold

more acetaldehyde and 30-fold more acetate than a reference strain (197). This production of acetaldehyde and acetate was attributed to an *in vivo* overcapacity of the key enzymes of the PRK-RuBisCO bypass. Reduction of the copy number of the expression cassette for RuBisCO led to lower acetaldehyde and acetate production in slow-growing cultures and a corresponding increase in ethanol yield (197). The production of acetaldehyde and acetate was further decreased by reducing PRK activity by lowering protein abundance by a C-terminal extension of PRK, or by expressing the spinach *PRK* gene from the growth-rate-dependent *ANB1* promoter (197). However, the resulting strains still showed trade-offs in performance at low and high specific growth rates, which illustrated the challenges involved in tuning the activity of engineered pathways under dynamic conditions.

An alternative redox-engineering strategy is based on the expression of a heterologous gene encoding acetylating acetaldehyde dehydrogenase (A-ALD). Together with native acetyl-CoA synthetase and alcohol dehydrogenase, A-ALD can catalyse the NADH-dependent reduction of exogenous acetate to ethanol (91). In the presence of acetate, anaerobic cultures of engineered A-ALD-synthesizing strains carrying a deletion in *GPD2*, which encodes one of the two *S. cerevisiae* isoenzymes of glycerol-3-phosphate dehydrogenase, show reduced glycerol yields and improved ethanol yields on glucose (93). When also *GPD1* is deleted, A-ALD strains can even grow anaerobically in the presence of acetate without producing glycerol (95). Due to bacterial contamination, feedstocks for 'first-generation' ethanol processes typically contain up to 20 mmol L^{-1} of acetate (37, 100, 194, 216). This concentration of acetate is insufficient to reach the same ethanol yield improvement as PRK-RuBisCO strains (217).

Defined microbial consortia are already used as starter cultures in food fermentation (218, 219) and there is a growing interest in the potential advantages of this approach (220-222). Co-cultivation of PRK-RuBisCO and A-ALD-based strains may, in theory, prevent accumulation of acetaldehyde and acetate generated by PRK-RuBisCO strains while limiting reduced fermentation rates and increased glycerol yields of A-ALD-based strains when acetate in growth media is depleted (Fig. 1). To evaluate this strategy, the present study explores co-cultivation of PRK-RuBisCO and A-ALD-based strains in anaerobic batch cultures on glucose, grown in the presence and absence of acetate. In addition to an A-ALD-containing strain in which only *GPD2* is deleted and which can therefore still grow in the absence of exogenous acetaldehyde or acetate, co-cultures with an A-ALD strain lacking both glycerol-3-phosphate dehydrogenase isoenzymes are investigated.

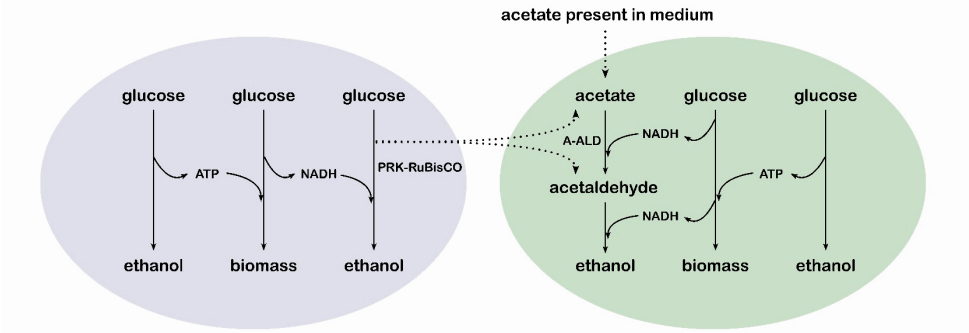

Figure 1: Schematic representation of NADH balances in anaerobic co-cultures of a PRK-RuBisCO-containing *S. cerevisiae* strain (left) and an A-ALD-containing strain (right). In both strains, re-oxidation of NADH generated during anaerobic biomass formation is coupled to ethanol production. Dotted arrows indicate use of the byproducts acetaldehyde and acetate, generated by the PRK-RuBisCO-based strain, as electron acceptors for NADH reoxidation by the A-ALD-dependent strain.

Results

Acetaldehyde and acetate as byproducts of PRK-RuBisCO-containing S. cerevisiae strains

In previous studies, growth and product formation by PRK-RuBisCO-containing *S. cerevisiae* strains were studied in anaerobic bioreactor batch cultures on 20 g L^{-1} glucose (77, 197). In such cultures, fast exponential growth continues until glucose is almost completely consumed. To capture some of the dynamics in large-scale processes, anaerobic bioreactor batch cultures of the reference strain IME324 and the PRK-RuBisCO-based strain IMX2736 (*Δgpd2* non-ox PPP↑ *PRK* 2x *cbbM groES/groEL*; non-ox PPP↑ indicates integration of the overexpression cassettes for the non-oxidative pentose phosphate pathway genes *RPE1*, *TKL1*, *TAL1*, *NQM1*, *RKI1* and *TKL2*, (197)), were grown on synthetic medium with 50 g L^{-1} glucose. In these cultures, both strains showed an initial exponential growth phase with a specific growth rate of 0.3 h^{-1}, after which the growth rate gradually declined to approximately 0.15 h^{-1} (Fig. 2, Fig. S1). These growth dynamics mimicked those in industrial fermentation processes for ethanol production from corn starch hydrolysates (215). Due to these changing growth rates, stoichiometries of glucose consumption and product formation could not be assumed constant throughout batch cultivation. Overall stoichiometries were therefore calculated from measurements on the first and final two time points of cultivation experiments.

Consistent with previous studies on PRK-RuBisCO-based *S. cerevisiae* strains, the glycerol yield on glucose of strain IMX2736, grown anaerobically on 50 g L^{-1} glucose, was 73% lower than that of the reference strain, while its ethanol yield on glucose was

7% higher ($p = 0.037$, Table 1). In these cultures of strain IMX2736, yields of the byproducts acetate and acetaldehyde on glucose were 0.030 and 0.018 mol (mol glucose)$^{-1}$, respectively (Table 1). This acetaldehyde yield was two-fold higher than reported for anaerobic cultures of strain IMX2736 on 20 g L^{-1} glucose, in which the specific growth rate remained 0.3 h^{-1} throughout batch cultivation (197). Since acetaldehyde production by anaerobic chemostat cultures of PRK-RuBisCO-based strains increases at low specific growth rates (197), the higher acetaldehyde yield of batch cultures grown on 50 g L^{-1} glucose was attributed to their declining specific growth rate.

In earlier batch experiments with PRK-RuBisCO-based *S. cerevisiae* strains grown on 20 g L^{-1} glucose, biomass yields on glucose were approximately 5% higher than in cultures of reference strains (197). Those observations were consistent with lower ATP costs for NADH regeneration via the RuBisCO bypass than via the native glycerol pathway (132). In cultures grown on 50 g L^{-1} glucose, biomass yields of strains IME324 and IMX2736 were not significantly different. Absence of a higher biomass yield of strain IMX2736 in these cultures may be related to the accumulation of 4.1 ± 0.4 mmol L^{-1} acetaldehyde and 7.8 ± 0.1 mmol L^{-1} acetate in the culture broth. Combined, formation of these metabolites already accounted for a loss of ca. 6 mmol L^{-1} glucose, while loss of acetaldehyde via the gas phase (136), toxicity effects of acetaldehyde and weak-acid uncoupling by acetate may affect biomass yield even further (31, 137, 223).

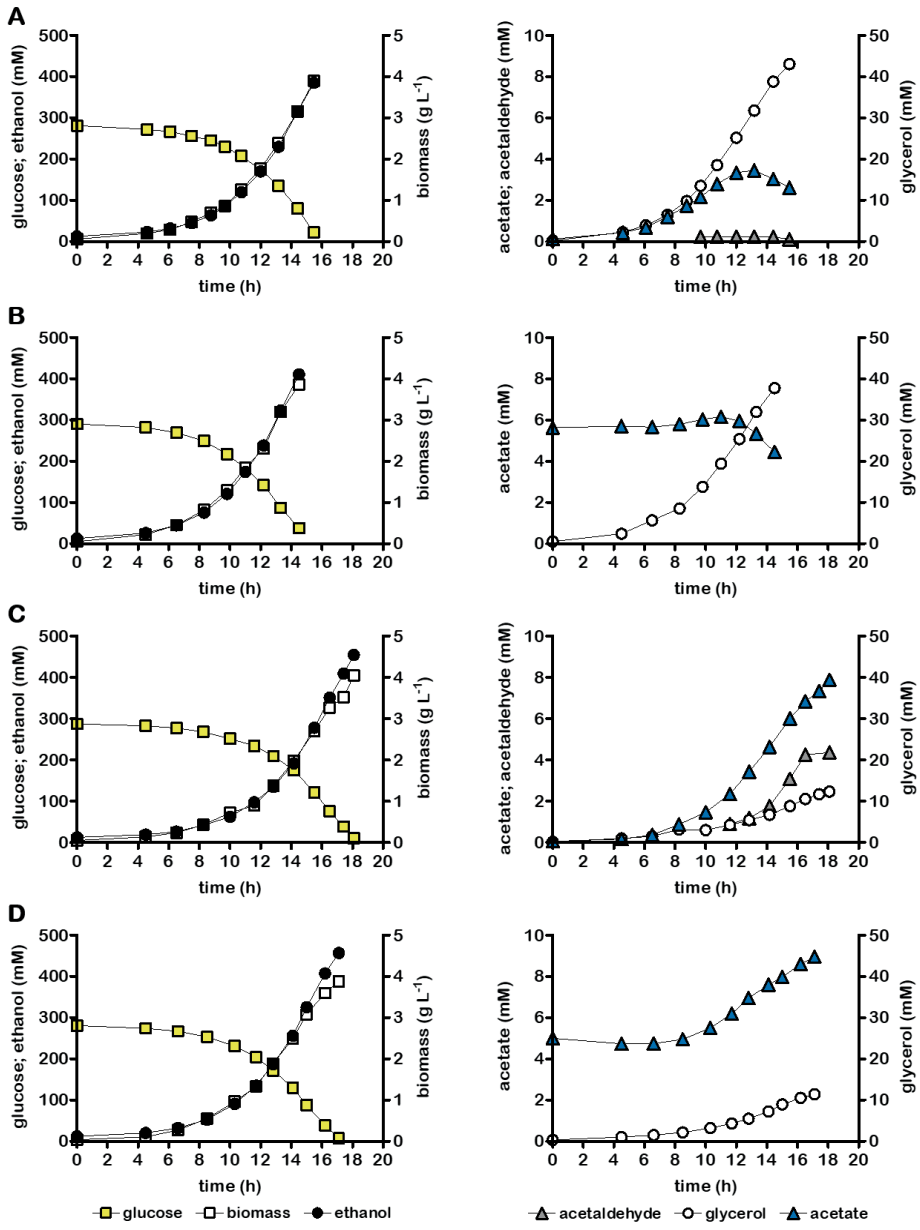

Figure 2: Growth, glucose consumption and product formation of anaerobic bioreactor batch cultures of individual *S. cerevisiae* strains, grown on SM with 50 g L^{-1} glucose (panels A and C) or on SM with 50 g L^{-1} glucose and 5 mmol L^{-1} acetate (panels B and D). Panels show data for *S. cerevisiae* strains IME324 (reference strain, A and B) and IMX2736 *(Δgpd2* non-ox PPP↑ *PRK* 2x *cbbM groES/groEL*, C and D). Representative cultures of independent duplicate experiments are shown, corresponding replicate of each culture shown in Fig. S2. Data on strain IME324 on SM with 50 g L^{-1} glucose and 5 mmol L^{-1} acetate were taken from (217).

Table 1: Key physiological parameters of anaerobic bioreactor batch cultures of *S. cerevisiae* strains IME324 (reference), IMX2736 *(Δgpd2* non-ox PPP↑ *PRK* 2x *cbbM groES/groEL*), IMX2503 (*Δgpd2 Δald6 eutE*) and IMS1247 *(Δgpd1 Δgpd2 Δald6 eutE*, evolved). Non-ox PPP↑ indicates integration of the overexpression cassettes for *RPE1, TKL1, TAL1, NQM1, RKI1 and TKL2*. Cultures were grown on synthetic medium with 50 g L^{-1} glucose, with or without addition of 5 mM acetate, at pH 5 and at 30 °C. Y indicates yield, subscript x denotes biomass. Acetate and acetaldehyde concentrations indicate values in the culture broth, measured at the end of the cultivation experiments. Negative acetate yields indicate net consumption and were calculated from data derived from sampling points before acetate depletion. Yields were calculated using the first two and last two sampling points. Degree-of-reduction balances (11) were used to verify data consistency. Values represent averages ± mean deviations of measurements on independent duplicate cultures for each combination of strain and medium. n.d., not determined.

Strain name Relevant genotype	**IME324** reference		**IMX2736** *Δgpd2 PRK* 2x *cbbM*		**IMX2503** *Δgpd2 Δald6 eutE*	**IMS1247** *Δgpd1 Δgpd2 Δald6 eutE*
Initial acetate concentration	0 mM	5 mM[a]	0 mM	5 mM	5 mM[a]	5 mM
$Y_{biomass/glucose}$ (g_x g^{-1})	0.084 ± 0.000	0.084 ± 0.000	0.082 ± 0.005	0.081 ± 0.001	0.085 ± 0.000	0.100 ± 0.001
$Y_{ethanol/glucose}$ (mol mol^{-1})	1.49 ± 0.02	1.55 ± 0.01	1.60 ± 0.00	1.64 ± 0.01	1.58 ± 0.00	1.78 ± 0.02
$Y_{acetaldehyde/glucose}$ (mol mol^{-1})	<0.001	n.d.	0.018 ± 0.001	n.d.	n.d.	n.d.
$Y_{glycerol/glucose}$ (mol mol^{-1})	0.169 ± 0.006	0.150 ± 0.000	0.046 ± 0.002	0.041 ± 0.001	0.125 ± 0.000	<0.001
$Y_{acetate/glucose}$ (mol mol^{-1})	0.012 ± 0.002	-0.004 ± 0.002	0.030 ± 0.002	0.017 ± 0.002	-0.064 ± 0.003	-0.100 ± 0.004
mmol glycerol per g_x	11.2 ± 0.3	9.9 ± 0.0	3.1 ± 0.0	2.8 ± 0.1	8.2 ± 0.0	0.1 ± 0.0
Final concentration acetaldehyde (mM)	0.1 ± 0.0	n.d.	4.1 ± 0.4	n.d.	n.d.	n.d.
Final concentration acetate (mM)	2.8 ± 0.3	4.4 ± 0.1	7.8 ± 0.1	9.3 ± 0.5	<0.01	<0.01
Electron recoveries (%)	99-101	99-99	98-98	99-100	99-99	101-102

[a]data on strain IME324 and IMX2503 on 50 g L^{-1} of glucose with 5 mM acetate were taken from (217).

Anaerobic co-cultivation of PRK-RuBisCO-based and A-ALD-based S. cerevisiae strains on acetate-containing medium

First-generation feedstocks for ethanol production such as corn mash can contain up to 20 mmol L^{-1} acetate (37) while glucose concentrations can reach 300 g L^{-1} (152). To mimic these acetate-to-glucose ratios, anaerobic bioreactor batch cultures of strains IME324 (reference) and IMX2736 (*Δgpd2* non-ox PPP↑ *PRK* 2x *cbbM groES/groEL*) were grown on 50 g L^{-1} glucose and 5 mmol L^{-1} acetate (Table 1, Fig. 2). Under these conditions, the reference strain IME324 consumed approximately 1.6 mmol L^{-1} acetate (Table 1), probably reflecting its conversion to the biosynthetic precursor molecule acetyl-Coenzyme A (198). In contrast, the PRK-RuBisCO-containing strain IMX2736 produced 2.8 mmol L^{-1} acetate. In these acetate-supplemented anaerobic cultures, the PRK-RuBisCO strain showed a 2.4% higher ethanol yield than in cultures grown without acetate supplementation ($p = 0.011$, Table 1), which may reflect an increased ATP demand caused by mild weak-acid uncoupling by acetate (31).

Introduction of a heterologous acetylating acetaldehyde dehydrogenase (A-ALD) enables anaerobic *S. cerevisiae* cultures to re-oxidize 'surplus' NADH from biosynthetic reactions by NADH-dependent reduction of exogenous acetate to ethanol (91, 217). In anaerobic batch cultures on 50 g L^{-1} glucose and 5 mmol L^{-1} acetate, the A-ALD-containing strain IMX2503 (*Δgpd2 Δald6 eutE*; (217)), had already converted all acetate after 12 h, when only 33% of the available glucose had been consumed (Fig. 4A). Moreover, the rate of acetate consumption already declined before this time point (Fig. 4A). This deceleration is likely to reflect Monod kinetics for acetate consumption, possibly influenced by the high K_m of Acs2 (ca. 8.8 mM, (143)). Consequently, glycerol formation via Gpd1 was the predominant mechanism for reoxidizing 'surplus' NADH in strain IMX2503 and its glycerol yield on glucose of was only 17% lower than that of the reference strain IME324 ($p < 0.001$, Table 1).

The PRK-RuBisCO strain IMX2736 (*Δgpd2* non-ox PPP↑ *PRK* 2x *cbbM groES/groEL;* (197)) does not depend on acetate for glycerol-independent NADH cofactor balancing and its byproducts acetate and acetaldehyde could potentially be used as electron acceptors for the A-ALD-strain IMX2503 (Fig. 1). We therefore investigated whether co-cultivation of these two strains could combine low-glycerol fermentation with complete conversion of acetate. Two unique single-nucleotide polymorphisms (SNPs) in strain IMX2736, on Chromosome 11 (location 331347) and Chromosome 15 (location 912014), allowed for estimation of the ratio of strains IMX2503 and IMX2736 in co-cultures by counting reads containing and lacking these SNPs in whole-genome sequence data (Fig. 3).

When strains IMX2503 (A-ALD) and IMX2736 (PRK-RuBisCO) were inoculated at a ratio of 1.4:1 (IMX2503:IMX2736) in medium containing 50 g L^{-1} glucose and 5 mmol L^{-1} acetate, acetate was completely consumed when, after 14 h, ca. 50% of the glucose was still unused (Fig. 4B). When the initial abundance of the A-ALD-based strain was decreased by changing the inoculum ratio to 0.8:1 (IMX2503:IMX2736), complete consumption of glucose and acetate almost coincided (Fig. 4C). As a consequence, acetate limitation of A-ALD strain was delayed and the glycerol yield of the co-culture on glucose was 20% lower than at the higher inoculum ratio ($p < 0.001$, Table 2). Glycerol yields in co-cultures grown at inoculum ratios of 0.8 and 1.4 were 49% and 34% lower than in corresponding monocultures of the reference strain IME324 (Tables 1 and 2). Ethanol yields of the co-cultures were not significantly different from that of a monoculture of the PRK-RuBisCO strain IMX2736 and 6% higher than that of monocultures of the reference strain IME324 ($p = 0.015$, Tables 1 and 2). Biomass yields on glucose of these co-cultures were 6.7% higher than those of a monoculture of the PRK-RuBisCO strain IMX2736 grown on the same medium ($p = 0.002$, Tables 1 and 2). The higher biomass yield of the consortium cultures is likely to reflect consumption of acetaldehyde and acetate by the A-ALD strain.

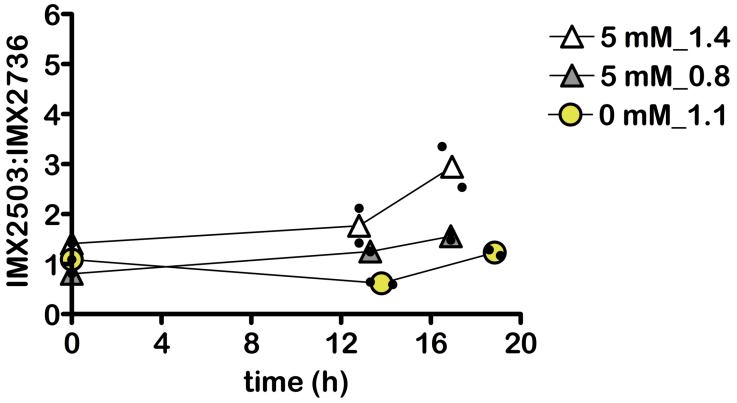

Figure 3: Ratio of *S. cerevisiae* strains IMX2503 *(Δgpd2 Δald6* eutE) relative to IMX2736 *(Δgpd2* non-ox PPP↑ *PRK* 2x *cbbM groES/groEL*) in anaerobic bioreactor batch co-cultures on synthetic medium containing 50 g L^{-1} glucose, with or without the addition of 5 mM acetate (indicated in the Figure as either 5 mM or 0 mM). Ratios were calculated based on whole genome sequencing. Values represent means and individual values of measurements on independent batch duplicate cultures. Cultures were inoculated at ratios of strain IMX2503 relative to strain IMX2736 of 1.4:1, 0.8:1 or 1.1:1 as indicated in the Figure.

Table 2: Key physiological parameters of anaerobic bioreactor batch co-cultures of *S. cerevisiae* strains IMX2736 (*Δgpd2* non-ox PPP↑ *PRK* 2x *cbbM groES/groEL*) and IMX2503 (*Δgpd2 Δald6 eutE*). Inoculum ratios of the two strains were calculated by genome sequencing. Cultures were grown on synthetic medium with 50 g L^{-1} glucose, with or without addition of 5 mM acetate. Y indicates yield, subscript x denotes biomass. Acetate and acetaldehyde concentrations indicate values in the culture broth, measured at the end of the cultivation experiments. Negative acetate yields indicate net consumption and were calculated from data derived from sampling points before acetate depletion. Yields were calculated using the first two and last two sampling points. Degree-of-reduction balances (11) were used to verify data consistency. Values represent averages ± mean deviations of measurements on independent duplicate cultures for each combination of strain and medium. n.d., not determined.

Strain name	**IMX2503 & IMX2736**		
Relevant genotype	*Δgpd2 Δald6 eutE & Δgpd2 PRK* 2x *cbbM*		
Initial acetate concentration	0 mM	5 mM	5 mM
Inoculum ratio IMX2503:IMX2736	1.1±0.0	1.4±0.2	0.8±0.1
$Y_{biomass/glucose}$ (g_x g^{-1})	0.090 ± 0.000	0.088 ± 0.001	0.090 ± 0.000
$Y_{ethanol/glucose}$ (mol mol $^{-1}$)	1.62 ± 0.00	1.63 ± 0.01	1.63 ± 0.01
$Y_{acetaldehyde/glucose}$ (mol mol $^{-1}$)	0.004 ± 0.001	n.d.	n.d.
$Y_{glycerol/glucose}$ (mol mol $^{-1}$)	0.070 ± 0.002	0.073 ± 0.002	0.058 ± 0.000
$Y_{acetate/glucose}$ (mol mol $^{-1}$)	0.007 ± 0.003	-0.045 ± 0.000	-0.030 ± 0.004
mmol glycerol per g_x	4.3 ± 0.1	4.6 ± 0.1	3.6 ± 0.0
Final acetaldehyde concentration (mM)	1.2 ± 0.1	n.d.	n.d.
Final acetate concentration (mM)	1.5 ± 0.23	0.3 ± 0.1	0.7 ± 0.2
Electron recoveries	99-100	99-99	98-101

Anaerobic co-cultivation of A-ALD-based and RuBisCO-based strains on glucose

In anaerobic batch cultures grown on glucose, the PRK-RuBisCO-based strain IMX2736 produced acetaldehyde and acetate as byproducts (Table 1, Fig. 2). To investigate whether co-cultivation with an A-ALD-based strain could reduce or eliminate this undesirable byproduct formation, anaerobic batch co-cultures of strains IMX2736 and IMX2503 were grown on glucose (50 g L^{-1}) as sole carbon source (Fig. 4). In these cultures, which were grown with an inoculum ratio of 1.1:1 (IMX2503:IMX2736), strain IMX2503 (*Δgpd2 Δald6 eutE*) can only use acetate and acetaldehyde generated by strain IMX2736. Yields of acetate and acetaldehyde were 84% and 72% lower, respectively, than in corresponding monocultures of the RuBisCO-based strain IMX2736 (Tables 1 and 2). Co-cultivation did not extend the fermentation time relative to monocultures of strain IMX2736, while the ethanol yield of the consortium was 1.5% higher than that of monocultures of strain IMX2736 and 8.8% higher than that of monocultures of the reference strain IME324 ($p = 0.026$ and $p = 0.034$, respectively, Fig. 2, Fig. 4, Tables 1 and 2). The glycerol yield of these co-cultures was 58% lower than that of monocultures of the reference strain IME324, but 55% higher than that of monocultures of the PRK-RuBisCO-containing strain IMX2736 (Fig. 2, Fig. 4, Tables 1 and 2).

In contrast to co-cultures of strains IMX2736 and IMX2503 on 50 g L^{-1} glucose and 5 mmol L^{-1} acetate, the co-culture on 50 g L^{-1} glucose still produced some acetate and acetaldehyde (Table 2, Fig. 4). A dependency of the A-ALD strain IMX2503 on acetate for fast growth (19, 217) was reflected by a decrease of its relative abundance in the mixed culture during the first phase of batch cultivation on 50 g L^{-1} glucose (Fig. 3). Such a decrease was not observed in co-cultures of these strains that, with a similar inoculum ratio of the two strains, were grown on 50 g L^{-1} glucose and 5 mmol L^{-1} acetate (Fig. 3).

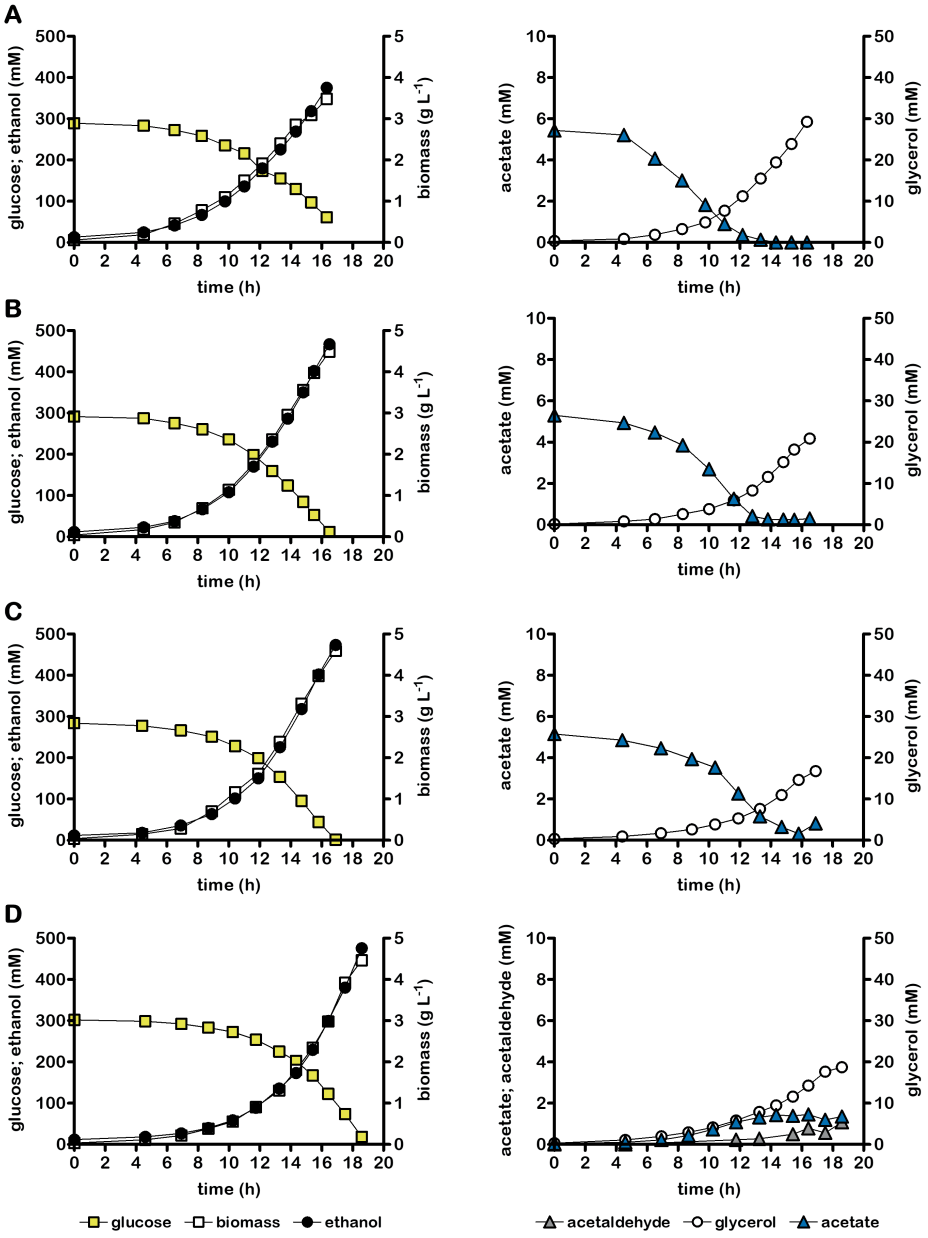

Figure 4: Growth, glucose consumption and product formation of anaerobic bioreactor batch cultures of *S. cerevisiae* strain IMX2503 (*Δgpd2 Δald6 eutE*) (A) and co-cultures of IMX2503 and IMX2736 (Δgpd2, non-ox PPP↑ *prk* 2x *cbbM groES/ groEL*). Cultures were grown on synthetic medium containing 50 g L^{-1} glucose (panel D) or 50 g L^{-1} glucose and 5 mmol L^{-1} acetate (panels A-C) and were inoculated at a ratio of 1.4±0.2 (B), 0.8±0.1 (C) or 1.1±0.0 (D). Representative cultures of independent duplicate experiments are shown, corresponding replicate of each culture shown in Fig. S3. Data for panel A were taken from (217).

Additional deletion of GPD1 in A-ALD-based strain prevents glycerol production in the absence of acetate

The A-ALD-synthesizing strain IMX2503 (*Δgpd2 Δald6 eutE*) retains a functional *GPD1* gene and therefore, albeit slower than the reference strain (19, 217) can grow in the absence of acetate. Therefore, when the inoculum of co-cultures with the RuBisCO strain IMX2736 contained a high fraction of strain IMX2503 and acetate was consumed before glucose was exhausted, the co-culture displayed a higher glycerol yield (Fig. 4; Table 2). Ideally, depletion of acetate should not lead to enhanced glycerol formation, since this goes at the expense of ethanol yield. Avoiding this requires that the A-ALD strain stops growing when acetate is depleted. We therefore constructed the A-ALD strain IMX2744 (*Δgpd1 Δgpd2 Δald6 eutE*) whose anaerobic growth, due to the elimination of both glycerol-3-phosphate-dehydrogenase isoenzymes, depended on external supply of acetate or acetaldehyde. We decided to not also delete *GPD1* in strain IMX2736 because of the role of glycerol in osmotolerance of *S. cerevisiae* (76, 224). In this way, glycerol can still be produced in co-cultures of strains IMS1247 and IMX2736.

As reported for previously constructed *Δgpd1 Δgpd2 EutE* strains (95), strain IMX2744 showed a suboptimal specific growth rate in anaerobic cultures grown on glucose and acetate (Fig. S4). A faster-growing single-cell isolate, IMS1247, was obtained by adaptive laboratory evolution of strain IMX2744 (initial specific growth rate of ca. 0.20 h^{-1}) in sequential batch reactors on 50 g glucose L^{-1} and 17 mmol L^{-1} acetate (Fig. S4). In anaerobic batch cultures on 50 g L^{-1} glucose and 5 mmol L^{-1} acetate, the evolved strain IMS1247 still grew slower than strain IMX2503 (*Δgpd2 Δald6 eutE*) (Fig. 5A and 4A, initial specific growth rates ca. 0.32 h^{-1} and 0.27 h^{-1}, respectively). After 19 h, when acetate had been completely consumed, anaerobic cultures of strain IMS1247 had only consumed a quarter of the glucose initially present in the culture (Fig. 5A). However, in contrast to strain IMX2503, strain IMS1247 did not produce any glycerol (Fig. 5A and 4A).

Whole-genome sequencing of the evolved strain IMS1247 revealed single-nucleotide mutations in *HXK2*, *GIS3* and in the intergenic region in front of *GUT1* (Table S1). The SNP on Chr. 7 location 30770 (*HXK2*) in IMS1247 was used in addition to the two previously described unique SNPs in strain IMX2736. These mutations were used to estimate the ratio of strains IMS1247 and IMX2736 in co-cultures (Fig. 6).

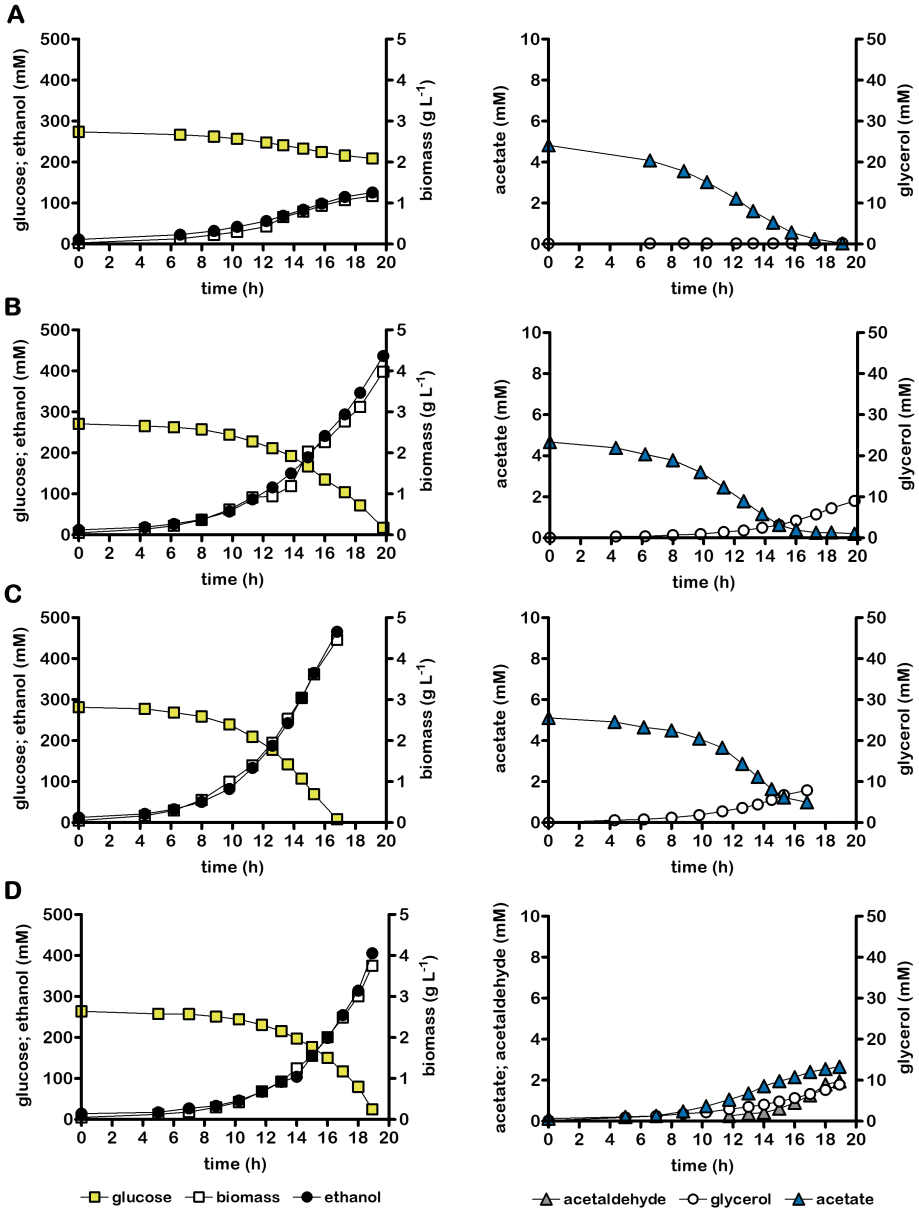

Figure 5: Growth, glucose consumption and product formation of anaerobic bioreactor batch cultures of *S. cerevisiae* strain IMS1247 (*Δgpd1 Δgpd2 Δald6 eutE*, evolved) (A) and co-cultures of IMS1247 and IMX2736 (*Δgpd2* non-ox PPP↑ *PRK* 2x *cbbM groES/groEL*). Non-ox PPP↑ indicates integration of overexpression cassettes for *RPE1*, *TKL1*, *TAL1*, *NQM1*, *RKI1* and *TKL2*. Cultures were grown on synthetic medium containing 50 g L^{-1} glucose (panel D) or 50 g L^{-1} glucose and 5 mmol L^{-1} acetate (panels A-C) and were inoculated at a ratio of 5.5±1.3 (B), 1.0±0.2 (C) or 1.3±0.4 (D). Representative cultures of independent duplicate experiments are shown, corresponding replicate of each culture shown in Fig. S5.

Table 3: Key physiological parameters of anaerobic bioreactor batch co-cultures of *S. cerevisiae* strains IMX2736 (*Δgpd2*, non-ox PPP↑ *PRK* 2x *cbbM groES/groEL*) and IMS1247 (*Δgpd1 Δgpd2 Δald6 eutE*, evolved). Inoculum ratios of the two strains were calculated by genome sequencing. Cultures were grown on synthetic medium with 50 g L^{-1} glucose, with or without addition of 5 mM acetate. Y indicates yield, subscript x denotes biomass. Acetate and acetaldehyde concentrations indicate values in the culture broth, measured at the end of the cultivation experiments. Negative acetate yields indicate net consumption and were calculated from data derived from sampling points before acetate depletion. Yields were calculated using the first two and last two sampling points. Degree-of-reduction balances (11) were used to verify data consistency. Values represent averages ± mean deviations of measurements on independent duplicate cultures for each combination of strain and medium. n.d., not determined.

Strain name	**IMS1247 & IMX2736**		
Relevant genotype	*Δgpd1 Δgpd2 Δald6 eutE & Δgpd2 PRK* 2x *cbbM*		
Initial acetate concentration	0 mM	5 mM	5 mM
Inoculum ratio IMS1247:IMX2736	1.33±0.36	5.51±1.26	1.00±0.15
$Y_{biomass/glucose}$ (g_x g^{-1})	0.088 ± 0.000	0.088 ± 0.002	0.091 ± 0.000
$Y_{ethanol/glucose}$ (mol mol $^{-1}$)	1.64 ± 0.01	1.67 ± 0.01	1.66 ± 0.00
$Y_{acetaldehyde/glucose}$ (mol mol $^{-1}$)	0.009 ± 0.000	n.d.	n.d.
$Y_{glycerol/glucose}$ (mol mol $^{-1}$)	0.037 ± 0.000	0.035 ± 0.000	0.029 ± 0.000
$Y_{acetate/glucose}$ (mol mol $^{-1}$)	0.012 ± 0.000	-0.049 ± 0.002	-0.019 ± 0.000
mmol glycerol per g_x	2.4 ± 0.1	2.2 ± 0.0	1.8 ± 0.0
Final concentration acetaldehyde (mM)	2.1 ± 0.2	n.d.	n.d.
Final concentration acetate (mM)	2.9 ± 0.3	0.2 ± 0.0	0.9 ± 0.1
Electron recoveries	98-99	99-100	98-99

To compensate for the slow growth of strain IMS1247, initial co-cultivation experiments with strain IMX2736 on 50 g L^{-1} glucose and 5 mmol L^{-1} acetate were grown with an inoculum ratio of 5.5. In these cultures, acetate was completely consumed after 16 h, when only half of the glucose had been consumed (Fig. 5B). Complete consumption of glucose occurred after 20 h, which was 3 h later than in monocultures of strain IMX2736 on the same medium (Fig. 2D). This slower conversion was anticipated due to the lower inoculum density of strain IMX2736 and the dependency of strain IMS1247 on exogenous acetate or acetaldehyde.

When the inoculum ratio of the two strains was changed to 1, approximately 1 mmol L^{-1} acetate was left in the culture when glucose was exhausted (Fig. 5C). As a consequence, growth arrest of IMS1247 was prevented and the overall fermentation time was close to that of monocultures of PRK-RuBisCO strain IMX2736 on the same medium (Fig. 6). Glycerol yields in co-cultures of strains IMS1247 and IMX2736 grown on acetate-supplemented medium at inoculum ratios of 5.5:1 and 1.0:1 were 77% and 82% lower, respectively, than in corresponding monocultures of the reference strain IME324 and 22% and 37% lower than the monocultures of PRK-RuBisCO strain IMX2736. Moreover, ethanol yields were 8.3% and 7.1% higher, respectively, for co-

cultures grown at inoculum ratios of 5.5 and 1.0, than for monocultures of the reference strain IME324 ($p = 0.002$ and $p = 0.014$, respectively, Tables 1 and 3).

During anaerobic co-cultivation on 50 g L^{-1} glucose as sole carbon source, growth of the glycerol-negative A-ALD strain IMS1247 was anticipated to depend on supply of acetate and acetaldehyde by the PRK-RuBisCO-based strain IMX2736. Acetate and acetaldehyde yields of the co-cultures of strains IMS1247 and the PRK-RuBisCO IMX2736 on 50 g L^{-1} glucose were 47% and 61% lower, respectively, than those of a monocultures of strain IMX2736 on 50 g L^{-1} and their ethanol yield was 2.7% higher ($p = 0.046$, Tables 1 and 3). These byproduct yields were 2.3- and 1.7-fold higher, respectively than observed in co-cultures of strain IMX2736 and strain IMX2503 (*Δgpd2 Δald6 eutE*) (Table 2). The latter observation probably reflects the population dynamics of the co-cultures of strains IMS1247 and IMX2736 on glucose as sole carbon source, which showed a 50% decrease of the relative abundance of strain IMS1247 during fermentation. In contrast, in co-cultures on 50 g L^{-1} glucose and 5 mmol L^{-1} acetate of the two strains with an inoculation ratio of 1, strain IMS1247 represented approximately half of the population throughout fermentation (Fig. 6).

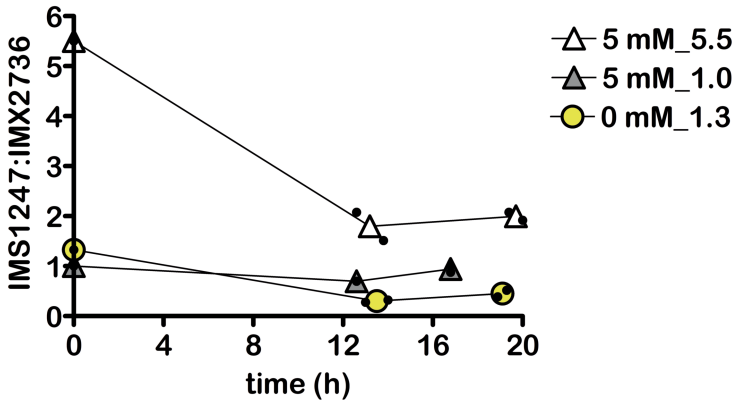

Figure 6: Ratio of *S. cerevisiae* IMS1247 *(Δgpd1 Δgpd2 Δald6 eutE*, evolved) relative to strain IMX2736 *(Δgpd2* non-ox PPP↑ *PRK* 2x *cbbM groES/groEL*) in anaerobic bioreactor batch co-cultures on synthetic medium containing 50 g L^{-1} glucose with or without the addition of 5 mM acetate (indicated in the Figure as either 5 mM or 0 mM). Ratios were calculated based on whole genome sequencing. Values represent means and individual values of measurements on independent batch duplicate cultures. Cultures were inoculated at ratios of strain IMS1247 relative to strain IMX2736 of 5.5:1, 1.0:1, 1.3:1 as indicated in the Figure.

Discussion

Advantages of microbial interactions are well described for multi-species natural microbial ecosystems and microbial consortia applied in food fermentation processes (225, 226). Previous laboratory studies on the use of consortia of different engineered *S. cerevisiae* strains for ethanol production focused on conversion of polysaccharides or sugar mixtures by consortia of engineered 'specialist' strains (227, 228). The present study focused on efficient conversion of glucose to ethanol, both in the absence and presence of low concentrations of acetate in growth media. Its results show that consortia of engineered PRK-RuBisCO-based and A-ALD-based *S. cerevisiae* strains enable higher ethanol yields than obtained with a non-engineered reference strain, while reducing net formation of byproducts originating from PRK-RuBisCO-based *S. cerevisiae* and removing acetate from growth media.

Introduction of PRK and RuBisCO, combined with modifications in the central metabolism of *S. cerevisiae*, enables improved ethanol yields in fast-growing anaerobic cultures (77). However, during slower anaerobic growth in continuous cultures (217), and in batch cultures on 50 g L^{-1} glucose (Fig. 2 CD), PRK-RuBisCO strains optimized for fast growth generate acetaldehyde and acetate as byproducts. In a recent study, PRK-RuBisCO strains into which an A-ALD pathway had been introduced showed inferior acetate reduction relative to a strain that only expressed the A-ALD pathway (217). A lack of *in vivo* reductive A-ALD activity in 'dual pathway' strains was attributed to the impact of acetaldehyde and a low $NADH/NAD^+$ ratio, both generated by activity of the PRK-RuBisCO bypass, on the reversible A-ALD reaction ($\Delta G^{0\prime}$ = 17.6 kJ mol^{-1} for the reductive reaction, (199)). Further engineering to adapt *in vivo* activity of PRK and RuBisCO in dual-pathway strains to NADH availability in dynamic industrial cultures would require introduction of dynamic regulation circuits (217). Alternatively, our results show that interference of the two pathways was mitigated by their compartmentation in separate co-cultivated strains. This co-cultivation approach enabled high ethanol yields while strongly reducing acetate and acetaldehyde production in glucose-grown batch cultures (Fig. 4D, Fig 5D). Minimizing acetaldehyde production is not only relevant for improving ethanol yield but also to prevent its toxicity to yeast cells (137, 223) and also in view of environmental and health issues (146, 147).

Consortia of PRK-RuBisCO and A-ALD-based strains removed essentially all acetate from media with acetate-to-glucose ratios similar to those in feedstocks for first-generation bioethanol production (Fig. 4 BC, Fig. 5 BC). The complete removal of acetate during fermentation does not only contribute to increased ethanol yields, but also prevents its recycling into subsequent fermentation runs and, potentially its

accumulation to inhibitory levels, as a result of recycling thin stillage and evaporator condensate (205).

Co-cultivation of the PRK-RuBisCO strain IMX2736 with the A-ALD strains IMX2503 (*Δgpd2 Δald6 eutE*) and IMS1247 (*Δgpd1 Δgpd2 Δald6 eutE*) revealed a trade-off between stoichiometry and kinetics (Fig. 4, Fig. 5). Co-cultivation of strain IMX2736 with strain IMS1247, which could not produce any glycerol, led to low glycerol formation but led to extended fermentation times (Fig. 5 B). Ideally, low-glycerol growth and vigorous fermentation by A-ALD-based strains should continue even when acetate availability in the medium becomes growth limiting. In addition to the option of supplying small amounts of acetate during fermentation, this goal may be pursued by further strain engineering to allow for a strongly constrained rate of glycerol production. Alternatively, *S. cerevisiae* strains may be used in which A-ALD reduces acetyl-CoA synthesized from glucose via engineered pathways that generates fewer than 2 mol of NADH per mol of acetyl-CoA. Such strategies can be based on introduction of a heterologous pyruvate-formate lyase (PFL) (101, 102), or of a heterologous phosphoketolase (PK) and phosphotransacetylase (PTA) (106-108).

With the exception of classical processes in Brazil, in which yeast biomass is recycled after each fermentation run (129, 229, 230), industrial batch fermentation processes for ethanol production are typically started with fresh pre-cultures of yeast strains provided by specialist companies (231). When exclusively relying on metabolic engineering of monocultures, adaptations to regular changes in feedstock and process configurations would require extensive strain engineering. Use of co-cultures enables fast adaptation of inoculation ratios of available strains to optimally balance ethanol yield, productivity and byproduct formation (Fig. 4, Fig. 5). For example, ethanol plants dealing with higher contamination levels, and therefore higher acetic acid levels, might increase the fraction of acetate-reducing yeast in strain blends. The readiness of the first-generation bioethanol industry to adopt this strategy is illustrated by a recent report that, without disclosing details on the strains involved, indicates that blends of engineered yeast strains are already applied at full industrial scale (232).

Materials and Methods

Strains, media and maintenance

The *S. cerevisiae* strains used in this study were derived from the CEN.PK lineage (168, 208) (Table 5). Synthetic medium (SM), containing 3.0 g L^{-1} KH_2PO_4, 0.5 g L^{-1} $MgSO_4 \cdot 7H_2O$, 5.0 g L^{-1} $(NH_4)_2SO_4$, trace elements and vitamins, was prepared as described previously (29). Shake-flask cultures were grown on SM supplemented with

20 g L^{-1} glucose (SMD) and bioreactor cultures on SM with 50 g L^{-1} glucose. Anaerobic growth media were supplemented with ergosterol (10 mg L^{-1}) and Tween 80 (420 mg L^{-1}) (179). Anaerobic cultures were grown on SMD in which the KH_2PO_4 concentration was raised to 14.4 g L^{-1} for extra pH buffering. Complex medium (YPD) contained 10 g L^{-1} Bacto yeast extract (Thermo Fisher Scientific, Waltham MA), 20 g L^{-1} Bacto peptone (Thermo Fisher Scientific) and 20 g L^{-1} glucose. To select for presence of an acetamidase marker cassette (210), $(NH_4)_2SO_4$ was replaced by 6.6 g L^{-1} K_2SO_4 and 0.6 g L^{-1} filter-sterilized acetamide. Where indicated, pure acetic acid solution (≥99.8%, Honeywell, Charlotte NC) was added to media at a concentration of 0.30 g L^{-1} or 1.0 g L^{-1}. *Escherichia coli* XL1-Blue cultures were grown on lysogeny broth (LB) (171) containing 10 g L^{-1} tryptone (Brunschwig Chemie B.V., Amsterdam, The Netherlands), 5.0 g L^{-1} yeast extract and 10 g L^{-1} NaCl. Where relevant, LB was supplemented with 100 mg L^{-1} ampicillin (Merck, Darmstadt, Germany). *E. coli* strains were grown overnight at 37 °C in 15-mL tubes containing 5 mL LB, shaken at 200 rpm in an Innova 4000 Incubator (Eppendorf AG, Hamburg, Germany). Solid media were prepared by adding 20 g L^{-1} agar (Becton Dickinson, Breda, The Netherlands) prior to heat sterilization. *S. cerevisiae* plate cultures were incubated at 30 °C until colonies appeared (1-5 d), while *E. coli* plates were incubated overnight at 37 °C. Frozen stock cultures were prepared by freezing samples from fully grown batch cultures at -80 °C after addition of 30% (v/v) glycerol.

Plasmid construction

Cas9 target sequences in *GPD1* and *GPD2* were identified as described previously (175). To construct plasmid pUDR203 (Table 4), a linear backbone fragment of pROS11 was first PCR amplified with primer 5793. Subsequently, DNA fragments encoding *GPD1*-targeting and *GPD2*-targeting gRNA cassettes were PCR-amplified using primers 6965/6966. Phusion high-fidelity DNA Polymerase (Thermo Fisher) was used as specified by the manufacturer. Plasmid-backbone and insert fragments were isolated from gels with the Zymoclean Gel DNA Recovery kit (Zymo Research, Irvine CA). DNA concentrations were measured with a NanoDrop 2000 spectrophotometer (Thermo Fisher) at a wavelength of 260 nm. Plasmid assembly was performed by in vitro Gibson Assembly using a HiFi DNA Assembly master mix (New England Biolabs, Ipswich, MA), downscaled to 5 µL reaction volumes. 1 µL of the reaction mixture was used to transform *E. coli* XL-1 Blue cells with a heat-shock protocol (211). Plasmid pUDR203 was isolated from *E. coli* XL-I Blue cells with the Sigma GenElute Plasmid Miniprep Kit (Sigma-Aldrich) as specified by the manufacturer.

Table 4: Plasmids used in this study.

Plasmid	Characteristics	Reference
pROS11	2 µm ori , *AmdS*, gRNA-*CAN1*.Y gRNA-*ADE2*.Y	(175)
pUDR203	2 µm ori, *AmdS*, gRNA.*GPD1*.Y gRNA.*GPD2*.Y	This work

Genome editing

A dsDNA-repair fragment for deletion of *GDP1* was obtained by mixing primers 6969/6970 in a 1:1 molar ratio. This mixture was heated to 95 °C for 5 min and allowed to cool to room temperature. *S. cerevisiae* IMX2744 was constructed by co-transforming strain IMX2503 with gRNA-plasmid pUDR203 and the *GPD1* repair fragment, using the lithium-acetate method (178). Transformants were selected on SM supplemented with 20 g L^{-1} glucose (SMD) and acetamide (210), after which correct deletion of *GPD1* was checked by diagnostic colony PCR with DreamTaq polymerase (Thermo Fisher). pUDR203 was removed by growing non-selectively on SMD, while pUDR774 was retained to support uracil prototrophy. A correct transformant was restreaked thrice on SMD and stored at -80 °C.

Table 5: *S. cerevisiae* strains used in this study. *Kl* denotes *Kluyveromyces lactis*.

Strain name		Parental strain	origin
CEN.PK113-5D	*MATa ura3-52*	-	(168)
IMX581	*MATa ura3-52 can1::cas9-natNT2*	CEN.PK113-5D	(175)
IME324	*MAT*a *ura3-52 can1::cas9-natNT2* p426-*TEF*(empty)	IMX581	(77)
IMX2503	*MATa ura3-52 can1::cas9 natNT2 ALD6::*p*TDH3-eutE gpd2Δ* pUDR774	IMX581	(217)
IMX2744	*MATa ura3-52 can1::cas9 natNT2 ALD6::*p*TDH3-eutE gpd2Δ gpd1Δ* pUDR774	IMX2503	This study
IMS1247	Strain IMX2744 evolved for faster anaerobic growth on 50 g L^{-1} glucose and 1 g L^{-1} acetic acid	IMX2744	This study
IMX2736	*MATa ura3-52 can1::cas9 natNT2 gpd2::*(p*TDH3-RPE1,* p*PGK1-TKL1,* p*TEF1-TAL1,* p*PGI1-NQM1,* p*TPI1-RKI1,* p*PYK1-TKL2*) *sga1::*(p*DAN1-PRK,* p*TDH3-cbbM* (2 copies) *pTPI1-groES*, *pTEF1-groEL*) pUDR103 (*KlURA3*)	-	(197)

Anaerobic shake-flask cultivation

Anaerobic shake-flask cultures of single-colony isolates from sequential-batch-reactor (SBR) evolution experiments with *S. cerevisiae* IMX2744 were grown at 30 °C in 50-mL round-bottom shake-flasks containing 30 mL extra buffered SM supplemented with vitamins, 50 g L^{-1} glucose, 1 g L^{-1} acetic acid and Tween 80/ergosterol. Seven

single-colony isolates from each reactor isolated after 38 repeated-batch cycles, along with four isolates from reactor I and seven from reactor II isolated after 63 cycles, were analysed for their specific growth rates. Of these 25 single colony isolates, IMS1247 was selected with the fastest growth rate (0.27 h^{-1}), which was isolated from reactor I after 63 cycles. Shake-flasks were placed on an IKA KS 260 basic shaker (Dijkstra Verenigde BV, Lelystad, The Netherlands, 200 rpm) in a Bactron anaerobic chamber (Sheldon Manufacturing Inc., Cornelius, OR) under an atmosphere of 5% (v/v) H_2, 6% (v/v) CO_2 and 89% (v/v) N_2 (179).

Bioreactor cultivation

Anaerobic bioreactor batch and sequential-batch cultures were grown at 30 °C in 2-L bioreactors (Applikon, Delft, The Netherlands). Culture pH was maintained at 5.0 by automatic addition of 2 M KOH. Bioreactor cultures were grown on SM, supplemented with glucose (50 g L^{-1}), acetic acid (0.3 g L^{-1} or 1 g L^{-1} as indicated), Tween 80 (420 mg L^{-1}) and ergosterol (10 mg L^{-1}), and antifoam C (0.2 g L^{-1}) (Sigma-Aldrich). Bioreactor cultures were operated at a working volume of 1 L and sparged at 0.5 L min^{-1} with an N_2/CO_2 (90/10%) gas mixture, except for the laboratory-evolution cultures of strain IMX2744 and the anaerobic bioreactor batch of strains IMX2744 and IMS1247 on 50 g L^{-1} of glucose and 1 g L^{-1} of acetic acid, which were sparged with pure N_2. The outlet gas stream was cooled to 4 °C in a condenser to minimize evaporation. Oxygen diffusion was minimized by use of Norprene tubing (Saint-Gobain, Amsterdam, The Netherlands) and Viton O-rings (ERIKS, Haarlem, The Netherlands) (179). Inocula for bioreactor cultures were prepared in 500-mL shake-flasks containing 100 mL SMD. A first preculture, inoculated with a frozen stock culture and grown aerobically at 30 °C for 15-18 h, was used to inoculate a second preculture. Upon reaching mid-exponential phase (OD_{660} of 3-6), the second preculture was used to inoculate a bioreactor culture at an initial OD_{660} of 0.2-0.4. For inoculation of the co-culture, the OD_{660} was used to calculate how much volume from each strain needed to be added into the reactor. DNA isolated from the mix containing both strains, used for inoculation, was sequenced to determine the estimated starting inoculum ratio.

Laboratory evolution of *S. cerevisiae* IMX2744 was performed in sequential batch reactor (SBR) set-ups on SM supplemented with 50 g L^{-1} glucose and 1 g L^{-1} acetic acid. Cultures were sparged at 0.5 L min^{-1} with pure N_2. When, after having peaked, the CO_2 concentration in the off-gas had decreased to 60% of the highest CO_2-value measured during a batch cycle, an effluent pump was automatically switched on for 20 min. After this emptying phase only 0.05 L broth remained in the reactor. The effluent pump was then stopped and the inflow pump activated to supply fresh sterile medium from a 20-

L reservoir vessel. This refill phase was stopped via an electrical level sensor calibrated at a 1-L working volume.

Analytical methods

The optical density of cultures was measured at 660 nm on a Jenway 7200 spectrophotometer (Bibby Scientific, Staffordshire, UK). Biomass dry weight was measured as described previously (109). Metabolite concentrations were determined by high-performance liquid chromatography and a first-order evaporation rate constant of 0.008 h^{-1} was used to correct ethanol concentrations (109). Acetaldehyde concentrations in culture broth were determined after derivatization with 2,4-dinitrophenylhydrazine as described previously (197). As carbon recoveries could not be accurately calculated due to the high concentration of CO_2 in the inlet gas of bioreactor cultures, electron recoveries were used instead (11).

Whole-genome sequencing

Genomic DNA was extracted from an 100-mL aerobic, late-exponential-phase (OD_{660} of 10–15) shake-flask culture on SMD of *S. cerevisiae* strain IMX2503, using a Qiagen Blood & Cell Culture DNA kit and 100/G Genomics-tips (Qiagen, Hilden, Germany). Custom paired-end sequencing of genomic DNA was performed by Macrogen (Amsterdam, The Netherlands) on a 350-bp PCR-free insert library using Illumina SBS technology. Sequence reads were mapped against the genome of *S. cerevisiae* CEN.PK113-7D (212) to which a virtual contig containing p*TDH3-eutE* had been added, and processed as described previously (140).

To determine relative abundancy of strains IMX2736 and IMX2503 in bioreactor batch co-cultivation experiments, 50-mL culture samples were centrifuged for 10 minutes at 5,000 x *g* and biomass pellets temporarily stored at -20 °C. These pellets were used for genomic DNA extraction and Illumina sequencing. Sequence reads were mapped against the genome of *S. cerevisiae* CEN.PK113-7D to which a virtual contig containing p*TDH3-eutE*, p*DAN1-PRK*, p*TDH3-cbbM*, p*TPI1-groES* and p*TEF1-groEL* had been added. Unique SNPs in strains IMX2736 and IMS1247 were identified and used to quantify the percentage of each strain present in the sample.

Statistical analysis

Significance was assessed by performing a two-sided unpaired Student's t-test. Differences were considered to be significant if a p-value < 0.05 was obtained.

Availability of data and materials

Short read DNA sequencing data of the *Saccharomyces cerevisiae* strain IMS1247 were deposited at NCBI under BioProject accession number PRJNA972873. All measurement data used to prepare Figure 2, Figure 3, Figure 4, Figure 5, Figure 6, Table 1, Table 2 and Table 3 of the manuscript and Figure S1, Figure S2, Figure S3, Figure S4 and Figure S5 are available in Additional files 1, 2 and 3, which can be accessed online via https://doi.org/10.1101/2023.07.04.547682.

Funding

This work was supported by DSM Bio-based Products & Services B.V. (Delft, The Netherlands).

Acknowledgements

We want to thank Rinke van Tatenhove-Pel for stimulating discussions.

Supplementary information

Additional supplementary information

Available online via: https://doi.org/10.1101/2023.07.04.547682.

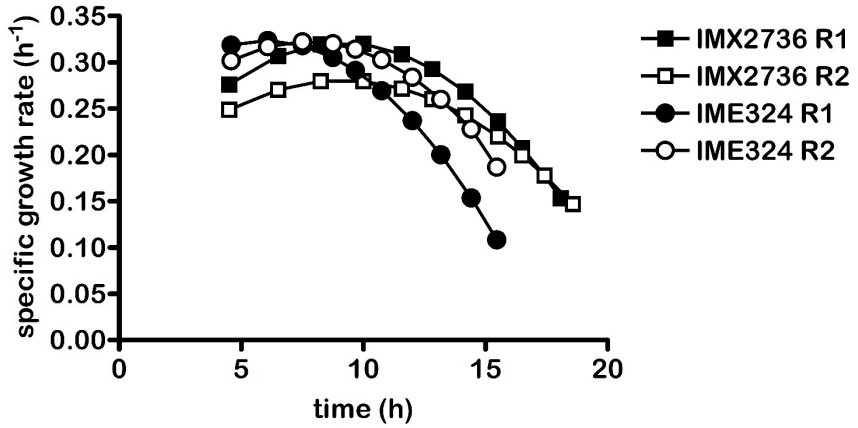

Figure S1: Specific growth rates at different timepoints of anaerobic duplicate batch cultures of *S. cerevisiae* strains IME324 (reference) and IMX2736 (non-ox PPP↑ *Δgpd2* p*DAN1-PRK* 2x p*TDH3-cbbM* p*TPI1-groES* p*TEF1-groEL*). Cultures were grown on synthetic medium containing 50 g L^{-1} glucose.

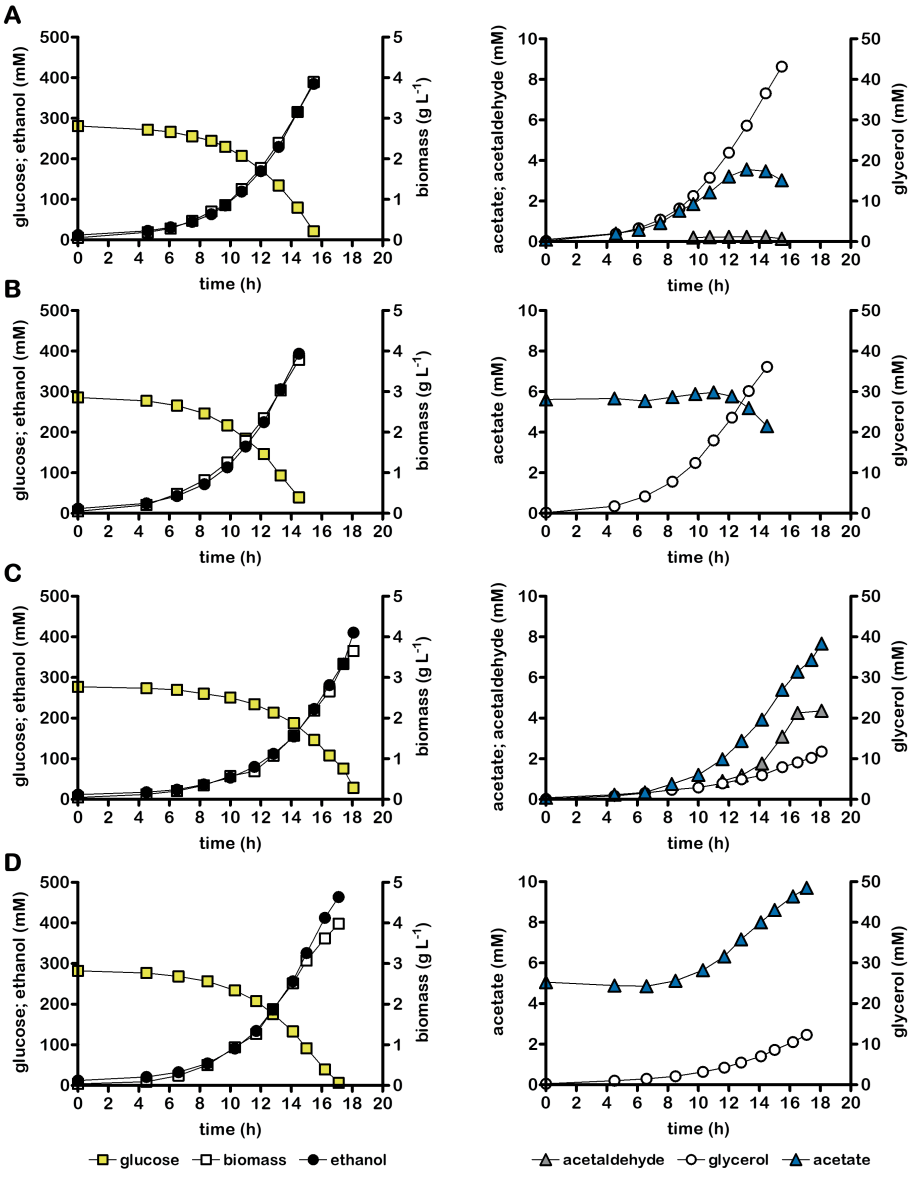

Figure S2: Growth, glucose consumption and product formation of anaerobic bioreactor batch cultures of individual *S. cerevisiae* strains, grown on SM with 50 g L^{-1} glucose (panels A and C) or on SM with 50 g L^{-1} glucose and 5 mmol L^{-1} acetate (panels B and D). Panels show data for *S. cerevisiae* strains IME324 (reference strain, A and B) and IMX2736 *(Δgpd2* non-ox PPP↑ *PRK* 2x *cbbM groES/groEL*, C and D). Representative cultures of independent duplicate experiments are shown, corresponding replicate of each culture shown in Fig. 2.

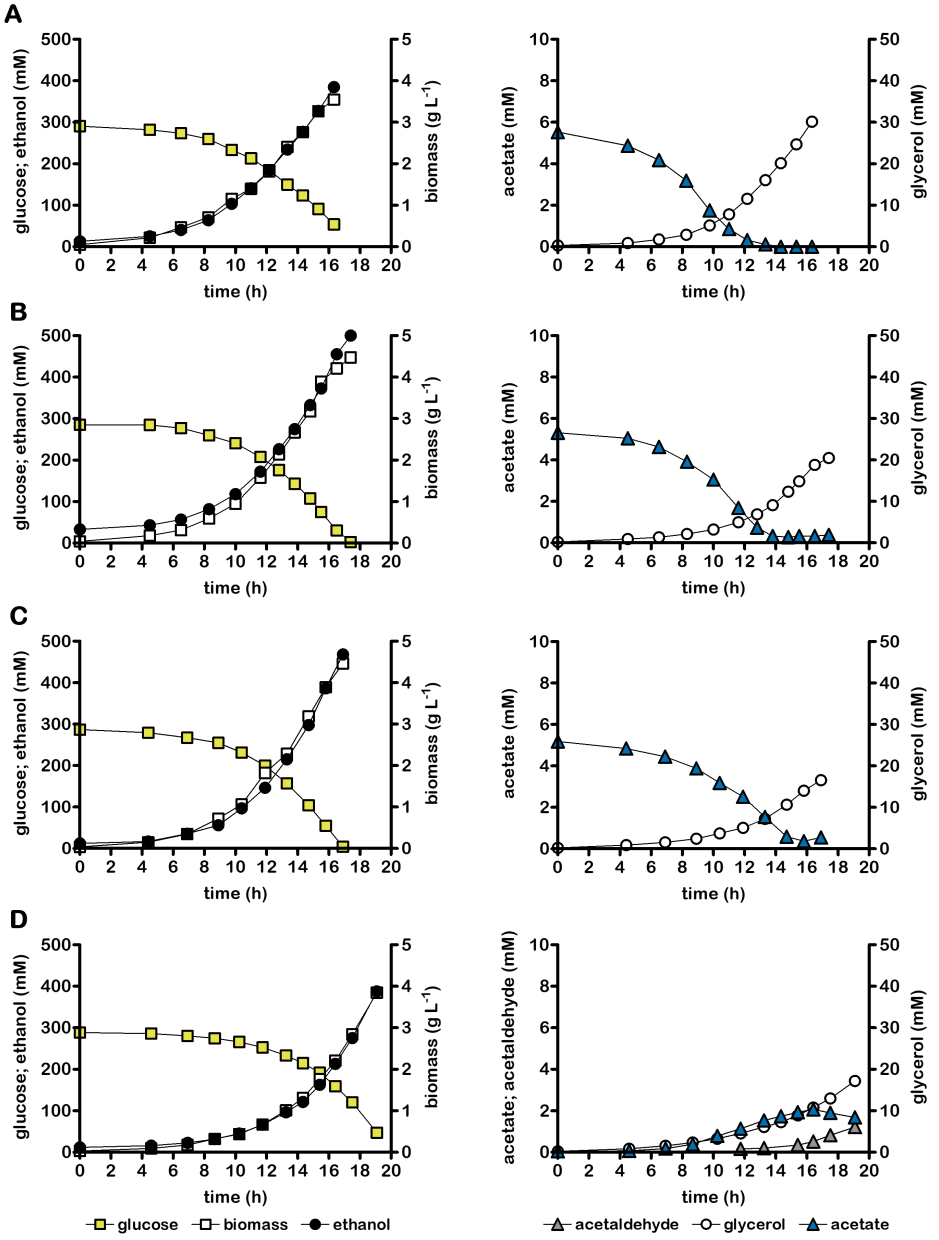

Figure S3: Growth, glucose consumption and product formation of anaerobic bioreactor batch cultures of S. cerevisiae strain IMX2503 (*Δgpd2 Δald6 eutE*) (A) and co-cultures of IMX2503 and IMX2736 (*Δgpd2* non-ox PPP↑ *prk* 2x *cbbM groES/ groEL*). Cultures were grown on synthetic medium containing 50 g L^{-1} glucose (panel D) or 50 g L^{-1} glucose and 5 mmol L^{-1} acetate (panels A-C) and were inoculated at a ratio of 1.4±0.2 (B), 0.8±0.1 (C) or 1.1±0.0 (D). Representative cultures of independent duplicate experiments are shown, corresponding replicate of each culture shown in Fig. 4.

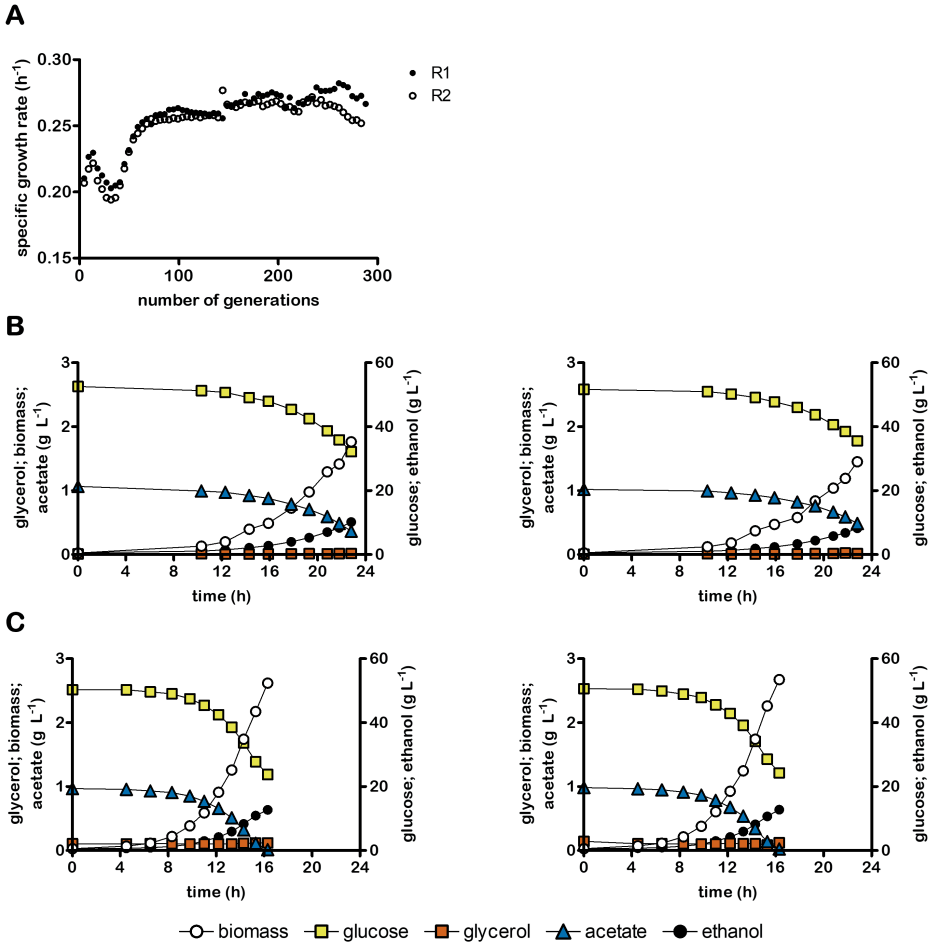

Figure S4: Evolution performed in SBR set-up to increase the specific growth rate of IMX2744 in anaerobic batch bioreactors on 50 g L^{-1} glucose and 1 g L^{-1} acetate. Overview of the specific growth rate as function of the number of generations (A). Growth, glucose consumption and product formation of both replicate anaerobic bioreactor batch cultures of *S. cerevisiae* strain IMX2744 (*Δgpd1 Δgpd2 Δald6 eutE*) (B) and evolved single colony isolate IMS1247 (C).

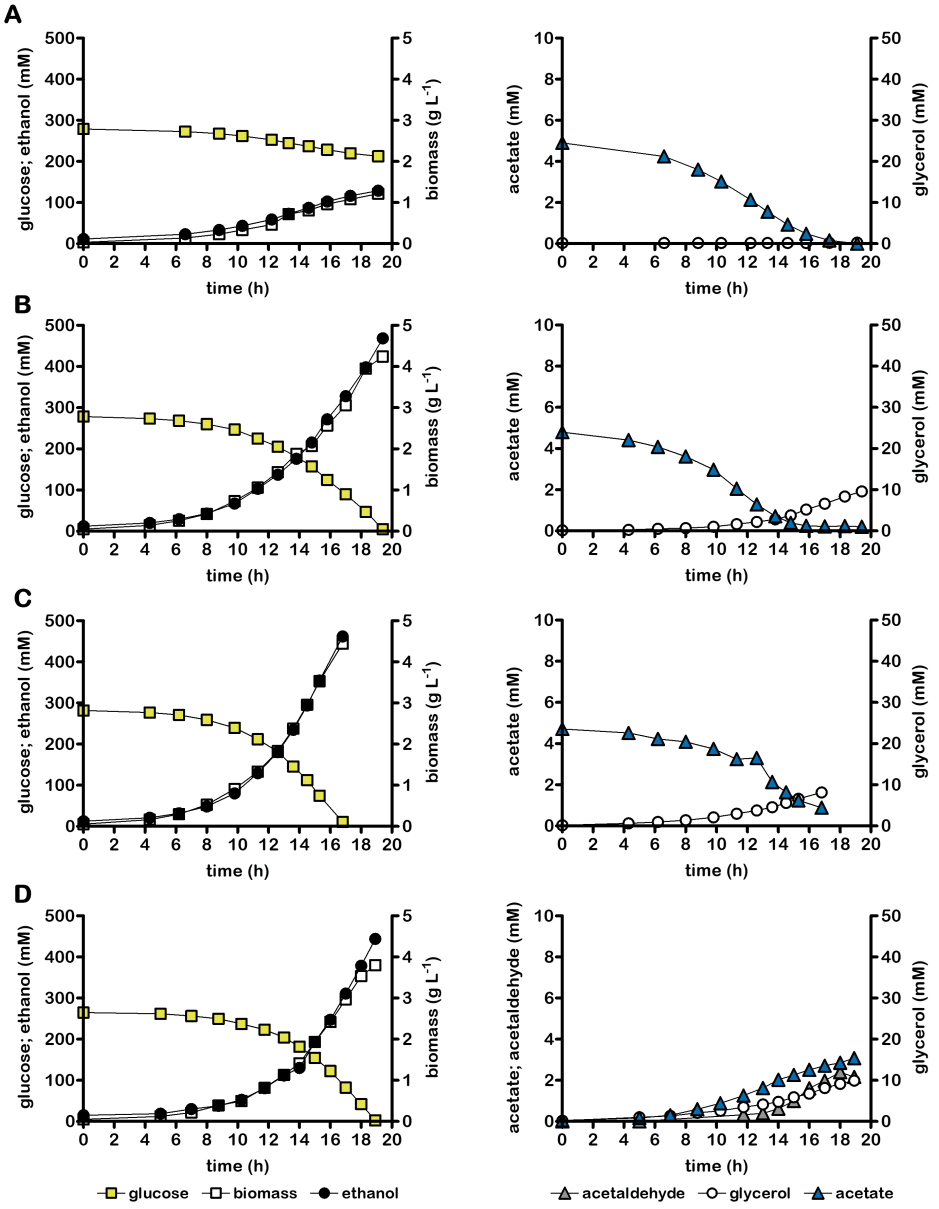

Figure S5: Growth, glucose consumption and product formation of anaerobic bioreactor batch cultures of *S. cerevisiae* strain IMS1247 (*Δgpd1 Δgpd2 Δald6 eutE*, evolved) (A) and co-cultures of IMS1247 and IMX2736 (*Δgpd2* non-ox PPP↑ *PRK* 2x *cbbM groES/groEL*). Cultures were grown on synthetic medium containing 50 g L^{-1} glucose (panel D) or 50 g L^{-1} glucose and 5 mmol L^{-1} acetate (panels A-C) and were inoculated at a ratio of 5.5±1.3 (B), 1.0±0.2 (C) or 1.3±0.4 (D). Representative cultures of independent duplicate experiments are shown, corresponding replicate of each culture shown in Fig. 5.

Table S1: Identified mutation based on whole genome sequencing in IMS1247 (*Δgpd1 Δgpd2 Δald6 eutE*) compared to IMX2503 (*Δgpd2 Δald6 eutE*).

Position	Location annotation	Mutation	Altered aa	Gene annotation
Chromosome 7, position 30790	Coding sequence of *HXK2*	G → A	G177S	Hexokinase isoenzyme 2
Chromosome 8, position 35455	Intergenic, in front of *GUT1*	A → T	n.a.	n.a.
Chromosome 8, position 35456	Intergenic, in front of *GUT1*	T → A	n.a.	n.a.
Chromosome 12, position 307396	Coding sequence of *GIS3*	C → T	S288S	Protein of unknown function

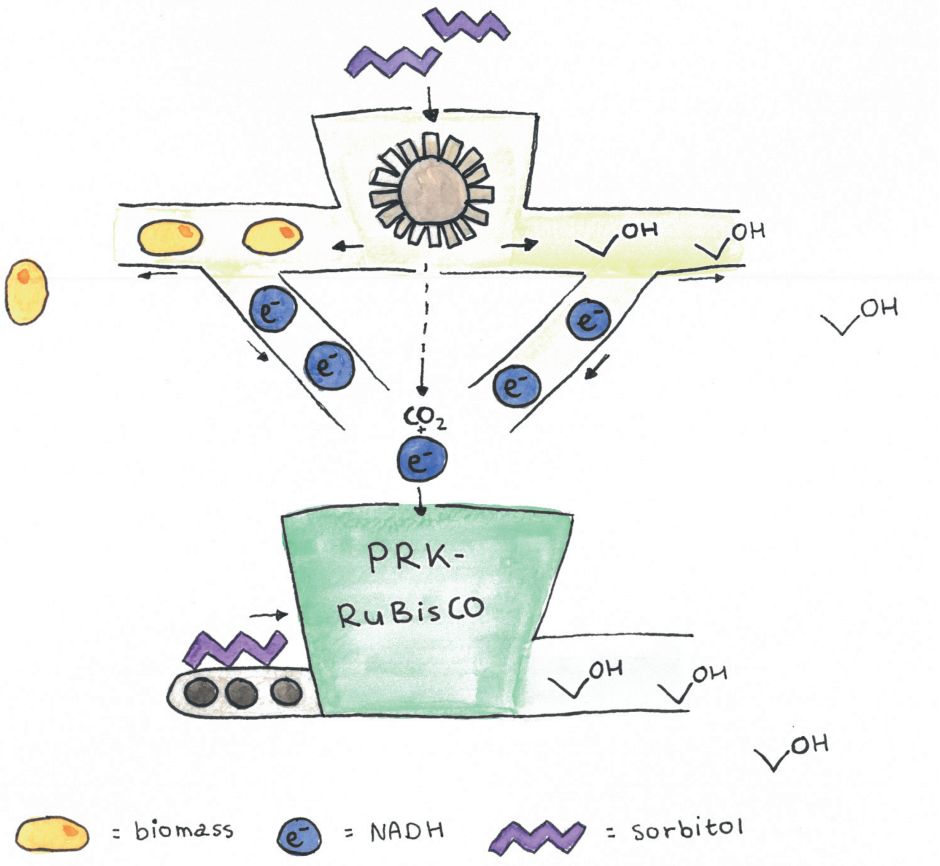
OH
OH
OH
e⁻
e⁻
e⁻
e⁻
CO2
e⁻
PRK-
RuBisCO
OH
OH
OH
= biomass
e⁻
= NADH
= sorbitol

Chapter 5

An engineered non-oxidative glycolytic bypass based on Calvin-cycle enzymes enables anaerobic co-fermentation of glucose and sorbitol by *Saccharomyces cerevisiae*

Aafke C.A. van Aalst, Robert Mans and Jack T. Pronk

This chapter is essentially as published in Biotechnology for Biofuels and Bioproducts (2022), 15(1):1-15.

Abstract

Saccharomyces cerevisiae is intensively used for industrial ethanol production. Its native fermentation pathway enables a maximum product yield of 2 moles of ethanol per mol of glucose. Based on conservation laws, supply of additional electrons could support even higher ethanol yields. However, this option is disallowed by the configuration of the native yeast metabolic network. To explore metabolic engineering strategies for eliminating this constraint, we studied alcoholic fermentation of sorbitol. Sorbitol cannot be fermented anaerobically by *S. cerevisiae* because its oxidation to pyruvate via glycolysis yields one more NADH than conversion of glucose. To enable re-oxidation of this additional NADH by alcoholic fermentation, sorbitol metabolism was studied in *S. cerevisiae* strains that functionally express heterologous genes for ribulose-1,5-bisphosphate carboxylase/oxygenase (RuBisCO) and phosphoribulokinase (PRK). Together with the yeast non-oxidative pentose-phosphate pathway, these Calvin-cycle enzymes enable a bypass of the oxidative reaction in yeast glycolysis.

Consistent with earlier reports, overproduction of the native sorbitol transporter Hxt15 and the NAD^+-dependent sorbitol dehydrogenase Sor2 enabled aerobic, but not anaerobic growth of *S. cerevisiae* on sorbitol. In anaerobic, slow-growing chemostat cultures on glucose-sorbitol mixtures, functional expression of PRK-RuBisCO-pathway genes enabled a 12-fold higher rate of sorbitol co-consumption than observed in a sorbitol-consuming reference strain. Consistent with the high K_m for CO_2 of the bacterial RuBisCO that was introduced in the engineered yeast strains, sorbitol consumption and increased ethanol formation depended on enrichment of the inlet gas with CO_2. Prolonged chemostat cultivation on glucose-sorbitol mixtures led to loss of sorbitol co-fermentation. Whole-genome resequencing after prolonged cultivation suggested a trade-off between glucose-utilization and efficient fermentation of sorbitol via the PRK-RuBisCO pathway.

Combination of the native sorbitol assimilation pathway of *S. cerevisiae* and an engineered PRK-RuBisCO pathway enabled RuBisCO-dependent, anaerobic co-fermentation of sorbitol and glucose. This study demonstrates the potential for increasing the flexibility of redox-cofactor metabolism in anaerobic *S. cerevisiae* cultures and, thereby, to extend substrate range and improve product yields in anaerobic yeast-based processes by enabling entry of additional electrons.

Background

With an estimated global output of 103 billion litres in 2021 (1), fuel ethanol produced from plant carbohydrates with the yeast *Saccharomyces cerevisiae* remains the largest process in microbial biotechnology based on product volume. Yeast-based ethanol production is predominantly performed in the USA and Brazil, using corn starch and cane sugar, respectively, as feedstocks (1, 233). Since carbohydrate feedstocks can contribute up to 70% to the overall process costs of industrial ethanol production, optimization of the ethanol yield on carbohydrates is of paramount importance for process economics (7, 234).

Hydrolysis of corn starch yields glucose as fermentable sugar, while sucrose, the predominant sugar in sugar cane, is hydrolysed to glucose and fructose by yeast invertase (66, 235). In *S. cerevisiae*, the conversion of these hexoses to ethanol and carbon dioxide occurs via the Embden-Meyerhof glycolysis (9) and the fermentation enzymes pyruvate decarboxylase and alcohol dehydrogenase (10). By producing two moles of ethanol per mol of hexose, this pathway conserves the entire degree of reduction of the substrate in ethanol and, thereby, reaches the theoretical maximum yield of ethanol on hexose sugars (131). In practice, this theoretical maximum is approached at near-zero growth rates in anaerobic retentostat cultures, in which the impact of yeast biomass formation on carbon and redox metabolism is negligible (23).

To achieve ethanol yields above 2 moles per mol of hexose, additional electrons would have to be fed into alcoholic fermentation, for example in the form of NADH. However, the configuration of the metabolic network of wild-type *S. cerevisiae* precludes this option. This constraint is illustrated by experiments in which formate was co-fed to anaerobic, glucose-limited cultures of *S. cerevisiae* strains overproducing the native NAD^+-dependent formate dehydrogenase Fdh1. In these cultures, the additional electrons provided by formate were channelled into glycerol production rather than into alcoholic fermentation (236). In *S. cerevisiae*, glycerol production occurs by NADH-dependent reduction of the glycolytic intermediate dihydroxyacetone phosphate to glycerol-3-phosphate by NAD^+-dependent glycerol-3-phosphate dehydrogenase (Gpd1 or Gpd2). This redox reaction is followed by dephosphorylation of glycerol-3-phosphate by glycerol-3-phosphatase (Gpp1 or Gpp2) (15, 78). In anaerobic cultures of wild-type *S. cerevisiae* strains, glycerol formation is essential for re-oxidation of 'surplus' NADH generated in biosynthetic reactions and has an economically significant negative impact on ethanol yields in industrial processes (19).

The rigidity of the *S. cerevisiae* metabolic network that prevents use of formate-derived NADH for alcoholic fermentation and necessitates glycerol production under anaerobic conditions for redox balancing, also prevents anaerobic fermentation of polyols such as mannitol and sorbitol. Mannitol is a main component of brown seaweed, which is investigated as a potential feedstock for ethanol production (237). Sorbitol occurs in flowering plants (238) and is industrially produced by catalytic hydrogenation of glucose (239). Although *S. cerevisiae* genomes harbour structural genes for polyol transporters and dehydrogenases, aerobic growth on mannitol and sorbitol typically requires prolonged adaptation (240, 241). Instantaneous aerobic growth is observed upon combined overexpression of either of the native hexose-transporter genes *HXT13*, *HXT15* or *HXT17* and a native gene encoding mannitol dehydrogenase (*MAN1* or *MAN2*) or sorbitol dehydrogenase (*SOR1* or *SOR2*) (242, 243). Since these polyol dehydrogenases are NAD^+-dependent, conversion of mannitol or sorbitol to pyruvate yields one more NADH than glucose upon conversion to pyruvate via the glycolytic pathway. Use of polyols as (co-)substrates therefore provides an interesting model to explore metabolic engineering strategies for feeding additional electrons into yeast-based ethanol production. Such additional electrons could alternatively be provided by, for example, co-feeding of electrochemically produced formate (244, 245) or cathode-associated electrobiotechnology (246, 247).

Our group explored expression of heterologous genes encoding the Calvin-cycle enzymes ribulose-5-phosphate kinase (PRK) and ribulose-1,5-bisphosphate carboxylase/oxygenase (RuBisCO) in yeast to re-route re-oxidation of 'surplus' NADH from glycerol formation to ethanol formation (109). This metabolic engineering strategy encompasses a bypass of the NADH-yielding glyceraldehyde-3-phosphate-dehydrogenase reaction in glycolysis, involving the native non-oxidative pentose-phosphate pathway, PRK and RuBisCO. This bypass allows for redox-neutral synthesis of 3-phosphoglycerate from glucose and CO_2. Subsequent conversion of 3-phosphoglycerate to ethanol via the regular yeast pathway for alcoholic fermentation then enables re-oxidation of NADH. Implementation of this strategy in engineered strains led to strongly reduced glycerol yields and correspondingly increased ethanol yields on sugar (109). Strains were further optimized by combined overexpression of non-oxidative pentose-phosphate pathway enzymes (139) to increase supply of ribulose-5-phosphate and deleting the structural gene encoding for the Gpd2 isoenzyme of glycerol-3-phosphate dehydrogenase. This approach yielded *S. cerevisiae* strains with an over 10% higher ethanol yield on glucose in anaerobic batch cultures, while showing the same rates of growth and ethanol production as a non-engineered parental strain (77).

The goal of the present study was to explore whether introduction of a functional PRK-RuBisCO bypass can accommodate the NADH generated upon the entry of sorbitol into glycolysis and, thereby, enable anaerobic (co-)fermentation of this polyol. To this end, Cas9-mediated genome editing was used to construct *S. cerevisiae* strains containing overexpression cassettes for *HXT15* and *SOR2* with or without a simultaneously introduced PRK-RuBisCO bypass. Anaerobic growth and product formation of the resulting engineered strains were quantitatively analysed in anaerobic mixed-substrate batch and chemostat cultures on glucose and sorbitol.

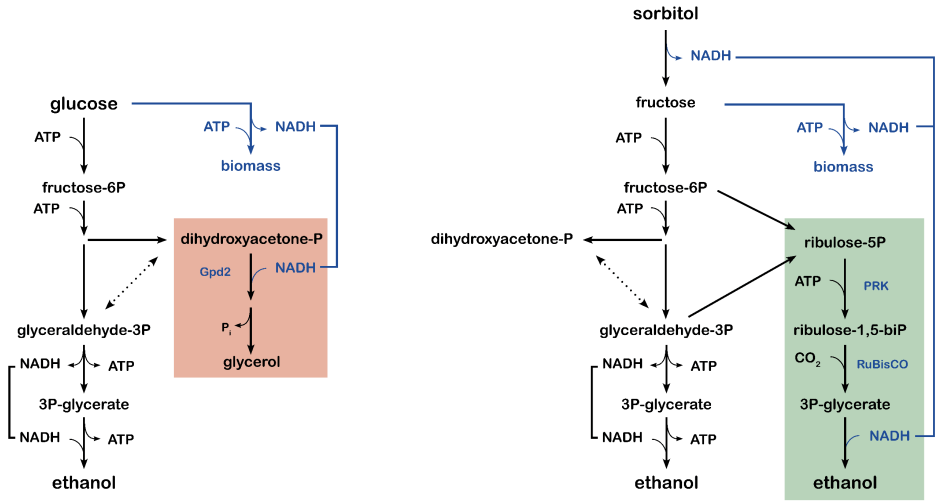

Figure 1: Schematic representation of NADH redox-cofactor balances during glucose fermentation by wild-type *S. cerevisiae* (left) and during sorbitol fermentation by an engineered PRK-RuBisCO-synthesizing strain (right). Coloured boxes indicate pathways used for anaerobic reoxidation of NADH generated in biosynthesis. The red box indicates the native *S. cerevisiae* glycerol pathway for NADH reoxidation, while the green box indicates the engineered PRK-RuBisCO bypass. in the last scenario, re-oxidation of 'surplus' NADH generated during biomass formation and/or sorbitol fermentation is coupled to ethanol production. This scenario involves an engineered strain expressing a gene for a membrane transporter that enables energy-independent uptake of sorbitol, together with an NAD^+-dependent sorbitol dehydrogenase and an optimized PRK-RuBisCO pathway. Gpd2: NAD^+-dependent glycerol-3-phosphate dehydrogenase; PRK: ribulose-5-phosphate kinase; RuBisCO: ribulose-1,5-bisphosphate carboxylase/oxygenase.

Results

Theoretical analysis of glucose or sorbitol fermentation by wild-type and engineered S. cerevisiae

Introduction of a PRK-RuBisCO-based 'bypass' of the oxidative reaction in glycolysis, as previously applied for improving ethanol yields of anaerobic glucose-grown cultures (77, 109), could theoretically enable redox-neutral fermentation of sorbitol (Fig. 1). Simultaneous operation of the native yeast glycolytic pathway and this bypass should then be redox-cofactor balanced according to the following 'redox half reactions':

3.5 sorbitol	→ 7 ethanol + 7 CO_2 + 3.5 NADH + 7 ATP	via native glycolysis
2.5 sorbitol + 3.5 NADH	→ 6 ethanol + 3 CO_2	via PRK-RuBisCO

The combined reaction would then provide a redox-balanced, net ATP-generating pathway for anaerobic fermentation of sorbitol (Fig 1) or, by analogy, mannitol:

6 sorbitol	→ 13 ethanol + 10 CO_2 + 7 ATP	combined

Functional expression of this pathway in a host organism could, in the absence of growth, support a theoretical maximum yield of 13:6 = 2.17 moles of ethanol per mol of sorbitol, which is 8.5% higher than the theoretical yield of ethanol on glucose. Compared to alcoholic fermentation of glucose, this pathway for sorbitol fermentation would yield 42% less ATP per mol of substrate. Provided that sufficient rates of alcoholic fermentation can be achieved to maintain industrially relevant productivities, a low ATP yield on sorbitol could be interesting as it should divert carbon substrate from biomass formation to ethanol production (70, 132).

To further assess the predicted impact of the proposed metabolic engineering strategy, it was implemented in a stoichiometric model of the core metabolic network of *S. cerevisiae* (118, 132). The model was then used to calculate biomass and ethanol yields at different specific growth rates. Calculations were based on the assumption that NADH from biomass formation (15), as well as NADH from the reaction catalysed by sorbitol dehydrogenase (Sor2) (Fig. 1), was exclusively re-oxidized by ethanol formation via the PRK-RuBisCO route. Consistent with the calculations presented above, sorbitol fermentation via the engineered pathway was predicted to result in a theoretical maximum yield of 2.17 mol ethanol (mol sorbitol)$^{-1}$ (Fig. 2, supplementary Table S1). Up to a specific growth rate of 0.1 h^{-1}, the predicted molar yield of ethanol on sorbitol remained above the theoretical maximum yield on glucose (Fig. 2, Supplementary Table S1). As anticipated based on the lower ATP yield from sorbitol fermentation, predicted biomass yields on this substrate (g biomass (mol sorbitol)$^{-1}$)

were 42% lower at all specific growth rates than corresponding biomass yields in glucose-grown cultures. At the same specific growth rate, the required biomass-specific rate of sorbitol fermentation was therefore predicted to be 71% higher than in glucose-grown anaerobic cultures.

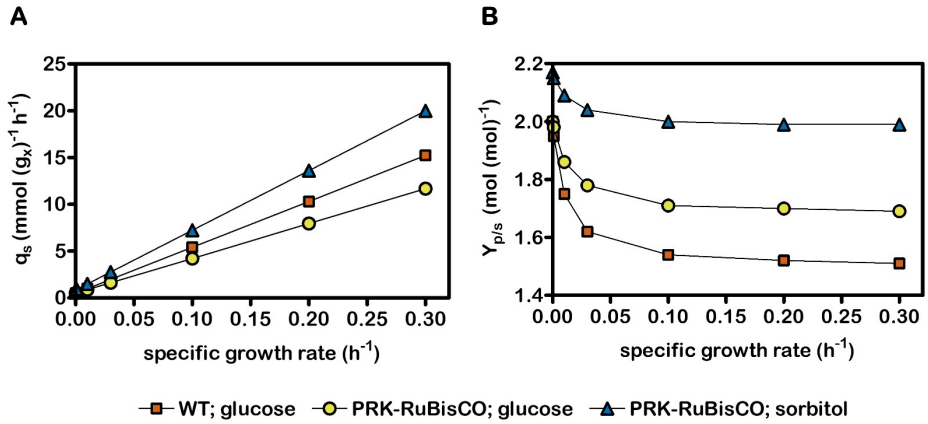

Figure 2: Model-based predictions on kinetics and stoichiometry of anaerobic growth of a reference *S. cerevisiae* strain on glucose and of a strain carrying a functional PRK-RuBisCO-based glycolytic bypass on glucose or on sorbitol as sole carbon source. (A) Biomass-specific substrate-uptake rates and (B) ethanol yield at different growth rates were simulated with an extended stoichiometric model of the core metabolic network of *S. cerevisiae* (118, 132).

Characterization of S. cerevisiae strains overexpressing HXT15 and SOR2

Consistent with results from an earlier study (243), aerobic batch cultures of *S. cerevisiae* IME611, which carried overexpression cassettes for *HXT15* and *SOR2*, grew on synthetic medium (SM) with sorbitol as sole carbon source at a specific growth rate of 0.23 h^{-1}. Under the same conditions, cultures of the congenic reference strain IME324 showed virtually no growth (Table S2). Strain IMX2506, in which overexpression of *HXT15* and *SOR2* was combined with deletion of *GPD2* and introduction of a PRK-RuBisCO pathway optimized for reduced glycerol production in anaerobic glucose-grown batch cultures (77), showed a similar growth rate on sorbitol (0.25 h^{-1}). Specific growth rates of these strains on sorbitol were approximately 33% lower than on glucose (0.36 h^{-1} and 0.35 h^{-1}, respectively; Table S2). However, despite the fast aerobic growth of strain IMX2506 on sorbitol, no growth was observed after up to 50 days of anaerobic incubation in SM with sorbitol as sole carbon source.

Co-utilization of glucose and sorbitol in anaerobic batch cultures

The inability of *S. cerevisiae* IMX2506 to grow anaerobically on sorbitol as sole carbon source suggested that the *in vivo* capacity of Hxt15, Sor2 and/or the engineered PRK-RuBisCO bypass was too low to sustain the rate of ATP production required for cellular maintenance. Such a scenario might still allow for anaerobic co-consumption of sorbitol and glucose. We therefore investigated growth in anaerobic bioreactor batch cultures on a mixture of 20 g L^{-1} glucose and 30 g L^{-1} sorbitol (Fig. 3, Table 1). No co-consumption of sorbitol was observed in mixed-substrate cultures of strains IME324 (reference) and IMX1489, which expressed an optimized PRK-RuBisCO bypass and carried a *gpd2Δ* mutation (Fig. 3, Table 1). In contrast, upon reaching stationary phase, strain IME611 , which carried overexpression cassettes for *HXT15* and *SOR2* had consumed 1.5 g L^{-1} (4.3 mmol g_x^{-1}; subscript x denotes biomass) sorbitol. Co-consumption coincided with a higher glycerol production (16.3 mmoL g_x^{-1}) than observed in strains IME324 and IMX1489 (11.8 mmol g_x^{-1} and 3.1 mmol g_x^{-1}, respectively, Table 1). This observation indicated that, in strain IME611, the surplus NADH generated during sorbitol co-fermentation (Fig. 1) was predominantly re-oxidized by glycerol formation. In contrast, when strain IMX2506, which combined the genetic modifications carried by strains IME611 and IMX1489, reached stationary phase, consumption of 2.3 g L^{-1} sorbitol (5.4 mmol g_x^{-1}) was accompanied by production of only 3.5 mmol g_x^{-1} glycerol. In addition, co-consumption of sorbitol by strain IMX2506 coincided with a higher apparent ethanol yield on glucose than observed for the three other strains (Table 1). These results indicated that overexpression of *HXT15* and *SOR2* in a strain with an active PRK-RuBisCO pathway enabled a modest co-fermentation of glucose and sorbitol in anaerobic batch cultures.

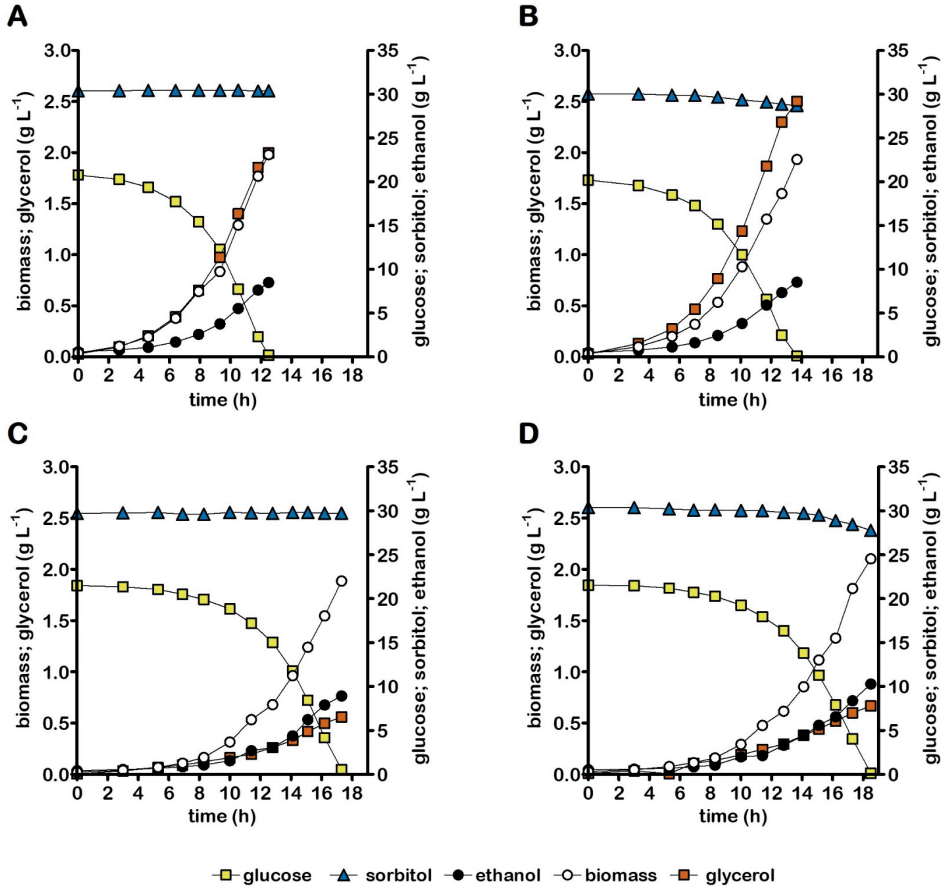

Figure 3: Growth, glucose consumption, sorbitol consumption, ethanol formation and glycerol formation in anaerobic bioreactor batch cultures of *S. cerevisiae* strains IME324 (reference strain) (A), IME611 (p*TEF1-HXT15* p*ACT1-SOR2*) (B), IMX1489 (optimized PRK-RuBisCO bypass and *gpd2Δ* mutation, (77)) (C) and IMX2506 (optimized PRK-RuBisCO bypass and *gpd2Δ* mutation, p*TEF1-HXT15* p*ACT1-SOR2*) (D). Cultures were grown anaerobically at pH 5 and at 30 °C on synthetic medium containing 20 g L^{-1} glucose and 30 g L^{-1} sorbitol as carbon sources. Representative cultures of independent duplicate experiments are shown, corresponding replicate of each culture shown in Fig. S3.

Table 1: Yields of biomass and ethanol on glucose, sorbitol consumption, stoichiometric relationships between glycerol production and biomass formation and specific growth rates in anaerobic bioreactor batch cultures of *S. cerevisiae* strains IME324 (reference strain), IME611 (p*TEF1-HXT15* p*ACT1-SOR2*), IMX1489 (optimized PRK-RuBisCO bypass and *gpd2Δ* mutation, *(77)*) and IMX2506 (optimized PRK-RuBisCO bypass and *gpd2Δ* mutation, p*TEF1-HXT15* p*ACT1-SOR2*). Cultures were grown on 20 g L^{-1} glucose and 30 g L^{-1} sorbitol. 'Substrates' refers to the combination of glucose and sorbitol. Specific growth rates and stoichiometries were calculated from at least 7 sampling points in the exponential growth phase. Values represent averages ± mean deviations of measurements on independent duplicate cultures for each strain.

Strain Relevant genotype	**IME324** reference	**IME611** *HXT15↑ SOR2↑*	**IMX1489** *gpd2*Δ PRK-RuBisCO	**IMX2506** *HXT15↑ SOR2↑gpd2*Δ PRK-RuBisCO
Specific growth rate (h^{-1})	0.31 ± 0.01	0.31 ± 0.00	0.30 ± 0.00	0.27 ± 0.00
Biomass yield on glucose (g g^{-1}) *	0.091 ± 0.001	0.089 ± 0.001	0.090 ± 0.005	0.095 ± 0.001
Ethanol yield on glucose (mol mol^{-1})*	1.47 ± 0.02	1.51 ± 0.01	1.64 ± 0.04	1.80 ± 0.05
Ethanol yield on substrates (mol mol^{-1})	1.47 ± 0.02	1.42 ± 0.01	1.64 ± 0.04	1.65 ± 0.05
Glycerol produced (mmol (g_x^{-1}))	11.8 ± 0.2	16.3 ± 0.2	3.1 ± 0.1	3.5 ± 0.0
Sorbitol consumed (mmol (g_x^{-1}))	<0.3	4.3 ± 0.1	<0.3	5.4 ± 0.2
Degree of reduction recovery (%)	100-102	100-101	100-104	95-99

* These yield values on glucose also include ethanol and biomass formed by the additional consumption of sorbitol.

Co-fermentation of sorbitol by anaerobic mixed-substrate chemostat cultures

In anaerobic mixed-substrate batch cultures of strain IMX2506, sorbitol consumption predominantly occurred when the supplied glucose was already nearly consumed (Fig. 3, panel D). Based on this observation, we hypothesized that glucose and sorbitol competed for Hxt transport proteins. Sorbitol co-consumption at low glucose concentrations was investigated in anaerobic chemostat cultures. In chemostat cultures, culture broth is removed at a fixed flow rate (F_{out}) while the culture volume (V_L) is kept constant by continuous supply of fresh medium, thus controlling the specific growth rate (248, 249). The anaerobic chemostat cultures were grown on a mixture of 10 g L^{-1} glucose and 10 g L^{-1} sorbitol at a dilution rate (F_{out}/V_L which, in steady-state cultures, equals specific growth rate) of 0.025 h^{-1}. In these chemostat cultures, residual glucose concentrations were below 0.036 g L^{-1}. In chemostat cultures of strain IMX2506, anaerobic sorbitol conversion rates were 12-fold higher than in cultures of strain IME611, which carried overexpression cassettes for *HXT15* and *SOR2* but did not harbor a PRK-RuBisCO bypass (Table 2). In cultures of the congenic reference strain IME324, which carried no PRK-RuBisCO bypass or *HXT15*

and *SOR15* overexpression cassettes (Table 2), glucose was virtually completely consumed but sorbitol concentrations in the chemostat cultures equalled those in the medium inflow. This observation reflected the reference strain's inability to anaerobically consume sorbitol. However, the PRK-RuBisCO-based reference strain IMX1489, which did not contain overexpression cassettes for *HXT15* and *SOR15*, did co-consume sorbitol (Table 2, Fig. 4B).

The *Thiobacillus denitrificans* form-II RuBisCO present in strains IMX1489 and IMX2506 has a high K_m for CO_2 (0.26 mM; (110)). To verify involvement of the PRK-RuBisCO pathway in the increased sorbitol consumption by engineered yeast strains, the inlet gas, which routinely consisted of a mixture of 90% N_2 and 10% CO_2, was switched to pure N_2 during fermentation runs. This switch led to an instantaneous, progressive increase of the residual sorbitol concentration, with a profile that closely corresponded to wash-in kinetics in the complete absence of sorbitol consumption (Fig. 4). These results, in combination with the absence of sorbitol consumption in strain IME611 lacking the PRK-RuBisCO pathway (Table 2), confirmed involvement of *in vivo* RuBisCO activity in anaerobic sorbitol co-fermentation.

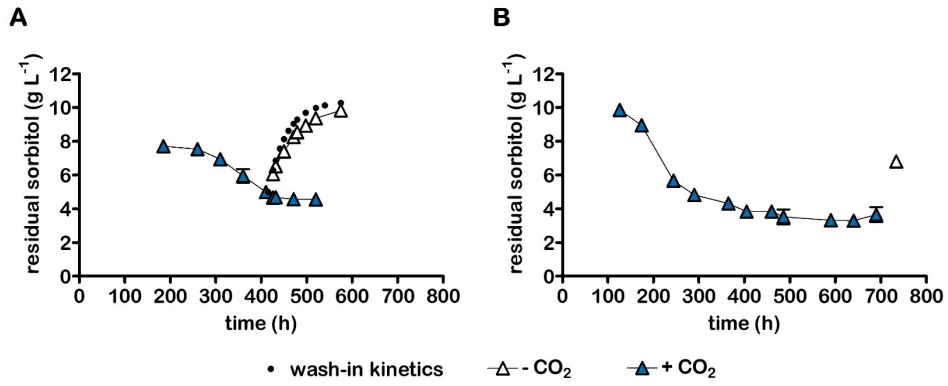

Figure 4: Sorbitol consumption by anaerobic chemostat cultures of *S. cerevisiae* strains IMX2506 (optimized PRK-RuBisCO bypass and *gpd2*Δ mutation, p*TEF1-HXT15* p*ACT1-SOR2*) (A) and IMX1489 (optimized PRK-RuBisCO bypass and *gpd2*Δ mutation (77)) (B). Chemostat cultures were grown at a dilution rate of 0.025 h^{-1} on 10 g L^{-1} of glucose and 10 g L^{-1} of sorbitol. A: Average residual sorbitol concentration ± standard deviation in four chemostat cultures of strain IMX2506. After 400 h, the CO_2 content of the inlet gas was reduced to zero in two of the four cultures. The dotted line represents expected wash-in kinetics of sorbitol in the absence of sorbitol consumption: $c(t)=c_{in}-((c_{in}-c_{400})*e^{(-D*t)})$ with c = residual sorbitol concentration, c_{400} = sorbitol concentration at 400 h, c_{in} = sorbitol concentration in medium feed and D = dilution rate. B: Average sorbitol concentration ± standard deviation in two chemostats of strain IMX1489. CO_2 supplementation was stopped at 700 h.

Table 2: Yields of biomass and ethanol on glucose, sorbitol consumption, biomass-specific sorbitol uptake rates and stoichiometric relationships between glycerol production and biomass formation in anaerobic bioreactor chemostat cultures of *S. cerevisiae* strains IME324 (reference strain), IME611 (p*TEF1-HXT15* p*ACT1-SOR2*), IMX1489 (optimized PRK-RuBisCO bypass and *gpd2*Δ mutation, (77)) and IMX2506 (optimized PRK-RuBisCO bypass and *gpd2*Δ mutation, p*TEF1-HXT15* p*ACT1-SOR2*). 'Substrates' refers to the combination of glucose and sorbitol. Cultures were grown at a dilution rate of 0.025 h^{-1} on 10 g L^{-1} of glucose and 10 g L^{-1} of sorbitol (pH 5). Values represent averages ± mean deviations of measurements on independent steady-state triplicate cultures of strain IME611 and duplicate cultures of strain IMX2506.

Strain Relevant genotype	**IME324** Reference	**IME611** *HXT15↑ SOR2↑*	**IMX1489** *gpd2*Δ PRK-RuBisCO	**IMX2506** *HXT15↑ SOR2↑ gpd2*Δ PRK-RuBisCO
Biomass yield on substrates (g g^{-1})	0.079 ± 0.00	0.079 ± 0.003	0.067 ± 0.005	0.074 ± 0.002
Yield of ethanol on glucose (mol mol^{-1})*	1.62 ± 0.03	1.66 ± 0.07	2.96 ± 0.00	2.86 ± 0.02
Ethanol yield on substrates (mol mol^{-1})	1.63 ± 0.04	1.61 ± 0.06	1.76 ± 0.01	1.83 ± 0.04
Glycerol/biomass (mmol g_x^{-1})	8.1 ± 0.2	10.8 ± 0.5	0.6 ± 0.2	1.0 ± 0.0
Sorbitol consumed (mmol g_x^{-1})	<0.5	2.2 ± 1.1	33.9 ± 3.0	27.0 ± 0.1
Biomass-specific sorbitol uptake rate (mmol g_x^{-1} h^{-1})	<0.02	0.06 ± 0.03	0.89 ± 0.08	0.67 ± 0.00
Degree of reduction recovery (%)	99-100	98-102	98-99	100-101

*These yield values on glucose also include ethanol and biomass formed by the additional consumption of sorbitol.

Prolonged continuous cultivation on a glucose-sorbitol mixture does not select for improved sorbitol fermentation

During anaerobic chemostat cultivation of strain IMX2506 on sorbitol and glucose, sorbitol co-consumption increased during the first 10 volume changes. After this point, it stabilized for approximately 3 volume changes (Fig. 4A), leaving ~4 g L^{-1} of sorbitol unused. Based on the assumption that improved co-consumption of sorbitol by spontaneous mutants would confer a selective advantage, two new anaerobic continuous cultures were grown on a glucose and sorbitol mixture for over 80 generations. During the first approximately 40 generations, sorbitol consumption by the mixed-substrate chemostat cultures improved. However, contrary to expectation, sorbitol co-consumption deteriorated rather than improved further in both evolution experiments. In evolution line 1, sorbitol co-consumption completely ceased, while in evolution line 2 its rate declined by approximately 3.5 fold (Fig. 5A). In both prolonged continuous cultures, glycerol production increased, indicating a decline of the *in vivo* activity of the PRK-RuBisCO pathway (Fig. 5B).

To explore underlying mechanisms for the reduced sorbitol co-consumption observed during prolonged mixed-substrate cultivation, whole-genome sequencing was performed on culture samples. After 86 generations, sequence data from both chemostat cultures showed an identical non-synonymous point mutation in the open-reading frame of the spinach *PRK* sequence, which caused an alanine-to-aspartate change at position 193 in PRK (A193D). In evolution line 1, in which sorbitol co-consumption was virtually completely abolished, 73% of the *PRK* sequence reads carried the mutation. A lower percentage (45%) of reads carrying this mutation was identified in evolution line 2, in which some sorbitol co-consumption was still observed after 86 generations. Sequence alignment showed that the mutation in *PRK* involves a highly conserved amino acid residue in type II PRK proteins from 49 different species (Archaea, Eukaryotes and Cyanobacteria; position 372 in the multiple sequence alignment as identified in supplementary figure 6 of the publication by Gurrieri et al. (2019) (250)). In these dimeric type II PRK enzymes (including the spinach PRK expressed in this study), an alanine residue is invariably found at this position, while the bacterial allosterically regulated and octameric type I PRK enzymes, either have an alanine or a threonine in this position. For both PRK types, this residue is located on the edge of a β-sheet (250, 251). We hypothesize that exchange of a neutral residue (alanine/threonine) for a negatively charged residue (aspartate) in a highly conserved position disrupted protein folding and thereby reduced or even abolished PRK activity.

No sequence changes were found in other coding regions in the analysed culture samples where sorbitol consumption was greatly reduced after prolonged cultivation. However, sequence data from both evolution experiments displayed segmental aneuploidy in multiple chromosomes (Fig. S1, Table S3). Some amplifications differed between the two experiments or, based on read coverages, only occurred in part of the population. Since the duplicated regions carried multiple genes, no definitive interpretation is possible without extensive reverse engineering studies (203, 252). However, we note that ca. 100 kb duplication of a fragment of chromosome IV (~1,075,000-1,175,000) that was found in both evolution experiments carried the *HXT6* and *HXT7* genes. These genes, which encode the major high-affinity glucose transporters of *S. cerevisiae*, are highly expressed in glucose-limited chemostat cultures (253). A large duplication of a centromeric region of chromosome XV (~0-495,000) carried the *GPD2* locus into which the overexpression cassettes for six genes encoding non-oxidative pentose-phosphate-pathway enzymes had been integrated. In addition, this region harboured *HXT11* which, like *HXT15*, encodes a functional sorbitol transporter (243).

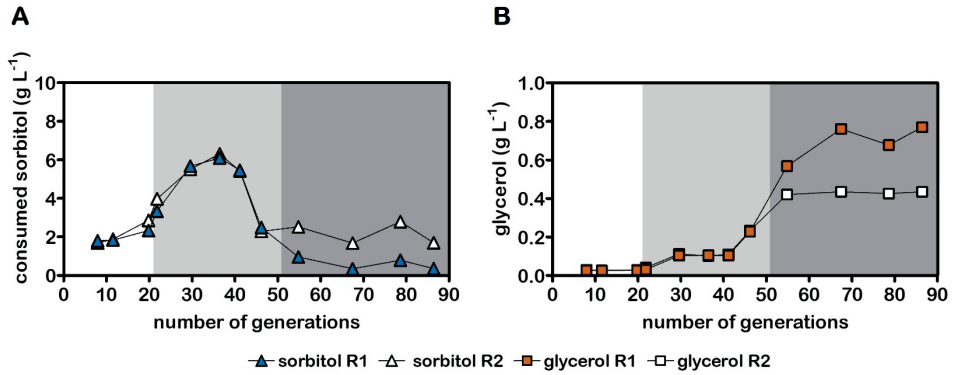

Figure 5: Sorbitol consumption (A) and glycerol production (B) in duplicate anaerobic chemostat cultures of strain IMX2506 (optimized PRK-RuBisCO bypass and *gpd2*Δ mutation, p*TEF1-HXT15* p*ACT1-SOR2*). For the first 20 generations, the cultures were grown on a mixture of 10 g L^{-1} sorbitol and 10 g L^{-1} glucose at a dilution rate of 0.05 h^{-1}. After 20 generations, the dilution rate was decreased to 0.025 h^{-1} and after 50 generations the substrate mixture was changed to 20 g L^{-1} sorbitol and 10 g L^{-1} glucose.

Discussion

Introduction of functional Calvin-cycle enzymes in *S. cerevisiae* was previously shown to couple re-oxidation of 'surplus' NADH, generated during biomass formation in anaerobic cultures, to ethanol formation, thereby reducing glycerol production and enhancing ethanol yield on sugars (77, 109, 115, 116). The present study demonstrates that expression of a non-oxidative, PRK-RuBisCO bypass of glycolysis enabled a 12-fold higher rate of sorbitol conversion in anaerobic chemostat cultures grown on glucose-sorbitol mixtures than observed in cultures of a reference *S. cerevisiae* strain.

As reported for aerobic growth of *S. cerevisiae* on sorbitol (243), overexpression of *HXT15* and *SOR2* was required to achieve a modest co-utilization of sorbitol by anaerobic batch cultures of *S. cerevisiae* grown on glucose-sorbitol mixtures (Fig. 3). In contrast, constitutive overexpression of these genes was not required for a much more extensive sorbitol co-consumption by slow-growing, glucose-limited anaerobic chemostat cultures of PRK-RuBisCO-synthesizing strains (Fig. 4B). Acquisition of the ability to aerobically consume sorbitol in batch cultures was previously attributed to mutations in the Tup1-Cyc8 complex, that relieve transcriptional repression of many genes, including *HXT15* and *SOR2* (254). However, whole-genome sequencing did not identify such mutations in steady-state chemostat cultures of the PRK-RuBisCO-synthesizing reference strain IMX1489, which co-consumed sorbitol but did not contain overexpression cassettes for *HXT15* and *SOR15*. Gene expression patterns in

S. cerevisiae are strain dependent (255) and glucose concentrations strongly affect transcriptional regulation of *HXT* transporter genes (253). Furthermore, expression of *HXT13* and *HXT15* (two polyol transporters) has been linked to growth on non-fermentable carbon sources (256). We hypothesize that the conditions in our chemostat setup, which combined low residual glucose concentrations with the presence of sorbitol, stimulated expression of native *HXT13* and *HXT15* genes and thereby enabled sorbitol utilization in strain IMX1489 (Fig. 4B).

Although expression of the PRK-RubisCO bypass enabled anaerobic co-consumption of sorbitol and glucose, anaerobic growth of *S. cerevisiae* on sorbitol as sole carbon source was not yet achieved. In order for sorbitol fermentation to sustain anaerobic growth, the biomass-specific rate of ATP formation should exceed the cellular ATP requirement of anaerobic cultures for cellular maintenance processes (approximately 1 mmol ATP (g biomass)$^{-1}$ h^{-1}; (23)). At an ATP stoichiometry of 1.17 mol ATP (mol sorbitol)$^{-1}$ calculated for the PRK-RuBisCO-based pathway, the threshold biomass-specific rate of sorbitol fermentation for anaerobic growth would then equal 0.86 mmol (g biomass)$^{-1}$ h^{-1}. The biomass-specific sorbitol uptake rate of strain IMX2506 in anaerobic mixed-substrate chemostat cultures of 0.67 mmol sorbitol g_x^{-1} h^{-1} (Table 2) remained below this threshold.

In aerobic batch cultures of *HXT15*- and *SOR2*-overexpressing *S. cerevisiae* strains (IME611 and IMX2506) (Fig. S2) a specific growth rate of 0.22 h^{-1} was observed. At an estimated biomass yield of 0.07 g_x^{-1} (mmol sorbitol)$^{-1}$ in these respiro-fermentative cultures, this growth rate would correspond to a biomass-specific sorbitol-consumption rate of 3.0 mmol (g biomass)$^{-1}$ h^{-1}. In anaerobic cultures, such an *in vivo* activity of sorbitol transport and oxidation to fructose would be over 3-fold higher than required to meet maintenance-energy requirements. Alternatively, *in vivo* capacity of the PRK-RuBisCO pathway might be too low to support anaerobic growth on sorbitol alone. Since form-II RuBisCO enzymes such as *T. denitrificans* cbbM exhibit low k_{cat} values (110) and require chaperones for functional expression, high-level expression is required to support the *in vivo* fluxes required for anaerobic growth on sorbitol as sole carbon source. Implementation of RuBisCO variants with a higher k_{cat} (257), potentially in combination with increased expression of PRK, may enable anaerobic growth on sorbitol.

Instead of targeted engineering of the PRK-RuBisCO pathway, we tried to use adaptive laboratory evolution to identify key genes involved in its *in vivo* capacity. While, in two parallel evolution experiments, the degree of sorbitol co-consumption initially increased, it subsequently deteriorated. This deterioration was accompanied by an

increase of the glycerol concentration in the cultures that indicated loss of functionality of the PRK-RuBisCO pathway. No mutations or reduction of copy number of the *cbbM* expression cassettes were observed upon prolonged cultivation. This observation suggested that protein burden caused by RuBisCO overexpression was unlikely to be a key factor in the unexpected loss of pathway functionality. Instead, a mutation in the *PRK* gene, duplication of overexpression cassettes for non-oxidative pentose phosphate pathway enzymes and duplication of a genomic region carrying the *HXT6* and *HXT7* genes that both encode the high-affinity glucose transporters, were found. These mutations may indicate a trade-off between kinetics of sorbitol fermentation via the PRK-RuBisCO bypass and kinetics of glucose uptake at the very low residual glucose concentrations in the chemostat cultures. Further research is required to investigate whether this trade-off is impacted by the reported toxic effects of PRK overexpression (142).

This study provides a proof of principle for engineering a redox-cofactor-neutral bypass of glycolysis to enable entry of additional electrons in the main yeast alcoholic fermentation pathway and. This strategy enabled a higher theoretical maximum yield of ethanol than possible with sugars as sole source of electrons. In addition to further analysis of the rate-controlling steps in the PRK-RuBisCO pathway, alternative bypasses of the oxidative step in glycolysis with a better ATP stoichiometry may be explored. A particularly interesting option is offered by the combined expression of a heterologous phosphoketolase, phosphotransacetylase and acetylating acetaldehyde dehydrogenase (107, 108). In contrast to the PRK-RuBisCO strategy, this redox-cofactor-neutral bypass of glyceraldehyde-3-phosphate dehydrogenase has a net positive ATP yield (132). In addition to improving polyol fermentation, further research on extending flexibility of redox-cofactor balancing in yeast may ultimately enable the co-consumption of auxiliary electron donors such as formic acid and/or hydrogen (82, 236, 258) to boost ethanol yields on sugars beyond current limits.

Materials and methods

Strains and maintenance

S. cerevisiae strains used in this study (Table 4) belong to the CEN.PK lineage (168, 208) and were propagated in YPD medium (10 g L^{-1} Bacto yeast extract, 20 g L^{-1} Bacto peptone, 20 g L^{-1} glucose). *Escherichia coli* XL-I Blue-derived strains were propagated in LB medium (10 g L^{-1} Bacto tryptone, 5 g L^{-1} Bacto yeast extract, 20 g L^{-1} glucose) supplemented with 100 µg mL^{-1} ampicillin. After addition of sterile glycerol (30% v/v) to late-exponential-phase *S. cerevisiae* cultures or overnight *E. coli* cultures, 1-mL aliquots were frozen and stored at -80 °C.

Molecular biology techniques

Cas9-based genome editing (175) was employed for markerless integration of expression cassettes in the intergenic region X-2 (259). Oligonucleotide primers used in this study are listed in Table S4 (available online). Plasmid fragments and yeast integration cassettes were PCR amplified with Phusion High Fidelity DNA polymerase (Thermo Fisher Scientific, Waltham MA) and Dreamtaq polymerase (Thermo Fisher) was used for diagnostic PCR. Yeast genomic DNA was isolated as described by (173). PCR-amplified DNA fragments were purified from agarose gels with a ZymoClean Gel DNA kit (Zymo Research, Irvine CA) or purified directly from the PCR mix with a GeneJET kit (Thermo Fisher). Purified plasmid backbone and insert fragments were assembled with a Gibson assembly cloning kit (New England Biolabs, Ipswich MA), downscaled to 5-µL reaction volume. After plasmid assembly, 1 µL of the resulting mixture was used for heat-shock transformation of *E. coli* XL-I Blue (211). Plasmids were isolated from *E. coli* using Sigma GenElute Plasmid kit (Sigma-Aldrich).

Construction of plasmids

Plasmids used and constructed in this study are listed in Table 3. To remove its p*TEF1* and t*CYC1* promoter and terminator sequences, p426-*TEF* (177) was used as template for PCR amplification with primer pairs 15514/10901 and 15515/7388. The amplified fragments were purified and digested with KpnI and PfoI (Thermo Fisher). Digestion products were repurified and ligated with T4 DNA ligase (Thermo Fisher), yielding pUD968. p*ACT1* and t*CPS1* sequences were amplified from genomic DNA of strain CEN.PK113-7D with primer pairs 15548/15549 and 15550/15551, respectively. Gibson assembly of the resulting fragments with KpnI-linearized pUD968 yielded plasmid pUDE885. Primers 16709 and 16710, with sequence homology to the 5' and 3' regions of the coding region of *SOR2* and to the 3' and 5' termini of the p*ACT1* and t*CPS1* sequences, respectively, were used to amplify the coding region of *SOR2* from genomic DNA of strain CEN.PK113-7D. Gibson assembly of KpnI-linearized pUDE885 with the resulting DNA fragment yielded pUDE941.

Construction of expression cassettes

A p*TEF1*-*HXT15*-t*CYC1* expression cassette was obtained by assembling three DNA fragments. A *TEF1* promoter fragment and a *CYC1* terminator fragment were amplified from p426-*TEF* (177) with primer pairs 16711/17031 and 17032/16712, respectively. The coding region of *HXT15* ORF was amplified with primer pair 16705/16706 from genomic DNA of strain CEN.PK113-7D. Assembly of these three fragments by homologous recombination of terminal sequences introduced during amplification yielded a p*TEF1*-*HXT15*-t*CYC1* expression cassette for integration at the X-2 locus (259). Amplification of the p*ACT1*-*SOR2*-t*CPS1* expression cassette from

pUDE941 with primer pair 16715/16716 added terminal sequences homologous to the X-2 integration site on Chromosome X of *S. cerevisiae* (259) and to synthetic homologous recombination sequence A (SHR-A) (176). These terminal sequences allowed for simultaneous *in vivo* assembly and integration into the X-2 locus with the p*TEF1*-*HXT15*-t*CYC1* cassette.

Table 3: Plasmids used and constructed in this study.

Name	Characteristics	Origin
pUDR538	*Hyg*, gRNA.*X-2*-2 µm-gRNA.*X-2*	(260)
p426-*TEF*	2 µm, *URA3*, p*TEF1*-t*CYC1* (empty vector)	(177)
pUD968	2 µm, *URA3*	This study
pUDE885	2 µm, *URA3*, p*ACT1*-t*CPS1*	This study
pUDE941	2 µm, *URA3*, p*ACT1*-*SOR2*-t*CPS1*	This study

Yeast genome editing

The lithium-acetate method (178) was used for yeast transformation. *S. cerevisiae* IMX2411 was constructed by transforming strain IMX581 with pUDR538, along with p*ACT1*-*SOR2*-t*CPS1*, p*TEF1*, *HXT15* and t*CYC1* DNA fragments. Transformants were selected on YPD plates (10 g L^{-1} Bacto yeast extract, 20 g L^{-1} Bacto peptone, 20 g L^{-1} glucose and 20 g L^{-1} agar) supplemented with 200 mg L^{-1} hygromycin B. After verification of correct assembly by diagnostic PCR, single colony isolates were restreaked thrice and stored. The empty-vector reference strain IME611 was constructed by transforming strain IMX2411 with p426-*TEF* (*URA3*). Uracil prototrophic transformants were selected on synthetic medium with vitamins [SM, (29)] supplemented with 20 g L^{-1} agar and 20 g L^{-1} sorbitol. A p*TEF1*-*HXT15*-t*CYC1* expression cassette was amplified from genomic DNA of strain IMX2411 with primer pair 16711/16712. Strain IMX2495 was obtained by transforming strain IMX1489 with pUDR538 together with p*ACT1*-*SOR2*-t*CPS1* and p*TEF1*-*HXT15*-t*CYC1* fragments. Transformants were selected on YPD-hygromycin plates. Strain IMX2506 was obtained by transforming strain IMX2495 with p426-*TEF* (*URA3*). Transformants were selected on SM plates supplemented with 20 g L^{-1} sorbitol.

Table 4: *S. cerevisiae* strains used in this study. Non-ox PPP↑ indicates the integration of the expression cassettes of p*TDH3-RPE1*-t*RPE1*, p*PGK1-TKL1*-t*TKL1*, p*TEF1-TAL1*-t*TAL1*, p*PGI1-NQM1*-t*NQM1*, p*TPI1-RKI1*-t*RKI1*, p*PYK1-TKL2*-t*TKL2*. *Kl* denotes *Kluyveromyces lactis*.

Strain name	Relevant genotype	Parental strain	Origin
CEN.PK113-7D	*MATa URA3 GPD2*	-	(168)
IMX581	*MATa ura3-52 GPD2 can1::cas9-natNT2*	CEN.PK113-5D	(175)
IME324	*MATa ura3-52 GPD2 can1::cas9-natNT2* p426-*TEF* (*URA3*)	IMX581	(77)
IMX1489	*MAT2 ura3-52 can1::cas9-natNT2 gpd2::*non-ox PPP↑ *sga1::*(p*DAN1-PRK,* p*TDH3-cbbM*-t*CYC1* (9 copies), p*TPI1-groES*-t*PGI1*, p*TEF1-groEL*-t*ACT1*) pUDR103 (*KlURA3*)	IMX581	(77)
IMX2411	*MATa ura3-52 GPD2 can1::cas9-natNT2 X-2::*p*TEF1-HXT13-tCYC1,* p*ACT1-SOR2*-t*CPS1*	IMX581	This study
IMX2495	*MAT2 ura3-52 can1::cas9-natNT2 gpd2::*non-ox PPP↑ *sga1::*(p*DAN1-PRK,* p*TDH3-cbbM*-t*CYC1* (9 copies), p*TPI1-groES*-t*PGI1*, p*TEF1-groEL*-t*ACT1*) *X-2::*(p*TEF1-HXT13-tCYC1,* p*ACT1-SOR2*-t*CPS1*)	IMX1489	This study
IMX2506	*MAT2 ura3-52 can1::cas9-natNT2 gpd2::*non-ox PPP↑ *sga1::*(p*DAN1-PRK,* p*TDH3-cbbM*-t*CYC1* (9 copies), p*TPI1-groES*-t*PGI1*, p*TEF1-groEL*-t*ACT1*) *X-2::*(p*TEF1-HXT13-tCYC1,* p*ACT1-SOR2*-t*CPS1*) p426-*TEF* (*URA3*)	IMX2495	This study

Shake-flask cultivation

Aerobic shake-flask cultures were grown in 500-mL round-bottom shake-flasks containing 100 mL medium, placed in an Innova incubator shaker (Eppendorf Nederland B.V., Nijmegen, The Netherlands) at 30 °C and 200 rpm. Anaerobic cultures were grown in 50-mL round-bottom shake-flasks containing 30 mL medium, incubated at 30 °C in a Bactron anaerobic chamber (Sheldon Manufacturing Inc., Cornelius, OR) with an atmosphere of 5% (v/v) H_2, 6% (v/v) CO_2 and 89% (v/v) N_2. Flasks were shaken on a IKA KS 260 basic shaker (Dijkstra Verenigde BV, Lelystad, The Netherlands) at 200 rpm (179).

Bioreactor cultivation

Anaerobic chemostat cultures and batch cultures were grown at 30 °C in 2-L bioreactors (Applikon, Delft, The Netherlands), with 1-L working volume. Anaerobic chemostat cultures were grown at a dilution rate of 0.025 L h^{-1} and the effluent pump

was controlled by an electrical level sensor to maintain a 1.0-L working volume. The pH was kept constant at 5.0 by automatic addition of 2 M KOH. Chemostat cultures were grown on SM with 10 g L^{-1} glucose and 10 g L^{-1} sorbitol and bioreactor batch cultures were grown on SM with 20 g L^{-1} glucose and 30 g L^{-1} sorbitol. Media was supplemented with the anaerobic growth factors Tween 80 (420 mg L^{-1}) and ergosterol (10 mg L^{-1}) (179), and 0.2 g L^{-1} antifoam C (Sigma-Aldrich). Unless otherwise indicated, cultures were sparged at 0.5 L min^{-1} with an N_2/CO_2 (90/10%) gas mixture. The outlet gas stream was cooled to 4 °C in a condenser to minimize evaporation. Oxygen diffusion was minimized by use of Norprene tubing (Saint-Gobain, Amsterdam, The Netherlands) and Viton O-rings (ERIKS, Haarlem, The Netherlands). Steady state was assumed when, after at least 5 volume changes of operation under constant conditions, biomass dry weight, ethanol, glycerol and acetate concentrations varied by less than 5% over at least two additional volume changes. Inocula for chemostat and bioreactor batch cultures were prepared in 500-mL shake flasks containing 100-mL SM with 20 g L^{-1} glucose. A first starter culture was inoculated with frozen stock culture, grown aerobically for 15-18 h at 30 °C and used to inoculate precultures on SM. Upon reaching mid-exponential phase (OD_{660} of 3-5), these were used as inocula for bioreactor cultures at an initial OD_{660} of 0.2-0.3. Bioreactor batch cultures that preceded the chemostat-cultivation phase were grown on SM with 20 g L^{-1} glucose.

Analytical methods

Biomass dry weight measurements, analysis of metabolite concentrations and correction for ethanol evaporation were performed as described previously (109). Metabolite concentrations in steady-state chemostat cultures were analysed after rapid quenching of the culture samples using cold steel beads (181). Carbon recoveries could not be accurately calculated due to the high concentration of CO_2 in the inlet gas of bioreactor cultures of PRK-RuBisCO-mediated strains (77, 109). Instead, balances of degree of reduction of substrates and products (11) were calculated. These calculations were based on concentrations of relevant components in medium feed and culture samples and on a published value for the elemental composition of yeast biomass (182).

High-throughput analysis of specific growth rates

A Growth-Profiler system (EnzyScreen, Heemstede, The Netherlands) was used for parallel analysis of specific growth rates of multiple *S. cerevisiae* strains. Cultures were grown under air on SM supplemented with either 20 g L^{-1} glucose or 20 g L^{-1} sorbitol, in a culture volume of 250 µL, at 30 °C and at an agitation rate of 250 rpm. The

measurement interval was set at 30 min and specific growth rates were calculated from raw green values (261).

Whole-genome sequencing

100 mL aerobic shake-flask cultures *S. cerevisiae* strains IMX1489 and IMX2506 on YPD were centrifuged for 10 minutes at 5,000 x *g* in late exponential phase (OD_{660} of 10-15). For genomic DNA isolation from chemostat cultures of strain IMX1489, 50 mL samples were harvested. Genomic DNA extracted with a Qiagen Blood & Cell Culture NDA kit and 100/G Genomics-tips (Qiagen, Hilden, Germany) was quantified with a Qubit Fluorometer 2.0 (Thermo Fisher). The genome of strain IMX1489 was sequenced in-house as described previously (262) on an Illumina Miseq sequencer (Illumina, San Diego, CA, USA) with a minimum of 50-fold read coverage. Custom paired-end sequencing of genomic DNA of duplicate chemostat cultures of IMX1489 was performed by Macrogen (Amsterdam, The Netherlands) on a 350-bp PCR-free insert library using Illumina SBS technology. Genomic DNA of strain IMX2506 was sequenced by Genomescan (Leiden, The Netherlands) with Illumina SBS technology yielding 151 bp reads with at least 50-fold read coverage. Sequence reads were mapped against the genome of *S. cerevisiae* CEN.PK113-7D (212) to which a virtual contig containing the sequences of p*DAN1-PRK*-t*PGK1*, p*TDH3-cbbM*-t*CYC1*, p*TEF1-groEL*-t*ACT1* and p*TPI1-groES*-t*PGI1* had been added, and processed as described previously (262).

Stoichiometric analysis

Quantitative estimates of the ethanol yield, biomass yield and biomass-specific rate of substrate consumption were obtained using a stoichiometric model of the core metabolic network of *S. cerevisiae* (118). This model was adjusted as described previously, by including a PRK-RuBisCO-based bypass of the oxidative reaction in glycolysis (Fig. 1, (132)). For sorbitol-grown cultures, three additional reactions were implemented, corresponding to a sorbitol facilitator (eq. 1), a sorbitol dehydrogenase (eq. 2) and a fructose kinase (eq. 3):

sorbitol (external) → sorbitol (cytosolic)	eq. 1
sorbitol + NAD+ → fructose + NADH	eq. 2
fructose + ATP → fructose-6P + ADP	eq. 3

Availability of data and materials

DNA sequencing data of the *Saccharomyces cerevisiae* strains IMX1489, IMX2506 and evolved population of evolution line 1 (deposited as IMS1232) and evolution line 2

(deposited as IMS1233) were deposited at NCBI under BioProject accession number PRJNA818459. All measurement data used to prepare Figure 3, Tables 1 and 2, Figure 5, Figure S2, Figure S3 and Tables S2 and S3 of the manuscript are available in Additional file 1, Additional file 2, Additional file 3 and Additional file 4, respectively (accessible online via https://doi.org/10.1186/s13068-022-02200-3).

Funding

This work was supported by DSM Bio-based Products & Services B.V. (Delft, The Netherlands).

Acknowledgements

We thank Mickel Jansen for many stimulating discussions and Walter van Gulik for his assistance in modelling the impact on product yields and substrate uptake rates. We thank Maaike Remeijer for her help in the construction of strain IMX2411 and Nicolò Baldi for the construction of pUD968 and pUDE885.

Supplementary information

Additional supplementary information

Available online via: https://doi.org/10.1186/s13068-022-02200-3.

Table S1: Predicted ethanol yields on substrate, biomass-specific substrate-uptake rates ($q_{substrate}$) and biomass yields on substrate for wild-type *S. cerevisiae* (WT) and strains with an engineered PRK-RuBisCO bypass of the oxidative reaction in glycolysis on both glucose and on sorbitol. Rates and yields were predicted for cultures growing at different specific growth rates, using an extended stoichiometric model of the core metabolic network of *S. cerevisiae* (118, 132). A Cmol biomass ($CH_{1.8}O_{0.5}N_{0.2}$, (182)) corresponds to 26.4 g dry biomass. Gluc indicates glucose, sor indicates sorbitol.

Specific growth rate (h^{-1})	**$Y_{ethanol/substrate}$ (mol/mol)**			**$q_{substrate}$ (mmol/g_x/h)**			**$Y_{x/substrate}$ (g_x/mol)**		
	WT	PRK-RuBisCO		WT	PRK-RuBisCO		WT	PRK-RuBisCO	
	gluc	gluc	sor	gluc	gluc	sor	gluc	gluc	sor
0.0001	2.00	2.00	2.17	0.504	0.504	0.864	0.211	0.211	0.106
0.001	1.95	1.98	2.15	0.549	0.538	0.921	1.822	1.874	1.082
0.01	1.75	1.86	2.09	0.992	0.872	1.496	10.08	11.46	6.679
0.03	1.62	1.78	2.04	1.974	1.618	2.765	15.21	18.56	10.82
0.1	1.54	1.71	2.00	5.417	4.205	7.235	18.51	23.71	13.83
0.2	1.52	1.70	1.99	10.30	7.955	13.60	19.40	25.19	14.70
0.3	1.51	1.69	1.99	15.23	11.67	20	19.72	25.74	15.02

Table S2: Maximum specific growth rates in aerobic batch cultures of *S. cerevisiae* strains IME611 and IMX2506. Strains were grown on synthetic medium, supplemented with either 20 g L^{-1} of glucose or 20 g L^{-1} of sorbitol. Specific growth rates were calculated from quadruplicate cultures in a Growth Profiler, using at least 9 measurement points obtained during the exponential growth phase. Strain IME324, was inoculated in duplicate aerobic shake-flask cultures containing synthetic medium supplemented with 20 g L^{-1} of sorbitol as sole carbon source. No growth was observed after 4 weeks of incubation. N.D.: not determined.

strain	Relevant genotype	Specific growth rate on glucose (h^{-1})	Specific growth rate on sorbitol (h^{-1})
IME324	Reference	N.D.	<0.001
IME611	*HXT15*↑ *SOR2*↑	0.36 ± 0.01	0.23 ± 0.00
IMX2506	*gpd2*Δ non-ox PPP↑ p*DAN1-PRK cbbM HXT15*↑ *SOR2*↑	0.35 ± 0.01	0.25 ± 0.00

Table S3 Segmental aneuploidies observed in two prolonged anaerobic chemostat cultivation experiments with *S. cerevisiae* strain IMX2506 (optimized PRK-RuBisCO bypass and *gpd2*Δ mutation, overexpression cassettes for *HXT15* and *SOR2*) on glucose-sorbitol mixtures.

Partial aneuploidy on chromosome and coordinates	Found in	Genes located on duplicated region
IV (~1,075,000 – 1,185,000)	Evolution experiment 1 Evolution experiment 2	*OMS1*, *HIM1*, *MCM21*, *YFT2*, *SWA2*, *DAD4*, *ASP1*, *MRPL35*, *TIM11*, *PEP7*, *UTP4*, *YCG1*, *YSP2*, *SKP1*, *PEX3*, *UBX5*, *GPI8*, *IRC3*, *YDR333C*, *SWR1*, *MSN5*, *YDR336W*, *MRPS28*, *YDR338C*, *FCF1*, *YDR341C*, *HXT7*, *HXT6*, *HXT3*, *SVF1*, *MRP1*, *PAL1*, *YPS7*, *ATP22*, *SBE2*, *YDR352W*, *TRR1*, *TRP4*, *SPC110*, *CLN1*, *GGA1*, *EAF1*, *BCP1*
VIII (~250,000-end)	Evolution experiment 2	>100 genes
IX (~180,000-215,000)	Evolution experiment 2	*PRK1*, *LYS12*, *RSM25*, *YIL092W*, *UTP25*, *ICE2*, *YIL089W*, *AVT7*, *AIM19*, *KTR7*, *SDS3*, *THS1*, *YIL077C*, *SEC28*, *RPN2*, *SER33*, *SPO22*
X (~415,00-435,00)	Evolution experiment 1	*CYR1*, *SYS1*, *COX16*, *OST1*, *PRE3*, *AVT1*, *MPP10*, *YJR003C*, *SAG1*
XV (~0-200,000)	Evolution experiment 1 Evolution experiment 2	>100 genes
XV (~215,000-495,000)	Evolution experiment 1 Evolution experiment 2	>100 genes

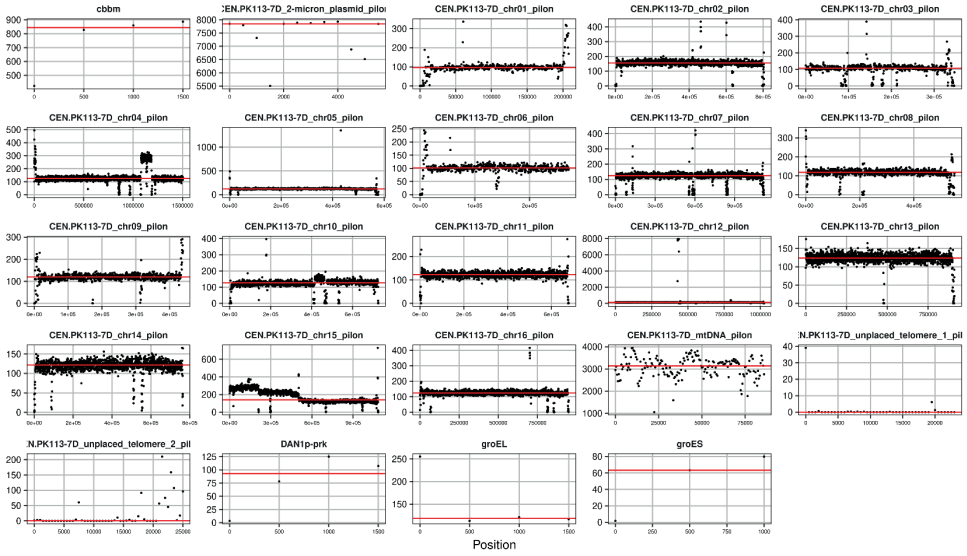

Figure S1A Copy number variation across yeast chromosomes in prolonged anaerobic chemostat cultivation experiment 1 with *S. cerevisiae* IMX2506 (optimized PRK-RuBisCO bypass and *gpd2*Δ mutation, overexpression cassettes for *HXT15* and *SOR2*) on glucose-sorbitol mixtures (see Fig. 5). Copy number variations were visualized with the Magnolya (208).

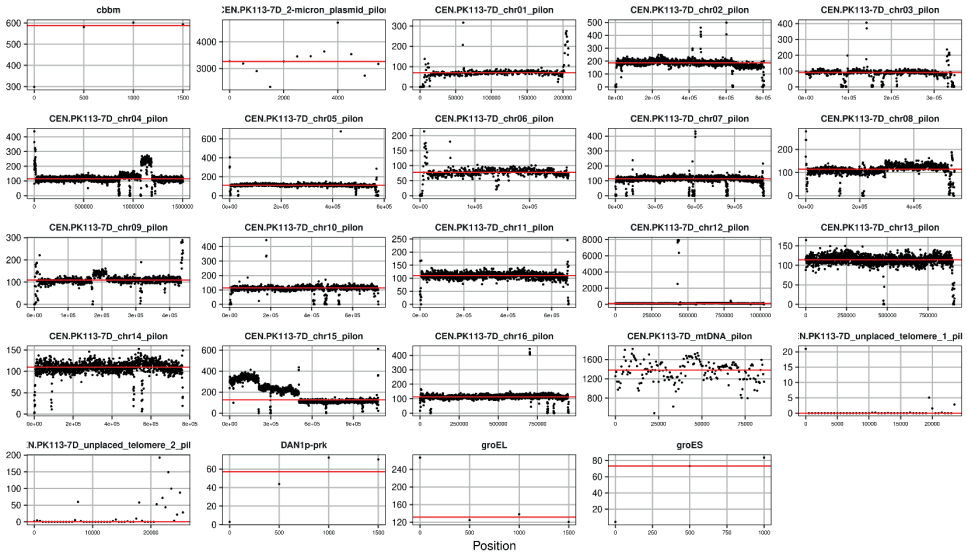

Figure S1B Copy number variation across yeast chromosomes in prolonged anaerobic chemostat cultivation experiment 2 with *S. cerevisiae* IMX2506 (optimized PRK-RuBisCO bypass and *gpd2*Δ mutation, overexpression cassettes for *HXT15* and *SOR2*) on glucose-sorbitol mixtures (see Fig. 5). Copy number variations were visualized with the Magnolya algorithm (208).

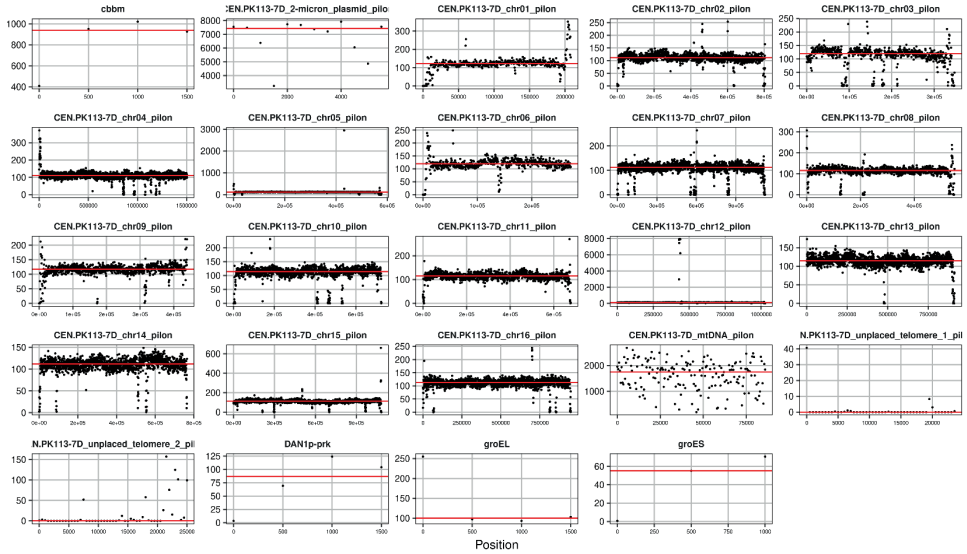

Figure S1C Reference data for copy-number assessment with the Magnolya algorithm (208) for the reference strain *S. cerevisiae* IMX2506 (optimized PRK-RuBisCO bypass and *gpd2*Δ mutation, overexpression cassettes for *HXT15* and *SOR2*).

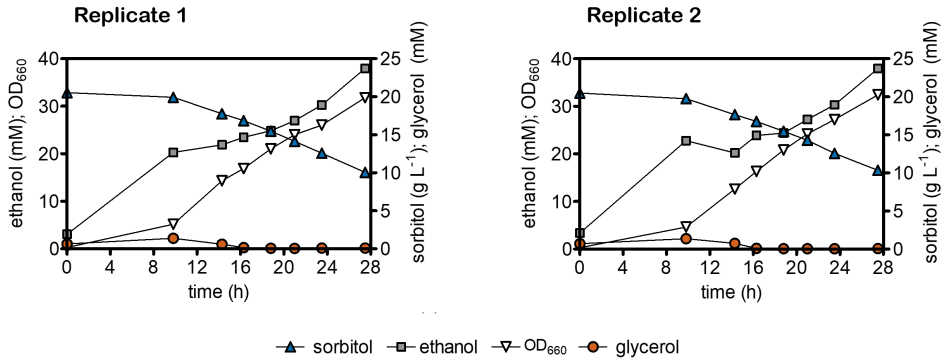

Figure S2: Optical density at 660 nm (OD_{660}), sorbitol concentration, ethanol concentration and glycerol concentration in duplicate aerobic shake-flask cultures of *S. cerevisiae* IMX2506 (optimized PRK-RuBisCO bypass and *gpd2Δ* mutation, overexpression cassettes for *HXT15* and *SOR2*) on 20 g L^{-1} sorbitol.

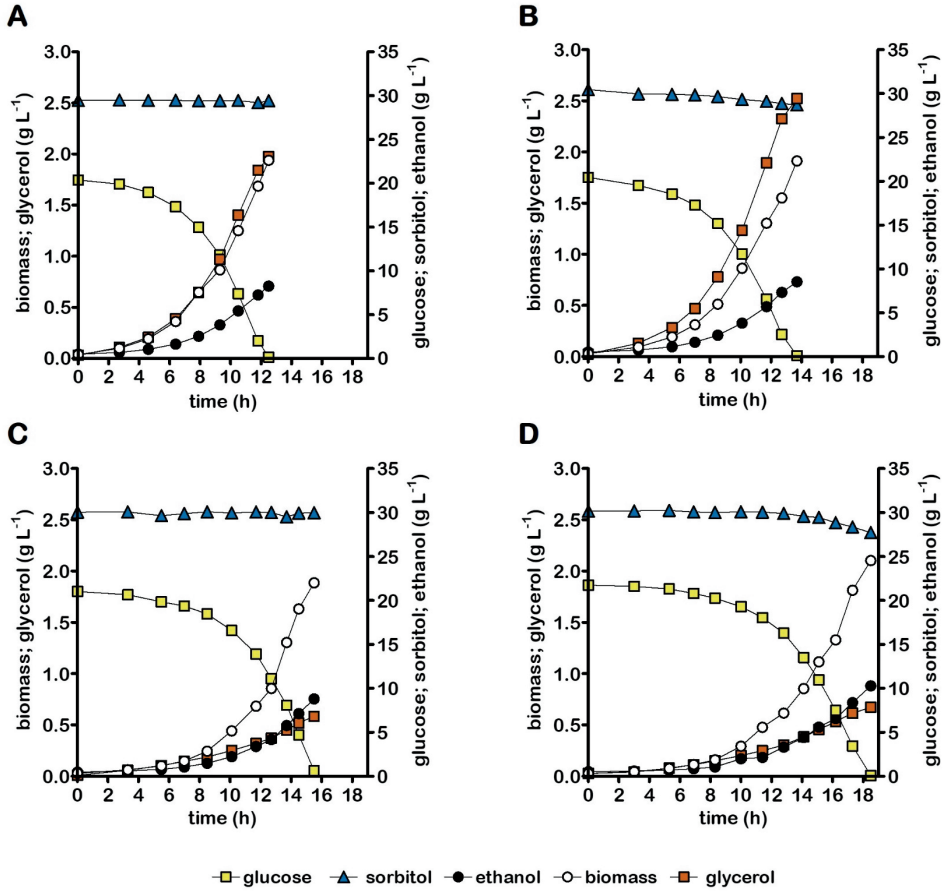

Figure S3: Growth, glucose consumption, sorbitol consumption, ethanol formation and glycerol formation in anaerobic bioreactor batch cultures of *S. cerevisiae* strains IME324 (reference strain) (A), IME611 (overexpression cassettes for *HXT15* and *SOR2*) (B), IMX1489 (optimized PRK-RuBisCO bypass and *gpd2Δ* mutation, (77)) (C) and IMX2506 (optimized PRK-RuBisCO bypass and *gpd2Δ* mutation, overexpression cassettes for *HXT15* and *SOR2*) (D). Cultures were grown anaerobically at pH 5 and at 30 °C on synthetic medium containing 20 g L^{-1} glucose and 30 g L^{-1} sorbitol as carbon sources. Representative cultures of independent duplicate experiments are shown, corresponding replicate of each culture shown in main manuscript Fig. 2.

Outlook

Biofuels provide storable forms of renewable energy that are to varying extents compatible with the current, still predominantly fossil-fuel-based energy infrastructure of industrialized countries. Brazil was the first country that, during the 20th century, started a nation-wide program to stimulate the use of biologically produced ethanol ('bioethanol') as a transport fuel. Already in 1931 a law was implemented which prescribed that ethanol should be mixed to gasoline at 5% (v/v), with the aim to reduce Brazil's dependence on oil imports (229). This policy was strengthened when, in 1975 and in response to the 1970's oil crisis, the Brazilian government launched the 'Proalcool' program (129, 190). In addition to blending ethanol with gasoline for use in regular car engines, flex-fuel cars were produced for the Brazilian market that can run on either 100% ethanol or on mixes of ethanol and gasoline (190, 229). Since the early 1980's, substantial growth of global yeast-based ethanol production primarily relied on the United States of America and Brazil. While, since 2007, the bioethanol industry also gained ground in Asia and Europe, these two countries remain the major fuel ethanol producers (263). Since 2010, world fuel ethanol production levelled off at an annual production volume of around 100 billion litres (1). Further growth was limited by different factors, including the so-called ''blend wall'', which limits the percentage of fuel ethanol that can be blended with gasoline (usually 5-15%) without adaptations to car engines (263). In addition, the ethanol market still depends on the price of competing non-renewable fossil resources (263). Continued efforts to make the bioethanol industry more cost-efficient and sustainable are essential to improve its competitiveness with fossil alternatives. Cheap, sustainable processing would, moreover, enable applications of ethanol beyond its use in automotive fuels. Ethylene is already produced on an industrial scale via the dehydration of ethanol from first generation biorefineries (264), while catalytic upgrading of ethanol to jet fuel may soon leave the pilot phase (265, 266).

Boosting ethanol yields

Currently, bioethanol is almost exclusively made via the fermentation of plant carbohydrates by the yeast *Saccharomyces cerevisiae*. As the costs of carbohydrate feedstock can account for up to 70% of the total production costs (7), maximizing ethanol yield on sugar remains important. Due to the extensive knowledge on the responsible metabolic pathways and excellent genetic accessibility of *S. cerevisiae*, yeast-based ethanol production provides a near-ideal model system for experimental and modelling studies on this subject. While not solving all relevant questions,

the research presented in this thesis and in recent related work by other scientists helps to identify some new and promising research directions. **Chapter 1** discusses previously published metabolic engineering strategies for maximizing the yield of ethanol on sugars in anaerobic fermentation processes with the yeast *Saccharomyces cerevisiae*. Based on altering the ratio of the formation of ethanol, biomass and glycerol by engineering redox metabolism, several of these strategies have been shown to enable economically significant improvements (up to ca. 10%) of ethanol yields in laboratory studies. Using these strategies, 'high-ethanol-yield' yeast strains have been developed, which approach maximum yields of 2 mol ethanol/mol hexose.

Theoretically, ethanol yields beyond 2 mol ethanol per mol hexose might become possible if additional electrons can be fed into alcoholic fermentation. As a proof-of-principle, **Chapter 5** explores anaerobic conversion of the polyol sorbitol by *S. cerevisiae*. This polyol cannot be fermented anaerobically by *S. cerevisiae* because its oxidation to pyruvate via glycolysis yields an additional NADH than the conversion of glucose to pyruvate. Slow-growing anaerobic cultures of *S. cerevisiae* strains expressing the genes for the Calvin-cycle enzymes phosphoribulokinase (PRK) and ribulose-1,5-bisphosphate carboxylase/oxygenase (RuBisCO) displayed a 12-fold higher anaerobic sorbitol conversion rate and 91% lower glycerol production on a mixture of glucose and sorbitol, resulting in a 15% higher ethanol yield, compared to a sorbitol-consuming reference strain. Anaerobic growth of *S. cerevisiae* on sorbitol as the sole carbon source was not yet achieved. Further research in this direction could exploit the use of an alternative non-oxidative bypass of glycolysis with a better ATP stoichiometry than the PRK-RuBisCO route. A particularly interesting option is offered by the combined expression of a heterologous phosphoketolase (PK), phosphotransacetylase (PTA) and acetylating acetaldehyde dehydrogenase (A-ALD) (106-108). Preliminary experiments in our lab indicate that under anaerobic conditions the PK-PTA-A-ALD pathway still requires further engineering to improve the *in vivo* capacity to enable sorbitol fermentation. Alternatively, *Thermoanaerobacter kivui* has been described to ferment the polyol mannitol to acetate (267). Pathway engineering in this acetogenic microorganism might enable the fermentation of mannitol into ethanol instead.

Polyols are not commonly used as substrates in the bioethanol industry. However, in the future polyols might become more common in industry as sorbitol can be produced by the catalytic hydrogenation of glucose (239, 268) and is abundant in nature in flowering plants (238). Metabolic engineering in corn might enable the development of crop varieties with increased abundance of sorbitol in the future. Moreover, sorbitol can be produced from lignocellulosic biomass (269, 270), while

mannitol is abundantly present in macroalgae, a promising third generation feedstock (237, 242, 271, 272).

Alternatively, soluble electron carriers which can be obtained from the reduction of CO_2 (273) can be an interesting alternative for co-feeding of electrons. Such soluble electron carriers include carbon monoxide, formic acid, formaldehyde, methanol and methane (244, 245). Formic acid can be converted by formate dehydrogenase into NADH and CO_2 (105). Generation of NADH via co-feeding of formic acid has been demonstrated to either provide reducing power in yeast cultures grown under anaerobic conditions (236, 274) or metabolic energy via aerobic respiration (82, 275-277). A set-up in which CO_2 emitted from microbial processes is recycled as formic acid (278-280) and subsequently implemented into an ethanol pathway might be envisioned for the future.

Metabolic engineering: from laboratory to dynamic industrial processes

As demonstrated in **Chapters 2-4**, improved performance under controlled laboratory conditions does not guarantee that the same improvements can also be achieved under the conditions that occur in large-scale industrial processes. One contributing factor is that, in large-scale industrial batch processes for ethanol production, a vigorous anaerobic growth phase is followed by a growth deceleration phase due to increasing ethanol concentrations and/or depletion of essential nutrients (215). In addition, extensive engineering for improved yield can result in trade-off situations where an improved product yield is or appears to be coupled to a lower productivity. Lastly, the yeast encounters different stresses when growing on industrial corn mash, including but not limited to bacterial contamination causing the production of acids, and inadequate nutrition (215, 281). Understanding and improving performance of engineered strains under real-life industrial conditions and addressing these rate-yield trade-offs will, for the coming years, continue to present interesting challenges for metabolic engineering research.

In **Chapter 2**, we analysed the performance of an *S. cerevisiae* strain expressing heterologous genes encoding the Calvin-cycle enzymes PRK and RuBisCO that had been optimized for fast growth, low glycerol production and high ethanol yield. Lowering the specific growth rate, which during large-scale fermentation occurs due to nutrient depletion and/or ethanol accumulation, resulted in a discrepancy between the rate of biomass formation and the rate of pyruvate formation via PRK and RuBisCO. This discrepancy caused formation of acetaldehyde and acetate as byproducts and thereby contributed to suboptimal biomass and ethanol yields. Metabolic engineering studies showed that 'tuning' the *in vivo* capacity of PRK and

RuBisCO mitigated this undesirable byproduct formation. Experiments in which PRK synthesis was controlled by a growth-rate-dependent promoter illustrated the potential of using dynamic regulation strategies to further optimize strain performance under the growth-rate dynamics encountered in industrial batch processes. In addition to testing native growth-rate-dependent promoters of *S. cerevisiae* genes, genetic regulatory loops controlled by biosensors based on allosterically regulated transcription factors (aTFs) hold great promise for dynamic adaptation of *in vivo* pathway activity in response to dynamic process conditions (282). In addition, such regulatory control loops can be implemented to ensure genetic stability of engineered pathways during long-term propagation and fermentation processes (283).

In addition to the growth deceleration the yeast encounters under industrial conditions, acetate naturally occurs in several industrial feedstocks due to bacterial contamination (37, 100, 216). As acetate is normally not consumed during the fermentation process, this compound is recycled into subsequent fermentation runs via thin stillage and evaporator condensate and the concentration of acetate therefore gradually increases per fermentation run (205). At the low pH values at which yeast-based fermentation processes for ethanol production are usually run at, weak organic acids readily become toxic to yeast cells, due to uncoupling of the plasma-membrane pH gradient (215, 281). *In situ* acetate detoxification by yeast-mediated reduction of acetate into ethanol is a very promising strategy as it simultaneously contributes to improved ethanol yields (91). Especially for conversion of feedstocks that contain only low concentrations of acetate, this approach can be combined with other redox-engineering strategies, as discussed in **Chapter 3** and **4**.

Corn mash, which is the predominant feedstock for the USA-based ethanol industry, lacks nitrogen, minerals and vitamins and oxygen needed for yeast cell membrane synthesis and unsaturated fatty acids is quickly depleted throughout the fermentation (215, 281). Academic studies have shown promising results in the development of vitamin-independent strains (262, 284, 285) and oxygen-independent strains (260, 286), which might soon be adopted by industry.

Process intensification

Bioethanol production processes increasingly use very-high-gravity (VHG) fermentation (i.e., use of very high sugar concentrations, 250 g L^{-1} and up) as a strategy to optimize volumetric productivity and, thereby, minimize production costs (281, 287). Apart from the challenges related to the engineered pathways, VHG processes expose yeast cells to multiple stress factors, including high temperatures in

combination with high ethanol concentrations (215, 281). Research has indicated the synergistic effect of high temperatures and high ethanol concentration, resulting in greatly reduced strain performance (288). Temperature staging is therefore often applied, which requires a drop in temperature late in the fermentation when ethanol concentrations are high, to mitigate the negative effects of the combined intolerance to high ethanol concentrations and temperatures above 30°C (215). Exploration of natural biodiversity of *S. cerevisiae* strains (289) or (evolutionary) engineering strategies can be used to develop yeast strains with improved tolerance to VHG conditions (290). Looking beyond *S. cerevisiae*, thermotolerant yeasts with temperature maxima of up to 50 °C (291-293), as well as thermophilic bacteria (294, 295), are being explored for bioethanol production.

Consolidated Bioprocessing

The majority of the current ethanol production is derived from corn or from sugar cane. In the case of corn, starch is the predominant carbohydrate, which can be hydrolysed by amylases, and hemicellulose and cellulose are the dominant carbohydrate polymers in the fiber residue (296). '1.5-G ethanol processes' involve the additional use, in existing first-generation bioethanol plants, of enzymes other than amylases. These enzymes, which for example can include cellulases and xylanases, are added to release additional fermentable sugar from the fiber residues present in the feedstock (297). The use of additional enzymes in the existing corn ethanol process has been shown to increase ethanol yields and reduce water usage and greenhouse gas emissions. A large corn-ethanol plant typically spends more than US$1 million on purchased glucoamlyase in a single year (298) and the enzyme costs for cellulosic substrates are even higher (299). Therefore, process economics can greatly benefit from the development of new crop varieties which contain less fibre and/or consist of more readily-accessible starch or sugar (300, 301). As an alternative approach, yeasts have been developed to produce and excrete hydrolytic enzymes during the fermentation process, which is referred to as consolidated bioprocessing (CBP) principle (298, 299, 302, 303). While the ideal amylolytic CBP strain can express both α-amylase and glucoamylase, currently commercialized industrial amylolytic yeast strains express only one of these amylases, resulting in so-called partial-CBP strains that require supplementation with one or both of the amylases to fully hydrolyze the substrate (303). A major hurdle for industrial full-CBP strain development is achieving high levels of enzyme production without compromising ethanol productivity (303). In an alternative and potentially transformative approach, ethanol-tolerant cellulolytic bacteria are being selected and engineered for their use in consolidated bioprocesses that only require mechanical pre-treatment of plant biomass. Although impressive progress has been made, these processes do not yet

reach the ethanol titres and yields that are reached in industrial yeast-based processes (304-306).

Consortia in bioethanol industry

As alternative to the development of single 'all-in-one' CBP strains, further improvements in CBP might be possible using multiple (micro)-organisms. Syngenta has developed and commercialized a corn variety which synthesizes α-amylase in the corn kernel (307, 308) and other corn varieties are being developed which synthesize cellulolytic enzymes (309). Combining α-amylase producing corn with gluco-amylase producing yeast, was found to replace the need for exogenous α-amylase addition and reduce the gluco-amylase dose by 25% (308). Additionally, cooperation between cellulolytic bacteria (310) and high-ethanol producer yeast strains is explored, in which pre-treatment of lignocellulosic biomass is done by the cellulolytic bacteria followed by fermentation performed by high-ethanol producing yeast strains (311). Similarly, mixed cultures of hemicellulase-displaying xylose-utilizing yeast strains were applied for efficient utilization of xylan substrates (227).

Chapter 4 describes the use of co-cultures for ethanol production, in which consortia of previously characterised PRK-RuBisCO- and A-ALD-based strains removed essentially all acetate from media with acetate-to-glucose ratios similar to those in first generation feedstocks. The co-cultures thereby enabled higher ethanol yields and lower glycerol yields than obtained with a non-engineered reference strain. Changes in inoculation ratios and co-culture composition were demonstrated as a means to 'tune' the kinetics of the fermentation process. Further glycerol reductions, without extending fermentation times, may involve the use of an A-ALD-based strain, in which acetyl-CoA can be synthesized from glucose via heterologous pyruvate-formate lyase (PFL) (101), or via heterologous PK and PTA (106). While the USA-based bioethanol industry has long stuck to pure cultures of single *S. cerevisiae* strains, a recent publication indicates that blends of yeast strains, optimized for substrate utilization and ethanol yield, are already successfully applied in first-generation bioethanol industry (232). Optimizing interactions between the strains in such synthetic consortia opens up a new and exciting area in industrial biotechnology.

Acknowledgements

During my PhD I have had the opportunity to work with a lot of great and inspiring people, whom I would like to thank for all of their contributions to my time at IMB. I am grateful for all of you!

I would like to start by thanking **Jack** and **Robert**, my two supervisors. First of all, **Jack**, you have written up an amazing research proposal and it has been a great and interesting project to work on. We have come across a number of unexpected but interesting observations and you have always been supportive and reassuring. I want to thank you for the numerous feedback rounds on all of my work, all the interesting scientific discussions and for all your involvement and enthusiasm! **Robert**, after a few weeks I was already adopted into the energetics group, and you have been intensively involved in my project. Your very application-oriented mindset really inspired me and I have learned a lot from you! Moreover, I believe you have a special talent for motivating and encouraging people. I am really excited about your career switch for you, and I wish you all the best in Canada or anywhere else. Thank you for joining me on the trip to Vancouver, I really enjoyed the conference! **Jack** and **Robert**, I have been extremely lucky to have had such a strong supervisory team I am grateful for all the input and help I have received, with so much patience. I have learned so much during these four years and I have had a lot of fun as well!

Special thanks to **Mickel**, I really enjoyed working with you. I learned a lot about the industry and thanks to all your effort, I was able to perform experiments in the very beautiful labs of DSM, which I enjoyed a lot! Moreover, I appreciated all the useful feedback and input on the publications we collaborated on and thank you for your willingness to answer all my industry-related questions.

Jean-Marc, thank you for being my stand-in supervisor for my final PhD-year. Moreover, as head of IMB you ensured a stimulating and well-organized working environment. Additionally, I really appreciated your valuable input during the work discussions or during the few but very useful meetings we have had. **Walter**, thank you for your contributions to my research with the metabolic model and I wish you all the best. **Pascale**, thank you as well for your contribution to a great working environment at IMB and good luck with all your future research. **Rinke**, thank you for all the input during the MEC-meetings and outside of these meetings. Thank you for all your help with flow cytometry data analysis and I wish you all the best with your

future plans! **Djorge**, I am really curious to find out about your future research plans and I wish you all the best.

Arthur, **Mark**, **Xin** and **Willem-Jan**, you have been very important during my BSc, MSc and industrial internships. You encouraged me and helped me to develop into an independent researcher, and my experiences under your supervision have been an important reason why I decided to apply for a PhD. Having to supervise students myself during my PhD made me even more grateful for and impressed by your supervision during my internships. **Xin**, thank you for making me feel so at home in Sweden. **Mark** and **Arthur**, I am really grateful that, even after my internship ended, you continued to help me with my application for an industrial internship, applications for PhD-positions and PostDoc-grant.

During my PhD I received a lot of help from my students. **Maaike**, **Maarten**, **Rosalie**, **Suzanne**, **Ellen**, **Iris**, **Luca**, **Miriam** and **Igor**. It has been a real privilege to supervise all of you during my PhD-project. Thank you for your commitment to my PhD and all the help. Thank you for showing up each day, staying late when needed, and for all the interesting and fun conversations. Apart from scientific knowledge, each one of you has helped me grow as a person and as a manager. I am sure you will do great things in the future and do not hesitate to reach out to me. **Rosalie**, **Miriam**, **Iris** and **Luca**, good luck at IMB, I hope you will enjoy your time at IMB as much as I did!

I would never have been able to finish my PhD without all the help and support from the technical staff of IMB. **Erik**, we have worked together a lot in the fermentation lab and without you, my project would not have been possible. You are very fun to hang out with, and I have really enjoyed the surfing trip and the 'wadloop' trip. When people approach you in the lab, they usually need something fixed. Though you might not always be in the mood for problems, you are always approachable and always willing to help. I really appreciate your patience and your positive attitude, and with your innovative mindset there is never a problem you cannot fix! Thank you to **Christiaan**, **Flip** and **Maria**, as you have been of great help in the fermentation lab as well! An additional thanks to **Christiaan** for staying late with me for my very first late-night experiment and for the fun at the surfing trip. **Maria**, it was fun being office mates and I enjoyed the surfing trip. Your vast knowledge helped me a lot with many different issues, from HPLC, to strain construction, to bioreactor sampling. **Flip**, you are a very accommodating person and you always try to think along and help solve problems. Thank you **Marijke**, for all the help and effort with the 'left-HPLC' and with enzyme assays. Also for all your important life lessons including: 'zonder blanco gaat 'ie manco!'. **Susan W.**, thank you for your help with the HPLC as well. **Pilar**, I really

enjoyed my tour through Sevilla and thank you for all your help with RNA extraction and whole genome sequencing. **Augustina**, you have only been at our group for a short time, but I was one of the lucky ones to have received some training from you: thank you for your help with nanopore sequencing. **Clara**, thank you for your help with whole genome sequencing and for all the fun car rides! **Jordi**, you are a very approachable person and you were always willing to help. Thank you for answering many of my lab-related questions. **Marcel**, you have helped me so much with many different bioinformatics quests. I really appreciate your patience and willingness to help me understand abstract concepts and without your help, many analyses would not have been performed. **Susan B.**, thank you for all your quick responses and help with labservant, lab access and scheduling,

Astrid, **Apilena**, **Jannie** and **Gea**, thank you for all the support in the lab, with all the media components, bioreactors, medium vessels, waste vessels and whatnot. You have always been super accommodating and your help has been essential for my experiments. Moreover, I really enjoyed our chats in the lab!

When I just started my PhD, I got adopted immediately by the energetics group. **Nicolo**, **Hannes** and **Sophie**, thank you for helping me get started and integrated into the group. **Hannes**, I only worked with you for a couple of months, but in this short time you gave me great advice on chemostat runs and steady states, which I have used throughout my PhD. **Nicolò**, thank you for staying late with me during a long experiment and for all your enthusiasm and help during and outside of the energetics meetings and I really enjoyed the surfing trip! **Sophie**, thank you for all your advice and help in the fermentation lab and for being a great example of how to finish your PhD on time and for organizing an amazing surfing trip! I also enjoyed writing a review together  and thank you for all your tips and tricks on Endnote. I really enjoyed being your paranymph, which has been very special! It was great getting to know you in- and outside of the lab!

Thank you to **Charlotte** for being my office mate, all the fun during the surfing trip and other activities, and good luck in Wageningen! **Mario**, I really enjoyed supervising a student together with you. **Anna**, thank you for offering your room to me for one of my late-night experiments, while you were in Denmark and thanks for all the good talks and fun during the 'wadloop'-tocht. **Sanne**, thank you for all your advice and for the fun during the surfing trip. **Jonna**, thank you for collecting and delivering our DNA samples, despite your flat tyre. **Ewout**, I want to thank you for all your help with the growth profiler and for all your advice on getting through your final year as a PhD. I am glad you are back at IMB! I want to thank all other 'old-IMB-ers' as well: **Aurin**,

Wijb, **Jasmijn**, **Eline**, **Thomas, Koen**, **Francine**. Thanks for all the fun events and for all the wisdom you have shared with me in the lab or during your presentations. Advice from experienced colleagues is very valuable, and you have made me feel very welcome at IMB.

A special mention of my fellow members of the BT PhD committee (**Alexandra**, **Marina**, **Philipp**, **Maxime** and **Sergio**). This was a great opportunity to meet people from outside IMB and I really enjoyed our online activities during the pandemic.
Maxime, I have really enjoyed getting to know you as a colleague and as a friend. Thank you for being my buddy on the many late-night experiments we both had to perform. I enjoyed working together in the BT PhD committee and I had so much fun in Vancouver at the conference and during our holiday afterwards. Moreover, it has been great to be your paranymph, you did an amazing job and I am really curious to find out about your next steps. Lastly, thank you for being my paranymph! Thanks to **Sagarika** as well, for being a nice office mate in my final months, and for the fun during the 'wadloop' trip. I met you early on in my PhD, when you were performing your MSc project and it has been really great to have gotten to know you over the years. I am impressed by your perseverance, skills and knowledge and I am sure you will successfully finish your PhD. Thank you for all the nice talks and of course thank you for being my paranymph!

Thanks to **Nicole** for all the fun while organizing the lab retreat and as co-paranymph for Sophie. And in my final months as my office mate. Also, thank you for all the talks and fun outside of work. **Celine**, I really appreciate all the effort you put into both research groups, to make sure you are involved in both of them! **Denzel**, I enjoyed all the game nights, especially with saboteur, and you are a positive presence in and around the lab. **Rozanne**, it is amazing how fast you integrated in our group, like you have always been there. I really appreciate having you around! **Yanfang**, thank you for being a positive presence in the fermentation lab. I wish you a lot of luck with your PostDoc! **Shree**, lots of luck to you too!

Tobias, thank you for all the interesting discussions, for all the fun and for all the enthusiasm you bring every day. I really enjoyed the 'wadloop' trip and the Leuven conference was unforgettable! I am looking forward to collaborating with you on co-cultures. **Marcel**, you are such a kind person and very knowledgeable. IMB is very lucky to have you as PI and I wish you all the best. Leuven conference will always be one of the many great memories of my time at IMB. Thank you as well for your help and patience with the python models and for all the useful input during the energetics/MEC/JAMM meetings. **Marieke**, you are a positive and energetic presence

at IMB, and I had so much fun at all the escape rooms and 'konijnenhokken' games. Working together on the A-ALD review went smooth and I always enjoyed listening to all your cool results. I hope we can continue to collaborate on cool stuff in the future!

During my PhD I entered into a collaboration with **Charles** and **Kevin Verstrepen** from KU Leuven, which was later enriched by **David**. Thank you for all the interesting discussions and also for the great time in Leuven during the conference! **David**, good luck with your PhD, do not hesitate to reach out to me.

I would like to thank all of my friends, I am so grateful for the times when you were able to distract me from work and energize me again. A special thanks to **Imke**, for brainstorming on my thesis cover. **Marloes** and **Demi**, though far away, always close in heart. I treasure our calls and visits and thank you for always thinking along with me to try and solve my PhD-related (or other) problems. **Frederique** and **Hanneke**, thank you for recharging me during our sauna visits. **Kelly**, your positive attitude in life inspires me and our coaching session at the start of my PhD made me more efficient. **Jeroen** and **Amária**, thank you for letting me stay in your room in Delft during my late-night experiments.

Then I would like to thank my family: **mam**, **pap**, **Joris**, **Floor** and **Wies**. I am so grateful for our bond and unconditional love and support. As the youngest of 4, I felt protected and at the same time encouraged and supported. **Floor** and **Joris**, I feel like I am finally catching up to you and I really appreciate all the interest and support you have shown throughout my PhD. **Wies**, we are closest in age and growing up we have always been a strong team. I have really enjoyed the talks, boardgames, ski trip, carnaval and all the other fun activities. Thank you for your input on my thesis cover and propositions and for all the moral support. Most importantly, I would like to thank my parents, as they have been supportive of me throughout my life. Thank you for all your encouragement during my education and my PhD. Thank you for all the help during multiple moving sessions, thank you for all the prepared meals and thank you for all your love and support in general. I would not have been here if it wasn't for you!

Finally, my dear **Thomas**, you are my rock. I am so proud of you, and I am so grateful to have you in my life. Thank you for celebrating with me all the minor and major milestones, and listening to and comforting me during the lesser days. You really helped me get through my PhD with all your advice and support, and I will help you get through yours. Our holidays and time together are memories for a life-time and helped me energize again to continue my PhD. Thank you for all the cooking and cleaning and thank you for just always being there for me!

Curriculum vitae

Aafke van Aalst was born on the 13th of October 1994 in Breda, The Netherlands. She followed bilingual education at Menzia de Mendoza and graduated summa cum laude in 2013. After graduating she moved to Leiden to study Life Science & Technology, a joint BSc programme of Leiden University and Delft University of Technology. As a BSc student, Aafke followed a minor in Biological and Environmental Sciences at the University of East Anglia in Norwich, UK. In 2016, she finalized her BSc program with a research project at the Industrial Microbiology Section at TU Delft under the supervision of dr. ir. Arthur Gorter de Vries. This project focused on lager brewing yeast strains, evolved under different brewing conditions. She went on to enroll for the MSc program of Life Science & Technology at TU Delft, choosing the biocatalysis specialization. As an MSc student, she participated in the iGEM competition the 2017 TU Delft team. At the final event in Boston, the team won the Grand Prize and 9 additional awards. After the iGEM competition, Aafke performed a 9-month inter-laboratory research internship at the Industrial Microbiology Section at TU Delft and at the Systems and Synthetic Biology group at Chalmers University of Technology in Gothenburg, Sweden. During this project, which focused on the role of autophagy in maintenance-energy metabolism, she was supervised by dr. ir. Mark Bisschops in Delft and dr. Xin Chen in Gothenburg. Aafke finalized her MSc study with a 6- month internship at ZoBio in Leiden, during which she focused on protein domain expression and purification. In June 2019, Aafke started her PhD project in the Industrial Microbiology section at TU Delft under the supervision of professor Jack Pronk and dr. ir. Robert Mans, in collaboration with DSM. The results of this project, which focused on engineering redox metabolism in *Saccharomyces cerevisiae* to improve ethanol yields, are described in this dissertation.

Publication list

van Aalst, A. C. A., van der Meulen, I., Jansen, M., Mans, R., & Pronk, J. T. (2023). Co-cultivation of *Saccharomyces cerevisiae* strains combines advantages of different metabolic engineering strategies for improved ethanol yield. BioRxiv, 07. https://doi.org/10.1101/2023.07.04.547682

van Aalst, A. C. A., Geraats., E.H., Jansen, M., Mans, R., & Pronk, J. T. (2023). Optimizing the balance between heterologous acetate- and CO_2-reduction pathways in anaerobic cultures of *Saccharomyces cerevisiae* strains engineered for low glycerol production. BioRxiv, 05. https://doi.org/10.1101/2023.05.21.541164.

van Aalst, A. C. A., Jansen, M., Mans, R., & Pronk, J. T. (2023). Quantification and mitigation of byproduction formation by low-glycerol-producing *Saccharomyces cerevisiae* strains containing Calvin-cycle enzymes. Biotechnology for Biofuels and Bioproducts, 16 (1), 1-17. https://doi.org/10.1186/s13068-023-02329-9.

Chen, X.*, van Aalst, A.C.A.*, Petranovic, D. & Bisschops, M.M.M. (2023). Loss of kinase Atg1 increases yeast maintenance energy requirement. bioRxiv, 03. https://doi.org/10.1101/2023.03.06.531285.

van Aalst, A. C. A., Mans, R., & Pronk, J. T. (2022). An engineered non-oxidative glycolytic bypass based on Calvin-cycle enzymes enables anaerobic co-fermentation of glucose and sorbitol by *Saccharomyces cerevisiae*. Biotechnology for Biofuels and Bioproducts, 15(1), 1-15. https://doi.org/10.1186/s13068-022-02200-3.

van Aalst, A. C. A.*, de Valk, S. C.*, van Gulik, W. M., Jansen, M. L., Pronk, J. T., & Mans, R. (2022). Pathway engineering strategies for improved product yield in yeast-based industrial ethanol production. Synthetic and Systems Biotechnology, 7(1), 554-566. https://doi.org/10.1016/j.synbio.2021.12.010.

Gorter de Vries, A. R., Voskamp, M. A, van Aalst, A. C. A., Kristensen, L. H., Jansen, L., Van den Broek, M., Salazar, A.N., Brouwers, N., Abeel, T., Pronk, J.T. & Daran, J. M. G. (2019). Laboratory evolution of a *Saccharomyces cerevisiae*× *S. eubayanus* hybrid under simulated lager-brewing conditions. Frontiers in genetics, 10, 242. https://doi.org/10.3389/fgene.2019.00242

*authors contributed equally

Patent list

van Aalst, A. C. A., Mans, R., & Pronk, J. T., inventor; DSM IP Assets B.V., assignee. Mutant Yeast Cell and Process for the Production of Ethanol. European patent EP22169812; 2022 April 25.

Selected conference contributions

van Aalst, A.C.A. Minimizing byproduct formation at sub-maximal growth rates by engineered 'low-glycerol' *Saccharomyces cerevisiae* strains expressing heterologous genes encoding Calvin-cycle enzymes [oral presentation]. Fuel Ethanol Workshop (FEW). 12 June, 2023. Omaha, USA.

van Aalst, A.C.A. CO_2-dependent anaerobic co-fermentation of glucose and sorbitol to increase ethanol yields [oral presentation]. Emerging Applications of Microbes: 2nd edition. 7 December, 2022. Leuven, Belgium.

van Aalst, A.C.A. CO_2-dependent anaerobic conversion of sorbitol and glucose in *Saccharomyces cerevisiae* [oral presentation]. MB8.0 Microbial Biotechnology Symposium. 28 November, 2022. Amsterdam, The Netherlands.

van Aalst, A.C.A. CO_2-dependent anaerobic co-fermentation of glucose and sorbitol to increase ethanol yields [poster presentation]. ISSY36: Yeast in the genomic era. 12 June, 2022. Vancouver, Canada.

References

1. Renewable Fuels Association: Annual Ethanol Production. https://ethanolrfa.org/markets-and-statistics/annual-ethanol-production. Accessed 7 Jan 2022.
2. Capaz R, Posada J, Seabra J, Osseweijer P, editors. Life cycle assessment of renewable jet fuel from ethanol: an analysis from consequential and attributional approaches. Proceedings of the 26th European Biomass Conference and Exhibition, Copenhagen, Denmark; 2018.
3. Mohsenzadeh A, Zamani A, Taherzadeh MJ. Bioethylene production from ethanol: a review and techno-economical evaluation. ChemBioEng Reviews. 2017;4:75-91.
4. Ruchala J, Kurylenko OO, Dmytruk KV, Sibirny AA. Construction of advanced producers of first-and second-generation ethanol in *Saccharomyces cerevisiae* and selected species of non-conventional yeasts (*Scheffersomyces stipitis*, *Ogataea polymorpha*). Journal of Industrial Microbiology and Biotechnology. 2020;47:109-32.
5. Devantier R, Pedersen S, Olsson L. Characterization of very high gravity ethanol fermentation of corn mash. Effect of glucoamylase dosage, pre-saccharification and yeast strain. Applied Microbiology and Biotechnology. 2005;68:622-9.
6. Thomas K, Ingledew W. Production of 21%(v/v) ethanol by fermentation of very high gravity (VHG) wheat mashes. Journal of Industrial Microbiology. 1992;10:61-8.
7. Pfromm PH, Amanor-Boadu V, Nelson R, Vadlani P, Madl R. Bio-butanol vs. bio-ethanol: a technical and economic assessment for corn and switchgrass fermented by yeast or *Clostridium acetobutylicum*. Biomass and Bioenergy. 2010;34:515-24.
8. Lian J, Mishra S, Zhao H. Recent advances in metabolic engineering of *Saccharomyces cerevisiae*: new tools and their applications. Metabolic Engineering. 2018;50:85-108.
9. Cori CF. Embden and the glycolytic pathway. Trends in Biochemical Sciences. 1983;8:257-9.
10. de Smidt O, du Preez JC, Albertyn J. The alcohol dehydrogenases of *Saccharomyces cerevisiae*: a comprehensive review. FEMS Yeast Research. 2008;8:967-78.
11. Roels J. Simple model for the energetics of growth on substrates with different degrees of reduction. Biotechnology and Bioengineering. 1980;22:33-53.

12. Russell JB, Cook GM. Energetics of bacterial growth: balance of anabolic and catabolic reactions. Microbiological Reviews. 1995;59:48-62.
13. Conroy BB, Bittner CJ, MacDonald JC, Luebbe MK, Erickson GE. 373 Effects of feeding isolated nutritional components in distillers grains on growing cattle performance. Journal of Animal Science. 2016;94:174-5.
14. Bakker BM, Overkamp KM, van Maris AJ, Kötter P, Luttik MA, van Dijken JP, et al. Stoichiometry and compartmentation of NADH metabolism in *Saccharomyces cerevisiae*. FEMS Microbiology Reviews. 2001;25:15-37.
15. Verduyn C, Postma E, Scheffers WA, van Dijken JP. Physiology of *Saccharomyces cerevisiae* in anaerobic glucose-limited chemostat cultures. Microbiology. 1990;136:395-403.
16. Albertyn J, Hohmann S, Thevelein JM, Prior BA. *GPD1*, which encodes glycerol-3-phosphate dehydrogenase, is essential for growth under osmotic stress in *Saccharomyces cerevisiae*, and its expression is regulated by the high-osmolarity glycerol response pathway. Molecular and Cellular Biology. 1994;14:4135-44.
17. Eriksson P, André L, Ansell R, Blomberg A, Adler L. Cloning and characterization of *GPD2*, a second gene encoding *sn*-glycerol 3-phosphate dehydrogenase (NAD^+) in *Saccharomyces cerevisiae*, and its comparison with *GPD1*. Molecular Microbiology. 1995;17:95-107.
18. Norbeck J, Påhlman A-K, Akhtar N, Blomberg A, Adler L. Purification and characterization of two isoenzymes of DL-glycerol-3-phosphatase from *Saccharomyces cerevisiae*: Identification of the corresponding *GPP1* and *GPP2* genes and evidence for osmotic regulation of Gpp2p expression by the osmosensing mitogen-activated protein kinase signal transduction pathway. Journal of Biological Chemistry. 1996;271:13875-81.
19. Nissen TL, Hamann CW, Kielland-Brandt MC, Nielsen J, Villadsen J. Anaerobic and aerobic batch cultivations of *Saccharomyces cerevisiae* mutants impaired in glycerol synthesis. Yeast. 2000;16:463-74.
20. den Haan R, Kroukamp H, Mert M, Bloom M, Görgens JF, van Zyl WH. Engineering *Saccharomyces cerevisiae* for next generation ethanol production. Journal of Chemical Technology and Biotechnology. 2013;88:983-91.
21. Jansen ML, Bracher JM, Papapetridis I, Verhoeven MD, de Bruijn H, de Waal PP, et al. *Saccharomyces cerevisiae* strains for second-generation ethanol production: from academic exploration to industrial implementation. FEMS Yeast Research. 2017;17.
22. Laluce C, Schenberg ACG, Gallardo J, Coradello L, Pombeiro-Sponchiado S. Advances and developments in strategies to improve strains of *Saccharomyces cerevisiae* and processes to obtain the lignocellulosic ethanol–A review. Applied Biochemistry and Biotechnology. 2012;166:1908-26.

23. Boender LG, de Hulster EA, van Maris AJ, Daran-Lapujade PA, Pronk JT. Quantitative physiology of *Saccharomyces cerevisiae* at near-zero specific growth rates. Applied and Environmental Microbiology. 2009;75:5607-14.
24. Tännler S, Decasper S, Sauer U. Maintenance metabolism and carbon fluxes in *Bacillus* species. Microbial Cell Factories. 2008;7:1-13.
25. Vos T, de la Torre Cortés P, van Gulik WM, Pronk JT, Daran-Lapujade P. Growth-rate dependency of de novo resveratrol production in chemostat cultures of an engineered *Saccharomyces cerevisiae* strain. Microbial Cell Factories. 2015;14:1-15.
26. Abbott DA, Suir E, van Maris AJ, Pronk JT. Physiological and transcriptional responses to high concentrations of lactic acid in anaerobic chemostat cultures of *Saccharomyces cerevisiae*. Applied and Environmental Microbiology. 2008;74:5759-68.
27. Taherzadeh MJ, Niklasson C, Lidén G. Acetic acid—friend or foe in anaerobic batch conversion of glucose to ethanol by *Saccharomyces cerevisiae*? Chemical Engineering Science. 1997;52:2653-9.
28. Verduyn C, Postma E, Scheffers WA, van Dijken JP. Energetics of *Saccharomyces cerevisiae* in anaerobic glucose-limited chemostat cultures. Microbiology. 1990;136:405-12.
29. Verduyn C, Postma E, Scheffers WA, van Dijken JP. Effect of benzoic acid on metabolic fluxes in yeasts: a continuous-culture study on the regulation of respiration and alcoholic fermentation. Yeast. 1992;8:501-17.
30. Viegas CA, Isabel S-C. Activation of plasma membrane ATPase of *Saccharomyces cerevisiae* by octanoic acid. Journal of General Microbiology. 1991;137:645-51.
31. Narendranath NV, Thomas KC, Ingledew WM. Acetic acid and lactic acid inhibition of growth of *Saccharomyces cerevisiae* by different mechanisms. Journal of the American Society of Brewing Chemists. 2001;59:187-94.
32. Serrano R. Energy requirements for maltose transport in yeast. European Journal of Biochemistry. 1977;80:97-102.
33. Weusthuis RA, Adams H, Scheffers WA, van Dijken JP. Energetics and kinetics of maltose transport in *Saccharomyces cerevisiae*: a continuous culture study. Applied and Environmental Microbiology. 1993;59:3102-9.
34. Cardoso H, Leão C. Mechanisms underlying the low and high enthalphy death induced by short-chain monocarboxylic acids and ethanol in *Saccharomyces cerevisiae*. Applied Microbiology and Biotechnology. 1992;38:388-92.
35. Santos J, Sousa MJ, Cardoso H, Inacio J, Silva S, Spencer-Martins I, et al. Ethanol tolerance of sugar transport, and the rectification of stuck wine fermentations. Microbiology. 2008;154:422-30.

36. Dunlop A. Furfural formation and behavior. Industrial and Engineering Chemistry. 1948;40:204-9.
37. Russell I. Understanding yeast fundamentals. In: The Alcohol Textbook. Jacques K, Lyons T, Kelsall D, editors. 4 ed. Nottingham. 2003. p. 85-120.
38. Ulbricht RJ, Northup SJ, Thomas JA. A review of 5-hydroxymethylfurfural (HMF) in parenteral solutions. Toxicological Sciences. 1984;4:843-53.
39. Monteiro G, Sá-Correia I, Supply P, Goffeau A. The *in vivo* activation of *Saccharomyces cerevisiae* plasma membrane H^+-ATPase by ethanol depends on the expression of the *PMA1* gene, but not of the *PMA2* gene. Yeast. 1994;10:1439-46.
40. Rosa MF, Sá-Correia I. In vivo activation by ethanol of plasma membrane ATPase of *Saccharomyces cerevisiae*. Applied and Environmental Microbiology. 1991;57:830-5.
41. Boles E, Hollenberg CP. The molecular genetics of hexose transport in yeasts. FEMS Microbiology Reviews. 1997;21:85-111.
42. Lagunas R. Sugar transport in *Saccharomyces cerevisiae*. FEMS Microbiology Reviews. 1993;10:229-42.
43. van Leeuwen C, Weusthuis R, Postma E, van den Broek P, van Dijken J. Maltose/proton co-transport in *Saccharomyces cerevisiae*. Comparative study with cells and plasma membrane vesicles. Biochemical Journal. 1992;284:441-5.
44. Nissen TL, Schulze U, Nielsen J, Villadsen J. Flux distributions in anaerobic, glucose-limited continuous cultures of *Saccharomyces cerevisiae*. Microbiology. 1997;143:203-18.
45. Albers E, Larsson C, Lid n G, Niklasson C, Gustafsson L. Influence of the nitrogen source on *Saccharomyces cerevisiae* anaerobic growth and product formation. Applied and Environmental Microbiology. 1996;62:3187-95.
46. Jørgensen H. Effect of nutrients on fermentation of pretreated wheat straw at very high dry matter content by *Saccharomyces cerevisiae*. Applied Biochemistry and Biotechnology. 2009;153:44-57.
47. Radler F, Schütz H. Glycerol production of various strains of *Saccharomyces*. American Journal of Enology and Viticulture. 1982;33:36-40.
48. Jensen P, Snoep J, Westerhoff H, inventors; Peter Ruhdal Jensen, assignee. Method for improving the production of biomass or a desired product from a cell. US 7250280B2; 2007 July 31.
49. Zahoor A, Messerschmidt K, Boecker S, Klamt S. ATPase-based implementation of enforced ATP wasting in *Saccharomyces cerevisiae* for improved ethanol production. Biotechnology for Biofuels. 2020;13:1-12.
50. Rogers D, Szostak J, inventors; Genetics Institute, Inc., assignee. Strains of yeast with increased rates of glycolysis. US 005268285A; 1993 Dec 7.

51. Semkiv MV, Dmytruk KV, Abbas CA, Sibirny AA. Increased ethanol accumulation from glucose via reduction of ATP level in a recombinant strain of *Saccharomyces cerevisiae* overexpressing alkaline phosphatase. BMC Biotechnology. 2014;14:1-9.
52. Navas MA, Cerdán S, Gancedo JM. Futile cycles in *Saccharomyces cerevisiae* strains expressing the gluconeogenic enzymes during growth on glucose. Proceedings of the National Academy of Sciences. 1993;90:1290-4.
53. Navas MA, Gancedo JM. The regulatory characteristics of yeast fructose-1,6-bisphosphatase confer only a small selective advantage. Journal of Bacteriology. 1996;178:1809-12.
54. Semkiv MV, Dmytruk KV, Abbas CA, Sibirny AA. Activation of futile cycles as an approach to increase ethanol yield during glucose fermentation in *Saccharomyces cerevisiae*. Bioengineered. 2016;7:106-11.
55. Lee K, Skotnicki M, Tribe D, Rogers P. Kinetic studies on a highly productive strain of *Zymomonas mobilis*. Biotechnology Letters. 1980;2:339-44.
56. Rogers P, Lee KJ, Tribe D. Kinetics of alcohol production by *Zymomonas mobilis* at high sugar concentrations. Biotechnology Letters. 1979;1:165-70.
57. Lancashire W, Dickinson J, Malloch R, inventors; cardiff university college consultants ltd whitbread PLC, assignee. DNA encoding enzymes of the glycolytic pathway of for use in alcohol producing yeast. US 005786186A; 1994 Jul 28.
58. Benisch F, Boles E. The bacterial Entner–Doudoroff pathway does not replace glycolysis in *Saccharomyces cerevisiae* due to the lack of activity of iron–sulfur cluster enzyme 6-phosphogluconate dehydratase. Journal of Biotechnology. 2014;171:45-55.
59. Morita K, Nomura Y, Ishii J, Matsuda F, Kondo A, Shimizu H. Heterologous expression of bacterial phosphoenol pyruvate carboxylase and Entner–Doudoroff pathway in *Saccharomyces cerevisiae* for improvement of isobutanol production. Journal of Bioscience and Bioengineering. 2017;124:263-70.
60. Gardner PR, Fridovich I. Superoxide sensitivity of the *Escherichia coli* 6-phosphogluconate dehydratase. Journal of Biological Chemistry. 1991;266:1478-83.
61. Biz A, Mahadevan R. Overcoming challenges in expressing iron–sulfur enzymes in yeast. Trends in Biotechnology. 2021;39:665-77.
62. Bro C, Regenberg B, Förster J, Nielsen J. In silico aided metabolic engineering of *Saccharomyces cerevisiae* for improved bioethanol production. Metabolic Engineering. 2006;8:102-11.
63. Guo Z-p, Zhang L, Ding Z-y, Shi G-y. Minimization of glycerol synthesis in industrial ethanol yeast without influencing its fermentation performance. Metabolic Engineering. 2011;13:49-59.

64. Zhang L, Tang Y, Guo Z-p, Ding Z-y, Shi G-y. Improving the ethanol yield by reducing glycerol formation using cofactor regulation in *Saccharomyces cerevisiae*. Biotechnology Letters. 2011;33:1375-80.
65. Carlson M, Botstein D. Two differentially regulated mRNAs with different 5′ ends encode secreted and intracellular forms of yeast invertase. Cell. 1982;28:145-54.
66. Gascón S, Lampen JO. Purification of the internal invertase of yeast. Journal of Biological Chemistry. 1968;243:1567-72.
67. Kruckeberg AL. The hexose transporter family of *Saccharomyces cerevisiae*. Archives of microbiology. 1996;166:283–92.
68. Santos E, Rodriguez L, Elorza MV, Sentandreu R. Uptake of sucrose by *Saccharomyces cerevisiae*. Archives of Biochemistry and Biophysics. 1982;216:652-60.
69. Stambuk BU, Batista AS, De Araujo PS. Kinetics of active sucrose transport in *Saccharomyces cerevisiae*. Journal of Bioscience and Bioengineering. 2000;89:212-4.
70. Basso TO, de Kok S, Dario M, do Espirito-Santo JCA, Müller G, Schlölg PS, et al. Engineering topology and kinetics of sucrose metabolism in *Saccharomyces cerevisiae* for improved ethanol yield. Metabolic Engineering. 2011;13:694-703.
71. de Kok S, Kozak BU, Pronk JT, van Maris AJ. Energy coupling in *Saccharomyces cerevisiae*: selected opportunities for metabolic engineering. FEMS Yeast Research. 2012;12:387-97.
72. Tiukova IA, Møller-Hansen I, Belew ZM, Darbani B, Boles E, Nour-Eldin HH, et al. Identification and characterisation of two high-affinity glucose transporters from the spoilage yeast *Brettanomyces bruxellensis*. FEMS Microbiology Letters. 2019;366:fnz222.
73. Athenstaedt K, Weys S, Paltauf F, Daum Gn. Redundant systems of phosphatidic acid biosynthesis via acylation of glycerol-3-phosphate or dihydroxyacetone phosphate in the yeast *Saccharomyces cerevisiae*. Journal of Bacteriology. 1999;181:1458-63.
74. Ansell R, Granath K, Hohmann S, Thevelein JM, Adler L. The two isoenzymes for yeast NAD+-dependent glycerol 3-phosphate dehydrogenase encoded by *GPD1* and *GPD2* have distinct roles in osmoadaptation and redox regulation. The EMBO Journal. 1997;16:2179-87.
75. Björkqvist S, Ansell R, Adler L, Liden G. Physiological response to anaerobicity of glycerol-3-phosphate dehydrogenase mutants of *Saccharomyces cerevisiae*. Applied and Environmental Microbiology. 1997;63:128-32.
76. Blomberg A, Adler L. Physiology of osmotolerance in fungi. Advances in Microbial Physiology. 1992;33:145-212.
77. Papapetridis I, Goudriaan M, Vázquez Vitali M, De Keijzer NA, Van Den Broek M, Van Maris AJ, et al. Optimizing anaerobic growth rate and fermentation kinetics in

Saccharomyces cerevisiae strains expressing Calvin-cycle enzymes for improved ethanol yield. Biotechnology for Biofuels. 2018;11:1-17.
78. van Dijken JP, Scheffers WA. Redox balances in the metabolism of sugars by yeasts. FEMS Microbiology Reviews. 1986;1:199-224.
79. Henriques D, Minebois R, Mendoza SN, Macías LG, Pérez-Torrado R, Barrio E, et al. A multiphase multiobjective dynamic genome-scale model shows different redox balancing among yeast species of the *Saccharomyces* genus in fermentation. mSystems. 2021;6:e00260-21.
80. Hubmann G, Guillouet S, Nevoigt E. Gpd1 and Gpd2 fine-tuning for sustainable reduction of glycerol formation in *Saccharomyces cerevisiae*. Applied and Environmental Microbiology. 2011;77:5857-67.
81. Bruinenberg PM, van Dijken JP, Scheffers WA. A theoretical analysis of NADPH production and consumption in yeasts. Journal of General Microbiology. 1983;129:953-64.
82. Bruinenberg PM, Jonker R, van Dijken JP, Scheffers WA. Utilization of formate as an additional energy source by glucose-limited chemostat cultures of *Candida utilis* CBS 621 and *Saccharomyces cerevisiae* CBS 8066. Archives of Microbiology. 1985;142:302-6.
83. Anderlund M, Nissen TL, Nielsen J, Villadsen J, Rydström J, Hahn-Hägerdal Br, et al. Expression of the *Escherichia coli* pntA and pntB genes, encoding nicotinamide nucleotide transhydrogenase, in *Saccharomyces cerevisiae* and its effect on product formation during anaerobic glucose fermentation. Applied Environmental Microbiology. 1999;65:2333-40.
84. Nissen TL, Anderlund M, Nielsen J, Villadsen J, Kielland-Brandt MC. Expression of a cytoplasmic transhydrogenase in *Saccharomyces cerevisiae* results in formation of 2-oxoglutarate due to depletion of the NADPH pool. Yeast. 2001;18:19-32.
85. Nissen TL, Kielland-Brandt MC, Nielsen J, Villadsen J. Optimization of ethanol production in *Saccharomyces cerevisiae* by metabolic engineering of the ammonium assimilation. Metabolic Engineering. 2000;2:69-77.
86. Nogae I, Johnston M. Isolation and characterization of the *ZWF1* gene of *Saccharomyces cerevisiae*, encoding glucose-6-phosphate dehydrogenase. Gene. 1990;96:161-9.
87. Vanrolleghem PA, de Jong-Gubbels P, van Gulik WM, Pronk JT, van Dijken JP, Heijnen S. Validation of a metabolic network for *Saccharomyces cerevisiae* using mixed substrate studies. Biotechnology Progress. 1996;12:434-48.
88. Navarrete C, Nielsen J, Siewers V. Enhanced ethanol production and reduced glycerol formation in *fps1Δ* mutants of *Saccharomyces cerevisiae* engineered for improved redox balancing. Amb Express. 2014;4:1-8.

89. Remize F, Barnavon L, Dequin S. Glycerol export and glycerol-3-phosphate dehydrogenase, but not glycerol phosphatase, are rate limiting for glycerol production in *Saccharomyces cerevisiae*. Metabolic Engineering. 2001;3:301-12.
90. Ciriacy M. Genetics of alcohol dehydrogenase in *Saccharomyces cerevisiae*: Isolation and genetic analysis of *adh* mutants. Mutation Research. 1975;29:315-25.
91. Guadalupe-Medina V, Almering MJ, van Maris AJ, Pronk JT. Elimination of glycerol production in anaerobic cultures of a *Saccharomyces cerevisiae* strain engineered to use acetic acid as an electron acceptor. Applied and Environmental Microbiology. 2010;76:190-5.
92. van den Berg MA, de Jong-Gubbels P, Kortland CJ, van Dijken JP, Pronk JT, Steensma HY. The two acetyl-coenzyme A synthetases of *Saccharomyces cerevisiae* differ with respect to kinetic properties and transcriptional regulation. Journal of Biological Chemistry. 1996;271:28953-9.
93. Papapetridis I, Van Dijk M, Van Maris AJ, Pronk JT. Metabolic engineering strategies for optimizing acetate reduction, ethanol yield and osmotolerance in *Saccharomyces cerevisiae*. Biotechnology for Biofuels. 2017;10:1-14.
94. Almeida JR, Modig T, Petersson A, Hähn-Hägerdal B, Lidén G, Gorwa-Grauslund MF. Increased tolerance and conversion of inhibitors in lignocellulosic hydrolysates by *Saccharomyces cerevisiae*. Journal of Chemical Technology and Biotechnology. 2007;82:340-9.
95. Papapetridis I, van Dijk M, Dobbe A, Metz B, Pronk JT, van Maris AJ. Improving ethanol yield in acetate-reducing *Saccharomyces cerevisiae* by cofactor engineering of 6-phosphogluconate dehydrogenase and deletion of *ALD6*. Microbial Cell Factories. 2016;15:1-16.
96. Henningsen BM, Hon S, Covalla SF, Sonu C, Argyros DA, Barrett TF, et al. Increasing anaerobic acetate consumption and ethanol yields in *Saccharomyces cerevisiae* with NADPH-specific alcohol dehydrogenase. Applied and Environmental Microbiology. 2015;81:8108-17.
97. Kim Y, Mosier NS, Hendrickson R, Ezeji T, Blaschek H, Dien B, et al. Composition of corn dry-grind ethanol by-products: DDGS, wet cake, and thin stillage. Bioresource Technology. 2008;99:5165-76.
98. de Bont J, Teunissen A, Klaassen P, Hartman W, van Beusekom S, inventors; DSM IP ASSETS B.V., assignee. Yeast strains engineered to produce ethanol from acetic acid and glycerol. US 009988649B2; 2018 Jun 5.
99. Klaassen P, Hartman W, inventors; DSM IP ASSETS B.V., assignee. Glycerol and acetic acid converting yeast cells with improved acetic acid conversion. US 010450588B2; 2019 Oct 22.

100. Rasmussen ML, Koziel JA, Jane J-l, Pometto III AL. Reducing bacterial contamination in fuel ethanol fermentations by ozone treatment of uncooked corn mash. Journal of Agricultural and Food Chemistry. 2015;63:5239-48.
101. Argyros A, Sillers W, Barrett T, Caiazza N, Shaw A, inventors; Lallemand Hungary Liquidity Management, assignee. Methods for the improvement of product yield and production in a microorganism through the addition of alternate electron acceptors. US 008956851B2; 2015 Feb 17.
102. de Bont J, Teunissen A, inventors; Yeast Company B.V., assignee. Yeast strains engineered to produce ethanol from glycerol. WO 2012/067510 A1; 2012 May 4. International patent WO 2012/067510 A1.
103. Kozak BU, van Rossum HM, Benjamin KR, Wu L, Daran J-MG, Pronk JT, et al. Replacement of the *Saccharomyces cerevisiae* acetyl-CoA synthetases by alternative pathways for cytosolic acetyl-CoA synthesis. Metabolic Engineering. 2014;21:46-59.
104. van Rossum HM, Kozak BU, Pronk JT, van Maris AJ. Engineering cytosolic acetyl-coenzyme A supply in *Saccharomyces cerevisiae*: pathway stoichiometry, free-energy conservation and redox-cofactor balancing. Metabolic Engineering. 2016;36:99-115.
105. Overkamp KM, Kötter P, van der Hoek R, Schoondermark-Stolk S, Luttik MA, van Dijken JP, et al. Functional analysis of structural genes for NAD^+-dependent formate dehydrogenase in *Saccharomyces cerevisiae*. Yeast. 2002;19:509-20.
106. Andrei M, Munos JW, inventors; Danisco US Inc, assignee. Altered host cell pathway for improved ethanol production. US 2017088861A1; 2017 Mar 30.
107. Bergman A, Siewers V, Nielsen J, Chen Y. Functional expression and evaluation of heterologous phosphoketolases in *Saccharomyces cerevisiae*. Amb Express. 2016;6:1-13.
108. Meadows AL, Hawkins KM, Tsegaye Y, Antipov E, Kim Y, Raetz L, et al. Rewriting yeast central carbon metabolism for industrial isoprenoid production. Nature. 2016;537:694-7.
109. Guadalupe-Medina V, Wisselink HW, Luttik MA, de Hulster E, Daran J-M, Pronk JT, et al. Carbon dioxide fixation by Calvin-Cycle enzymes improves ethanol yield in yeast. Biotechnology for Biofuels. 2013;6:1-12.
110. Hernandez JM, Baker SH, Lorbach SC, Shively JM, Tabita FR. Deduced amino acid sequence, functional expression, and unique enzymatic properties of the form I and form II ribulose bisphosphate carboxylase/oxygenase from the chemoautotrophic bacterium *Thiobacillus denitrificans*. Journal of Bacteriology. 1996;178:347-56.
111. Brandes HK, Hartman FC, Lu T-YS, Larimer FW. Efficient Expression of the Gene for Spinach Phosphoribulokinase in *Pichia pastoris* and Utilization of the Recombinant Enzyme to Explore the Role of Regulatory Cysteinyl Residues by Site-directed Mutagenesis. Journal of Biological Chemistry. 1996;271:6490-6.

112. Hudson G, Morell M, Arvidsson Y, Andrews T. Synthesis of spinach phosphoribulokinase and ribulose 1, 5-bisphosphate in *Escherichia coli*. Functional Plant Biology. 1992;19:213-21.
113. Kötter P, Ciriacy M. Xylose fermentation by *Saccharomyces cerevisiae*. Applied Microbiology and Biotechnology. 1993;38:776-83.
114. Roca C, Nielsen J, Olsson L. Metabolic engineering of ammonium assimilation in xylose-fermenting *Saccharomyces cerevisiae* improves ethanol production. Applied and Environmental Microbiology. 2003;69:4732-6.
115. Li Y-J, Wang M-M, Chen Y-W, Wang M, Fan L-H, Tan T-W. Engineered yeast with a CO_2-fixation pathway to improve the bio-ethanol production from xylose-mixed sugars. Scientific Reports. 2017;7:1-9.
116. Xia P-F, Zhang G-C, Walker B, Seo S-O, Kwak S, Liu J-J, et al. Recycling carbon dioxide during xylose fermentation by engineered *Saccharomyces cerevisiae*. ACS Synthetic Biology. 2017;6:276-83.
117. Sonderegger M, Schümperli M, Sauer U. Metabolic engineering of a phosphoketolase pathway for pentose catabolism in *Saccharomyces cerevisiae*. Applied and Environmental Microbiology. 2004;70:2892-7.
118. Daran-Lapujade P, Jansen ML, Daran J-M, van Gulik W, de Winde JH, Pronk JT. Role of transcriptional regulation in controlling fluxes in central carbon metabolism of *Saccharomyces cerevisiae*: a chemostat culture study. Journal of Biological Chemistry. 2004;279:9125-38.
119. Pirt S. The maintenance energy of bacteria in growing cultures. Proceedings of the Royal Society of London Series B. 1965;163:224-31.
120. Regueira A, Lema JM, Mauricio-Iglesias M. Microbial inefficient substrate use through the perspective of resource allocation models. Current Opinion in Biotechnology. 2021;67:130-40.
121. Sánchez BJ, Zhang C, Nilsson A, Lahtvee PJ, Kerkhoven EJ, Nielsen J. Improving the phenotype predictions of a yeast genome-scale metabolic model by incorporating enzymatic constraints. Molecular Systems Biology. 2017;13:935.
122. Hennaut C, Hilger F, Grenson M. Space limitation for permease insertion in the cytoplasmic membrane of *Saccharomyces cerevisiae*. Biochemical and Biophysical Research Communications. 1970;39:666-71.
123. Glick BR. Metabolic load and heterologous gene expression. Biotechnology Advances. 1995;13:247-61.
124. Gopal CV, Broad D, Lloyd D. Bioenergetic consequences of protein overexpression in *Saccharomyces cerevisiae*. Applied Microbiology and Biotechnology. 1989;30:160-5.
125. Daran-Lapujade P, Jansen MLA, Daran J-M, van Gulik WM, de Winde JH, Pronk JT. Role of Transcriptional Regulation in Controlling Fluxes in Central Carbon

Metabolism of *Saccharomyces cerevisiae*. The Journal of Biological Chemistry. 2004;279:9125–38.
126. Boender LGM, de Hulster E, van Maris AJA, Daran-Lapujade P, Pronk JT. Quantitative Physiology of *Saccharomyces cerevisiae* at Near-Zero Specific Growth Rates. Applied and Environmental Microbiology. 2009;75:5607-17.
127. Lange HC, Heijnen JJ. Statistical Reconciliation of the Elemental and Molecular Biomass Composition of *Saccharomyces cerevisiae*. Biotechnology and Bioengineering. 2001;75:334-44.
128. Dürre P, Eikmanns BJ. C1-carbon sources for chemical and fuel production by microbial gas fermentation. Current Opinion in Biotechnology. 2015;35:63-72.
129. Della-Bianca BE, Basso TO, Stambuk BU, Basso LC, Gombert AK. What do we know about the yeast strains from the Brazilian fuel ethanol industry? Applied Microbiology and Biotechnology. 2013;97:979-91.
130. Ingledew W, Lin Y. Ethanol from starch-based feedstocks. In: Comprehensive biotechnology. 2 ed. Amsterdam. Elsevier; 2011. p. 37-49.
131. Dugar D, Stephanopoulos G. Relative potential of biosynthetic pathways for biofuels and bio-based products. Nature Biotechnology. 2011;29:1074-8.
132. van Aalst AC, de Valk SC, van Gulik WM, Jansen ML, Pronk JT, Mans R. Pathway engineering strategies for improved product yield in yeast-based industrial ethanol production. Synthetic and Systems Biotechnology. 2022;7:554-66.
133. Cohen BD, Sertil O, Abramova NE, Davies KJ, Lowry CV. Induction and repression of *DAN1* and the family of anaerobic mannoprotein genes in *Saccharomyces cerevisiae* occurs through a complex array of regulatory sites. Nucleic Acids Research. 2001;29:799-808.
134. Zitomer RS, Lowry CV. Regulation of gene expression by oxygen in *Saccharomyces cerevisiae*. Microbiological Reviews. 1992;56:1-11.
135. Ingram LON, Buttke TM. Effects of alcohols on micro-organisms. Advances in Microbial Physiology. 1985;25:253-300.
136. Guan X, Rubin E, Anni H. An optimized method for the measurement of acetaldehyde by high-performance liquid chromatography. Alcoholism: Clinical and Experimental Research. 2012;36:398-405.
137. Stanley G, Douglas N, Every E, Tzanatos T, Pamment N. Inhibition and stimulation of yeast growth by acetaldehyde. Biotechnology Letters. 1993;15:1199-204.
138. Saint-Prix F, Bönquist L, Dequin S. Functional analysis of the *ALD* gene family of *Saccharomyces cerevisiae* during anaerobic growth on glucose: the NADP+-dependent Ald6p and Ald5p isoforms play a major role in acetate formation. Microbiology. 2004;150:2209-20.

139. Verhoeven MD, Lee M, Kamoen L, van Den Broek M, Janssen DB, Daran J-MG, et al. Mutations in *PMR1* stimulate xylose isomerase activity and anaerobic growth on xylose of engineered *Saccharomyces cerevisiae* by influencing manganese homeostasis. Scientific Reports. 2017;7:1-11.
140. van Aalst AC, Mans R, Pronk JT. An engineered non-oxidative glycolytic bypass based on Calvin-cycle enzymes enables anaerobic co-fermentation of glucose and sorbitol by *Saccharomyces cerevisiae*. Biotechnology for Biofuels and Bioproducts. 2022;15:1-15.
141. Salama SR, Hendricks KB, Thorner J. G1 cyclin degradation: the PEST motif of yeast Cln2 is necessary, but not sufficient, for rapid protein turnover. Molecular Cellular Biology. 1994;14:7953-66.
142. Wang D, Zhang Y, Pohlmann EL, Li J, Roberts GP. The poor growth of *Rhodospirillum rubrum* mutants lacking RubisCO is due to the accumulation of ribulose-1, 5-bisphosphate. Journal of Bacteriology. 2011;193:3293-303.
143. de Jong-Gubbels P, van den Berg MA, Steensma HY, van Dijken JP, Pronk JT. The *Saccharomyces cerevisiae* acetyl-coenzyme A synthetase encoded by the *ACS1* gene, but not the *ACS2*-encoded enzyme, is subject to glucose catabolite inactivation. FEMS Microbiology Letters. 1997;153:75-81.
144. Regenberg B, Grotkjær T, Winther O, Fausbøll A, Åkesson M, Bro C, et al. Growth-rate regulated genes have profound impact on interpretation of transcriptome profiling in *Saccharomyces cerevisiae*. Genome Biology. 2006;7:1-13.
145. Mehta K, Leung D, Lefebvre L, Smith M. The *ANB1* locus of *Saccharomyces cerevisiae* encodes the protein synthesis initiation factor eIF-4D. Journal of Biological Chemistry. 1990;265:8802-7.
146. Batista FR, Meirelles AJ. A strategy for controlling acetaldehyde content in an industrial plant of bioethanol. IFAC Proceedings Volumes. 2009;42:928-33.
147. Cohen G, Kreutzer N, Mowat K, Hassan AA, Dvorak B. Compliance with hand sanitizer quality during the SARS-CoV-2 pandemic: Assessing the impurities in an ethanol plant. Journal of Environmental Management. 2021;297:113329.
148. Cameron DE, Collins JJ. Tunable protein degradation in bacteria. Nature Biotechnology. 2014;32:1276-81.
149. Peng B, Plan MR, Chrysanthopoulos P, Hodson MP, Nielsen LK, Vickers CE. A squalene synthase protein degradation method for improved sesquiterpene production in *Saccharomyces cerevisiae*. Metabolic Engineering. 2017;39:209-19.
150. Mateus C, Avery SV. Destabilized green fluorescent protein for monitoring dynamic changes in yeast gene expression with flow cytometry. Yeast. 2000;16:1313-23.
151. Pyne ME, Narcross L, Melgar M, Kevvai K, Mookerjee S, Leite GB, et al. An engineered Aro1 protein degradation approach for increased cis, cis-muconic acid

biosynthesis in *Saccharomyces cerevisiae*. Applied and Environmental Microbiology. 2018;84:e01095-18.
152. Secches TO, Santos Viera CF, Pereira TK, Santos VT, Ribeirodos Santos J, Pereira GA, et al. Brazilian industrial yeasts show high fermentative performance in high solids content for corn ethanol process. Bioresources and Bioprocessing. 2022;9:1-9.
153. Skjoedt ML, Snoek T, Kildegaard KR, Arsovska D, Eichenberger M, Goedecke TJ, et al. Engineering prokaryotic transcriptional activators as metabolite biosensors in yeast. Nature Chemical Biology. 2016;12:951-8.
154. Zhang J, Sonnenschein N, Pihl TP, Pedersen KR, Jensen MK, Keasling JD. Engineering an NADPH/$NADP^+$ redox biosensor in yeast. ACS Synthetic Biology. 2016;5:1546-56.
155. Huang G, Zhang Y, Shan Y, Yang S, Chelliah Y, Wang H, et al. Circadian oscillations of NADH redox state using a heterologous metabolic sensor in mammalian cells. Journal of Biological Chemistry. 2016;291:23906-14.
156. Hung YP, Albeck JG, Tantama M, Yellen G. Imaging cytosolic NADH-NAD+ redox state with a genetically encoded fluorescent biosensor. Cell Metabolism. 2011;14:545-54.
157. Liu Y, Landick R, Raman S. A regulatory NADH/NAD+ redox biosensor for bacteria. ACS Synthetic Biology. 2019;8:264-73.
158. Lee C, Kim I, Lee J, Lee K-L, Min B, Park C. Transcriptional activation of the aldehyde reductase YqhD by YqhC and its implication in glyoxal metabolism of *Escherichia coli* K-12. Journal of Bacteriology. 2010;192:4205-14.
159. Frazão CR, Maton V, François JM, Walther T, Biotechnology. Development of a metabolite sensor for high-throughput detection of aldehydes in *Escherichia coli*. Frontiers in Bioengineering Biotechnology. 2018;6:118.
160. Turner PC, Miller EN, Jarboe LR, Baggett CL, Shanmugam K, Ingram LO. YqhC regulates transcription of the adjacent *Escherichia coli* genes yqhD and dkgA that are involved in furfural tolerance. Journal of Industrial Microbiology Biotechnology. 2011;38:431-9.
161. Qi LS, Larson MH, Gilbert LA, Doudna JA, Weissman JS, Arkin AP, et al. Repurposing CRISPR as an RNA-guided platform for sequence-specific control of gene expression. Cell. 2013;152:1173-83.
162. Williams T, Averesch N, Winter G, Plan M, Vickers C, Nielsen L, et al. Quorum-sensing linked RNA interference for dynamic metabolic pathway control in *Saccharomyces cerevisiae*. Metabolic Engineering. 2015;29:124-34.
163. Lu Z, Peng B, Ebert BE, Dumsday G, Vickers CE. Auxin-mediated protein depletion for metabolic engineering in terpene-producing yeast. Nature Communications. 2021;12:1-13.

164. D'ambrosio V, Jensen MK. Lighting up yeast cell factories by transcription factor-based biosensors. FEMS Yeast Research. 2017;17.
165. Ambri F, Snoek T, Skjoedt ML, Jensen MK, Keasling JD. Design, engineering, and characterization of prokaryotic ligand-binding transcriptional activators as biosensors in yeast. In: Synthetic Metabolic Pathways. Springer; 2018. p. 269-90.
166. Snoek T, Chaberski EK, Ambri F, Kol S, Bjørn SP, Pang B, et al. Evolution-guided engineering of small-molecule biosensors. Nucleic Acids Research. 2020;48:e3-e.
167. Ambri F, D'Ambrosio V, Di Blasi R, Maury J, Jacobsen SAB, McCloskey D, et al. High-resolution scanning of optimal biosensor reporter promoters in yeast. ACS Synthetic Biology. 2020;9:218-26.
168. Entian K-D, Kötter P. 25 yeast genetic strain and plasmid collections. Methods in Microbiology. 2007;36:629-66.
169. Nijkamp JF, van den Broek M, Datema E, de Kok S, Bosman L, Luttik MA, et al. De novo sequencing, assembly and analysis of the genome of the laboratory strain Saccharomyces cerevisiae CEN. PK113-7D, a model for modern industrial biotechnology. Microbial cell factories. 2012;11:36.
170. Boer VM, de Winde JH, Pronk JT, Piper MD. The genome-wide transcriptional responses of *Saccharomyces cerevisiae* grown on glucose in aerobic chemostat cultures limited for carbon, nitrogen, phosphorus, or sulfur. Journal of Biological Chemistry. 2003;278:3265-74.
171. Bertani G. Lysogeny at mid-twentieth century: P1, P2, and other experimental systems. Journal of Bacteriology. 2004;186:595-600.
172. Froger A, Hall JE. Transformation of plasmid DNA into E. coli using the heat shock method. Journal of visualized experiments: JoVE. 2007.
173. Lõoke M, Kristjuhan K, Kristjuhan A. Extraction of genomic DNA from yeasts for PCR-based applications. Biotechniques. 2011;50:325-8.
174. Mans R, Wijsman M, Daran-Lapujade P, Daran J-M. A protocol for introduction of multiple genetic modifications in *Saccharomyces cerevisiae* using CRISPR/Cas9. FEMS Yeast Research. 2018;18:foy063.
175. Mans R, van Rossum HM, Wijsman M, Backx A, Kuijpers NG, van den Broek M, et al. CRISPR/Cas9: a molecular Swiss army knife for simultaneous introduction of multiple genetic modifications in *Saccharomyces cerevisiae*. FEMS Yeast Research. 2015;15.
176. Kuijpers NG, Solis-Escalante D, Bosman L, van den Broek M, Pronk JT, Daran J-M, et al. A versatile, efficient strategy for assembly of multi-fragment expression vectors in *Saccharomyces cerevisiae* using 60 bp synthetic recombination sequences. Microbial Cell Factories. 2013;12:1-13.

177. Mumberg D, Müller R, Funk M. Yeast vectors for the controlled expression of heterologous proteins in different genetic backgrounds. Gene. 1995;156:119-22.
178. Gietz RD, Woods RA. Genetic transformation of yeast. Biotechniques. 2001;30:816-31.
179. Mooiman C, Bouwknegt J, Dekker WJ, Wiersma SJ, Ortiz-Merino RA, De Hulster E, et al. Critical parameters and procedures for anaerobic cultivation of yeasts in bioreactors and anaerobic chambers. FEMS Yeast Research. 2021;21:foab035.
180. Lange H, Eman M, Van Zuijlen G, Visser D, Van Dam J, Frank J, et al. Improved rapid sampling for in vivo kinetics of intracellular metabolites in *Saccharomyces cerevisiae*. Biotechnology and Bioengineering. 2001;75:406-15.
181. Mashego M, Van Gulik W, Vinke J, Heijnen J. Critical evaluation of sampling techniques for residual glucose determination in carbon-limited chemostat culture of *Saccharomyces cerevisiae*. Biotechnology and Bioengineering. 2003;83:395-9.
182. Lange H, Heijnen J. Statistical reconciliation of the elemental and molecular biomass composition of *Saccharomyces cerevisiae*. Biotechnology and Bioengineering. 2001;75:334-44.
183. Piper MD, Daran-Lapujade P, Bro C, Regenberg B, Knudsen S, Nielsen J, et al. Reproducibility of Oligonucleotide Microarray Transcriptome Analyses: an interlaboratory comparison using chemostat cultures of *Saccharomyces cerevisiae*. Journal of Biological Chemistry. 2002;277:37001-8.
184. Mendes F, Sieuwerts S, de Hulster E, Almering MJ, Luttik MA, Pronk JT, et al. Transcriptome-based characterization of interactions between *Saccharomyces cerevisiae* and *Lactobacillus delbrueckii* subsp. *bulgaricus* in lactose-grown chemostat cocultures. Applied and Environmental Microbiology. 2013;79:5949-61.
185. Tai SL, Boer VM, Daran-Lapujade P, Walsh MC, de Winde JH, Daran J-M, et al. Two-dimensional transcriptome analysis in chemostat cultures: combinatorial effects of oxygen availability and macronutrient limitation in *Saccharomyces cerevisiae*. Journal of Biological Chemistry. 2005;280:437-47.
186. Dobin A, Davis CA, Schlesinger F, Drenkow J, Zaleski C, Jha S, et al. STAR: ultrafast universal RNA-seq aligner. Bioinformatics. 2013;29:15-21.
187. Liao Y, Smyth GK, Shi W. featureCounts: an efficient general purpose program for assigning sequence reads to genomic features. Bioinformatics. 2014;30:923-30.
188. Robinson MD, McCarthy DJ, Smyth GK. edgeR: a Bioconductor package for differential expression analysis of digital gene expression data. Bioinformatics. 2010;26:139-40.
189. Koren S, Walenz BP, Berlin K, Miller JR, Bergman NH, Phillippy AM. Canu: scalable and accurate long-read assembly via adaptive k-mer weighting and repeat separation. Genome Research. 2017;27:722-36.

190. Lopes ML, Paulillo SCdL, Godoy A, Cherubin RA, Lorenzi MS, Giometti FHC, et al. Ethanol production in Brazil: a bridge between science and industry. Brazilian Journal of Microbiology. 2016;47:64-76.
191. Wei N, Quarterman J, Kim SR, Cate JH, Jin Y-S. Enhanced biofuel production through coupled acetic acid and xylose consumption by engineered yeast. Nature Communications. 2013;4:2580.
192. Taherzadeh MJ, Eklund R, Gustafsson L, Niklasson C, Lidén GJI, research ec. Characterization and fermentation of dilute-acid hydrolyzates from wood. Industrial and Engineering Chemistry Research. 1997;36:4659-65.
193. Thomas K, Hynes S, Ingledew WJA, microbiology e. Influence of medium buffering capacity on inhibition of *Saccharomyces cerevisiae* growth by acetic and lactic acids. Applied and Environmental Microbiology. 2002;68:1616-23.
194. Phibro Animal Health Corporation. https://fermfacts.com/ferm-facts/yeast-health/. Accessed 1 Dec 2022.
195. Kumar D, Jansen M, Basu R, Singh V. Enhancing ethanol yields in corn dry grind process by reducing glycerol production. Cereal Chemistry. 2020;97:1026-36.
196. Kumar D, Singh V. Dry-grind processing using amylase corn and superior yeast to reduce the exogenous enzyme requirements in bioethanol production. Biotechnology for Biofuels. 2016;9:1-12.
197. van Aalst AC, Jansen ML, Mans R, Pronk JT. Quantification and mitigation of byproduct formation by low-glycerol-producing *Saccharomyces cerevisiae* strains containing Calvin-cycle enzymes. Biotechnology for Biofuels and Bioproducts. 2023;16:1-17.
198. Flikweert MT, de Swaaf M, van Dijken JP, Pronk JT. Growth requirements of pyruvate-decarboxylase-negative *Saccharomyces cerevisiae*. FEMS Microbiology Letters. 1999;174:73-9.
199. Beber ME, Gollub MG, Mozaffari D, Shebek KM, Flamholz AI, Milo R, et al. eQuilibrator 3.0: a database solution for thermodynamic constant estimation. Nucleic Acids Research. 2022;50:603-9.
200. Shiba Y, Paradise EM, Kirby J, Ro D-K, Keasling JD. Engineering of the pyruvate dehydrogenase bypass in *Saccharomyces cerevisiae* for high-level production of isoprenoids. Metabolic Engineering. 2007;9:160-8.
201. Lian J, Si T, Nair NU, Zhao H. Design and construction of acetyl-CoA overproducing *Saccharomyces cerevisiae* strains. Metabolic Engineering. 2014;24:139-49.
202. Zhang GC, Kong II, Wei N, Peng D, Turner TL, Sung BH, et al. Optimization of an acetate reduction pathway for producing cellulosic ethanol by engineered yeast. Biotechnology and Bioengineering. 2016;113:2587-96.

203. Mans R, Daran J-MG, Pronk JT. Under pressure: evolutionary engineering of yeast strains for improved performance in fuels and chemicals production. Current Opinion in Biotechnology. 2018;50:47-56.
204. Guadalupe-Medina V, Metz B, Oud B, van der Graaf CM, Mans R, Pronk JT, et al. Evolutionary engineering of a glycerol-3-phosphate dehydrogenase-negative, acetate-reducing *Saccharomyces cerevisiae* strain enables anaerobic growth at high glucose concentrations. Microbial Biotechnology. 2014;7:44-53.
205. Ingledew WM. Water reuse in fuel alcohol plants: effect on fermentation. Is a 'zero discharge' concept attainable? In: The Alcohol Textbook. Jacques K, Lyons T, Kelsall D, editors. 4 ed. Nottingham. 2003. p. 343-54.
206. Renna M, Najimudin N, Winik L, Zahler S. Regulation of the *Bacillus subtilis* alsS, alsD, and alsR genes involved in post-exponential-phase production of acetoin. Journal of Bacteriology. 1993;175:3863-75.
207. Frädrich C, March A, Fiege K, Hartmann A, Jahn D, Härtig E. The transcription factor AlsR binds and regulates the promoter of the alsSD operon responsible for acetoin formation in *Bacillus subtilis*. Journal of Bacteriology. 2012;194:1100-12.
208. Nijkamp JF, van den Broek M, Datema E, de Kok S, Bosman L, Luttik MA, et al. De novo sequencing, assembly and analysis of the genome of the laboratory strain *Saccharomyces cerevisiae* CEN. PK113-7D, a model for modern industrial biotechnology. Microbial Cell Factories. 2012;11:1-17.
209. Pronk JT. Auxotrophic yeast strains in fundamental and applied research. Applied and Environmental Microbiology. 2002;68:2095-100.
210. Solis-Escalante D, Kuijpers NG, Nadine B, Bolat I, Bosman L, Pronk JT, et al. amdSYM, a new dominant recyclable marker cassette for *Saccharomyces cerevisiae*. FEMS Yeast Research. 2013;13:126-39.
211. Froger A, Hall JE. Transformation of plasmid DNA into *E. coli* using the heat shock method. JoVE. 2007:e253.
212. Salazar AN, Gorter de Vries AR, van den Broek M, Wijsman M, de la Torre Cortés P, Brickwedde A, et al. Nanopore sequencing enables near-complete de novo assembly of *Saccharomyces cerevisiae* reference strain CEN. PK113-7D. FEMS Yeast Research. 2017;17.
213. Kumar K, Bruheim P. Large dependency of intracellular NAD and CoA pools on cultivation conditions in *Saccharomyces cerevisiae*. BMC Research Notes. 2021;14:1-5.
214. Bekers K, Heijnen J, Van Gulik W. Determination of the in vivo NAD^+:NADH ratio in *Saccharomyces cerevisiae* under anaerobic conditions, using alcohol dehydrogenase as sensor reaction. Yeast. 2015;32:541-57.
215. Ingledew W. Yeast stress and fermentation. In: The Alcohol Textbook. Walker G, Abbas CA, Ingledew WM, Pilgrim C, editors. 6 ed. Duluth. 2017. p. 273-85.

216. van Zuyl F, Kauers K. Contaminant microbes and their control. In: The Alcohol Textbook. Walker G, Abbas CA, Ingledew WM, Pilgrim C, editors. 6 ed. Duluth. 2017. p. 377-400.
217. van Aalst AC, Geraats EH, Jansen ML, Mans R, Pronk JT. Optimizing the balance between heterologous acetate- and CO_2-reduction pathways in anaerobic cultures of *Saccharomyces cerevisiae* strains engineered for low glycerol production. *bioRxiv*. 2023;05.
218. Buckenhüskes HJ. Selection criteria for lactic acid bacteria to be used as starter cultures for various food commodities. FEMS Microbiology Reviews. 1993;12:253-71.
219. Coelho MC, Malcata FX, Silva CC. Lactic acid bacteria in raw-milk cheeses: From starter cultures to probiotic functions. Foods. 2022;11:2276.
220. Roell GW, Zha J, Carr RR, Koffas MA, Fong SS, Tang YJ. Engineering microbial consortia by division of labor. Microbial Cell Factories. 2019;18:1-11.
221. Zhou K, Qiao K, Edgar S, Stephanopoulos G. Distributing a metabolic pathway among a microbial consortium enhances production of natural products. Nature Biotechnology. 2015;33:377-83.
222. Shong J, Diaz MRJ, Collins CH. Towards synthetic microbial consortia for bioprocessing. Current Opinion in Biotechnology. 2012;23:798-802.
223. Stanley G, Pamment N. Transport and intracellular accumulation of acetaldehyde in *Saccharomyces cerevisiae*. Biotechnology and Bioengineering. 1993;42:24-9.
224. Nevoigt E, Stahl U. Osmoregulation and glycerol metabolism in the yeast *Saccharomyces cerevisiae*. FEMS microbiology reviews. 1997;21:231-41.
225. Lindemann SR, Bernstein HC, Song H-S, Fredrickson JK, Fields MW, Shou W, et al. Engineering microbial consortia for controllable outputs. The ISME Journal. 2016;10:2077-84.
226. Bachmann H, Pronk JT, Kleerebezem M, Teusink B. Evolutionary engineering to enhance starter culture performance in food fermentations. Current Opinion in Biotechnology. 2015;32:1-7.
227. Tabañag IDF, Chu I-M, Wei Y-H, Tsai S-L. Ethanol production from hemicellulose by a consortium of different genetically-modified *Sacharomyces cerevisiae*. Journal of the Taiwan Institute of Chemical Engineers. 2018;89:15-25.
228. Verhoeven MD, de Valk SC, Daran J-MG, van Maris AJ, Pronk JT. Fermentation of glucose-xylose-arabinose mixtures by a synthetic consortium of single-sugar-fermenting *Saccharomyces cerevisiae* strains. FEMS Yeast Research. 2018;18:foy075.
229. Basso LC, Basso TO, Rocha SN. Ethanol production in Brazil: the industrial process and its impact on yeast fermentation. Biofuel Production-Recent Developments and Prospects. 2011;1530:85-100.

230. Della-Bianca BE, Gombert AK. Stress tolerance and growth physiology of yeast strains from the Brazilian fuel ethanol industry. Antonie Van Leeuwenhoek. 2013;104:1083-95.
231. Jacobus AP, Gross J, Evans JH, Ceccato-Antonini SR, Gombert AK. *Saccharomyces cerevisiae* strains used industrially for bioethanol production. Essays in Biochemistry. 2021;65:147-61.
232. IFF: Your Needs Change, Your Yeast Can't. Ethanol Producer Magazine. 2022 January.
233. Lopes H, Rocha I. Genome-scale modeling of yeast: chronology, applications and critical perspectives. FEMS Yeast Research. 2017;17.
234. Maiorella B, Blanch H, Wilke C. Economic evaluation of alternative ethanol fermentation processes. Biotechnology and Bioengineering. 1984;26:1003-25.
235. Marques WL, Raghavendran V, Stambuk BU, Gombert AK. Sucrose and *Saccharomyces cerevisiae*: a relationship most sweet. FEMS Yeast Research. 2016;16.
236. Geertman J-MA, van Dijken JP, Pronk JT. Engineering NADH metabolism in *Saccharomyces cerevisiae*: formate as an electron donor for glycerol production by anaerobic, glucose-limited chemostat cultures. FEMS Yeast Research. 2006;6:1193-203.
237. Sharma S, Horn SJ. Enzymatic saccharification of brown seaweed for production of fermentable sugars. Bioresource Technology. 2016;213:155-61.
238. Noiraud N, Maurousset L, Lemoine R. Transport of polyols in higher plants. Plant Physiology and Biochemistry. 2001;39:717-28.
239. Jin X, Yin B, Xia Q, Fang T, Shen J, Kuang L, et al. Catalytic transfer hydrogenation of biomass-derived substrates to value-added chemicals on dual-function catalysts: opportunities and challenges. ChemSusChem. 2019;12:71-92.
240. Chujo M, Yoshida S, Ota A, Murata K, Kawai S. Acquisition of the ability to assimilate mannitol by *Saccharomyces cerevisiae* through dysfunction of the general corepressor Tup1-Cyc8. Applied Environmental Microbiology. 2015;81:9-16.
241. Tanaka H, Murata K, Hashimoto W, Kawai S. Hsp104-dependent ability to assimilate mannitol and sorbitol conferred by a truncated Cyc8 with a C-terminal polyglutamine in *Saccharomyces cerevisiae*. PLoS One. 2020;15:e0242054.
242. Enquist-Newman M, Faust AME, Bravo DD, Santos CNS, Raisner RM, Hanel A, et al. Efficient ethanol production from brown macroalgae sugars by a synthetic yeast platform. Nature. 2014;505:239-43.
243. Jordan P, Choe J-Y, Boles E, Oreb M. Hxt13, Hxt15, Hxt16 and Hxt17 from *Saccharomyces cerevisiae* represent a novel type of polyol transporters. Scientific Reports. 2016;6:1-10.

244. Inoue T, Fujishima A, Konishi S, Honda K. Photoelectrocatalytic reduction of carbon dioxide in aqueous suspensions of semiconductor powders. Nature. 1979;277:637-8.
245. Saeki T, Hashimoto K, Fujishima A, Kimura N, Omata K. Electrochemical reduction of CO_2 with high current density in a CO_2-methanol medium. The Journal of Physical Chemistry. 1995;99:8440-6.
246. Flexer V, Jourdin L. Purposely designed hierarchical porous electrodes for high rate microbial electrosynthesis of acetate from carbon dioxide. Accounts of Chemical Research. 2020;53:311-21.
247. Rosenbaum M, Aulenta F, Villano M, Angenent LT. Cathodes as electron donors for microbial metabolism: which extracellular electron transfer mechanisms are involved? Bioresource Technology. 2011;102:324-33.
248. Dykhuizen DE, Hartl DL. Selection in chemostats. Microbiological Reviews. 1983;47:150-68.
249. Novick A, Szilard L. Description of the chemostat. Science. 1950;112:715-6.
250. Gurrieri L, Del Giudice A, Demitri N, Falini G, Pavel NV, Zaffagnini M, et al. *Arabidopsis* and *Chlamydomonas* phosphoribulokinase crystal structures complete the redox structural proteome of the Calvin–Benson cycle. Proceedings of the National Academy of Sciences. 2019;116:8048-53.
251. Yu A, Xie Y, Pan X, Zhang H, Cao P, Su X, et al. Photosynthetic phosphoribulokinase structures: Enzymatic mechanisms and the redox regulation of the Calvin-Benson-Bassham cycle. The Plant Cell. 2020;32:1556-73.
252. Oud B, van Maris AJ, Daran J-M, Pronk JT. Genome-wide analytical approaches for reverse metabolic engineering of industrially relevant phenotypes in yeast. FEMS Yeast Research. 2012;12:183-96.
253. Diderich JA, Schepper M, van Hoek P, Luttik MA, van Dijken JP, Pronk JT, et al. Glucose uptake kinetics and transcription of *HXT* genes in chemostat cultures of *Saccharomyces cerevisiae*. Journal of Biological Chemistry. 1999;274:15350-9.
254. Sarthy AV, Schopp C, Idler KB. Cloning and sequence determination of the gene encoding sorbitol dehydrogenase from *Saccharomyces cerevisiae*. Gene. 1994;140:121-6.
255. Nadai C, Crosato G, Giacomini A, Corich V. Different gene expression patterns of hexose transporter genes modulate fermentation performance of four *Saccharomyces cerevisiae* strains. Fermentation. 2021;7:164.
256. Greatrix BW, van Vuuren HJ. Expression of the *HXT13*, *HXT15* and *HXT17* genes in *Saccharomyces cerevisiae* and stabilization of the *HXT1* gene transcript by sugar-induced osmotic stress. Current Genetics. 2006;49:205-17.

257. Davidi D, Shamshoum M, Guo Z, Bar-On YM, Prywes N, Oz A, et al. Highly active rubiscos discovered by systematic interrogation of natural sequence diversity. The EMBO Journal. 2020;39:e104081.
258. Schievano A, Sciarria TP, Vanbroekhoven K, De Wever H, Puig S, Andersen SJ, et al. Electro-fermentation–merging electrochemistry with fermentation in industrial applications. Trends in Biotechnology. 2016;34:866-78.
259. Mikkelsen MD, Buron LD, Salomonsen B, Olsen CE, Hansen BG, Mortensen UH, et al. Microbial production of indolylglucosinolate through engineering of a multi-gene pathway in a versatile yeast expression platform. Metabolic Engineering. 2012;14:104-11.
260. Bouwknegt J, Wiersma SJ, Ortiz-Merino RA, Doornenbal ES, Buitenhuis P, Giera M, et al. A squalene–hopene cyclase in *Schizosaccharomyces japonicus* represents a eukaryotic adaptation to sterol-limited anaerobic environments. Proceedings of the National Academy of Sciences. 2021;118:e2105225118.
261. Baldi N, de Valk SC, Sousa-Silva M, Casal M, Soares-Silva I, Mans R. Evolutionary engineering reveals amino acid substitutions in Ato2 and Ato3 that allow improved growth of *Saccharomyces cerevisiae* on lactic acid. FEMS Yeast Research. 2021;21:foab033.
262. Perli T, Vos AM, Bouwknegt J, Dekker WJ, Wiersma SJ, Mooiman C, et al. Identification of oxygen-independent pathways for pyridine nucleotide and Coenzyme A synthesis in anaerobic fungi by expression of candidate genes in yeast. mBio. 2021;12:e00967-21.
263. Pilgrim C, Vierhout R. Status of the worldwide fuel alcohol industry. In: The Alcohol Textbook. Walker G, Abbas CA, Ingledew WM, Pilgrim C, editors. 6 ed. Duluth. 2017. p. 1-22.
264. Lynd LR, Beckham GT, Guss AM, Jayakody LN, Karp EM, Maranas C, et al. Toward low-cost biological and hybrid biological/catalytic conversion of cellulosic biomass to fuels. Energy & Environmental Science. 2022;15:938-90.
265. Wang W-C, Tao L. Bio-jet fuel conversion technologies. Renewable and Sustainable Energy Reviews. 2016;53:801-22.
266. Mawhood R, Gazis E, de Jong S, Hoefnagels R, Slade R. Production pathways for renewable jet fuel: a review of commercialization status and future prospects. Biofuels, Bioproducts and Biorefining. 2016;10:462-84.
267. Moon J, Jain S, Müller V, Basen M. Homoacetogenic conversion of mannitol by the thermophilic acetogenic bacterium *Thermoanaerobacter kivui* requires external CO2. Frontiers in Microbiology. 2020;11:571736.
268. Van Gorp K, Boerman E, Cavenaghi C, Berben P. Catalytic hydrogenation of fine chemicals: sorbitol production. Catalysis Today. 1999;52:349-61.

269. Liu X, Wang X, Yao S, Jiang Y, Guan J, Mu X. Recent advances in the production of polyols from lignocellulosic biomass and biomass-derived compounds. RSC Advances. 2014;4:49501-20.
270. Galán G, Martín M, Grossmann IEJI, Research EC. Integrated renewable production of sorbitol and xylitol from switchgrass. Industrial & Engineering Chemistry Research. 2021;60:5558-73.
271. Ban C, Jeon W, Woo HC, Kim DH. Catalytic Hydrogenation of Macroalgae-Derived Alginic Acid into Sugar Alcohols. ChemSusChem. 2017;10:4891-8.
272. Guo H, Zhang H, Chen X, Zhang L, Huang C, Li H, et al. Catalytic upgrading of biopolyols derived from liquefaction of wheat straw over a high-performance and stable supported amorphous alloy catalyst. Energy Conversion and Management. 2018;156:130-9.
273. Noorman HJ, inventor; DSM IP Assets BV, assignee. Greenhouse gas improved fermentation. EP 3715464B1; 2021.
274. Kaup B, Bringer-Meyer S, Sahm H. Metabolic engineering of *Escherichia coli*: construction of an efficient biocatalyst for D-mannitol formation in a whole-cell biotransformation. Applied Microbiology and Biotechnology. 2004;64:333-9.
275. Harris DM, van der Krogt ZA, Van Gulik WM, van Dijken JP, Pronk JT. Formate as an auxiliary substrate for glucose-limited cultivation of *Penicillium chrysogenum*: impact on penicillin G production and biomass yield. Applied and environmental microbiology. 2007;73:5020-5.
276. Wang G, Wang X, Wang T, van Gulik W, Noorman HJ, Zhuang Y, et al. Comparative Fluxome and Metabolome Analysis of Formate as an Auxiliary Substrate for Penicillin Production in Glucose-Limited Cultivation of *Penicillium chrysogenum*. Biotechnology Journal. 2019;14:1900009.
277. van Winden WA, Mans R, Breestraat S, Verlinden RA, Mielgo-Gómez Á, de Hulster EA, et al. Towards closed carbon loop fermentations: Cofeeding of *Yarrowia lipolytica* with glucose and formic acid. Biotechnology and Bioengineering. 2022;119:2142-51.
278. Pérez-Gallent E, Vankani C, Sanchez-Martinez C, Anastasopol A, Goetheer E. Integrating CO_2 capture with electrochemical conversion using amine-based capture solvents as electrolytes. Industrial & Engineering Chemistry Research. 2021;60:4269-78.
279. Malkhandi S, Yeo BS. Electrochemical conversion of carbon dioxide to high value chemicals using gas-diffusion electrodes. Current Opinion in Chemical Engineering. 2019;26:112-21.
280. Claassens NJ, Cotton CA, Kopljar D, Bar-Even A. Making quantitative sense of electromicrobial production. Nature Catalysis. 2019;2:437-47.

281. Ingledew WM. Very high gravity (VHG) and associated new technologies for fuel alcohol production. In: The Alcohol Textbook. Walker G, Abbas CA, Ingledew WM, Pilgrim C, editors. 6 ed. Duluth. 2017. p. 363-76.
282. Zhang J, Jensen MK, Keasling JD. Development of biosensors and their application in metabolic engineering. Current Opinion in Chemical Biology. 2015;28:1-8.
283. D'ambrosio V, Dore E, Di Blasi R, van den Broek M, Sudarsan S, Ter Horst J, et al. Regulatory control circuits for stabilizing long-term anabolic product formation in yeast. Metabolic Engineering. 2020;61:369-80.
284. Wronska AK, van den Broek M, Perli T, de Hulster E, Pronk JT, Daran J-M. Engineering oxygen-independent biotin biosynthesis in *Saccharomyces cerevisiae*. Metabolic Engineering. 2021;67:88-103.
285. Wronska AK, Haak MP, Geraats E, Bruins Slot E, van den Broek M, Pronk JT, et al. Exploiting the diversity of *Saccharomycotina* yeasts to engineer biotin-independent growth of *Saccharomyces cerevisiae*. Applied and Environmental Microbiology. 2020;86:e00270-20.
286. Wiersma SJ, Mooiman C, Giera M, Pronk JT. Squalene-tetrahymanol cyclase expression enables sterol-independent growth of *Saccharomyces cerevisiae*. Applied and Environmental Microbiology. 2020;86:e00672-20.
287. Gomes D, Cruz M, de Resende M, Ribeiro E, Teixeira J, Domingues L. Very high gravity bioethanol revisited: main challenges and advances. Fermentation. 2021;7:38.
288. Aldiguier AS, Alfenore S, Cameleyre X, Goma G, Uribelarrea J, Guillouet S, et al. Synergistic temperature and ethanol effect on *Saccharomyces cerevisiae* dynamic behaviour in ethanol bio-fuel production. Bioprocess and Biosystems Engineering. 2004;26:217-22.
289. Pereira FB, Guimaraes PM, Teixeira JA, Domingues L. Selection of *Saccharomyces cerevisiae* strains for efficient very high gravity bio-ethanol fermentation processes. Biotechnology Letters. 2010;32:1655-61.
290. Wallace-Salinas V, Gorwa-Grauslund MF. Adaptive evolution of an industrial strain of *Saccharomyces cerevisiae* for combined tolerance to inhibitors and temperature. Biotechnology for Biofuels. 2013;6:1-9.
291. Kurylenko OO, Ruchala J, Hryniv OB, Abbas CA, Dmytruk KV, Sibirny AA. Metabolic engineering and classical selection of the methylotrophic thermotolerant yeast *Hansenula polymorpha* for improvement of high-temperature xylose alcoholic fermentation. Microbial Cell Factories. 2014;13:1-10.
292. Radecka D, Mukherjee V, Mateo RQ, Stojiljkovic M, Foulquie-Moreno MR, Thevelein JMJFyr. Looking beyond *Saccharomyces*: the potential of non-conventional yeast species for desirable traits in bioethanol fermentation. FEMS Yeast Research. 2015;15:fov053.

293. Voronovsky AY, Rohulya OV, Abbas CA, Sibirny AA. Development of strains of the thermotolerant yeast *Hansenula polymorpha* capable of alcoholic fermentation of starch and xylan. Metabolic Engineering. 2009;11:234-42.
294. Scully SM, Orlygsson J. Recent advances in second generation ethanol production by thermophilic bacteria. Energies. 2014;8:1-30.
295. Lynd LR, Weimer PJ, Van Zyl WH, Pretorius IS. Microbial cellulose utilization: fundamentals and biotechnology. Microbiology and Molecular Biology Reviews. 2002;66:506-77.
296. White P, Weber E. Lipids of the kernel. Corn: Chemistry and Technology. 2003:355-405.
297. Abbas CA, Langfelder K. Production of cellulosic ethanol at existing ethanol plants. In: The Alcohol Textbook. Walker G, Abbas CA, Ingledew WM, Pilgrim C, editors. 6 ed. Duluth. 2017. p. 237-56.
298. Argyros DA, Stonehouse EA. Yeast strain development for alcohol production. In: The Alcohol Textbook. Walker G, Abbas CA, Ingledew WM, Pilgrim C, editors. 6 ed. Duluth. 2017. p. 287-97.
299. Olson DG, McBride JE, Shaw AJ, Lynd LR. Recent progress in consolidated bioprocessing. Current Opinion in Biotechnology. 2012;23:396-405.
300. Chuck GS, Tobias C, Sun L, Kraemer F, Li C, Dibble D, et al. Overexpression of the maize Corngrass1 microRNA prevents flowering, improves digestibility, and increases starch content of switchgrass. Proceedings of the National Academy of Sciences. 2011;108:17550-5.
301. Lessard PA, Lanahan M, Samoylov V, Bougri O, Emery J, Raab RM, inventors; Agrivida Inc, assignee. Plants with altered levels of vegetative starch. US 9434954B2; 2016.
302. Lynd LR, Van Zyl WH, McBride JE, Laser M. Consolidated bioprocessing of cellulosic biomass: an update. Current Opinion in Biotechnology. 2005;16:577-83.
303. Cripwell RA, Rose SH, Favaro L, Van Zyl WH. Construction of industrial *Saccharomyces cerevisiae* strains for the efficient consolidated bioprocessing of raw starch. Biotechnology for Biofuels. 2019;12:1-16.
304. Yang S-J, Kataeva I, Hamilton-Brehm SD, Engle NL, Tschaplinski TJ, Doeppke C, et al. Efficient degradation of lignocellulosic plant biomass, without pretreatment, by the thermophilic anaerobe "*Anaerocellum thermophilum*" DSM 6725. Applied and Environmental Microbiology. 2009;75:4762-9.
305. Singh N, Mathur AS, Gupta RP, Barrow CJ, Tuli D, Puri M. Enhanced cellulosic ethanol production via consolidated bioprocessing by *Clostridium thermocellum* ATCC 31924☆. Bioresource Technology. 2018;250:860-7.

306. Lynd LR, Paye JM, Balch M, inventors; Dartmouth College, assignee. Systems and methods for enhancing microbial conversion of biomass using mechanical augmentation. US 10533194B2; 2020.
307. Lanahan MB, Basu SS, Batie CJ, Chen W, Craig J, Kinkema M, inventors; Syngenta Participation AG, assignee. Self-processing plants and plant parts. US 7102057B2; 2006.
308. Singh V, Batie CJ, Aux GW, Rausch KD, Miller C. Dry-grind processing of corn with endogenous liquefaction enzymes. Cereal Chemistry. 2006;83:317-20.
309. Shen B, Sun X, Zuo X, Shilling T, Apgar J, Ross M, et al. Engineering a thermoregulated intein-modified xylanase into maize for consolidated lignocellulosic biomass processing. Nature Biotechnology. 2012;30:1131-6.
310. Sharma HK, Xu C, Qin WJW, Valorization B. Biological pretreatment of lignocellulosic biomass for biofuels and bioproducts: an overview. Waste & Biomass Valorization. 2019;10:235-51.
311. Promon SK, Kamal W, Rahman SS, Hossain MM, Choudhury NJF. Bioethanol production using vegetable peels medium and the effective role of cellulolytic bacterial (*Bacillus subtilis*) pre-treatment. 2018;7.